

Identification of genetic interactors of *ypa2* in *Schizosaccharomyces pombe*

THÈSE N° 7158 (2016)

PRÉSENTÉE LE 19 AOÛT 2016

À LA FACULTÉ DES SCIENCES DE LA VIE

UNITÉ DU PROF. SIMANIS

PROGRAMME DOCTORAL EN APPROCHES MOLÉCULAIRES DU VIVANT

ÉCOLE POLYTECHNIQUE FÉDÉRALE DE LAUSANNE

POUR L'OBTENTION DU GRADE DE DOCTEUR ÈS SCIENCES

PAR

Manuela MORARU

acceptée sur proposition du jury:

Prof. O. Hantschel, président du jury

Prof. V. Simanis, directeur de thèse

Prof. I. Hagan, rapporteur

Prof. F. Stutz, rapporteuse

Prof. Y. Barral, rapporteur



ÉCOLE POLYTECHNIQUE
FÉDÉRALE DE LAUSANNE

Suisse
2016

Table of contents	
Acknowledgements	5
Abstract	6
Résumé	7
List of abbreviations	9
Chapter 1 Introduction	11
1.1 Overview of the mitotic cell cycle	11
1.2 <i>Schizosaccharomyces pombe</i> as a model organism	12
1.3 The mitotic cell cycle in fission yeast	13
1.4 Organization of the actin and MT cytoskeletons and the MTOC of fission yeast	17
1.5 Cytokinesis in fission yeast	18
1.5.1 CAR assembly	19
1.5.2 SIN components	20
1.5.3 Localization of the SIN proteins to the SPB	22
1.5.4 SIN regulators	23
1.5.5 The MOR network	24
1.5.6 CK II in <i>S. pombe</i>	25
1.5.7 Synthesis of the division septum and cell separation in fission yeast	25
1.5.8 The cytokinesis checkpoint in <i>S. pombe</i>	28
1.6 Phosphatases	29
1.6.1 Cdc25p	29
1.6.2 PP1	29
1.6.3 PP2A	30
1.6.4 PP2B/Calcineurin	35
1.7 Cytokinesis in other organisms	35
1.7.1 Cytokinesis in plants	35
1.7.2 Cytokinesis in budding yeast	36
1.7.3 Cytokinesis in metazoans	38
1.8 Homologs of SIN and MEN proteins in metazoans	39

Aim of this study.....	41
Chapter 2 Materials and Methods	42
2.1 Nomenclature.....	42
2.2 Fission yeast techniques and reagents.....	42
2.2.1 Fission yeast growth and crossing	42
2.2.2 Cell viability assays of haploid strains.....	42
2.2.3 Creation of diploid strains and cell viability assays	43
2.3 Yeast transformation.....	43
2.4 Synthetic Genetic Array (SGA)	44
2.4.1 Growth and mating of the Bioneer library	44
2.4.2 Spotting spores onto selective plates	44
2.4.3 Data analysis	44
2.5 Molecular biology techniques.....	47
2.5.1 Integration of <i>ypa2-S2</i> at <i>leu1</i> and <i>lys1</i>	47
2.5.2 Insertion of <i>nat^R</i> upstream of <i>ypa2-S2</i>	47
2.6 Imaging and cell length and width measurements.....	48
2.7 Confocal imaging	48
2.7.1 Imaging and analysis of GFP tagged SIN proteins	48
2.7.2 Imaging and analysis of <i>gfp-atb2</i>	48
Chapter 3 Results.....	49
3.1 <i>sup2*</i> , a suppressor of the SIN mutant <i>spg1-M19</i> , is an allele of <i>ypa2</i>	49
3.2 The <i>ypa2-S2</i> mutation lies in a domain required for PTPA ATPase activity	51
3.3 Is <i>ypa2-S2</i> dominant over <i>ypa2⁺</i> ?	51
3.4 Validation of <i>ypa2-S2</i> , as an allele of <i>ypa2</i>	53
3.5 Genetic tagging of the <i>ypa2-S2</i> locus	54
3.6 Characterization of the allele <i>ypa2-S2</i>	55
3.6.1 Is <i>ypa2-S2</i> advanced into mitotic commitment?	55
3.6.2 Does <i>nat^R-ypa2-S2</i> have altered cell polarity?.....	56
3.6.3 Analysis of the genetic interaction of <i>nat^R-ypa2-S2</i> with PP2A mutants	57
3.6.4 Does <i>nat^R-ypa2-S2</i> interact with the SIP?	59
3.6.5 Is the localization of SIN proteins altered in the <i>nat^R-ypa2-S2</i> allele? ...	59

3.7	SGA, to identify genetic interactions of <i>nat^R-ypa2-S2</i>	61
3.7.1	Screening and identification of control interactions.....	61
3.7.2	Bioinformatics analysis	64
3.7.3	Validation of the hits found at 29°C.....	67
3.7.4	Characterization of the interaction between <i>flp1-Δ</i> and PP2A/PTPA mutants	72
3.7.5	Characterization of the interaction between <i>ckb1-Δ</i> and alleles of PP2A/PTPA/Dis2p, SIN and Cdc2p.....	76
4	Discussion	81
4.1	What are the characteristics of the <i>nat^R-ypa2-S2</i> allele?.....	81
4.2	SGA, to identify non-essential genes that show a negative genetic interaction with <i>nat^R-ypa2-S2</i>	81
4.2.1	Concept of the SGA.....	81
4.2.2	Analysis of the hits	82
4.2.3	The validation of hits from the SGA	84
4.2.4	Characterization of the genetic interactions between Flp1p and PP2A/PTPA.....	85
4.2.5	Characterization of the genetic interaction between Ckb1p and PP2A/PTPA.....	88
4.2.6	Concluding remarks.....	90
4.2.7	Future directions	90
5	References.....	91
	Appendix	125
	Table 3:1 List of strains used in this study	125
	Table 3:2 Information on the hits from the SGA (attached to the online version of this document)	126
	Table 3:3 BP of the hits from the SGA (attached to the online version of this document)	126
	Table 3:4 FYPO of the deletion mutants identified as hits in the SGA (attached to the online version of this document)	126
	Table 3:5 Information on the non-growers from the SGA (attached to the online version of this document).....	126
	Table 3:6 BP of the non-growers from the SGA (attached to the online version of this document)	126
	Table 3:7 FYPO of the deletion mutants, which did not grow in the SGA (attached to the online version of this document)	126

Table 3:8	Information on the genes that generated a reduced number of colonies in the SGA (attached to the online version of this document).....	126
Table 3:9	BP of the genes that generated a reduced number of colonies in the SGA (attached to the online version of this document).....	126
Table 3:10	FYPO of the deletion mutants, for the genes that generated a reduced number of colonies in the SGA (attached to the online version of this document)	126
Table 3:11	Summary of the reconstructed interactions found in the SGA (section 3.7.3)	126
Table 3:12	List of primers used in this study.....	126

Acknowledgements

I express my gratitude to Viesturs, for offering me the chance to do my PhD studies in his laboratory and for inspiring me scientifically during my time here. Also, I thank Viesturs for the support he offered during thesis writing and throughout my applications for a postdoc position.

To Moira and Viesturs I thank for the fun events they organized outside the laboratory, in the last four years.

I thank Andrea for scientific discussions, for teaching me laboratory techniques and for sharing laboratory protocols.

I thank Elena for technical assistance and for keeping organized laboratory protocols, which were of great help throughout my time here.

I thank Claudia for being a fun colleague during the last year and to Paulina and Evelyn, for the help they offered to me in the first months of my arrival in the laboratory.

I wish to thank Jonathan Sobel, Julie Russeil and Romain Hamelin for their input into my projects.

I thank Prof. Yves Barral, Prof. Iain Hagan, Prof. Olivier Hantschel, Prof. Joachim Lingner and Prof. Françoise Stutz for accepting to be examiners in my candidacy and/or PhD exams.

I thank Prof. Joachim Lingner, Dr. Boris Egger and Prof. Simon Sprecher for writing recommendation letters during the period that I applied for a postdoc position.

I thank my friends and family for supporting me at all times. I thank my mother, who changed her life to make my dreams possible and to Seydar for everything that we achieved together.

Abstract

In this study, the fission yeast *Schizosaccharomyces pombe* was used as a model system to study the cellular signaling that underlies cell cycle progression. Phosphorylation plays an important part in the regulation of this process. Kinases catalyze the transfer of a phosphate group to a substrate, which may regulate its activity. Protein phosphatases oppose the activity of protein kinases; the balance of their activities regulates signaling flux in many signaling pathways.

The **Septation Initiation Network (SIN)** is a signaling cascade that regulates cytokinesis in fission yeast. SIN signaling is triggered by a GTPase and is transduced by three protein kinases; phosphorylation plays an important role in controlling SIN signalling. Numerous genetic screens and biochemical analyses have identified phosphatases and kinases that regulate the SIN. The protein phosphatases Calcineurin/**Protein Phosphatase 2B (PP2B)** and Flp1p promote SIN signaling, while PP2A is a SIN inhibitor. PP2A is conserved and is activated by the chaperone **Phosphatase Two A Phosphatase Activator (PTPA)**. *S. pombe* has two PTPA-related genes, *ypa1* and *ypa2*; the deletion mutant of the latter rescues SIN mutants which cannot undergo cytokinesis, consistent with PP2A opposing SIN signaling.

The phenotype of the deletion mutant of *ypa2*, indicates that it is involved in the control of cell polarity, cell growth, mitotic commitment and cytokinesis. In this study, we characterized the hypomorphic allele *ypa2-S2* which rescues SIN mutants, but is otherwise largely normal. *ypa2-s2* was used as bait in a synthetic genetic array screen, to identify genes whose products compensate for reduced function of Ypa2p.

A large number of hits were identified, of which approximately ninety percent are novel genetic interactors of *ypa2*. Validation studies indicated that eighty percent of the interactions seen in the high-throughput screen can be reconstructed. The identified genes regulate several biological processes, including signal transduction and protein phosphorylation. This prompted us to further characterize the roles of Ckb1p and Flp1p, in regulating cytokinesis signaling.

Ckb1p is a regulatory subunit for **Casein Kinase II (CK II)**, which was previously implicated in polar growth. The phenotype of the mutant *ypa2-S2 ckb1-Δ* indicates that Ckb1p, similar to Ypa2p, contributes to the regulation of mitotic commitment and cytokinesis signaling. Furthermore, *ckb1-Δ* showed negative genetic interaction with PP2A and SIN mutants.

Flp1p is a protein phosphatase that was reported to regulate mitotic commitment and to promote SIN signaling. The double mutant between *ypa2-S2* and *flp1-Δ* showed cell separation defects and phenotypic analysis of double mutants between *flp1-Δ* and PP2A mutants indicates that these phosphatases cooperate in cell separation.

Overall, this work has uncovered novel facets of the regulation of cytokinesis in *S. pombe*, implicating CK II in controlling SIN signaling, and uncovering cooperative interactions between different phosphatases in controlling cytokinesis.

Keywords: *Schizosaccharomyces pombe*, cell cycle, cytokinesis, SIN, PP2A, PTPA, Ypa2p, CK II, Ckb1p, Flp1p

Résumé

Dans cette étude, nous utilisons la levure à fission *Schizosaccharomyces pombe* comme organisme modèle pour étudier la signalisation cellulaire permettant la progression du cycle cellulaire. La phosphorylation joue un rôle important dans la régulation de ce processus. Les protéines kinases catalysent le transfert d'un groupe phosphate au substrat, ce qui permet de réguler l'activité de ce dernier. Les protéines phosphatases ont une activité opposée à celle des kinases; la balance de ces deux activités antagonistes régule de nombreuses voies de signalisation.

Le réseau d'initiation de la septation (Septation Initiation Network or SIN) est une cascade de signalisation qui régule la cytotérière chez *S. pombe*. La signalisation du SIN est initiée par une GTPase et transduite par trois kinases; la phosphorylation joue un rôle important dans le contrôle de la signalisation du SIN. De nombreux criblages génétiques et analyses biochimiques ont permis d'identifier des phosphatases et des kinases qui régulent le SIN. Les phosphatases Calcineurin/PP2B et Flp1p promeuvent la signalisation du SIN, alors que la phosphatase PP2A (Protein Phosphatase Two A) est un inhibiteur du SIN. PP2A est conservée et activée par la chaperone PTPA (Phosphatase Two A Phosphatase Activator). *S. pombe* possède 2 gènes associés à PTPA, *ypa1* et *ypa2*; la délétion de cette dernière restaure les mutants du SIN qui ne peuvent pas effectuer de cytotérière, montrant l'opposition de rôles de PP2A dans la signalisation du SIN.

Le phénotype du mutant dont le gène *ypa2* est délété indique qu'il est impliqué dans le contrôle de la polarité cellulaire, la croissance cellulaire, l'entrée en mitose et la cytotérière. Dans cette étude, nous avons caractérisé l'allèle hypomorphe *ypa2-S2* qui restaure les mutants SIN, mais qui se comporte par ailleurs normalement. *ypa2-S2* a été utilisé comme gène cible dans un essai de criblage génétique synthétique pour identifier des gènes dont les produits compensent les fonctions réduites de Ypa2p.

Un grand nombre de candidats ont été identifiés, parmi lesquels quatre-vingt-dix pour cent sont de nouveaux partenaires génétiques de *ypa2*. Les études de validation montrent que quatre-vingts pour cent des interactions identifiées dans le criblage haut-débit peuvent être reconstituées. Les gènes identifiés régulent différents processus biologiques, parmi lesquels la transduction du signal et la phosphorylation de protéines. Ceci nous a amené à mieux caractériser les rôles de Ckb1p et Flp1p dans la régulation de la signalisation de la cytotérière.

Ckb1p est une sous-unité régulatrice de CKII (Casein Kinase II), protéine impliquée également dans la croissance polaire. Le phénotype du mutant *ypa2-S2 ckb1-Δ* indique que Ckb1p, comme Ypa2p, contribue à la régulation de l'entrée en mitose et de la signalisation de la cytotérière. De plus, *ckb1-Δ* présente une interaction génétique négative avec PP2A et des mutants du SIN.

Flp1p est une protéine phosphatase impliquée dans la régulation de l'entrée en mitose et dans la promotion de la signalisation du SIN. Le double mutant *ypa2-S2* et *flp1-Δ* montre des défauts de division cellulaire et l'analyse phénotypique du double mutant *flp1-Δ* and PP2A indique que les phosphatases coopèrent dans la division cellulaire.

Globalement, cette étude a permis de découvrir de nouvelles facettes de la régulation de la cytotodiérèse chez *S. pombe*, impliquant la protéine CKII dans le contrôle de la signalisation du SIN et la découverte d'interactions coopératives entre différentes phosphatases dans le contrôle de la cytotodiérèse.

Mots-clés: *Schizosaccharomyces pombe*, cycle cellulaire, cytotodiérèse, SIN, PP2A, PTPA, Ypa2p, CK II, Ckb1p, Flp1p

List of abbreviations

Ade	Adenine
A	Adenosine
aa	aminoacid
APC	Anaphase Promoting Complex
Asp	Aspartic acid
AVG	Average
BP	Biological Process
CAK	Cdk Activating Kinase
CAR	Contractile Acto-myosin Ring
CDK	Cyclin-Dependent Kinase
CDKI	Cyclin Dependent Kinase Inhibitor
CDS	Coding Sequence
CK	Casein Kinase
cM	centimorgan
cs	cold sensitive
CYH	Cycloheximide
DAPI	4',6-Diamidino-2-Phenylindole
DMSO	Dimethyl Sulfoxide
FEAR	Fourteen Early Anaphase Release
Fig.	Figure
5-FOA	5-Fluoroorotic Acid
5-FU	5-Fluorouracil
FYPO	Fission Yeast Phenotype Ontology
G	Guanine
G1/G2	Gap phase 1 and 2
G418	Geneticin
GEF	Guanine Nucleotide Exchange Factor
GFP	Green Fluorescent Protein
GO	Gene Ontology
HDAC	Histone Deacetylase
hs	heat sensitive
<i>kan^R</i>	kanamycin/G418 resistance gene
kb	kilobases
Leu	Leucine
Lys	Lysine
EMM2	Edinburgh Minimal Medium
Ile	Isoleucine
M	Median
MAPK	Mitogen Activated Protein Kinase
MCC	Mitotic Checkpoint Complex
MEN	Mitotic Exit Network
MOR	Morphogenesis Orb6 Network
MS	Multiseptated
MT	Microtubule
MTOC	Microtubule Organizing Center
NAT	Nourseothricin
<i>nat^R</i>	nourseothricin resistance gene
NDR	Nuclear Dbf2-Related
nt	nucleotide
ORF	Open Reading Frame
OE	Overexpression
PAA	Post-Anaphase Array
PB	Phloxine B

PEM	Pombe Epistasis Mapper
PP	phosphatase
PPI	Peptidyl Prolyl Isomerase
PTPA	Phosphatase Two A Phosphatase Activator
PP2A	Protein Phosphatase Two A
S	Synthesis
SAC	Spindle Assembly Checkpoint
Ser	Serine
SGA	Synthetic Genetic Array
SIN	Septation Initiation Network
SIP	SIN Inhibitory Phosphatase Complex
SNP	Single Nucleotide Polymorphism
SPB	Spindle Pole Body
ST DEV	Standard Deviation
ts	temperature sensitive
TBZ	Thiabendazole
TOR	Target of Rapamycin
Thr	Threonine
Tyr	Tyrosine
UTR	Untranslated Region
Val	Valine
vs	versus
<i>WT</i>	<i>Wild Type</i>
YE	Yeast Extract
YT	Yeast Extract and Tryptone

Chapter 1 Introduction

1.1 Overview of the mitotic cell cycle

Living organisms perpetuate by means of cell division. The cell cycle comprises the sequential events that lead to cell division, which allows a cell to replicate itself. Although there are differences between the steps of the eukaryotic cell cycle as compared to prokaryotes, the main events that a cell has to accomplish are cell growth, DNA replication and segregation of the cellular content, between the two resulting cells. In eukaryotes, the mitotic cell cycle is involved in development and homeostasis, while meiosis is required for gamete production (Dewey et al., 2015; Verlhac and Terret, 2016). Mitotic division is intensively studied, due to its implication in disease (Malumbres and Barbacid, 2009). My work dealt with regulation that occurs in the mitotic cell cycle, therefore the subsequent sections focus on this type of division.

The phases of the eukaryotic cell cycle are interphase, mitosis and cytokinesis. Interphase is comprised of three phases: G₁, S and G₂, during which a cell grows and duplicates its DNA content. Mitosis is subdivided into prophase, metaphase, anaphase and telophase. In mitosis, chromosomes condense and each of the two copies of a chromosome is pulled to one of the two poles of the mitotic spindle. Cytokinesis ensures the partitioning of the cytoplasm and the physical separation of the two resulting cells. The newly created cells will choose whether to enter a mitotic cell cycle or a quiescent state (known as G₀), dependent upon the environmental and intrinsic conditions (De Virgilio, 2012; Dominguez-Brauer et al., 2015; Hug and Lingner, 2006; Vermeulen et al., 2003).

Progression through the cell cycle is achieved by changes in the periodic activity of CDK enzymes, which are bound and activated by cyclin proteins. Different cyclin/CDK complexes were shown to phosphorylate substrates that effect processes specific to the each cell cycle phase; the canonical stage at which each CDK is involved is listed in Table 1:1 (Bloom and Cross, 2007; Loog and Morgan, 2005; Vermeulen et al., 2003). To ensure unidirectional cell cycle progression, the localization, expression and degradation of cyclins and CDKs is regulated (King et al., 1996; Yang and Kornbluth, 1999).

CDK		Cyclin	Cell cycle phase activity
CDK4		Cyclin D	G ₁ phase
CDK6		Cyclin D	G ₁ phase
CDK2		Cyclin E	G ₁ /S phase transition
CDK2		Cyclin A	S phase
CDK1	(cdc2)	Cyclin A	G ₂ /M phase transition
CDK1	(cdc2)	Cyclin B	Mitosis
CDK7		Cyclin H	CAK, all cell cycle phases

Table 1:1 Cyclin/CDK complexes specific to the cell cycle stages of metazoan cells. Different CDKs are activated by cell cycle phase-specific cyclins as indicated, to regulate mitotic progression. CDK1 is also known as Cdc2p. Modified after (Vermeulen et al., 2003).

In early G₁, in response to nutrient supply and growth factors, a cell decides whether to enter the mitotic cell cycle or a G₀ state; once it has passed the so-called restriction point (or START), a cell is committed to mitosis (Hartwell and Unger, 1977; Pardee, 1974). Cell cycle checkpoints increase the fidelity of the cell cycle events

and maintain their order. There are two DNA damage checkpoints. At the G1/S transition, checkpoint activation leads to the inhibition of CDK by CDKI (Agarwal et al., 1998; Ko and Prives, 1996; Levine, 1997), which delays DNA replication (Painter, 1986; Paulovich and Hartwell, 1995). The DNA damage checkpoint that operates at G2/M transition blocks entry into mitosis by inhibiting a CDK1 activating phosphatase (Sanchez et al., 1997; Zeng et al., 1998) and by sequestration of cyclin B (Hermeking et al., 1997; Taylor and Stark, 2001). Another control within the cell cycle monitors cell size at division, such that a certain size is attained before the G1/S transition (Godin et al., 2010; Kafri et al., 2013; Son et al., 2012). The antephasis checkpoint delays mitotic entry and progression if cells are subjected to stresses that may affect chromosome integrity, the MT cytoskeleton or the growth temperature (Chin and Yeong, 2010). The cell also monitors the abscission process, blocking it if there is DNA in the bridge between the cells (Carmena et al., 2012; Norden et al., 2006).

1.2 *Schizosaccharomyces pombe* as a model organism

The advantages of using *S. pombe* (also known as fission yeast) to study basic processes in the eukaryotic cell are the short generation time, annotated genome, well-established methods for classical and molecular genetics, cell biology and biochemistry. In fission yeast studies were made on processes conserved in humans, such as cell division cycle, chromosome structure, cytoskeletal organization, DNA recombination, organelle biogenesis, RNA splicing and translation (Hoffman et al., 2015; Smith, 2009).

Fission yeast preferentially propagates in a haploid state, however diploids can be selected for and propagated. Mating of fission yeast requires fusion between cells of opposite mating types, known as h^+ and h^- . While heterothallic strains stably express the character of one of the two mating types (due to mutations at the mating type loci), homothallic (h^{90}) cells can switch to h^- or h^+ , by expressing *mat2* (for h^+) or *mat3* (for h^-) from the mating type locus *mat1*. This allows h^{90} strains to undergo meiosis at high frequency and is thus, preferred in meiosis-related studies. Mating between heterothallic strains allows the construction of desired mutant genotypes. When starved for nitrogen, cells of opposite mating type fuse and a diploid zygote is

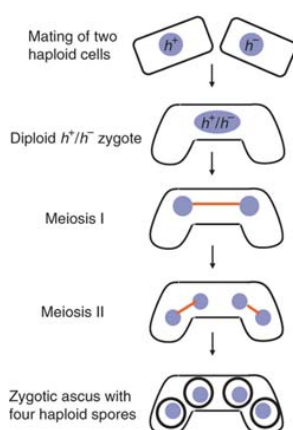


Fig 1:1 Schematic diagram of meiosis in *S. pombe*. Upon nitrogen starvation, cells of opposite mating type fuse and form a diploid zygote. If starvation persists, the zygote enters meiosis, which generates four spores embedded in an ascus. Taken from (Cipak et al., 2014).

generated. If starvation persists, the zygote undergoes meiosis (Fig. 1:1), whereas plating on rich medium allows them to re-enter mitosis and thus, propagate as diploids. Because they are genetically unstable, diploids often convert to the haploid state (Moreno et al., 1991; Smith, 2009).

1.3 The mitotic cell cycle in fission yeast

Similar to higher eukaryotes, one can distinguish that the fission yeast mitotic cell cycle comprises of interphase, mitosis and cytokinesis; however, the relative duration of the phases differs (Fig 1:2). In contrast to human cells, which spend a long time in the G1 and S phases, *S. pombe* spends 0.7 of the cell cycle in G2 and 0.1 in each of the other phases (Moreno et al., 1991; Smith, 2009).

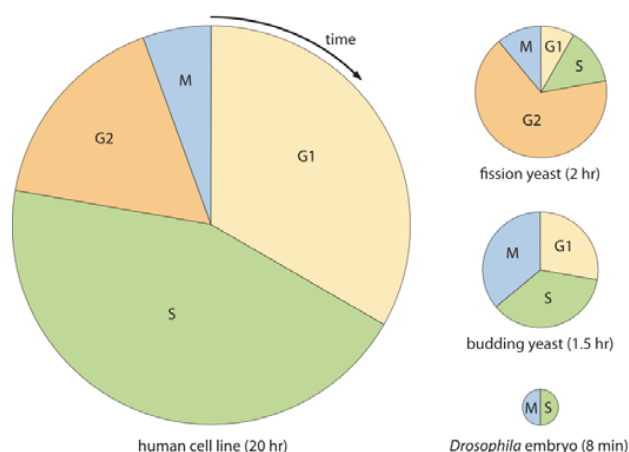


Fig 1:2 Representation of distribution of the cell cycle phases, in different eukaryotes. The cell cycle duration indicated for each organism, corresponds to that found under best growth conditions. The colored sections of each chart represent the proportion of each cell cycle phase indicated, in one mitotic cycle (source: <http://book.bionumbers.org/how-long-do-the-different-stages-of-the-cell-cycle-take/>).

Exponentially growing *S. pombe* cells, in rich medium, are about 7 μm long following cell separation. Fission yeast grows by tip elongation and initially cell growth occurs at the “old” cell end, which existed prior to cytokinesis. Once DNA replication completed, growth is also initiated at the “new” cell end. This process is known as “new end take off” (NETO); growth continues at both ends until the cell length reaches $\approx 14 \mu\text{m}$, which corresponds to 0.75 in the cell cycle. Growth then stops, the actin and MT cytoskeletons reorganize and the cell enters mitosis (Hagan and Yanagida, 1995; Hagan and Hyams, 1996; Mitchison and Nurse, 1985). The division plane is set at the cell center, therefore two equally sized daughter cells are generated (Fig. 1:3).

Since cells stop growing at mitotic commitment, the length of the dividing cell indicates whether it is advanced or delayed in mitotic commitment compared to *WT*. Cytokinesis normally occurs directly after mitosis and is characterized by the construction of a medially placed division septum, which is composed of cell wall material deposited at the site of cell separation. Therefore, the length of septated cells indicates the cell size at mitotic commitment (Mitchison, 1957, 1970; Mitchison and Nurse).

Two cell size checkpoints were identified, at the G1/S and G2/M transition points of the cell cycle. In early G1 a cell decides whether nutrient availability is sufficient to allow a mitotic cell cycle or whether to undergo mating. Transition of a cell through the restriction point (also called START) in G1, commits it to mitosis (Fantes and Nurse, 1977; Nasmyth, 1979; Nurse and Bissett, 1981; Nurse and Thuriaux, 1977). The G1/S control requires that a certain cell size is attained before progression into the S phase. This control is observed only when cells are grown in limiting nutrient conditions and in mutants that divide at reduced cell length. The cells grown in rich medium generate daughter cells that are already in G2, because G1 and S occur during cell separation. In this case only the G2/M size checkpoint is manifested (Sveiczer et al., 1996).

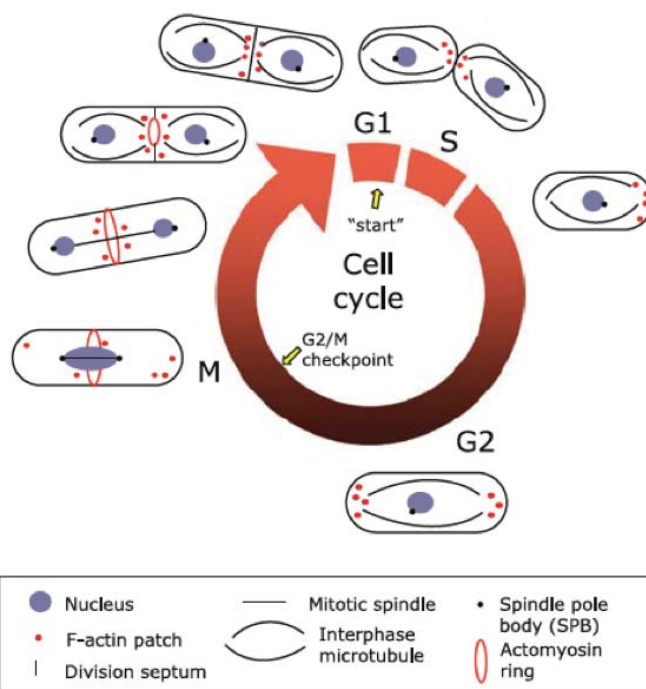


Fig. 1:3 Schematic of the cell cycle progression in fission yeast. Changes in cell length, reorganization of the actin and MT cytoskeletons and the nuclear division are indicated for each cell cycle phase. Yellow arrows indicate the cell size controls. Modified after (Ng et al., 2006).

Cell cycle progression is under the control of cyclins and CDKs (Nurse, 1990). Seven cyclins and two CDKs were identified in *S. pombe* (Bamps et al., 2004; Furnari et al., 1997; Nurse and Thuriaux, 1980; Tanaka and Okayama, 2000), however the B-type cyclin Cdc13p activates Cdc2p/CDK1 to promote both commitment to S phase and mitosis (Nurse and Bissett, 1981). The G1/S transition is achieved with low levels of Cdc2p, while high levels are required for mitotic commitment (Booher and Beach, 1988; Coudreuse and Nurse, 2010; Fisher and Nurse, 1995; Fisher and Nurse, 1996; Mitchison, 1957; Nurse and Bissett, 1981).

To achieve progression through the mitotic cycle, the Cdc2p kinase activity is regulated by 1) inhibition of its activating cyclin by Rum1p, until the required cell mass was attained for entry into the S phase (Labib and Moreno, 1996; Moreno and Nurse, 1994), 2) periodic degradation of Cdc13p regulated by the anaphase-

promoting complex, with high Cdc13p levels in G2 and low as the cell progresses through mitosis and early interphase (Blanco et al., 2000; Creanor and Mitchison, 1996; Yamaguchi et al., 2000) and 3) regulation of Cdc2p by phosphorylation.

The regulation of Cdc2p by phosphorylation modulates its ability to bind Cdc13p. Phosphorylation of Cdc2p Thr 167 is important for stable association to Cdc13p and is catalyzed by the activity of CAKs (Buck et al., 1995; Damagnez et al., 1995; Gould et al., 1991; Hermand et al., 1998). Phosphorylation of Tyr 15, on Cdc2p, is inhibitory and is catalyzed by the kinases Wee1p and Mik1p. To allow mitotic entry, this phosphorylation is reversed by the phosphatase Cdc25p (Fig. 1:4) (Fantès, 1979; Featherstone and Russell, 1991; Gould and Nurse, 1989; Lundgren et al., 1991; Millar et al., 1991; Russell and Nurse, 1986, 1987b).

Cdc2p, Wee1p, Mik1p and Cdc25p are conserved in all eukaryotes (Morgan, 1997). This regulatory network controls cell size at division in fission yeast and the relationship between these gene products (Fig. 1:4) was uncovered by altering their activity. OE of Cdc25p and deletion of *wee1*, as well as mutations in *cdc2* advances cells into mitosis, because the cells divide at reduced cell length (Nurse and Thuriaux, 1980; Russell and Nurse, 1986). Deletion of *cdc25* is lethal and generates elongated mononucleated G2 cells, a phenotype similar to OE of Wee1p (Russell and Nurse, 1986, 1987b).

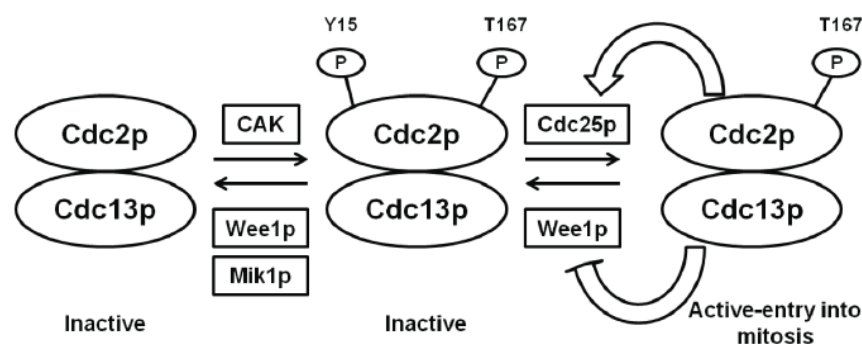


Fig. 1:4 The regulatory network that controls commitment to mitosis. Wee1p and Mik1p phosphorylate and inhibit Cdc2p, thus mitotic commitment is delayed and cell growth continues. Cdc25p dephosphorylates Cdc2p, which is then phosphorylated by CAK. This promotes Cdc2p binding to Cdc13p; active Cdc2p kinase activates Cdc25p and downregulates Wee1p. Taken from doi:10.5075/epfl-thesis-5292.

Cdc25p and Wee1p are considered to be upstream regulators of Cdc2p, because *cdc2* mutants exist that do not respond to *wee1* and *cdc25* (Fantès, 1981; Nurse and Thuriaux, 1980); also, Wee1p and Cdc25p function in different pathways, because the phenotypes resulting from altering these genes are additive (Fantès, 1979; Russell and Nurse, 1986, 1987b). Deletion of Wee1p-like kinase, Mik1p, does not generate an obvious phenotype in unperturbed cells, however the double mutant with the hypomorphic allele *wee1-50* is lethal (Lundgren et al., 1991). A second phosphatase that targets Tyr 15 and activates Cdc2p is Pyp3p; disruption of *pyp3* leads to mitotic delay and this effect is strongly enhanced in a background with reduced *cdc25* function (Millar et al., 1992).

The regulation of Cdc25p and Wee1p is achieved by posttranslational modification. Wee1p is phosphorylated and inhibited by the kinases Nim1p/Cdr1p and Cdr2p (Feilotter et al., 1991; Kanoh and Russell, 1998; Russell and Nurse, 1987a; Wu and Russell, 1993) and dephosphorylation is mediated by the phosphatases Pyp1p and Pyp2p (Hannig et al., 1994; Navarro and Nurse, 2012). At mitotic entry, Cdc25p is activated by phosphorylation, which depends upon Cdc2p (Fig. 1:4) (Kovelman and Russell, 1996). The reciprocal activation between Cdc2p and Cdc25p was suggested to be promoted by the Plo1p kinase (Tanaka et al., 2001).

PP2A and its activator (PTPA) inhibit mitotic progression, because mutations in PP2A subunits and PTPA advance cells into mitosis and there is a strong negative genetic interaction between these and *wee1-50* (Bernal et al., 2012; Chica et al., 2016; Goyal and Simanis, 2012). Input from the environmental conditions controls mitotic commitment. When grown in media with low nitrogen, the TOR signaling pathway is turned off, which leads to advancement into mitosis by inhibition of PP2A (Chica et al., 2016) and by modulation of Pyp2p activity (Fantes and Nurse, 1977; Petersen and Nurse, 2007).

The protein kinase Pom1p functions in the mechanism responsible for sensing cell growth and regulates commitment to mitosis, upstream of Cdr2p (Fig 1:5). This regulation is known as “the cell geometry model”, in which Pom1p forms a gradient whereby it strongly localizes at cell ends and diminished towards the cell center.

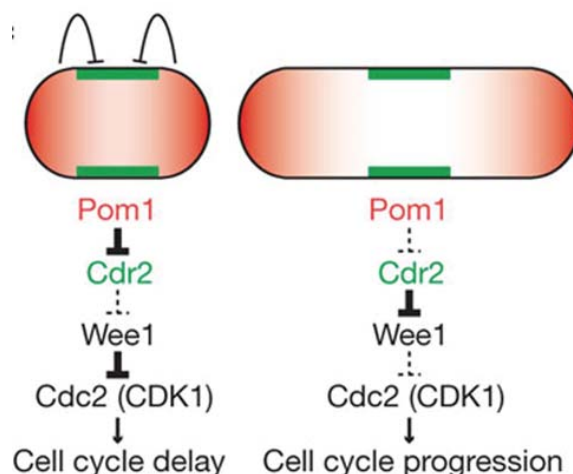


Fig. 1:5 The cell geometry model of mitotic commitment regulation in fission yeast. Pom1p kinase localizes at the cell ends and creates a gradient towards the cell center. In short cells the Pom1p levels that reach the cell center inhibit the medially located Cdr2p kinase. This allows Wee1p to inhibit Cdc2p activation and thus, delay mitotic commitment. As cell length increases, Pom1p activity at the cell center diminishes, which allows Cdr2p activation, further inhibition of Wee1p and activation of Cdc2p. Taken from (Martin and Berthelot-Grosjean, 2009).

Cdr2p localizes at the cortex of the cell center, as a broad band, in interphase; upon entry into mitosis Cdr2p delocalizes from the cell center and reappears in the cells generated by cell separation (Martin and Berthelot-Grosjean, 2009; Morrell et al., 2004a; Moseley et al., 2009). It was proposed that in short cells Pom1p activity is strong at the cell center and inhibits Cdr2p; as cells elongate, Pom1p activity diminishes at the cell center and Cdr2p gets activated. Further, Cdr2p inhibits Wee1p,

which is an inhibitor of Cdc2p activity (Martin and Berthelot-Grosjean, 2009; Moseley et al., 2009).

1.4 Organization of the actin and MT cytoskeletons and the MTOC of fission yeast

The actin cytoskeleton is essential in most eukaryotes and the assembly and disassembly of actin occurs under the activity of a large number of proteins. Actin can be globular, monomeric (G-actin) or filamentous, polymeric (F-actin). Actin monomers organize into polymers and polymers are further organized into filaments (or cables). F-actin cables form by incorporation of ATP-bound G-actin, which is promoted by formins and the Arp2/3 complex and is inhibited by profilin. Three types of F-actin structures have been reported in fission yeast: cortical actin patches, actin cables and the CAR (Mishra et al., 2014). Actin patches and cables are involved in cell polarity establishment and localization of actin patches correlates with growing cell ends (Marks et al., 1986; Martin and Arkowitz, 2014). Actin cables span along the cell length (Fig 1:6) and provide tracks for the delivery of exocytic vesicles. For3p is required for nucleation of actin cables and is activated by the GTPase Cdc42p (Martin and Arkowitz, 2014). MTs are important in polarity establishment, by delivering the proteins Tea1p and Tea4p at the cell tips, where they associate with For3p and Tea4p is believed to also activate For3p (Martin and Chang, 2005).

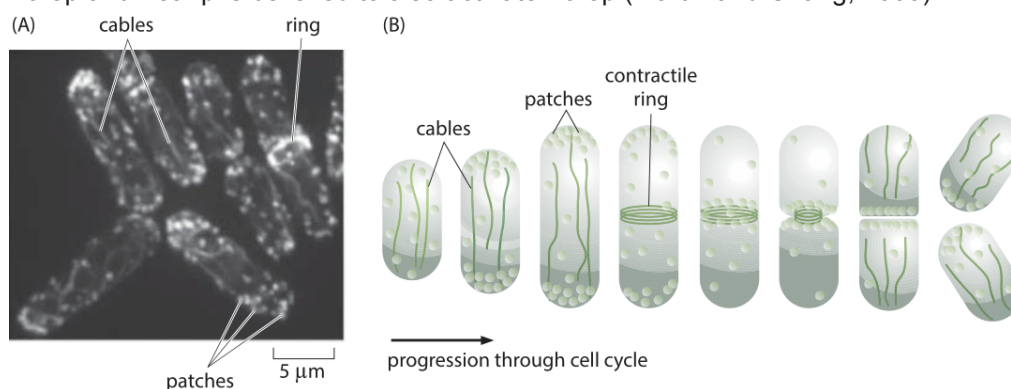


Fig. 1:6 Organization of the actin cytoskeleton throughout the mitotic cell cycle in fission yeast cells. A) Fluorescence imaging of the F-actin associated protein GFP-CHD (calponin homology domain of Rng2). B) Schematic of the cell cycle specific distribution of actin throughout the cell cycle. In interphase and early mitosis, actin patches are found at the cell tips and actin cables are distributed along the cell length. In mitosis actin patches and cables reorganize at the cell center, to form the CAR. Ring constriction brings about cell separation and the actin cytoskeleton takes the interphasic specific distribution in the generated cells (Kovar et al., 2011) (source: <http://book.bionumbers.org/what-are-the-concentrations-of-cytoskeletal-molecules/>).

MTs are polarized structures, which form by polymerization of α and β -tubulin heterodimers. The “plus” end of a MT is oriented towards the cell membrane and its growth is highly dynamic, while the “minus” end is oriented towards the nucleus, where it attaches to the centrosome (Cassimeris, 1999). Nucleation of MTs is initiated from the centrosomes (also known as MTOCs) and requires γ -tubulin and associated proteins (Schiebel, 2000; Stearns et al., 1991).

Similar to other eukaryotes, γ -tubulin is an integral component of the centrosome counterpart in *S. pombe*, which is known as the SPB (Stearns et al., 1991). MTs

function in the spatial organization of the cell and in cell division, and they undergo a cell-cycle specific reorganization: in interphase MT bundles span the cell in antiparallel arrays (Hagan, 1998) and keep the nucleus at the cell middle by “pushing” forces resulting from their polymerization (Tran et al., 2001). Upon mitotic entry, MTs are nucleated both inwards and outwards, from the separating SPBs.

Nucleation of MTs towards the cell membrane generates the astral MTs, whereas inwards nucleation of MTs, between the separating SPBs gives rise to the mitotic spindle. Astral MTs contribute to the pulling of the mitotic spindle towards the cell ends and to keep the mitotic spindle correctly oriented. In anaphase, upon separation of the two nuclei at the opposite cellular poles, the mitotic spindle breaks down and MTs distribute in a ring-like structure at the cell center, which colocalizes with the CAR (Heitz et al., 2001). This pattern of MTs distribution is known as PAA. Upon cell separation, the MT organization changes to an interphase-specific one (Fig. 1:7) (Hagan, 1998).

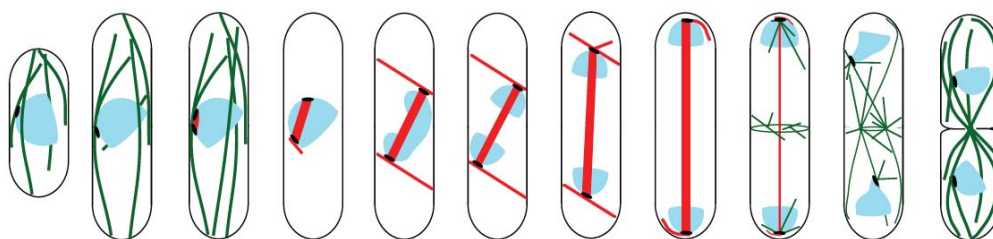


Fig 1:7 Organization of the MT cytoskeleton throughout the mitotic cell cycle in fission yeast. MTs are depicted in green, when interphasic and in red, if mitotic; chromatin is shown in blue and the SPBs are represented by black, ovals. Described from left to right: in interphase, MTs are organized along the cell. As the cell enters mitosis, SPBs separate and the mitotic spindle and astral MTs are organized. Upon separation of the nuclei at the opposite cellular poles, the mitotic spindle breaks and organizes in a ring-like structure at the cell middle. Subsequently, the MTs emanate out of the ring, towards the cell poles; this is known as the PAA. As cells progress to cell separation, MTs reorganize in the interphase-specific array. Taken from (Hagan, 1998).

The SPB is not only involved in MT nucleation but is also a docking site for molecules that signal cell cycle progression and cytokinesis (Hagan, 2008). In interphase the SPB is located adjacent to the nuclear membrane, in the cytoplasm. In late G2 the SPB duplicates and invagination of the nuclear membrane forms fenestrae, which allow insertion of the SPBs into the nucleus. At mitotic exit the closure of fenestrae leads to relocation of the SPBs into the cytoplasm (Ding et al., 1997). The protein Brr6p localizes to the SPB at mitotic commitment and mitotic exit and is essential for the nuclear insertion of the SPBs (Tamm et al., 2011).

1.5 Cytokinesis in fission yeast

In fission yeast, cytokinesis is promoted by the assembly and constriction of a medially placed CAR. In addition to CAR constriction, cell wall material is deposited at the site of cell division, which forms a structure known as the division septum; progressive degradation of the inner part of the division septum allows cell separation (Perez et al., 2016; Thiyagarajan et al., 2015; Zhou et al., 2015).

1.5.1 CAR assembly

CAR assembly at the medial region is guided by the anilin-related protein Mid1p (Balasubramanian et al., 1998; Chang et al., 1996; Sohrmann et al., 1996). Mid1p is restricted at the cell center by inhibitory cues, which emanate from the cell tips (Celton-Morizur et al., 2006; Padte et al., 2006) and positive signaling, provided by the position of the nucleus (Daga and Chang, 2005; Tolic-Norrelykke et al., 2005). In interphase, Mid1p is localized in the nucleus and as a faint band, at the medial region. Upon mitotic commitment, Plo1p mediates nuclear exclusion of Mid1p, which forms a node-like band at the medial cell cortex. Cdr2p attaches Mid1p at the cortex and both recruit CAR components (Almonacid et al., 2009; Bahler et al., 1998a; Sohrmann et al., 1996; Wu et al., 2003). At mitotic entry, several ring components are recruited to the nodes; Mid1p recruits the acto-myosin protein Rng2p, which further recruits the F-bar protein Cdc15p and the heavy chain protein of myosin II, Myo2p (Almonacid et al., 2011; Laporte et al., 2011; Padmanabhan et al., 2011; Wu et al., 2003). Other proteins that are recruited early at the cortical nodes are the light chain proteins of myosin II, Cdc4p and Rlc1p and the formin Cdc12p (Coffman et al., 2009; Laporte et al., 2011; Moteji et al., 2000; Padmanabhan et al., 2011; Wu et al., 2006). As the SPBs separate, F-actin cables are stabilized and crosslinked into the CAR by tropomyosin Cdc8p and the actin filament cross-linker protein Ain1p (Fig. 1:8) (Laporte et al., 2012; Wu et al., 2003).

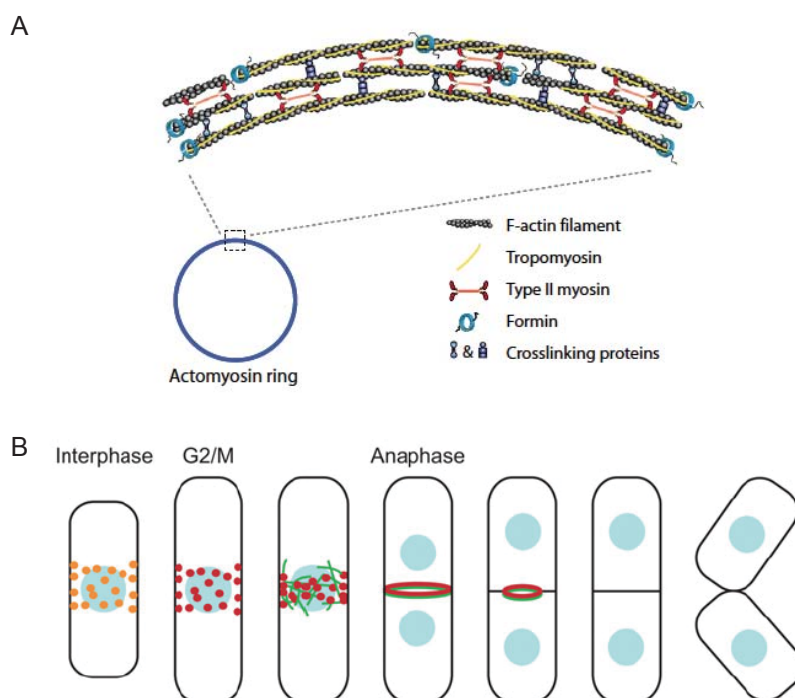


Fig. 1:8 Schematic representation of CAR formation and cytokinesis, in fission yeast. A) F-actin cables are organized in antiparallel arrays; formin nucleates actin at the ends of the filaments. Tropomyosin and crosslinking proteins assemble a compact CAR. Myosin II contributes in CAR assembly and constriction (Mishra et al., 2014). B) Interphase nodes (orange) guide the recruitment of CAR proteins (red nodes). Actin cables (green) and mitotic nodes merge, to form the CAR (green and red circles). Upon nuclear (blue) separation the CAR constricts and directs the synthesis of the division septum (black line, at the cell center). Septum dissolution brings about cell separation. Taken from (Lee et al., 2012a).

Two modes of CAR assembly were proposed: the search-capture-pull-release (SCPR) and the leading cable models (Roberts-Galbraith and Gould, 2008). The SCPR model explains the condensation of the nodes into a CAR structure by spontaneous meeting of myosin II from one node with a growing actin filament, nucleated by Cdc12p, from another node (search). Next, myosin II binds the actin filament (capture) and walks on it, which generates the energy to pull the two nodes together (pull). The interaction of myosin II with the actin filament is labile (release) and thus, a repeated number of such attempts would bring the nodes close together (Vavylonis et al., 2008). A second mechanism was revealed by study of CAR organization in mutants that do not organize node structures; such as *mid1-Δ* and OE the ring components Cdc12p and Cdc15p and of the SIN protein Spg1p (for Spg1p, see section 1.5.2) (Fankhauser et al., 1995; Hachet and Simanis, 2008; Yonetani and Chang, 2010). The second model proposes that actin filaments are nucleated from one spot at the cell division plane. Aster like structures nucleate a large number of actin filaments, organized in two bundles of antiparallel directionality, which merge together and form the CAR (Arai and Mabuchi, 2002; Kamasaki et al., 2007; Roberts-Galbraith and Gould, 2008; Wu et al., 2003). The SIN is a signaling network essential for proper CAR assembly and constriction and also functions in the CAR checkpoint (for CAR checkpoint, see section 1.5.6) (Simanis, 2015).

1.5.2 SIN components

The SIN is comprised of a GTPase and its GAP, three protein kinases, regulatory subunits for the kinases and three scaffold proteins. The association of all SIN proteins with the SPB is essential for cytokinesis signaling (Simanis, 2015). The GTPase Spg1p is a Ras superfamily GTPase, whose nucleotide status controls SIN signaling. When bound to GTP Spg1p is active and triggers SIN signaling, while GDP-bound Spg1p correlates with repressed signaling (Schmidt et al., 1997). The nucleotide status of Spg1p is regulated by a bipartite GAP, which is constituted of the scaffold Byr4p and the catalytic subunit Cdc16p. Byr4p mediates the interaction of Spg1p with Cdc16p, which forces Spg1p to hydrolyze GTP and thus, to become inactive (Furge et al., 1999; Furge et al., 1998). GEFs contribute to the activation of small GTPases by stimulating them to exchange GDP for GTP (Cherfils and Zeghouf, 2013; Vigil et al., 2010), however, no GEF has yet been identified for Spg1p (Simanis, 2015). GTP-bound Spg1p activates and recruits at the SPB the protein kinase Cdc7p (Schmidt et al., 1997). Cdc7p was proposed to activate the downstream kinases Sid1p and Sid2p (Guertin et al., 2000; Sparks et al., 1999). These have each a regulatory subunit, Cdc14p and Mob1p respectively, which are required for the localization and function of the kinases (Fig. 1:9) (Fankhauser and Simanis, 1993; Guertin et al., 2000; Hou et al., 2000; Salimova et al., 2000).

Localization at the SPB of the three kinases, their regulatory subunits, the GTPase and its GAP is mediated by the scaffold proteins Ppc89p, Sid4p and Cdc11p. Ppc89p is most upstream and anchors Sid4p to the SPB (Rosenberg et al., 2006); furthermore, Sid4p mediates binding of Cdc11p, which serves as platform for the binding of the SIN proteins mentioned above (Fig. 1:9) (Krapp et al., 2004; Krapp et al., 2001; Morrell et al., 2004b).

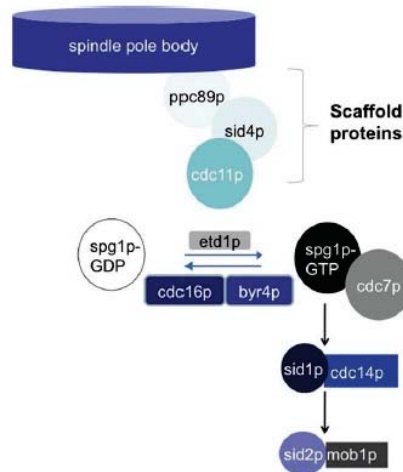


Fig. 1:9 The SIN components. The SIN core components are the GTPase Spg1p, its bipartite GAP Cdc16p-Byr4p, the protein kinases Cdc7p, Sid1p and Sid2p and the regulatory subunits Cdc14p and Mob1p. The nucleotide status of Spg1p controls SIN. When inhibited by the GAP complex, Spg1p is inactive (GDP-bound); upon switch into an active state (GTP-bound) Spg1p activates the network, which is characterized by SPB-association of the downstream kinases. The core SIN components depend on the tripartite scaffold Ppc89p-Sid4p-Cdc11p for the localization to the SPB. The dependency of the scaffold proteins and of the SIN kinases on each other for SPB localization is as depicted. Etd1p is a regulator of the SIN, that is required for signaling (for Etd1p, see section 1.5.4). Taken from (Goyal et al., 2011).

Consistent with their function in regulation of cytokinesis signaling, multiple septa form at any stage of the cell cycle when expressing any of the following genes from a strong promoter: *spg1* (Guertin et al., 2002; Schmidt et al., 1997), *cdc7* (Fankhauser and Simanis, 1994) and *plo1* (Ohkura et al., 1995) or when deleting *byr4* (Song et al., 1996) and *cdc16* (Fankhauser et al., 1993). The hypomorphic alleles *cdc16-116* (Minet et al., 1979) and *cdc13-117* (Nurse et al., 1976) show also a MS phenotype, when incubated at the restrictive temperature. Deletion or hypomorphic alleles of *spg1*, *cdc7*, *sid1*, *cdc14*, *sid2*, *mob1*, *cdc11* and *sid4* arrest the cells as elongated and multinucleated. This is known as “SIN phenotype” and arises from failure of cells to undergo cytokinesis (Fig. 1:10) (Balasubramanian et al., 1998; Chang and Gould, 2000; Fankhauser and Simanis, 1993; Salimova et al., 2000; Schmidt et al., 1997; Simanis, 2015)

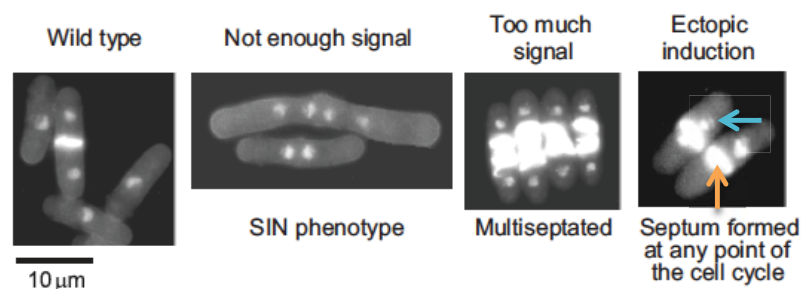


Fig 1:10 Phenotype of *WT* and mutants with altered SIN signaling. Appropriate SIN signaling directs the synthesis of one medially placed division septum (*WT*), after nuclear separation. Failure of SIN signaling generates the SIN phenotype. Continuously active SIN gives rise to MS cells; activation of the network at any stage of the cell cycle triggers septation in interphase (see the orange arrow) or before nuclear separation (see the blue arrow). Taken from (Simanis, 2015).

1.5.3 Localization of the SIN proteins to the SPB

The scaffold proteins Ppc89p, Sid4p and Cdc11p localize at the SPB(s) throughout the cell cycle (Fig. 1:11) (Chang and Gould, 2000; Krapp et al., 2001; Rosenberg et al., 2006; Wachowicz et al., 2015). Spg1p also associates continuously to the SPB(s), in a Cdc7p or GAP-dependent manner (Furge et al., 1999; Krapp et al., 2008; Mehta and Gould, 2006; Sohrmann et al., 1998). In interphase, Spg1p and Cdc16p-Byr4p co-localize to the SPB (Cerutti and Simanis, 1999; Furge et al., 1998; Li et al., 2000; Sohrmann et al., 1998). Upon mitotic entry, Cdc16p leaves the SPBs or shows a faint signal. Byr4p localizes at the SPBs of early mitotic cells; later, its signal diminishes or is no longer detectable. Both GAP proteins relocalize to the old SPB in late anaphase (Fig. 1:11), to inactivate Spg1p (Cerutti and Simanis, 1999; Grallert et al., 2004; Li et al., 2000; Wachowicz et al., 2015).

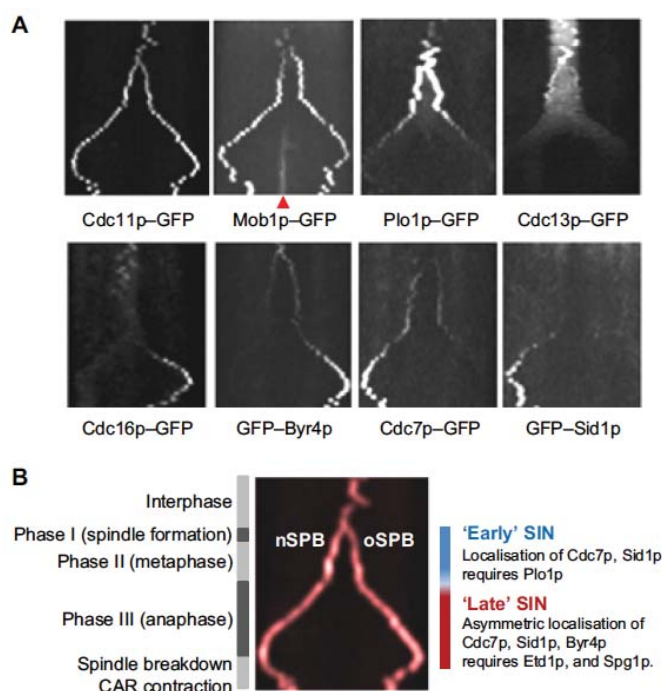


Fig. 1:11 Kymographs of the localization pattern of SIN proteins and of the SIN regulators Plo1p and Cdc13p at the SPBs, throughout the cell cycle. A) GFP-tagged fusion proteins were imaged throughout the mitotic cell cycle and kymographs were assembled as the cells progressed towards cell separation. The corresponding cell cycle phases are as indicated in B). Cdc11p associates to the SPB(s) throughout the cell cycle. Mob1p-GFP is found on both SPBs throughout mitosis and to the CAR (red arrow, under the kymograph). Cdc16p leaves the SPB at mitotic onset; in contrast, Byr4p localizes at SPB(s) until metaphase. Cdc16p and Byr4p relocalize at the old SPB in anaphase. Cdc7 localizes on both metaphase SPBs and only to the new SPB, in anaphase. Sid1p localizes to the new SPB in anaphase. The SIN regulators Plo1p and Cdc13p (see section 1.5.4) localize at the SPBs until the early phases of mitosis, with Plo1p persisting longer than Cdc13p. B) Kymograph of Cdc11p-GFP, with indications on the cell cycle phases (left side of the kymograph) and the “early” and “late” states of the SIN (right side). The kymograph shows (from up to bottom) the single SPB found in the interphase cell (Simanis, 2015). After mitotic entry the SPBs separate, with increasing distance between them as the mitotic spindle elongates. Upon mitotic spindle breakdown and CAR constriction, the SPBs come closer to each other, because the interphase nucleus of the generated cells localizes at the cell center (Hagan, 1998). Taken from (Simanis, 2015).

Cdc7p is recruited on early mitotic SPBs (Fig. 1:11); after Byr4p disappearance from the SPBs in anaphase, Cdc7p localizes at the new SPB and this localization depends on Spg1p (Cerutti and Simanis, 1999; Li et al., 2000; Sohrmann et al., 1998; Wachowicz et al., 2015). When asymmetry of Cdc7p is established, Sid1p and Cdc14p are recruited to the new SPB (Fig. 1:11) and Sid1p disappears from the SPB prior to cell separation (Garcia-Cortes and McCollum, 2009; Grallert et al., 2004; Guertin et al., 2000; Wachowicz et al., 2015).

Sid2p and Mob1p localize at the SPB(s) throughout mitosis (Fig. 1:11) and also to the cell division plane during CAR constriction and before septum formation (Hou et al., 2000; Salimova et al., 2000; Sparks et al., 1999; Wachowicz et al., 2015). The kinase activity of Sid2p peaks at the time of septation and it is believed to transmit the signal for cytokinesis (Sparks et al., 1999); consistent with such a role, the CAR-specific formin Cdc12p was identified as a substrate of Sid2p (Bohnert et al., 2013). Furthermore, the proteins Sid2p (Sparks et al., 1999), Sid4p and Ppc89p (Rosenberg et al., 2006) were observed on the SPB side that resides in the cytoplasm, which indicates that SIN signaling occurs there.

1.5.4 SIN regulators

Cdc2p is a SIN inhibitor in interphase and early mitosis. In interphase septation is thought to be prevented by synergistic activities of Cdc2p and Cdc16p (Cerutti and Simanis, 1999; Yamano et al., 1996), while inactivation of Cdc2p in early mitosis allows SIN activation (Chang et al., 2001; Dischinger et al., 2008; Guertin et al., 2000; He et al., 1997; Yamano et al., 1996). It is worth noting also that Cdc13p associates physically with Cdc11p (Morrell et al., 2004b) and localization of Sid1p-Cdc14p to the SPB occurs when CDK1 activity declines (Guertin et al., 2000). In anaphase Cdc2p promotes SIN signaling activation, because Cdc2p and the protein kinase Plo1p contribute to the removal of Byr4p from the SPBs (Rachfall et al., 2014).

Plo1p localizes to the SPB in late G2 and its localization here is considered as the earliest mitotic event (Mulvihill et al., 1999); it localizes at the SPBs (Fig. 1:11), mitotic spindle and CAR in early mitosis (Bahler et al., 1998a; Mulvihill et al., 1999). Although it binds Sid4p, the SPB localization of Plo1p is not entirely Sid4p-dependent (Morrell et al., 2004b). Plo1p is also involved in the proper formation of the mitotic spindle, and has multiple binding partners at the SPB (Bahler et al., 1998a; Grallert and Hagan, 2002; MacIver et al., 2003; Ohkura et al., 1995; Walde and King, 2014). A Plo1p shut-off mutant has a SIN phenotype, whereas OE gives rise to MS cells (Ohkura et al., 1995). GFP-tagged SIN proteins were imaged in the background of a *plo1* hypomorphic allele that is mainly altered in SIN regulation and it was found that it regulates the metaphase recruitment of Cdc7p to the SPBs, the symmetry of Mob1p and the asymmetry of Sid1p. Also, late anaphase asymmetry of Byr4p depends on Plo1p (Wachowicz et al., 2015).

Etd1p is a protein required for the localization of Cdc7p to the SPB in anaphase (Garcia-Cortes and McCollum, 2009) and for the CAR localization of Sid2p-Mob1p (Daga et al., 2005). *etd1-Δ* and Etd1p OE both give rise to a SIN phenotype (Daga et al., 2005; Garcia-Cortes and McCollum, 2009); the protein localizes at the cell tips, cell division site (Daga et al., 2005; Garcia-Cortes and McCollum, 2009) and in the cytoplasm, in the late stages of mitosis (Garcia-Cortes and McCollum, 2009). Etd1p maintains SIN signaling (Daga et al., 2005; Garcia-Cortes and McCollum, 2009) and

the SIN inhibits Etd1p (Garcia-Cortes and McCollum, 2009). Recently, it has been shown that Etd1p also promotes the activity of the GTPase Rho1p, which is involved in septum formation; an activating feedback loop was proposed between the SIN and Rho1p, whereby Etd1p could function as a link between the two (Alcaide-Gavilan et al., 2014).

Fin1p is a protein kinase, which requires SIN activity to localize to the SPB and inhibits SIN signaling on one of the two anaphase SPBs (Grallert et al., 2004). To prevent SIN activation in mitotically arrested cells, the ubiquitin ligase Dma1p (Murone and Simanis, 1996) targets Sid4p, which influences Plo1p binding to the SPB (Guertin et al., 2002; Johnson and Gould, 2011); Dma1p OE has a SIN phenotype (Guertin et al., 2002). The nucleolar protein Dnt1p regulates Dma1p and is a SIN signaling antagonist (Jin et al., 2007; Wang et al., 2012).

Modulation of gene expression was shown to affect SIN signaling. Mutating the C terminal domain of the RNA polymerase II (CTD) and the CDK family CTD kinase Lsk1p (for Lsk1p see also section 1.5.8) or Lsc1p, its activating cyclin, results in cytokinetic defects, suggesting that they promote SIN signaling (Karagiannis and Balasubramanian, 2007; Karagiannis et al., 2005). *zfs1-Δ* and *scw1-Δ* rescue mutants with a SIN phenotype, which indicates that their product inhibits SIN signaling. Zfs1p and Scw1p encode RNA-binding proteins, however it was not determined whether the rescue of SIN mutants by *zfs1-Δ* and *scw1-Δ* is direct or indirect (Beltraminelli et al., 1999; Cuthbertson et al., 2008; Jin and McCollum, 2003; Karagiannis et al., 2002). γ -tubulin is a SIN inhibitor, because mutants that do not localize Alp4p (a protein of the γ -tubulin complex) at the SPB undergo septation, which might be the result of early SPB recruitment of Sid1p (Vardy et al., 2002).

SIN signaling is also controlled by phosphorylation; hyperphosphorylated Cdc11p is associated with active SIN and it was previously shown that Plo1p, Cdc7 and Sid2p phosphorylate Cdc11p. The phosphorylation of Cdc11p by Sid2p was proposed to be a mechanism of positive feedback regulation of SIN signaling (Feoktistova et al., 2012). Biochemical analysis showed that Cdc11p is hyperphosphorylated in the mutant background of one of the PP2A regulatory subunits (Feoktistova et al., 2012; Krapp et al., 2003). Genetic interactions revealed a link between most SIN components and the phosphatases Flp1p, PP2A and SIP (Cueille et al., 2001; Goyal and Simanis, 2012; Jiang and Hallberg, 2000, 2001; Le Goff et al., 2001; Singh et al., 2011; Trautmann et al., 2001).

1.5.5 The MOR network

MOR is the second NDR-related signaling pathway in fission yeast and controls cell separation and polarized cell growth (Kanai et al., 2005), a network homologous to the RAM (Regulation of Ace2p activity and cellular Morphogenesis) in budding yeast (Liu and Young, 2012; Nelson et al., 2003) and to the Ndr and Lats kinases in mammals (for Ndr and Lats kinases see section 1.8) (Gupta et al., 2013; Kanai et al., 2005; Simanis, 2015). The core components of MOR are the MO25-like protein Pmo25p (Kanai et al., 2005; Leonhard and Nurse, 2005; Mendoza et al., 2005), Mor2p (Hirata et al., 2002), the protein kinases Nak1p/Orb3p (Kanai et al., 2005; Leonhard and Nurse, 2005), Orb6p (Verde et al., 1995; Verde et al., 1998) and Mob2p, which is a Mob1p-like protein that associates to Orb6p (Hou et al., 2003).

The SIN and the MOR are mutually antagonistic (Gupta et al., 2013; Ray et al., 2010); the SIN inhibits Nak1p (Gupta et al., 2013; Ray et al., 2010) and potentially its associated protein Sog2p (Cipak et al., 2013; Gupta et al., 2013). The subunits of CK II also interact with Nak1p (Cipak et al., 2013) and a mutant that reduces the kinase activity of CK II was found to have similar cell morphology defects as described for MOR mutants (Gupta and McCollum, 2011; Snell and Nurse, 1994).

1.5.6 CK II in *S. pombe*

CK II is highly conserved (Snell and Nurse, 1994) and is required in several processes in budding yeast, among which progression into the S phase and at the G2/M transition (Glover, 1998; Hanna et al., 1995). In *S. pombe*, CK II is encoded by the catalytic subunit Cka1p and the regulatory proteins Ckb1p and Ckb2p (Cipak et al., 2013; Roussou and Draetta, 1994). *cka1* is essential (Hayles et al., 2013; Kim et al., 2010; Snell and Nurse, 1994), *ckb1-Δ* is cs and has cell polarity and cell separation defects at permissive temperature (Hayles et al., 2013; Roussou and Draetta, 1994), while *ckb2-Δ* has normal cell morphology (Hayles et al., 2013) but longer telomeres (Liu et al., 2010). Cka1p-GFP localizes at the SPB throughout the mitotic cell cycle, at the cell tips, in the nucleolus and at the cell division site (Cipak et al., 2013). Ckb1p was also found at SPB and, similar to Ckb2p, in the nucleus (Matsuyama et al., 2006).

1.5.7 Synthesis of the division septum and cell separation in fission yeast

In fission yeast, successful cytokinesis is achieved by deposition of cell wall material behind the constricting CAR (Perez et al., 2016). In fixed samples of *S. pombe* dividing cells, the division septum can be visualized with Calcofluor staining (Mitchison and Nurse, 1985; Streiblova and Wolf, 1972).

The septum is composed of a primary and two secondary septa; the primary septum is found in the middle of the division plane and is degraded, to ensure separation of the resulting cells. The secondary septa are found on each side of the primary septum and remain in the cell wall structure upon cell separation. The major constituents of the cell wall are polysaccharides, about half of which are branched β -1,3-glucan and an estimated thirty percent is α -1,3-glucan; reviewed by (Perez et al., 2016). Both primary and secondary septa contain branched β -1,3-glucan, linear α -1,3-glucan and α -galactomannan. In addition, the primary septum contains linear β -1,3-glucan and the secondary septum incorporates β -1,6-glucan (Horisberger and Rouvet-Vauthey, 1984; Humbel et al., 2001; Sugawara et al., 2003).

Several genes encode for α -1,3-glucan synthases, of which *mok1* (also known as *ags1*) is essential (Hochstenbach et al., 1998; Katayama et al., 1999). The β -1,3-glucan synthase is constituted of a catalytic and a regulatory subunit. Four genes encode for the catalytic subunit, *bgs1-4*, of β -1,3-glucan synthase, all of which are essential (Perez et al., 2016). The gene *bgs1* (also known as *cps1*, *swl1* or *drc1*) is involved in the synthesis of linear β -1,3-glucan (Cortes et al., 2007; Ishiguro et al., 1997) and localizes to the division plane and at the growing cell ends (Cortes et al., 2002; Katayama et al., 1999). *bgs1* mutants arrest the cell cycle upon failure of cytokinesis (Ishiguro et al., 1997); this implicates Bgs1p in the cytokinesis checkpoint

(see section 1.5.6). SIN mutants do not synthesize a septum (Simanis, 2015) and Bgs1p localization requires SIN activity (Liu et al., 2002). Genetic interaction was found between SIN alleles and *bgs1* mutants (Le Goff et al., 1999); it is noteworthy that *bgs1-12* is dominant to the SIN mutant *cdc16-116*, which indicates that Bgs1p is involved in septum synthesis during cytokinesis (Cortes et al., 2002). The regulatory subunits of β -glucan synthase are the Rho-family GTPases Rho1p and Rho2p (Arellano et al., 1996; Calonge et al., 2000). An interaction between Rho1p and the SIN was found, whereby OE of Rho1p rescued SIN mutants (Alcaide-Gavilan et al., 2014; Jin et al., 2006).

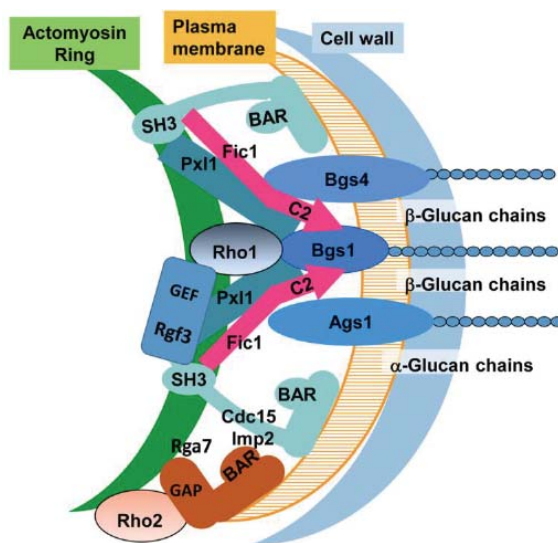


Fig1:12 Schematic representation of the interaction between the CAR and the cell wall. The PCH proteins Cdc15p, Imp2p and Rga7p bind the CAR with their SH3 domains and the plasma membrane through the F-bar domains. Cdc15p and Imp2p bind the proteins Fic1p, Rgf3p and Pxl1p, which contribute in septation. Rgf3p activates Rho1p, which further activates Bgs1p (Jin et al., 2006). Rga7p binds to Cdc15p and Imp2p and negatively regulates Rho2p, to promote correct septum synthesis. Taken from (Perez et al., 2016).

The CAR is required to recruit the cell wall polymerization machinery at the division site and to initiate this process (Proctor et al., 2012; Thiyagarajan et al., 2015). The force for and the rate of CAR constriction is provided by the polymerization of the division septum (Proctor et al., 2012; Thiyagarajan et al., 2015), which explains why the *bgs1-191* mutant arrests with an intact, unconstricted CAR (Liu et al., 1999). The link between CAR and the cell wall is thought to be proteins of the PCH family; these have an F-BAR domain, which interacts with the cellular membrane and an SH3 domains that binds the actin cytoskeleton (Roberts-Galbraith et al., 2009). Cdc15p is involved in CAR formation where it binds the formin Cdc12p, through the F-BAR domain (Carnahan and Gould, 2003; Willet et al., 2015). The SH3 domain of Cdc15p interacts with the proteins Fic1p, Rgf3p and Pxl1p, which contribute in different aspects of septation. (Ren et al., 2015; Roberts-Galbraith et al., 2009). For example, Pxl1p binds myosin II at the CAR and contributes in the stabilization and maintenance of CAR position (Ge and Balasubramanian, 2008; Pinar et al., 2008). The GEF Rgf3p activates the Rho1p GTPase, which promotes the activity of glucan synthases (Arellano et al., 1996; Tajadura et al., 2004). Two other F-BAR proteins

might provide a link between the CAR and the cell wall machinery; Imp2p, which binds Pxl1p, Fic1p and Rgf3p (Demeter and Sazer, 1998; Ren et al., 2015; Roberts-Galbraith et al., 2009) and Rga7p, which interacts with Imp2p and Cdc15p. Rga7p has a GAP domain, which regulates the Rho2p GTPase and contributes to CAR maintenance and septum synthesis (Fig. 1:12) (Martin-Garcia et al., 2014).

Cell separation is achieved by the activity of glucanases, septins, Rho GTPases and of the exocyst (Martin-Garcia and Santos, 2016). The glucanases Agn1p and Eng1p mediate the dissolution of the primary septum from the division site; Agn1p is involved in the initiation of cell wall degradation, which starts on the outer sides of the septum (Dekker et al., 2004). Next the activity of Eng1p and the turgor pressure lead to PS degradation (Fig. 1:13 A) (Alonso-Nunez et al., 2005; Martin-Cuadrado et al., 2003; Sipiczki and Bozsik, 2000). The localization of Agn1p and Eng1p is mediated by the exocyst, the anilin-related protein Mid2p and septins (Berlin et al., 2003; Martin-Cuadrado et al., 2005; Tasto et al., 2003). The exocyst is a complex of proteins that brings and tethers secretory vesicles at the cellular membrane; Agn1p and Eng1p are transported by the exocyst next to the division site (Jourdain et al., 2012; Martin-Cuadrado et al., 2005; Perez et al., 2015), where they localize in ring-like structures on each side of the septum. The formation, maintenance and correct localization of the ring structures also requires Mid2p and septins (Martin-Cuadrado et al., 2005). Furthermore, Mid2p and the septins depend on each other for correct localization at the cell separation plane (Berlin et al., 2003). Septins are GTP-binding proteins which localize at the cell division plane, in late mitosis; seven genes encode for septins (*spn1-7*), with *spn5-7* being expressed during meiosis (Onishi et al., 2010).

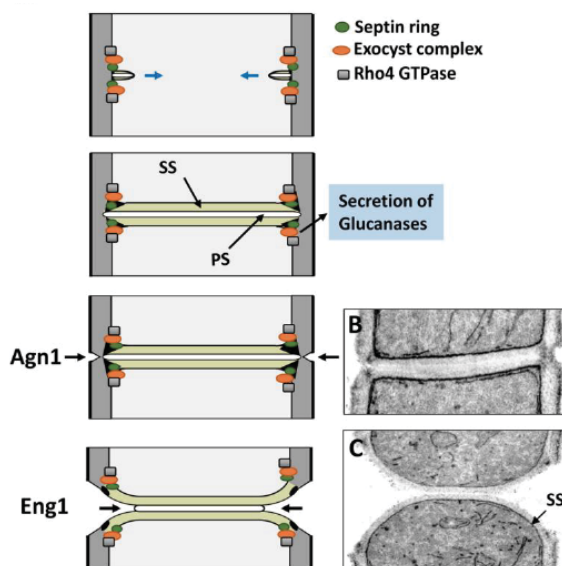


Fig 1:13 Representation of the cell wall at the division plane and the steps of primary septum degradation. A) Schematic representation of the cell wall at division site and of the factors that contribute in primary septum (PS) degradation. Secondary septum, SS. B) and C) Transmission electron micrograph shows the degradation of the PS. Notice the rounding of the cell ends, in the separated cells. Taken from (Perez et al., 2016).

Although none of the mitotic septins (Spn1p- Spn4p) is essential, mutants in these genes have cell separation defects (Berlin et al., 2003; Longtine et al., 1996; Sipiczki

et al., 1993; Tasto et al., 2003; Zilahi et al., 2000).

The GTPase Rho4p is activated by Gef3p and is involved in secretion of Agn1p and Eng1p, probably by targeting the exocyst (Perez et al., 2015; Santos et al., 2005). Gef3p localization at the site of exocyst activation by Rho4p is mediated by septins (Munoz et al., 2014; Perez et al., 2015; Wang et al., 2015). Rgf3p (see above, Rho1p GEF) modulates signaling of Rho3p, which also regulates the exocyst, for cell separation (Munoz et al., 2014; Wang et al., 2003a)

The gene expression of *agn1*, *eng1* and *mid2* is regulated by the transcription factor Ace2p, which was implicated in the transcription of genes required during cytokinesis and M/G1 transition. Ace2p is itself transcriptionally regulated by Sep1p, which regulates transcription of genes required in mitosis (Alonso-Nunez et al., 2005; Bahler, 2005; Ribar et al., 1997; Rustici et al., 2004). Ace2p interacts with the SIN, because the deletion mutant rescues SIN alleles (Jin et al., 2006).

1.5.8 The cytokinesis checkpoint in *S. pombe*

Conditional mutants of *bgs1* that cannot make a division septum (*drc1-191* and *swl-N12*) arrest with two G2 nuclei, PAA MT array and unconstricted CAR, which indicates the presence of a cytokinesis checkpoint. The arrest requires Wee1p, Cdc2p, the CAR, Flp1p and the SIN, which implicates them in the cytokinesis checkpoint (Cueille et al., 2001; Le Goff et al., 1999; Liu et al., 2000; Liu et al., 1999; Trautmann et al., 2001).

The double mutants between *bgs1* alleles and SIN mutants retain the SIN phenotype, which shows the involvement of SIN signaling in the checkpoint (Le Goff et al., 1999; Liu et al., 2000). The CAR is also essential for checkpoint maintenance, because alteration of CAR integrity with actin depolymerizing drugs releases the arrest of *bgs1-191* (Alcaide-Gavilan et al., 2014; Liu et al., 2000).

Flp1p is involved in the cytokinesis checkpoint, because double mutants between *bgs1-191* and *flp1-Δ* become multinucleated. When treated with an actin depolymerizing drug, *flp1-Δ* is not able to arrest in a binucleate state and becomes multinucleated. Some SIN mutants were found to have similar defects to *flp1-Δ*, when the CAR was perturbed, therefore it was proposed that Flp1p and SIN monitor CAR integrity and block cell cycle progression (Mishra et al., 2004; Trautmann and McCollum, 2005).

The localization of Flp1p changes throughout the cell cycle (see section 1.6.5.1) and cytoplasmic Flp1p is required for the cytokinesis checkpoint (Trautmann and McCollum, 2005). Phosphorylation of Flp1p by Sid2p and subsequent binding to the 14-3-3 protein Rad24p ensure retention of Flp1p in the cytoplasm. Consistent with its involvement in the cytokinesis checkpoint, *rad24-Δ* is sensitive to actin depolymerizing drugs (Chen et al., 2008; Mishra et al., 2005).

Another cytokinesis checkpoint protein is the CTD kinase Lsk1p (for Lsk1p see also section 1.5.4), whose deletion mutant does not maintain the CAR, upon perturbation of actin. Lsk1p was proposed to function in a parallel pathway to Flp1p, because in contrast to *flp1-Δ*, the *lsk1* deletion mutant was able to block mitotic progression.

Genetic interaction between *Isk1-Δ* and *cdc16-116* indicated that it is a positive regulator of the SIN (Karagiannis et al., 2005).

1.6 Phosphatases

As described above, protein phosphorylation is a mechanism that controls signaling of cellular events, with protein kinases catalyzing phosphorylation of a substrate and protein phosphatases to reversing this process (Cheng et al., 2011). Proteins are phosphorylated on nine aminoacids, of which phosphorylation on Ser, Thr and Tyr is most abundant. PPs were grouped into Ser/Thr PPs (PPPs), Mg²⁺ or Mn²⁺ dependent PPs (PPMs), protein Tyr phosphatases (PTPs) and Asp-based phosphatases. The following PPs belong to the former group: PP1, PP2A, PP2B, PP4, PP5, PP6 and PP7. PP2C is a PPM, while SCP (small CTD phosphatase) and HAD trigger the nucleophilic attack of γ -phosphate based on the activity of an Asp from the catalytic site. The dual specificity phosphatases belong, together with Tyr phosphatases, into the PTPs group (Moorhead et al., 2009; Moorhead et al., 2007).

PP1, PP2A, PP4, PP6 and the dual-specificity phosphatases Cdc25p and Cdc14p have functions in mitosis (Bollen et al., 2009; De Wulf et al., 2009; Sur and Agrawal, 2016; Trinkle-Mulcahy and Lamond, 2006; Zeng et al., 2010). The phosphatases relevant to this study are described in detail in the remaining part of this section.

1.6.1 Cdc25p

Cdc25p is a highly conserved protein phosphatase, whose activity is required for mitotic entry (Sur and Agrawal, 2016), by activating the highly conserved cyclin dependent kinase Cdc2p (Morgan, 1995). Although not formally proven in fission yeast, Cdc25p probably encodes for a dual-specificity phosphatase (Moreno and Nurse, 1991), which counteracts the inhibitory effect of Wee1p, on Cdc2p (Gould and Nurse, 1989; Millar et al., 1991; Russell and Nurse, 1986). Cdc25p activity is regulated by phosphorylation, with active Cdc25p found in a hyperphosphorylated form (Kovelman and Russell, 1996; Lopez-Girona et al., 1999; Lu et al., 2012). To activate Cdc2p and promote mitotic entry, Cdc25p has to enter the nucleus; accordingly, except for the cytoplasmic signal, a stronger nuclear signal was reported in G2 (Booher et al., 1989; Lopez-Girona et al., 1999). If there is DNA damage, the checkpoint protein Chk1p phosphorylates Cdc25p, to halt mitotic entry until DNA repair occurred (Raleigh and O'Connell, 2000). In addition to its regulation by phosphorylation, Cdc25p is under translational control (Daga and Jimenez, 1999) and is periodically expressed and degraded (Ducommun et al., 1990; Moreno et al., 1990; Nefsky and Beach, 1996).

1.6.2 PP1

The PP1 phosphatase (see also section 1.6.3.4) is involved in the control of several processes, including cell cycle progression. PP1 is comprised of a catalytic and a regulatory subunit, and large number of PP1 enzymes form through differential assortment of the subunits (Peti et al., 2013). Fission yeast PP1 has two catalytic subunits, Dis2p/Bws1p and Sds21p (Booher and Beach, 1989; Ohkura et al., 1988; Ohkura et al., 1989) and a regulatory subunit encoded by *sds22* (Ohkura and Yanagida, 1991; Stone et al., 1993). Dis2p is the major form of the PP1 catalytic subunit (Kinoshita et al., 1990) and is inhibited in mitosis by Cdc2p, through phosphorylation on Thr 316 (Grallert et al., 2015; Yamano et al., 1994). Single

deletion mutants of the genes that encode the catalytic subunit are viable, while the double deletion mutant arrests in metaphase (Booher and Beach, 1989; Ohkura et al., 1989). Metaphase arrest was also reported for a *ts* allele of *sds22* (Stone et al., 1993). The phenotypes of mutants in the PP1 subunits indicate the involvement of this phosphatase in mitotic exit. *dis2* was also implicated in the exit from DNA damage checkpoint arrest, in G2 (den Elzen et al., 2004; den Elzen and O'Connell, 2004). Dis2p and Sds21p localize in the nucleus, with a stronger signal in the nucleolus (Ohkura et al., 1989), but also at centromeres, cell tips and endocytic vesicles (Alvarez-Tabares et al., 2007), while Sds22p was observed in the nucleus (Peggie et al., 2002).

1.6.3 PP2A

1.6.3.1 Structure of the PP2A complex

PP2A is a highly conserved, heterotrimeric PP, which assembles by association of one catalytic and one regulatory subunit, with a scaffold protein. Up to one hundred PP2A trimeric complexes are expected to form, by differential assortment of its subunits (Sangodkar et al., 2016; Wlodarchak and Xing, 2016). The scaffold and the catalytic subunits are each encoded by one gene; however, alternative splicing leads to translation of two variants, for each subunit. The regulatory subunits of PP2A are encoded by fifteen genes, which are translated into twenty-three isoforms. The regulatory subunits are grouped into four families: B/PR55, B'/PR61, B''/PR72 and B'''/PR110, the latter of which is also known as the Striatin (Sents et al., 2013; Sontag and Sontag, 2014). PP2A was shown to regulate all steps of the cell cycle and has been linked to cancer and neurological diseases (Lee et al., 2011; Seshacharyulu et al., 2013; Sontag and Sontag, 2014; Wlodarchak and Xing, 2016). Of particular interest in this work is the involvement of PP2A in the control of mitotic events; PP2A and PP1 were shown to regulate mitotic progression and exit, in higher eukaryotes and fission yeast. Although conserved in budding yeast, PP2A is not the main phosphatase that reverses the phosphorylation of CDK1 substrates. Cdc14p is essential for mitotic exit in *S. cerevisiae*, but not in vertebrates and fission yeast (Bollen et al., 2009; Grallert et al., 2015; Trinkle-Mulcahy and Lamond, 2006; Wlodarchak and Xing, 2016).

1.6.3.2 Regulation of PP2A

PP2A assembly and activity is regulated by: posttranslational modifications (phosphorylation, methylation, ubiquitination and nitration), the Phosphatase Two A Phosphatase Activator (PTPA), association of regulatory subunits, binding to $\alpha 4$ and to target of rapamycin signaling pathway regulator-like (TIPRL)-1, Greatwall and the type of regulatory subunit it associates with.

Ubiquitination of the catalytic subunit targets it for degradation, while tyrosine nitration increases its activity. Phosphorylation was identified on all PP2A subunits, however among the regulatory subunits modification of only the B' family was reported. Phosphorylation of the scaffold was shown to affect its binding to the catalytic subunit. Phosphorylation of the catalytic subunit on Thr 304 and Tyr 307 modulates binding of specific B subunits. Also, the phosphorylation of Tyr 307 inhibits methylation of the catalytic subunit (Sangodkar et al., 2016; Sents et al., 2013; Sontag and Sontag, 2014); reversible methylation of Leu 309 of the catalytic

subunit is catalyzed by the methyltransferase LCMT-1 and the methylesterase PME-1. This is an essential process in mammals that is required for the assembly with B subunits and facilitates association of B' in heterotrimeric complexes (Sents et al., 2013; Sontag and Sontag, 2014). Decreased methylation of Leu 309 was associated with cancer progression and with Alzheimer's disease. PME-1 is associated with a pool of inactive catalytic subunit, whose reactivation is mediated by PTPA (Sangodkar et al., 2016; Sontag and Sontag, 2014).

PTPA is an activating chaperone for the catalytic subunit of PP2A. Together, PTPA and PP2A form an ATP-binding pocket that orients the γ -phosphate of ATP in the PP2A catalytic site. Upon ATP hydrolysis, metal ions are chelated to the catalytic subunit, which modulate the substrate specificity of PP2A (Guo et al., 2014; Wlodarchak and Xing, 2016). PTPA has also peptidyl-proline cis/trans isomerase activity, which modifies Pro 190 of the PP2A catalytic subunit; this conformational change is thought to reactivate PME-1 bound catalytic subunit (Jordens et al., 2006; Leulliot et al., 2006).

$\alpha 4$, also known as yeast phosphatase 2A-associated protein of 42kDa (Tap42) binds partially folded catalytic subunit, to protect it against degradation (Wlodarchak and Xing, 2016). Association of $\alpha 4$ to the catalytic subunit forms a stable complex, which might be enhanced by lack of methylation on the catalytic subunit (Sents et al., 2013).

TIPLR-1 binds and inhibits free PP2A catalytic and structural subunits and it is thought to have an allosteric effect on these. TIPLR-1 regulates PP2A during DNA damage and repair, to permit checkpoint activated phosphorylation (Sents et al., 2013).

To allow mitotic entry, MPF activates Greatwall/MAST-L, a protein kinase that phosphorylates ARPP-19 and α -Endosulphine (ENSA), which inhibit PP2A-B holoenzymes. Once Cdk1 is inactivated, PP2A becomes active and reverses the substrates phosphorylated by MPF, which allows the cell to return into an interphasic state (Haccard and Jessus, 2011; Wang et al., 2014).

The regulatory subunits control substrate specificity, by localizing the core dimer (constituted of the scaffold and catalytic subunit) to specific cellular locations. For example, B' subunits are responsible for localization of PP2A to the nucleus and to the centrosome, while B subunits target PP2A to the MTs (Sontag and Sontag, 2014).

1.6.3.3 PP2A in *S. pombe*

Similar to higher eukaryotes, fission yeast PP2A is constituted of a scaffold, to which catalytic and regulatory proteins associate; however, the reduced number of proteins that encode for these subunits makes *S. pombe* a good model for the study of PP2A function and regulation (see below and section 1.6.3).

The scaffold protein is encoded by *paa1*, whose disruption generates one rounded cell following spore germination (Kinoshita et al., 1996). Three genes were reported to encode for catalytic subunits: *ppa1*, *ppa2* and *ppa3*. The major subunit is Ppa2p; each single deletion mutant is viable. *ppa1- Δ ppa2- Δ* is the only lethal double mutant, in compound mutants deleted for more than one catalytic subunit (Kinoshita et al.,

1990; Singh et al., 2011). *ppa2-Δ* is advanced into mitotic commitment, because it divides at a cell length that is approximately twenty percent smaller than that of *WT* (Chica et al., 2016; Goyal and Simanis, 2012; Kinoshita et al., 1990; Kinoshita et al., 1993). A small reduction in cell length was also reported for *ppa1-Δ* (Chica et al., 2016; Goyal and Simanis, 2012); however, a synthetic lethal interaction with *wee1-50* was only reported for *ppa2-Δ* (Kinoshita et al., 1993). PP2A probably inhibits mitotic commitment in part by influencing the phosphorylation status of Wee1p and Cdc25p (Bollen et al., 2009; Chica et al., 2016; Jeong and Yang, 2013; Kinoshita et al., 1993).

The B and the B' regulatory subunits in *S. pombe*, are encoded by *pab1* and *par1* and *par2* respectively. Par1p is the major B' regulatory subunit, since it is expressed at higher levels. Neither regulatory gene is essential, however their disruption or deletion showed different phenotypes.

pab1-Δ cells are short and round, cannot mate or sporulate and show sensitivity to the cell wall damaging enzyme β-glucanase; also, this strain does not grow at 22°C and 36°C (Kinoshita et al., 1996). Although in the studies presented in this thesis and in (Goyal and Simanis, 2012) this strain was found to have the previously described morphological and mating phenotypes, the mutant grew at 36°C; also, despite being slow growing, *pab1-Δ* grew at 19°C (section 3.6.3) (Goyal and Simanis, 2012). An allele of *pab1* (*pab1-4*) that introduces a STOP codon before the region predicted to perform substrate recognition, has been reported to grow slower at 25°C and to have morphological phenotypes similar to those described for *pab1-Δ* (Lahoz et al., 2010).

Disruption of *par1* suggests its involvement in the control of medial positioning the division septum, perpendicular orientation (on the short axis of the cell) of the cell separation plane, inhibition of septation and cell morphology establishment, while *par2-Δ* is phenotypically similar to *WT*. The mutant *par1-Δ par2-Δ* has the phenotypes of *par1-Δ*, however the percentage of abnormal cells rises from ten percent, observed in the single mutant cultures, to fifty percent. Consistent with the defects observed in the double mutant, colony formation is impaired (Jiang and Hallberg, 2000). The same study showed that *par1-Δ* and *par1-Δ par2-Δ* do not properly enter stationary phase and that *par1-Δ* does not grow at 37°C. Although the deletion of *par1* leads to morphology defects similar to those described by (Jiang and Hallberg, 2000), this strain is able to grow at high temperature (Le Goff et al., 2001).

Studies of the cellular localization of PP2A subunits showed that some of these proteins also localize at the SPB, CAR and the cell separation site. Indirect immunofluorescence revealed that Ppa2p is excluded from the nucleus and localizes throughout the cytoplasm (Kinoshita et al., 1993); Ppa1p localization has not been reported. Paa1p-GFP localizes weakly to the SPBs and to the CAR in late mitosis (Singh et al., 2011).

Localization of GFP-tagged Pab1 in living cells indicated that it is found throughout the cell, with stronger signal in the nucleus and at the mitotic spindle (Lahoz et al., 2010). A similar localization pattern was reported by Goyal in doi:10.5075/epfl-thesis-5292, as well as the localization at the cell division site, in late anaphase and septating cells. This difference is probably due to the reagents used; (Lahoz et al.,

2010) expressed GFP-Pab1p under the *nmt41* promoter, from the *leu1* locus, while in the second study GFP-Pab1p was expressed under the *pab1* promoter, from *lys1*.

Immunofluorescence of Par1p-3HA showed a signal in the cytoplasm and at the center of mitotic cells (Jiang and Hallberg, 2000). In living cells, Par1p-GFP also changed its localization, as the cell progressed through the cell cycle: in interphase the signal is cytoplasmic and upon progression through mitosis, Par1p localizes on the SPBs, CAR (Le Goff et al., 2001) and at the cell ends of separating cells (doi:10.5075/epfl-thesis-5292). The latter study also reported that Par1p-GFP is also found at the cell tips in interphase.

Localization studies of Par2p indicated that in interphase, it is found in the cytoplasm and more is also strongly associated to the growing ends of the cells. In mitosis, the signal disperses during nuclear separation and next becomes visible at the cell division site. Cells that have separated from each other localize Par2p at the site of septum dissolution but also at the old end of the cell (Jiang and Hallberg, 2000) (doi:10.5075/epfl-thesis-5292).

Although there are allele specific differences, the PP2A mutants described above rescue hypomorphic alleles of SIN components. A negative genetic interaction was found between both *ppa2-Δ* and *pab1-4* with the conditional mutant *cdc16-116*, that becomes MS at high temperature (Goyal and Simanis, 2012; Jiang and Hallberg, 2001; Lahoz et al., 2010; Le Goff et al., 2001). Also, the localization of the SIN proteins Cdc7p and Sid2p is altered in the mutants *ppa2-Δ* and *par1-Δ* (Goyal and Simanis, 2012; Wachowicz et al., 2015). These observations, together with the fact that PP2A subunits localize at cellular locations where SIN proteins were observed (this section), the altered phosphorylation status of SIN proteins in PP2A mutant backgrounds (Krapp et al., 2003) and the fact that PP2A-Par1p activity is low during septation (Grallert et al., 2015) suggest that PP2A inhibits cytokinesis.

1.6.3.4 Regulators of PP2A in fission yeast

The genes *ppm1* and *mrps2* encode the predicted methyltransferase and respectively methylesterase of the PP2A catalytic subunit (Wood et al., 2012). Although neither gene product has been characterized to date, Ppm1p physically interacted with Paa1p-PK (Bernal et al., 2012) and a negative genetic interaction was reported between *mrps2-Δ* and *ppa2-Δ* (Ryan et al., 2012).

PTPA is encoded by *ypa1* (*pta1*) and *ypa2* (*pta2*), and deletion of these genes showed that each is essential for survival at 19°C. At both restrictive and permissive temperature, the phenotypes differ between *ypa1-Δ* and *ypa2-Δ*; the morphology of *ypa1-Δ* is similar to *WT*, while *ypa2-Δ* is advanced into mitotic commitment, has altered cell polarity, and affects growth pattern and cytokinesis. Although their phenotypes differ, these genes control together an essential process, because the double deletion mutant is not viable at any temperature. GFP-tagged fusion proteins of Ypa1p and Ypa2p showed that both localize through the cytoplasm and nucleus, with Ypa2p being more enriched in the nucleus and in cytoplasmic motile foci (Bernal et al., 2012; Goyal and Simanis, 2012).

The deletion of *ypa2*, like the hypomorphic allele *ypa2-7*, is *cs* and has phenotypes that implicate Ypa2p in mitotic commitment, polar growth, medial placement of the division septum and cell separation (Bernal et al., 2012; Goyal and Simanis, 2012). Similar to the observations made in PP2A deletion mutants, SIN proteins are mislocalized in *ypa2-Δ* (Goyal and Simanis, 2012); also, a similar genetic interaction to *ppa2-Δ* was observed between *ypa2-Δ* and SIN mutants and with mutants that alter mitotic commitment. Ypa2p might also be involved in DNA repair, because *ypa2-Δ* was identified in a screen for genes required for tolerance to cadmium, a drug that indirectly causes DNA damage (Kennedy et al., 2008).

Analysis of the genetic interaction between *ypa1-Δ* and *ypa2-Δ* with PP2A deletion mutants showed that regardless of the double mutant combination no colony grew at 19°C; *ypa1-Δ* was synthetic sick with *pab1-Δ* and *par1-Δ*, whereas *ypa2-Δ* showed a strong negative genetic interaction with *ppa2-Δ*, *pab1-Δ* and *par1-Δ* (Goyal and Simanis, 2012). These results are consistent with a model where PTPA activates PP2A. However, examination of Pab1p-GFP and Par1p-GFP in the *ypa1-Δ* and *ypa2-Δ* background did not show any difference in the localization of these proteins, at the permissive or restrictive temperature of the deletion mutants (doi:10.5075/epfl-thesis-5292). Also, it is worth noting that *mrps2-Δ* had a negative genetic interaction with *ypa1-Δ* and *ypa2-Δ* (Ryan et al., 2012).

S. pombe has homologs of Greatwall and ENSA, of which Ppk18p and respectively Igo1p were shown to inhibit Pab1p-containing PP2A complexes. This allows cell division at reduced cell length, in media with low nitrogen source. Upstream of this regulation is TORC1 (Chica et al., 2016), the signaling pathway that is activated when cells are grown in rich nitrogen media (Petersen and Nurse, 2007). When active, TORC1 inhibits Greatwall and Endosulphine, which leads to inhibition of mitotic commitment by PP2A-Pab1p; hence cells divide at longer cell length (Chica et al., 2016).

Of the two PP1 (for PP1 see also section 1.6.2) isoforms, Dis2p was shown to contribute to the activation of PP2A-Pab1p and PP2A-Par1p phosphatase complexes, to promote progression through and exit from mitosis. High CDK1 activity inhibits Dis2p (Grallert et al., 2013; Ohkura et al., 1989); upon mitotic commitment, decreasing activity of CDK1 allows Dis2p autoreactivation. By docking to PP2A-Pab1p, Dis2p activates this phosphatase complex, which further contributes in the activation of PP2A-Par1p (Grallert et al., 2015).

Sds23p is an inhibitor of PP2A and of the PP2A-related phosphatase, PP6. Physical interaction was found between Sds23p and both PP6 and PP2A subunits. Phosphatase assays, using whole cell extracts, indicated that in the *sds23-Δ* background there is higher phosphatase activity; this can be reversed by okadaic acid, which inhibits both phosphatases (Hanyu et al., 2009).

1.6.3.5 Other phosphatases that regulate the SIN

1.6.3.5.1 Flp1p

Flp1p/Clp1p is the fission yeast homolog of the phosphatase Cdc14p (for Cdc14p, see section 1.7.1) but, in contrast to budding yeast, Flp1p is not essential for mitotic

exit (Cueille et al., 2001; Oliferenko and Balasubramanian, 2001; Trautmann et al., 2001). *flp1-Δ* divides at reduced cell length, which may be due to the fact that Cdc25p is hyperphosphorylated in this mutant (Cueille et al., 2001; Esteban et al., 2004); also, degradation of Cdc25p is delayed in *flp1-Δ* (Esteban et al., 2004; Lu et al., 2012). Localization studies showed that Flp1p is found in the nucleolus and on the SPB, in interphase; throughout mitosis Flp1p was observed on both spindle pole bodies, at the kinetochores, on the mitotic spindle, at the CAR and throughout the nucleus (Cueille et al., 2001; Trautmann et al., 2004; Trautmann et al., 2001) and Flp1p localization is important for its function (Trautmann and McCollum, 2005). Double mutants between *flp1-Δ* and SIN alleles indicated that Flp1p promotes SIN signaling (Cueille et al., 2001). Other studies have implicated Flp1p in the response to genotoxic stress (Broadus and Gould, 2012).

1.6.3.5.2 The SIP

The SIP is a PP2A-related phosphatase complex, that comprises of the scaffold Paa1p, the catalytic protein Ppa3p (for Paa1p and Ppa3p see section 1.6.3) and regulatory proteins, that are encoded by the genes *csc1-csc4* (Singh et al., 2011). The regulatory subunits Csc1p-Csc3p have homologs that are required in budding yeast for cell cycle arrest, during pheromone response (Kemp and Sprague, 2003; Singh et al., 2011), while for Csc4p there are no reported orthologs (Singh et al., 2011). The stoichiometry of this complex is not known and the distribution of Ppa3p and Csc4p was undetectable, while Csc1p, Csc2p and Csc3p localize to the SPB. The SIP has been implicated in regulation of SIN signaling; *csc1-Δ* was shown to interact genetically with *cdc11* and *cdc16* mutants (Singh et al., 2011). Loss of any SIP subunits renders Cdc7p symmetric in anaphase (Singh et al., 2011; Wachowicz et al., 2015); in *csc1-Δ*, Sid1p and Byr4p localization at the SPB is also altered and Cdc11p is hyperphosphorylated (Singh et al., 2011). It has been proposed that SIP inhibits SIN signaling (Singh et al., 2011).

1.6.4 PP2B/Calcineurin

PP2B is conserved from yeast to humans, and is involved in the regulation of several biological processes, among which regulation of transcription in response to Ca^{2+} ; PP2B is specifically inhibited by the drugs cyclosporin A and tacrolimus/FK-506 (Sugiura et al., 2002). In fission yeast PP2B is encoded by Ppb1p and Cnb1p, which encode for the catalytic and regulatory subunit respectively. Each deletion mutant is viable, but *cs* and sterile. At both restrictive and permissive temperature, the deletion mutants have defects that implicate Calcineurin in cell separation (Sio et al., 2005; Yoshida et al., 1994). Some SIN alleles are sensitive to FK-506, at permissive temperature and OE of a constitutively active version of PP2B rescues the conditional phenotype of some SIN alleles. These indicate that PP2B promotes SIN signaling (Lu et al., 2002).

1.7 Cytokinesis in other organisms

1.7.1 Cytokinesis in plants

Unlike yeasts and metazoans, plant cytokinesis does not rely on the constriction of an acto-myosin ring. Fusion of membrane vesicles at the division plane forms the cell plate and its lateral expansion towards the plasma membrane leads to cell separation (Muller and Jurgens, 2016). The division plane is established before

prophase by the preprophase band, a structure formed of actin filaments and anti-parallel arrays of MTs; the MT are stabilized in the preprophase band by MT cross-linkers (Ho et al., 2011; Ho et al., 2012).

The preprophase band is involved in the recruitment of proteins that direct the fusion of the cell plate to the plasma membrane and disassembles in pro-metaphase (Muller and Jurgens, 2016). After chromosomes segregation, the material of the mitotic spindle organizes into the phragmoplast, which mediates the delivery of membrane vesicles to the cell division plane (Smertenko et al., 2011; Staehelin and Hepler, 1996). The vesicles contain material for the synthesis of the cell wall (Samuels et al., 1995; Thiele et al., 2009).

The MTs found at the center of the phragmoplast are de-polymerized and their polymerization at the leading edge underlies phragmoplast expansion, from the cell center towards the plasma membrane. MT polymerization is under the control of the MAPK signaling pathway, whose activation before anaphase is restrained by CDK1 (Sasabe et al., 2011; Sasabe and Machida, 2006). Actin association into the phragmoplast contributes in positioning of the division plane (Rasmussen et al., 2013; Smertenko et al., 2010), together with the actin-sliding myosin VIII (Wu and Bezanilla, 2014). The vesicles that fuse to form the cell plate are derived from Golgi and through endocytosis of the plasma membrane (Dhonukshe et al., 2006; Staehelin and Hepler, 1996). Membrane fusion is preceded by formation of membrane bridges between the vesicles, a process mediated by SNARE and SM (Sec1p/Munc18p) proteins (Carr and Rizo, 2010; Jahn and Scheller, 2006; Rehman et al., 2014; Sudhof and Rothman, 2009). The fusion of membrane vesicles to the cell plate requires KNOLLE-SNARE protein complexes, while the fusion of vesicles to the plasma membrane is mediated by Qa-SNAREs (El Kasmi et al., 2013; Enami et al., 2009). TPLATE, an adaptin-related protein localizes to the leading edge of the growing cell plate and to the cortex of the division plane (Van Damme et al., 2011).

1.7.2 Cytokinesis in budding yeast

Similar to fission yeast and animal cells cytokinesis in budding yeast is directed by the constriction of a CAR, which drives cell separation (Cundell and Price, 2014; Guizetti and Gerlich, 2010). Ring contraction occurs when the mitotic spindle breaks down and is coupled to deposition of cell wall material at the site of cell separation (Schmidt et al., 2002; VerPlank and Li, 2005). In budding yeast, mitotic exit and cytokinesis are driven by the counterpart of the SIN, which is termed the MEN (Hotz and Barral, 2014).

In contrast to *S. pombe*, where the site of CAR assembly is chosen in early mitosis (Daga and Chang, 2005; Paoletti and Chang, 2000), in budding yeast the location of the cell division plane (also known as the bud site) is defined in G1 (Oliferenko et al., 2009). CAR assembly involves reorganization of the actin cytoskeleton to the bud neck and requires actin, septins, the Rho1p GTPase and the endocytosis machinery. The CAR is assembled progressively and starts by deposition of septins at the site of cell division, in G1 (Gladfelter et al., 2002; McMurray and Thorner, 2009).

In early mitosis ring assembly continues, by septin-mediated recruitment of myosin II (Bi et al., 1998; Lippincott and Li, 1998); next the myosin light chain protein, Mlc1p

(Boyne et al., 2000; Shannon and Li, 2000) and Iqg1p are recruited. Iqg1p is a IQGAP protein which has several domains that function in ring assembly and cytokinesis signaling; A GAP domain that might regulate the MEN GTPase Tem1p (Lippincott and Li, 1998; Shannon and Li, 1999), a calponin homology domain that is involved in actin recruitment at the site of cell division (Epp and Chant, 1997; Shannon and Li, 1999) and IQ domains that bind to the myosin light chain and to calmodulin (Cheney and Mooseker, 1992; Xie et al., 1994). The polo-like kinase Cdc5p controls the localization and the activation of the GTPase Rho1 (Yoshida et al., 2006), which is involved in CAR and secondary septum formation (Onishi et al., 2013; Tolliday et al., 2002). CAR constriction is triggered by MEN signaling, which also drives mitotic exit, by mediating the release of the phosphatase Cdc14p from the nucleolus which further counteracts Cdk1p phosphorylation (Hotz and Barral, 2014). When mitotic exit is initiated the proteins Inn1p and Cyk3p are recruited to the CAR, in a MEN-dependent manner (Meitinger et al., 2010); these, together with Hof1p contribute to the formation of the primary division septum (Nishihama et al., 2009). The chitin synthase Chs2p polymerizes the primary septum (Chuang and Schekman, 1996; Sburlati and Cabib, 1986; Zhang et al., 2006) on the sides of which secondary septa are synthesized, which contain glucan and mannan (Cabib et al., 1982). Cell separation is achieved by hydrolysis of the primary septum by chitinase and other hydrolases (Cabib, 2004).

Similar to the SIN, the MEN consists of a GTPase (Tem1p), a bipartite GAP (Bfa1p-Bub2p) (Pereira et al., 2000) and a putative GEF for the GTPase (Lte1p) (Bardin et al., 2000; Hofken and Schiebel, 2002; Jensen et al., 2002; Pereira et al., 2000), three protein kinases (Cdc15p, Dbf2p and Dbf20p) and Mob1p, the regulatory subunit of Dbf2p and Dbf20p (Hotz and Barral, 2014; Lee et al., 2001a). The MEN components are anchored at the SPB through the protein Nud1p (Gruneberg et al., 2000), the homolog of the SIN Cdc11p. In mitosis, Tem1p is kept inactive by Bfa1p-Bub2p and all three proteins localize to the SPBs (Pereira et al., 2000).

In contrast to the SIN, the GAP of Tem1p functions also in the spindle orientation checkpoint (Alexandru et al., 1999; Fraschini et al., 1999; Li, 1999); Bub2p prevents activation of the kinase Dbf2p (Fesquet et al., 1999) and CAR formation (Lee et al., 2001b) in metaphase-arrested cells. However, given that Bfa1p OE arrests cells in a postanaphase state, the GAP is also believed to play a role in cytokinesis (Lee et al., 1999; Li, 1999). Tem1p and Bfa1p-Bub2p localize strongly to the old SPB, which enters the bud (Bardin et al., 2000). Dbf2 and Dbf20 were implicated in the Kar9p-dependent mechanism of old SPB localization into the bud (Hotz et al., 2012a; Hotz et al., 2012b).

If the mitotic spindle is misoriented, the spindle orientation checkpoint becomes activated and delays mitotic progression (Bloecher et al., 2000; Falk et al., 2016). This is mediated by the protein kinase Kin4p that localizes in the mother cell and phosphorylates Bfa1p, which prevents the GAP dissociation from the SPBs (D'Aquino et al., 2005; Pereira and Schiebel, 2005; Pereira et al., 2001). The current model for the MEN/SPOC function is that correct orientation of the mitotic spindle brings one SPB into the bud, away from Kin4p activity. Here Cdc5p phosphorylates and inhibits the GAP (Geymonat et al., 2003; Hu et al., 2001) whose departure from the SPB, together with the activity of the bud cortical protein Lte1p leads to Tem1p

activation (Bardin et al., 2000; Hofken and Schiebel, 2002; Jensen et al., 2002; Pereira et al., 2000; Yoshida et al., 2003).

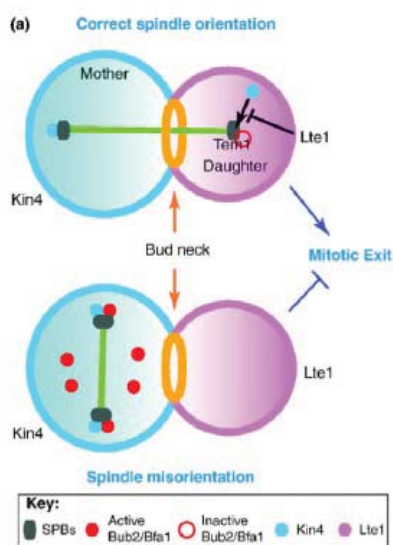


Fig. 1:14 Schematic representation of the spindle orientation checkpoint pathway in budding yeast. If one SPB segregates into the bud, Bub2p-Bfa1p gets inactivated and activation of Tem1p by Lte1p promotes mitotic exit. When the mitotic spindle is misoriented, both SPBs are found in the mother cell, where Kin4p phosphorylates and activates the Bub2p-Bfa1p; this keeps MEN inactive until the positioning of one SPB into the bud. Taken from (Pereira and Yamashita, 2011).

Active Tem1p recruits Cdc15p to the SPBs in anaphase, which further activates the Mob1p-Dbf2p complex (Lee et al., 2001a; Mah et al., 2001; Toyn and Johnston, 1994; Visintin and Amon, 2001). The three protein kinases and Mob1p localize at the site of cell division in late mitosis (Frenz et al., 2000; Luca et al., 2001; Xu et al., 2000; Yoshida and Toh-e, 2001). At the CAR, Cdc5p and Mob1p-Dbf2p phosphorylate Hof1p, which allows its binding to the CAR. Here, Hof1p initiates ring contraction (Meitinger et al., 2011). Active MEN contributes to the release of Cdc14p from the nucleolus (Shou et al., 1999; Stegmeier et al., 2002), which leads to the activation of the anaphase promoting complex that targets B-type cyclins for destruction (Baumer et al., 2000; Schwab et al., 1997; Shirayama et al., 1999; Yeong et al., 2000). However, the initial release of Cdc14p is under the control of the FEAR network; notably, the phosphorylation of Cdc14p and of its nucleolar anchor Cfi1p/Net1p, by the FEAR component Cdc5p promotes the release of Cdc14p (Shou et al., 2002; Visintin et al., 2003; Yoshida and Toh-e, 2002). The localization of Dbf20p and Dbf2p at the site of cell division is dependent upon Cdk1p inactivation (Hwa Lim et al., 2003). Upon completion of mitotic exit Cdc14p contributes to MEN inactivation, through several mechanisms, one of which is the contribution to Tem1p inactivation by dephosphorylating Bfa1p and Lte1p (Geymonat et al., 2003; Hu et al., 2001; Pereira et al., 2002) and by promoting the expression of Amn1p, a Tem1p inhibitor in the daughter cell (Wang et al., 2003b).

1.7.3 Cytokinesis in metazoans

Animal cells set the division plane in anaphase (Oliferenko et al., 2009), which is established by the MTs of the mitotic spindle (Dechant and Glotzer, 2003), as a

result of stimuli from the surrounding cells (Kumar et al., 2015). RhoA is a small GTPase that is required for the assembly of the CAR and the ingression of the cleavage furrow (Piekny and Glotzer, 2008). RhoA and its regulating GAPs and GEFs localize to the central spindle midzone (Somers and Saint, 2003; White and Glotzer, 2012) and active RhoA promotes actin polymerization by formins. Profilins and cofilins are actin-binding proteins which contribute in CAR formation (Glotzer, 2004). Anilin is a scaffold that fastens the CAR to the plasma membrane and is essential for completion of cytokinesis; recruitment of anilin to the cortex of the cell equator is mediated by RhoA and the RhoA GEF, ECT2 (Kumar et al., 2015).

Effector kinases of RhoA and anilin stabilize myosin into the ring (Kumar et al., 2015; Uehara et al., 2010), which mediates CAR constriction, by sliding along actin (Mierzwa and Gerlich, 2014). Factors required for cell membrane synthesis are delivered by transport vesicles, to the site of furrow ingression (McKay and Burgess, 2011). Maximal constriction of the CAR generates a dense structure termed the midbody (Mullins and Biesele, 1977; Skop et al., 2004), which comprises CAR components (among which anilin, septin and RhoA), spindle midzone proteins (such as the GAPs and GEFs for RhoA) and condensed MTs (Kumar et al., 2015).

Separation of the resulting cells occurs through abscission, a process mediated by reorganization of the cytoskeleton and membrane fusion (Chen et al., 2012). Disassembly of the CAR is achieved by regulation of RhoA and the rearrangements of the cortex leads to constriction on the sides of the midbody (Kumar et al., 2015).

During furrow ingression, cell membrane is remodeled by Golgi-derived/secretory and endocytic vesicles and by the activity of selective SNARE proteins. Secretory vesicles contribute membrane and proteins required for cell separation and their recruitment to the cell separation site is facilitated by centriolin, which localizes to the midbody. Endocytosis both removes and contributes membrane and is regulated by GTPases and proteins, that localize to the cell division site (Normand and King, 2010). SNARE proteins localize also to the midbody and are required for membrane fusion (Gromley et al., 2005; Jahn and Scheller, 2006). ESCRT proteins are also essential for cell separation, since they remodel the plasma membrane such that scission is promoted (Steigemann and Gerlich, 2009).

1.8 Homologs of SIN and MEN proteins in metazoans

Most SIN and MEN proteins are conserved in metazoans, with homologs of Cdc11p/Nud1p, Cdc7p/Cdc15p and Sid2p/Dbf2p-Mob1p in the Hippo signaling pathway (Fig. 1:15) (Hergovich et al., 2006; Simanis, 2015). Hippo is involved in tissue growth and regeneration, by controlling cell proliferation, differentiation and cell death. The key elements within this pathway are Lats1 and Lats2 (Warts, in *D. melanogaster*) kinases, MST1 and MST2 Ste20-like kinases (Hippo, in *D. melanogaster*), MOB1A/MOB1B and SAV1 (Salvador) (Fig. 1:15), which target the transcriptional regulators YAP and TAZ. Within this pathway MST1/2 associates to Sav1p, then phosphorylates Lats1/2 and MOB1p, which leads to complex formation between the two and thus, to the activation of Lats1/2 (Gomez et al., 2014; Harvey et al., 2013; Hergovich, 2013). Lats1 and Lats2 phosphorylate and inactivate YAP and TAZ, which would otherwise lead to a transcriptional program that promotes tissue

growth. Altered Hippo signaling has been associated with tumorigenesis, with YAP having been attributed an oncogenic role (Harvey et al., 2013).

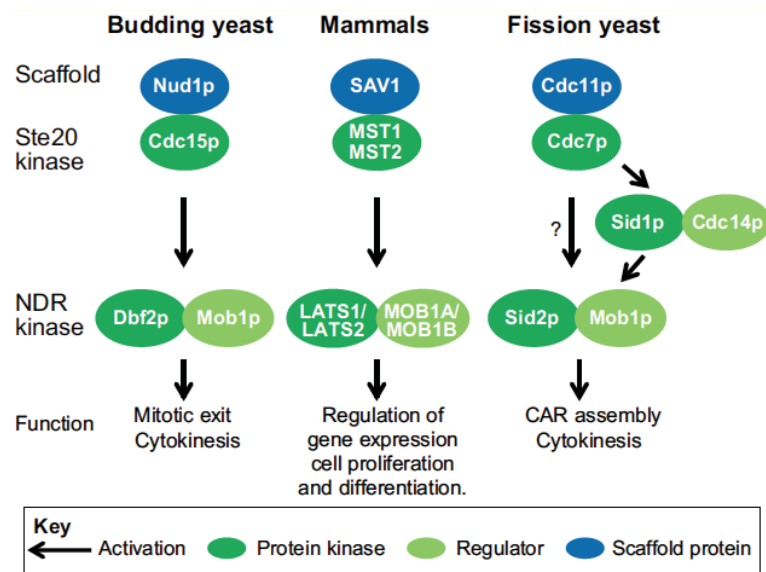


Fig. 1:15 Homologs of SIN core proteins, in budding yeast and mammals. Besides the common signaling modules, the SIN comprises the Sid1p kinase and its regulatory subunit, which might bring input from the MOR signaling pathway. Taken from (Simanis, 2015).

GAPcenA has homology domains that are also found in Cdc16p and Bub2p; GAPcenA is localized in the cytoplasm and on the centrosomes (Cuif et al., 1999) and was implicated in the metaphase to anaphase transition (Miserey-Lenkei et al., 2006).

Sequence homology indicates that human Centriolin is the equivalent of Cdc11p and Nud1p, which localizes to the centrosomes and the midbody. Centriolin is required for cytokinesis completion and entry into S phase; consistent with the similarities between centriolin and its yeast homologs, centriolin binds yeast Bub2p (Gromley et al., 2003; Gromley et al., 2005).

The homolog of Plo1p/Cdc5p is known as PLK1 (Polo-like kinase) in most metazoans, although Polo proteins are encoded in vertebrates by five genes (Zitouni et al., 2014). Based on the structure of their catalytic domains, Plk1-3, Plk4 and Plk5 differ; Plk1 is involved in DNA replication, centrosome maturation, mitotic entry, different aspects of chromosome segregation, mitotic exit and cytokinesis. Plk2 and Plk4 are required for centriole duplication, while Plk3 functions in G1/S and G2/M transition, DNA replication and cytokinesis (Barr et al., 2004; Zitouni et al., 2014). In humans, Plk5 lacks kinase activity and has antitumorigenic functions in the nervous system (de Carcer et al., 2011).

Aim of this study

ypa2 was previously found to regulate SIN signaling, probably by modulating PP2A activity (Goyal and Simanis, 2012). To identify potential regulatory links between the SIN and Ypa2p/ PP2A, we performed a synthetic genetic array analysis with the hypomorphic allele *ypa2-S2*. Characterization of this mutant indicated that it is largely altered in cytokinesis signaling, in contrast to *ypa2-Δ* in which other pathways are also affected. *ypa2-S2* was crossed to the genome wide, non-essential deletion library and synthetic sick/lethal interactions were scored. Given that *ypa2-S2* is a hypomorph, we expected to identify genes that compensate for the reduction in Ypa2p function. These genes would either activate the little activity of Ypa2p-S2 or would be required to inhibit it.

Chapter 2 Materials and Methods

2.1 Nomenclature

The genetic nomenclature follows the definition of (Kohli and Nurse, 1995). Gene names are designated as three lowercase letters followed by integers (for example, *ypa2*). For genes that do not have a standard name, the systematic ID is given (for example, *SPAC1782.05*). To indicate a *WT* gene, the superscript “+” follows the gene name (for example, *ypa2*⁺). Gene deletions or disruptions are represented as the gene name followed by 1) a hyphen and the symbol “Δ” (for example, *ypa2-Δ*) or by 2) “::” and the gene name of the marker used for replacement (for example, *ypa2::ura4*⁺). Mutant alleles are designated by gene name followed by a hyphen, and one or more uppercase letters and integers (for example, *ypa2-S2*). All gene nomenclature is italicized. Gene products are specified by non-italicized gene name, except that first letter is uppercase and is followed by “p” (standing for “protein”) (for example, Ypa2p). Tagged gene products are indicated by protein name followed by hyphen and the identity of the tag (for example, Ypa2p-GFP).

2.2 Fission yeast techniques and reagents

All strains used in the studies described herein are listed in Table 3:1. Note that in numbering of Microsoft Excel tables “:” was replaced by “.” (for example, Table 3:1 was named Table 3.1), due to the inability of the program to save this character.

2.2.1 Fission yeast growth and crossing

For the growth and manipulation of fission yeast cells, standard techniques were used (Moreno et al., 1991). Cells were grown in either YE or EMM2 medium supplemented with the required aa (at 100 μg/mL). The cell density of cultures was determined with a Neubauer hemocytometer (depth 0,100mm). Crosses were performed on EMM2 plates that lack a nitrogen source (Gutz and Doe, 1973) and tetrads were dissected on YE with a Singer MSM microdissector. The identity of selected genotypes was verified by outcrossing to *WT* or an appropriate strain. All growth medium components were purchased from Difco™.

Plates containing 5-FOA (at 0.66mg/mL; F595000, Toronto Research Chemicals) were prepared by mixing 250 mL agar 2X EMM2 to sterile filtered (0.22 μm GP Millipore Express® PLUS Membrane; SCGPT01RE, Millipore) 500 mg/200 mL 5-FOA (dissolved by heating at 60°C) and 10g glucose (G8270, Sigma)/50 mL water. The plates supplemented with TBZ (T-8904, Sigma) were made at the indicated concentrations, in agar YE, from a 5 mg/mL TBZ stock prepared in DMSO.

2.2.2 Cell viability assays of haploid strains

The strains used in cell viability assays were streaked to single colonies on YE, at 29°C. Exceptions from this temperature were the strains containing SIN mutations and the *cka1-12* allele, which were incubated at 19°C or 25°C, and strains with the mutation *etd1-Δ*, that were grown at 36°C.

The phenotype of the mutants was verified by appropriate replica plating and colonies were grown liquid YE; exponentially growing cultures, were diluted to 2x 10⁶ cells/mL. From this, four ten fold serial dilutions were made in YE. 5μL were spotted from each of the five dilutions on YE+ PB (at 10 μg/mL; P2759, Sigma) agar plates.

One plate was incubated at each of the following temperatures: 19°C, 25°C, 29°C, 32°C and 36°C. Images were taken (Nikon Coolpix 990 camera) three (for 29°C, 32°C and 36°C), five (for 25°C) and six days (19°C) later. Microscopic examination of cell morphology and PB colony color was also performed. The images were processed with Adobe Photoshop.

PB was used to better visualize synthetic negative interactions, because sick/dying mutants are not able to expel it and colonies become darker red. In contrast to sick mutants, *WT* colonies have a light pink color (Forsburg and Rhind, 2006).

2.2.3 Creation of diploid strains and cell viability assays

The stable diploids presented in Fig. 3:2 and Fig. 3:3 were obtained using the *mat2P-102* mutation and auxotrophies that allowed selection of diploids, when grown on EMM2 medium (for example, *ade6-M210* and *ade6-M216* or *leu1-32* and *lys1-131*).

The *mat2* locus contains the information for *h*⁺ mating type and is constituted of the Pc (c, for constitutive) and Pm (m, for meiosis) regions. Pc provides the message for mating, whereas Pm is required for meiosis (Willer et al., 1995). The mutation *mat2P-102* compromises the Pm function (Crandall et al., 1977; Kelly et al., 1988; Nurse and Bissett, 1981) and crossing *mat2P-102 h*⁹⁰ to an *h*⁺ strain allows meiosis to occur, because *h*⁺ information is provided. When mating *mat2P-102 h*⁹⁰ to an *h*⁻ strain, meiosis is blocked and a diploid zygote is generated (Kohli et al., 1977). Stable diploids can be mitotically propagated on YE plates (Moreno et al., 1991). To select diploids, each parental strain had an unique auxotrophy, which did not allow its growth on EMM2 plates. To obtain the diploids *ypa2-S2/ypa2⁺ cdc7-A20/cdc7-A20* and the control strains (Fig. 3:2), one parental strain was *leu1-32* and the other *lys1-131*. Only diploids of genotype *leu1-32/leu1⁺ lys1-131/lys1⁺* were able to form colonies on EMM2 plates (Moreno et al., 1991). A similar diploid selection system was used to obtain the genotypes presented in Fig. 3:3, except that the auxotrophies used were *ade6-M210* and *ade6-M216*. These Ade auxotrophes complement in *trans*, so diploids of genotype *ade6-M210/ade6-M216* grow on EMM2 (Szankasi et al., 1988).

Two days old matings of haploid strains were streaked to single colonies on EMM2 plates, at 25°C. Colonies were replica plated both to 25°C and to the restrictive temperature of *cdc7-A20* and *mob1-R4* (Fig. 3:1), on YE with PB. Diploids have darker pink colony color than haploid *WT* cells (Forsburg and Rhind, 2006), which was used to identify diploid colonies at 25°C. The phenotype was assessed at the restrictive temperature of the SIN mutants. Exponentially growing YE cultures of diploids (Fig. 3:2 and 3:3) were spotted and analyzed as described in section 2.2.2.

2.3 Yeast transformation

Transformation of fission yeast cells was done following the protocol described by (Bahler et al., 1998b), except that salmon sperm DNA (A2159, Applichem) was used instead of sheared herring testis DNA. Transformed cells were plated on M with appropriate supplements, or YE plates containing antibiotics.

2.4 Synthetic Genetic Array (SGA)

2.4.1 Growth and mating of the Bioneer library

The thirty-six 96 well plates of the Bioneer deletion library (Kim et al., 2010) (version 5) were screened against *nat^R-ypa2-S2* in batches of twelve plates. The “waking up” of the library from -78°C was done by robotically pipetting (TECAN Freedom Evo robot; MCA384 Disposable tips, TECAN) 10 µL library culture into 90 µL YE, in 96 well plates (780271, Greiner Bio One). The plates were covered with breathseal (676051, Greiner Bio One) and were incubated at 29°C. Three days later the volume of the liquid wells had decreased to 55 µL, with a cell density around 140×10^6 cells/mL. Cultures of the mutant *nat^R-ypa2-S2* were grown to 10×10^6 cells/mL in YE and were concentrated to 70×10^6 cells/mL; 55 µL were pipetted robotically into each well of the three days old library cultures and mixing was done by pipetting ten times the volume added.

A 96 well microplate replicator (140500, Boekel Scientific) was used to spot the cultures onto agar mating plates. The mating plates were prepared by pouring 50 mL agar medium into rectangular plates (PLU-001, Singer Instruments), one day before use. All plates were dried before use in the laminar flow hood, for 20`. The mixture of each library plate was spotted on two mating plates, which were incubated at 29°C. Eight days later, one mating plate was sealed with Parafilm (PM996, Pechiney Plastic Packaging) and was stored at 4°C. The second plate was processed as described in section 2.4.2.

2.4.2 Spotting spores onto selective plates

Eight to ten days old matings were resuspended in water, by passing the microplate replicator into the crosses and transferring into 50 µL water. This step was repeated, to ensure the transfer of a large number of spores. Resuspension was done by pipetting and the transfer onto selective plates was carried out with the microplate replicator. Four selective plates were spotted from each library plate: two YE supplemented with CYH (at 0.1mg/mL; C7698, Sigma) and G418 (at 0.1mg/mL; 11811023, ThermoFischer) and two YE supplemented with CYH, G418 and NAT (at 0.1mg/mL; Werner Bio Agents 5.001.000). The selective plates were prepared as described for the mating plates (see section 2.4.1). One of each selective plate was incubated at 19°C and 29°C.

2.4.3 Data analysis

2.4.3.1 Examination of the selective plates

The selective plates were examined four and eight days after spotting, for 29°C and 19°C, respectively. Growth on the selective plates was generally observed by spots of yeast with a diameter of about 3mm, resulting from a large number of colonies that grew next to each other. Interactions were scored as synthetic lethal if growth was observed on the selective plate that contained CYH and G418, with no colonies on the corresponding CYH, G418 and NAT plate. Synthetic sick interactions were characterized by colonies that grew slower (Kuzmin et al., 2016) on plates supplemented with CYH, G418 and NAT, as compared to CYH and G418 containing

plates. The synthetic lethal and sick interactions from 19°C and 29°C are listed in Table 3:2.

If no growth was observed on either selective plate of one or both temperatures assayed, the second mating plate (stored at 4°C; see section 2.4.1) was used to inoculate more of each cross into 50 µL water and selective plates were spotted as described above. A list of genes represented with a reduced number of colonies was obtained from 19°C, 29°C or both temperatures, with 1) mutants for which a spot of yeast grew on one selective plate, and less than three colonies, but at least one, grew on the second selective plate; 2) mutants for which one to four colonies grew on one plate but none on the second; 3) between one and three colonies grew on both selective plates. These too were respotted. After analysis of the second spotting, some mutants remained in the non-growers list or in that with a reduced number of colonies; they are mentioned in Tables 3:5 and 3:8 respectively. Some synthetic sick hits were identified based on only a small number of colonies, as indicated in Table 3:2. Note that among the screen hits there are *cs* mutants, thus, they are mentioned in the 29°C hits list and in the list with non-growers from 19°C.

2.4.3.2 Bioinformatic analysis of the hits

The bioinformatic analysis of the SGA was performed by Jonathan Aryeh Sobel, in the laboratory of Professor Felix Naef.

The BP and FYPO annotations corresponding to the systematic ID of hits, non-growers, genes that generated a reduced number of colonies and for the genes represented in the library were retrieved from Biomart and Pombase databases respectively (Smedley et al., 2015; Wood et al., 2012) and can be found in tables 3:3, 3:6, 3:9 (for BP) and respectively tables 3:4, 3:7, 3:10 (for FYPO). While BP is comprehensive, FYPO represents the reported phenotypes, resulting from the deletion of a specific gene. The previously reported genetic interactors of *ypa2* were retrieved from the Biogrid database (Chatr-Aryamontri et al., 2015; Stark et al., 2006). Note that in the Microsoft Excel tables the symbol “°C” was replaced by “degrees”. This is due to the inability of the program to save these characters.

To identify the BP and FYPO annotations enriched among the hits, non-growers and genes that generated a reduced number of colonies, these lists were sorted according to the log odds ratio and to the hypergeometric test (Rivals et al., 2007). The two values were calculated for each BP and FYPO annotation of the three categories of genes; the values corresponding to each statistical calculation can be found in tables 3:3, 3:6, 3:9, for BP and 3:4, 3:7, 3:10, for FYPO. The log odds ratio quantifies how strongly an annotation is associated with the list of genes analyzed, that will be generically referred to as “hits” in the below part of this section. The log odds ratio was generated with the formula:

$$\text{Log_Odds} = \log \left(\frac{\frac{Q_{\text{hits_annotated}}}{M_{\text{genes_annotated}} - Q_{\text{hits_annotated}}}}{\frac{N_{\text{hits}}}{P_{\text{genes_tot}} - N_{\text{hits}}}} \right), \text{ where:}$$

Q hits_annotated: the number of hits that belong to a specific annotation

M genes_annotated: the total number of library genes that belong to a specific annotation

N hits: the total number of hits

P genes_tot: the number of genes represented in the library

The hypergeometric test quantifies if specific annotations are over-represented among the hits, thus the statistical significance that a number of hits (out of the total number of hits) belong to a specific annotation. The hypergeometric distribution was first calculated with the formula:

$$1-P(X > k) = P(X \leq k) \approx \Phi\left(\frac{k-np}{\sqrt{np(1-p)}}\right), \text{ where:}$$

X: random variable

k: the number of annotated hits, for a given annotation

n: the number of hits

p: p-value/probability

Φ : the standard normal distribution

In section 3.7.2 the analysis of FYPO takes into consideration a hypergeometric test p-value below 0.0001 and a log odd ratio above 1.5, while a hypergeometric test p-value below 0.05 and a log odds ratio above 0.5 are discussed for the BP analysis. The filters used to generate the BP figures were less stringent, because the annotations for BP are less comprehensive compared to FYPO. All statistical analyses were performed using the statistical language R and various Bioconductor packages (<http://www.Bioconductor.org>).

2.4.3.3 Validation of hits

Validation of hits comprised PCR verification of the deletion mutants and the manual reconstruction and examination of the double mutants.

To verify whether the library strains were correctly deleted, PCR reactions were performed with the CP 5 primer provided from Bioneer for each deleted gene (Kim et al., 2010) and VS 713, from genomic DNA of the deletion mutants. Negative control reactions were set-up with the same primers, using *WT* DNA as the template.

The CP 5 primer maps upstream to the deleted gene, while VS 713 is internal to the *kan^R* construct used for gene deletion. The amplicon size expected for each deletion strain, when PCR amplifying with primers CP 5 and cp-N10, is provided on the website <http://pombe.kaist.ac.kr/nbtsupp/>. The primer cp-N10 spans from nt -45 to -21 nt upstream of *kan^R* ATG (Kim et al., 2010), while VS713 is complementary to nt 368- 385 downstream of START. Therefore, and extra 406 nt were added to the expected amplicon size.

The double mutants were reconstructed by tetrad dissection at 29°C and colony growth assays were spotted and analyzed as described in section 2.2.2. Synthetic

sick interactions were annotated if the double mutant colonies were smaller than the parental strains or when the double mutant showed an additive morphological phenotype.

2.5 Molecular biology techniques

Molecular biology techniques were performed following standard protocols described in (Sambrook et al., 1989). For all cloning manipulations, restriction digestion was used to assess correct cloning. The restriction enzymes used were purchased from New England Biolabs and used according to the manufacturer's recommendations. The primers used in PCR reactions are listed in Table 3:12.

2.5.1 Integration of *ypa2-S2* at *leu1* and *lys1*

The construct containing *ypa2-S2* CDS and 232 nt upstream as well as 262 nt downstream of the CDS, was PCR amplified from *ypa2-S2* genomic DNA with the primers VS 1598 and VS 1599. The 1552 nt long amplicon was digested with Sal I and EcoR I and was cloned into the plasmid DW232 (Weilguny et al., 1991). Sequencing (performed at Microsynth) showed the G to A change in nt 4764861. This corresponds to the mutation identified previously in the *ypa2* CDS, in whole-genome sequencing of *ypa2-S2*.

To integrate *ypa2-S2* at *lys1*, *ypa2-S2* was excised from DW232 with EcoR I (followed by filling of the overhang, by Klenow repair) and Sal I and was cloned into Sal I and Sma I digested INT K1 plasmid (Fennessy et al., 2014). To provide a functional promoter region to the *ypa2-S2* CDS cloned into INT K1, the following was done: 1) PCR amplification was performed with primers VS 1621 and VS 1622, from the cosmid containing the *WT* sequence. The amplicon, starting from nt -680 to nt +17 (referenced to the first nucleotide of *ypa2* START) contains the naturally occurring EcoR V and respectively Xba I restriction sites. This fragment was cloned into EcoR V and Xba I digested BSIIISK- plasmid (Stratagene). Sequencing confirmed that the amplicon is the *WT* promoter of *ypa2*. 2) The short promoter region of *ypa2-S2* was excised from INT K1 containing the *ypa2-S2* construct, with Sal I and Xba I; 3) the promoter region described at step 1) was excised Sal I and Xba I from the BSIIISK- vector and was cloned into INT K1. To express *ypa2-S2* from the *leu1* locus, the construct was excised with Pst I and Sac I from INT K1 and was cloned into INT A, digested with Pst I and Sac I.

To transform yeast cells with the appropriate fragments, a NotI digest was performed on either INT K1 or INT A, containing *ypa2-S2*, under *WT ypa2* promoter. Next, the fragment of interest was gel purified and was used to transform the *ura4-D18* auxotroph, as described in section 2.3. The construct used in transformation provided also *ura4+*, thus the transformants became auxotrophs for Lys or Leu.

2.5.2 Insertion of *nat^R* upstream of *ypa2-S2*

To target *nat^R* upstream of the *ypa2-S2* CDS, *nat^R* was cloned into the *ypa2⁺* promoter region (see section 2.5.1: BSIIISK-, containing the *ypa2⁺* promoter), in the naturally occurring BsrG I restriction site. BsrG I maps (direction 3'→5') starting at nt -341 upstream of the *ypa2* START.

The *nat^R* construct was amplified with primers VS 1649 and VS 1650 from the pFA6a *natMX6* plasmid (Hentges et al., 2005). The 1189 nt long amplicon was digested with BsrG I and was cloned into the same restriction site, in BSIISK-, containing the *ypa2⁺* promoter.

The functionality of the *nat^R* construct was tested in bacteria. Next, the construct was excised and yeast of genotype *ypa2-S2* was transformed. Transformation and selection was done as described in section 2.3.

2.6 Imaging and cell length and width measurements

Exponentially growing cultures were centrifuged (3000 RPM/3') and resuspended in 70% ethanol. For DAPI (DNA) and Calcofluor (cell wall material and the primary septum; chitin) staining, the fixed cells were washed once in 1x PBS pH 8 and were resuspended in 1x PBS pH 8, containing a final concentration of 1.2 ng/mL DAPI (D-9542, Sigma) and 5 µg/mL Calcofluor (F-6259, Sigma). Imaging was performed with Zeiss Axiophot microscope and Nikon Coolpix 990 camera.

One hundred cells with a division septum were measured for each genotype; images were analyzed using Adobe Photoshop. Cell width was measured along the division septum. AVG, ST DEV, M and P-values were calculated in Microsoft Excel.

2.7 Confocal imaging

2.7.1 Imaging and analysis of GFP tagged SIN proteins

Cultures grown in YE, at 29°C, to a cell density of 3×10^6 cells/mL were used for elutriation, imaging of living cells and data analysis as described in (Wachowicz et al., 2015), except that the experiments described in section 3.6.5 have only been done once. Mitotic progression was monitored by imaging Cherry-tagged Pcp1p, a SPB marker, and plotted the fraction between the separation of the SPBs and the cell length; early mitotic stages are indicated by values next to 0, while maximal elongation of the mitotic spindle gives values close to 1. The GFP signal was defined into three states: asymmetric (≥ 4 -fold difference between the SPBs), symmetric (≤ 2 -fold) and transition (> 2 and < 4 -fold). The data presented here was derived from 300 cells per genotype.

2.7.2 Imaging and analysis of *gfp-atb2*

Cultures grown in YE, at 29°C, to a cell density of 3×10^6 cells/mL were concentrated by filtration and were imaged as described by (Wachowicz et al., 2015). Image analysis was performed in ImageJ and Microsoft Excel and figure assembly was done in Adobe Photoshop CS6.

Chapter 3 Results

3.1 *sup2**, a suppressor of the SIN mutant *spg1-M19*, is an allele of *ypa2*

The mutant *spg1-M19* was identified as a suppressor of the MS phenotype of *cdc7-A20 cdc16-Δ*, at 19°C (Fournier et al., 2001). Outcrossing from the parental strain revealed that *spg1-M19* is viable at 19°C and 25°C and lyses with a SIN phenotype at higher temperatures (Fig. 3:1 and data not shown). This *spg1* allele changes Asp 65 to Asn (Grote, Krapp and Simanis, unpublished).

Mutation of the equivalent residue in the GTPase p21^{H-ras} (Asp 57 Ala) increased both the dissociation rate of GTP and its affinity for GDP (John et al., 1993). Given the SIN phenotype of *spg1-M19*, it is tempting to speculate that this mutant Spg1p binds preferentially to GDP.

To identify regulators of SIN signaling, a genetic screen was performed, to isolate spontaneous suppressors of *spg1-M19*, selecting for colony formation at 32°C. Forty-eight suppressor strains were generated, which defined five complementation groups (designated *sup1**-*sup5**). The second largest class, *sup2**, comprised eight alleles. Comparison of the whole genome sequences of *sup2**, in three SIN mutant backgrounds, identified several common SNPs, among which was the G to A change in nt 4764861, on chromosome I. This mutation results in the Gly 138 to Glu, in Ypa2p (Grote, Krapp, Wappet, Pepper, Hagan, Simanis, unpublished). Given that altered function of Ypa2p was shown to interact genetically with SIN mutants (Goyal and Simanis, 2012), we investigated whether *sup2** interacted with these alleles (Fig. 3:1). The mutants *spg1-B8*, *cdc7-24*, *cdc7-A20*, *sid2-1*, *sid2-250*, *mob1-R4*, *etd1-Δ*, *cdc14-118*, *cdc11-136*, *sid4-SA1* lyse with a SIN phenotype (Balasubramanian et al., 1998; Chang and Gould, 2000; Daga et al., 2005; Fankhauser and Simanis, 1993; Salimova et al., 2000; Schmidt et al., 1997; Simanis, 2015), while *cdc16-116* accumulates a large percentage of MS cells, at the restrictive temperature (Minet et al., 1979) (Fig 3:1).

Both *ypa2-Δ* and *sup2** rescued the mutants *cdc7-A20*, *mob1-R4*, *cdc11-136* and *etd1-Δ*; the latter mutant was rescued by *sup2** to 19°C, where *ypa2-Δ* does not form colonies (Bernal et al., 2012; Goyal and Simanis, 2012). The rescue of *cdc7-24* and *sid2-1* by *sup2** occurred one temperature lower than the one at which *ypa2-Δ* restored growth. The alleles *sid2-250*, *cdc14-118* and *spg1-B8* grew at their lowest restrictive temperature in *ypa2-Δ*, but not in the *sup2** background. Neither *ypa2-Δ*, nor *sup2** rescued *sid4-SA1*. In contrast to *ypa2-Δ*, that decreased the restrictive temperature of *cdc16-116* to lower than 29°C, *sup2* cdc16-116* had the phenotype of the SIN allele, however, with a reduction in colony size at the low restrictive temperature (Fig. 3:1) (Goyal and Simanis, 2012).

Although the degree of rescue differs from that of *ypa2-Δ*, *sup2** restored growth of SIN alleles, which suggested that it could be a hypomorphic allele. This indication is strengthened by the fact that *sup2** did not show a strong negative interaction with *cdc16-116*. The deletion of *ypa2*, like the hypomorphic allele *ypa2-7*, is cs, has polarity defects, it is advanced into mitosis and alters cytokinesis (Bernal et al., 2012; Goyal and Simanis, 2012). In contrast to *ypa2-Δ*, *sup2** is not cs (Fig. 3:5), is

morphologically similar to *WT* (Fig. 3:2) and interacted with SIN mutants (Fig. 3:1). These findings indicated that *sup2** an allele of *ypa2*, that is mainly affected in the regulation of cytokinesis.

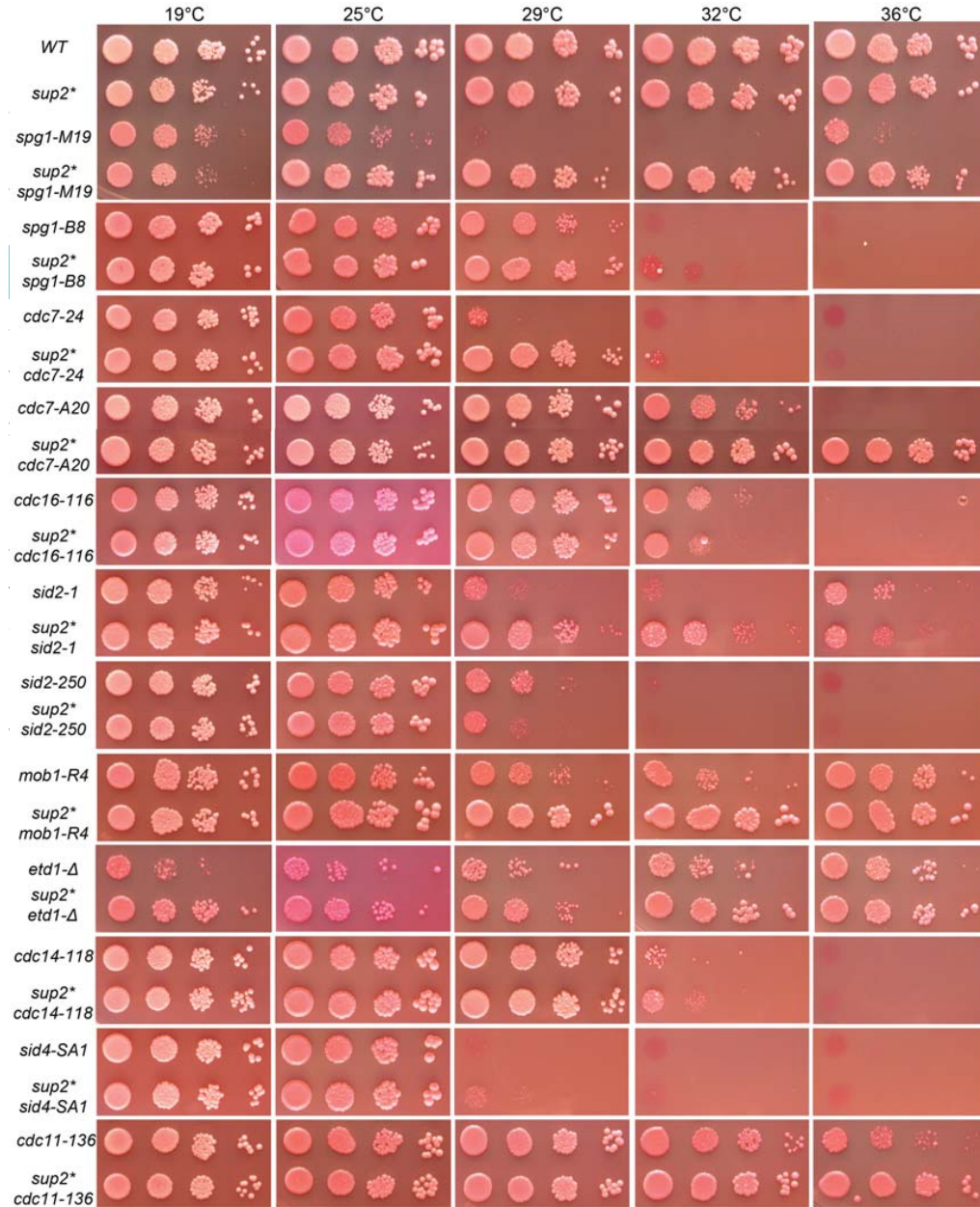


Figure 3:1 Cell growth assays showing the interaction between *sup2 and SIN mutants.** The cell growth assays were performed as described in section 2.2.2. Notice that *sup2** rescued the alleles *spg1-M19*, *cdc7-A20*, *mob1-R4*, *cdc11-136*, *etd1-Δ*, *cdc7-24*, *sid2-1* and *plo1-35*, although the latter three mutants only at their lower restrictive temperatures. No rescue of *spg1-B8*, *cdc14-118*, *sid4-SA1* or *sid2-250* was observed. A reduction in colony size was found for *sup2* cdc16-116*. Note that although a similar analysis to that presented here was initially performed with untagged *sup2**, the strain presented here is *nat^R*-tagged (see section 3.5).

To confirm that the ability of *sup2** to rescue SIN mutants is linked to the *ypa2* locus, we crossed it to *flp1-Δ*. The chromosomal location of *flp1+* is 4.48 kb away from the *ypa2* locus and 1 cM corresponds to 6 kb, in fission yeast (Hayles and Nurse, 1992). To follow *sup2**, the cross was dissected in the *cdc7-A20* background, because *sup2** rescues the SIN phenotype of *cdc7-A20*, at 36°C (data not shown and Fig. 3:1). In contrast to *sup2**, *flp1-Δ* does not rescue *cdc7-A20* and decreases its restrictive temperature to <32°C (data not shown). In each of the fifty-five tetrads dissected from *sup2* cdc7-A20 X flp1::kan^R cdc7-A20*, two colonies grew at 36°C, whereas the other two had SIN phenotype at 32°C (where *cdc7-A20* is viable *per se*). Since no colony of phenotype *cdc7-A20* was isolated, it is likely that *flp1-Δ* and *sup2** did not recombine. This is consistent with *sup2** being at the *ypa2* locus, therefore *sup2** was re-named *ypa2-S2*.

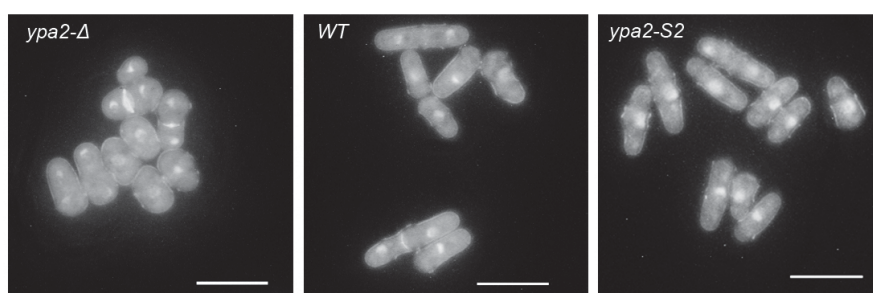


Figure 3:2 Phenotypic characterization of *sup2 and *ypa2-Δ* vs *ypa2⁺*.** Exponentially growing cultures from 29°C were imaged as described in section 2.6. *sup2** cells are rod-shaped, similar to *WT*. In contrast, *ypa2-Δ* cells divide at reduced cell length (compare septated cell from *WT* and *ypa2-Δ* panels) and cell polarity is altered. Scale bar: 10 μm.

3.2 The *ypa2-S2* mutation lies in a domain required for PTPA ATPase activity

The Gly 138 of fission yeast Ypa2p corresponds to Gly 152 of PTPA in humans (Leulliot et al., 2006). Mutational analysis of PTPA has demonstrated that Asp 150 Ala, His 155 Ala and Arg 148 Leu all reduce the *in vitro* ATPase activity, assessed when incubating PTPA and A-C dimers of PP2A (Chao et al., 2006). The double mutant *ypa2-Δ ypa1-Δ* is lethal (Bernal et al., 2012; Goyal and Simanis, 2012); we obtained the mutant *ypa2-S2 ypa1-Δ*, which formed microcolonies of about forty, short and round cells (data not shown). These cells lysed, which suggests that *ypa2-S2* is a hypomorphic allele. The current view concerning the role of PTPA is that it functions as an ATP-dependent chaperone in the activation of PP2A (Guo et al., 2014; Low et al., 2014). Therefore, it is possible that the biological outcome of Gly 138 Glu mutation encoded by *ypa2-S2* results in inefficient folding of PP2A complexes, reducing phosphatase activity.

3.3 Is *ypa2-S2* dominant over *ypa2⁺*?

In haploids, *ypa2-S2* rescues the hs, SIN phenotype of *cdc7-A20* and *mob1-R4* (Fig. 3:1 and data not shown). To investigate whether *ypa2-S2* is epistatic to *ypa2⁺* with respect to rescue of SIN mutants, we constructed diploids bearing either two, one or

no copies of *ypa2-S2* on a background of either *cdc7-A20* or *mob1-R4* (see section 2.2.3).

The mutation *cdc7-A20* is recessive, because *cdc7-A20/cdc7⁺* diploids grow at $\geq 32^{\circ}\text{C}$, in contrast to *cdc7-A20/cdc7-A20* (Fig. 3:3). Consistent with rescue of *cdc7-A20* by *ypa2-S2*, the diploids *ypa2-S2/ypa2-S2 cdc7-A20/cdc7-A20* formed colonies at $\geq 32^{\circ}\text{C}$, although this was impaired compared to haploids (*ypa2-S2/ypa2-S2 cdc7-A20/cdc7-A20*, Fig. 3:3 vs *ypa2-S2 cdc7-A20*, Fig. 3:1). The diploids *ypa2-S2/ypa2⁺ cdc7-A20/cdc7-A20* were able to form colonies at 32°C and 36°C , though with reduced fitness compared to the controls (Fig. 3:3). This result indicates that *ypa2-S2* is largely dominant over *ypa2⁺*.

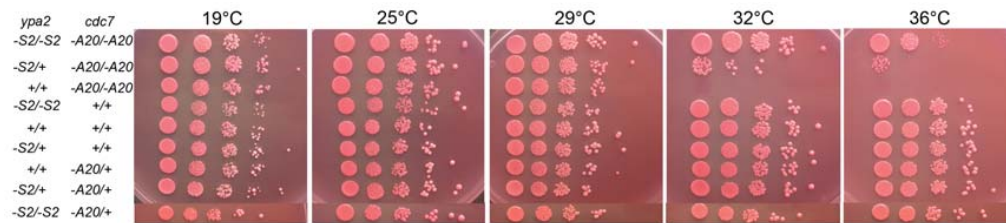


Figure 3:3 Cell growth assays of the diploids *ypa2-S2/ypa2⁺ cdc7-A20/cdc7-A20* and of the control strains. The cell growth assays were performed as described in section 2.2.3. Notice that *ypa2-S2/ypa2⁺* partially rescues the growth failure of *cdc7-A20/cdc7-A20*, at 32°C and 36°C .

The mutation *mob1-R4* is also recessive, since heterozygous diploids do not display the *hs* phenotype of *mob1-R4/mob1-R4* (Fig. 3:4). However, in contrast to *mob1-R4* haploids, the homozygous diploids not only grow poorly at 29°C and 32°C , but also at 36°C . Consistent with analysis of haploids, *ypa2-S2/ypa2-S2 mob1-R4/mob1-R4* diploids grow at all tested temperatures (Fig. 3:1, *ypa2-S2 mob1-R4* and Fig. 3:4, *ypa2-S2/ypa2-S2 mob1-R4/mob1-R4*). Similarly, *ypa2-S2/ypa2⁺ mob1-R4/mob1-R4* diploids are able to grow at the restrictive temperatures of *mob1-R4/mob1-R4* (Fig. 3:4), which indicates that *ypa2-S2* rescues *mob1-R4* in a dominant manner.

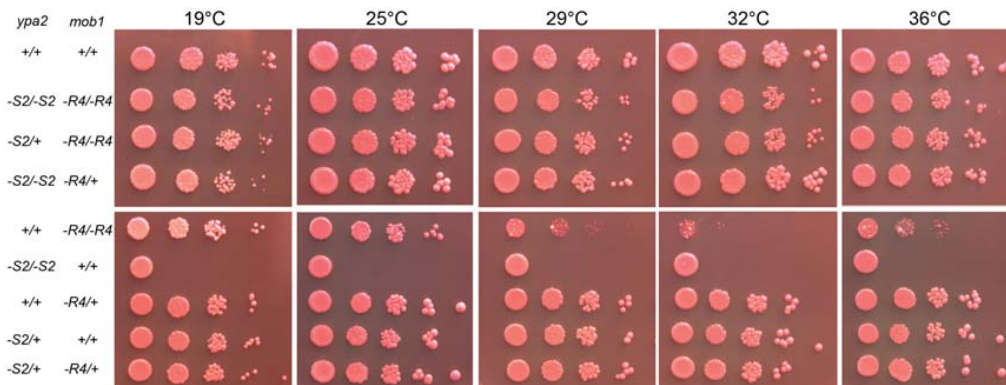


Figure 3:4 Cell growth assays of the diploids *ypa2-S2/ypa2⁺ mob1-R4/mob1-R4* and of the control strains. The cell growth assays were performed as described in section 2.2.3. Notice the rescue of *mob1-R4/mob1-R4* colony formation by *ypa2-S2/ypa2⁺*, at $\geq 29^{\circ}\text{C}$. The four lowest dilutions of *ypa2-S2/ypa2-S2* were not spotted, in error.

Both *ypa2-S2/ypa2-S2 cdc7-A20/cdc7-A20* and *mob1-R4/mob1-R4* diploids show differences in colony formation, as compared to haploids; this might be due to a hypersensitisation to these mutations in the diploid background, which is not the preferred ploidy state of fission yeast (Smith, 2009).

3.4 Validation of *ypa2-S2*, as an allele of *ypa2*

Because sequencing analysis of *ypa2-S2* has identified several SNPs in the genome, we wished to show that the nt change found in the *ypa2* CDS is responsible for the rescue of SIN mutants by *ypa2-S2*. To this end *ypa2-S2* CDS was purified from DW232 (see section 2.5.1) and was used to transform *ypa2::ura4⁺ ura4-D18*. This transformation aimed at replacing *ura4⁺* by *ypa2-S2*, thus rescue the *ypa2-Δ* phenotypes. Selection against *ypa2-Δ* was done on 5-FOA containing plates, because cells expressing a functional *ura4* gene convert 5-FOA into a toxic compound (Silar and Thiele, 1991; Watson et al., 2008). No colony of phenotype *ypa2-S2* was identified, due to a high background.

Next, the CDS of *ypa2-S2* was expressed from the *leu1* locus (referred to as *ypa2-S2@leu1*, in Fig. 3:5; see section 2.5.1) and we looked for its ability to rescue the SIN mutant *mob1-R4*. Expression of *ypa2-S2* from the *leu1* locus was able to rescue the cs phenotype and the morphological defects of *ypa2-Δ* (*ypa2-S2@leu1 ypa2-Δ*) but rescued poorly *mob1-R4* at 29°C and 32°C, in the *ypa2⁺* background (Fig. 3:5).

Diploid analysis shown above suggested that *ypa2-S2* is dominant over *ypa2⁺* (Fig. 3:3 and 3:4), therefore the failure to completely rescue *mob1-R4* in the *ypa2-S2@leu1 ypa2⁺ mob1-R4* strain may be due to competition between *WT* and mutant *Ypa2p*, in haploid cells. To test this, the triple mutant *ypa2-S2@leu1 ypa2-Δ mob1-R4* was constructed in which the rescue of *mob1-R4* by *ypa2-S2@leu1* was similar to that shown in Fig. 3:1, where *ypa2-S2* is expressed at the *ypa2* locus (Fig. 3:5). Similar rescue of *mob1-R4* and *ypa2-Δ* was observed when expressing *ypa2-S2* from the *lys1* locus (data not shown).

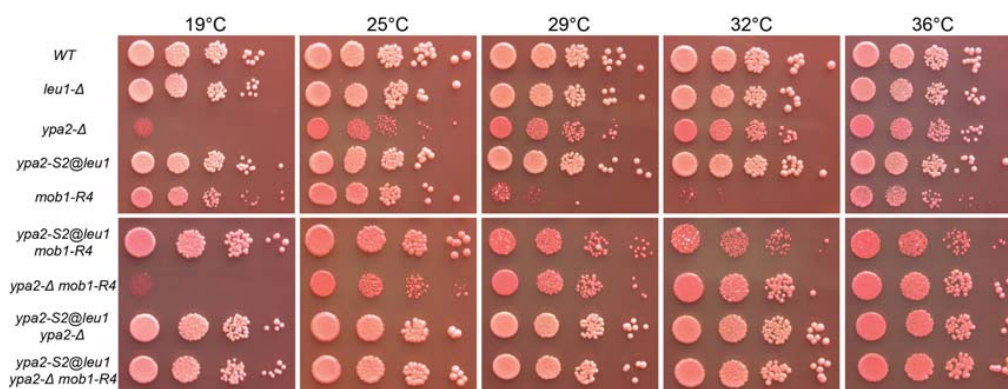


Figure 3:5 Cell growth assays showing the validation of *ypa2-S2*, as an allele of *ypa2*. The cell growth assays were performed as described in section 2.2.2. *ypa2-S2@leu1* partially rescues the hs phenotype of *mob1-R4*, in the presence of *ypa2⁺* (*ypa2-S2@leu1 mob1-R4*). The rescue is complete when the *Ypa2-S2p* form is the sole *Ypa2p* in the cell (*ypa2-S2@leu1 ypa2-Δ mob1-R4*). Notice that the cs phenotype of *ypa2-Δ* is also rescued by *ypa2-S2@leu1*.

3.5 Genetic tagging of the *ypa2-S2* locus

In the experiments described above *ypa2-S2* was identified through its TBZ-sensitivity or by keeping it in the background of a SIN allele, with which the genetic interaction had been characterized. However, different concentrations of TBZ are required to assess the sensitivity of *ypa2-S2*, depending on the temperature (data not shown), while using *ypa2-S2* in the background of a SIN allele would impose a large number of crosses, to validate the creation of a strain with the desired genotype.

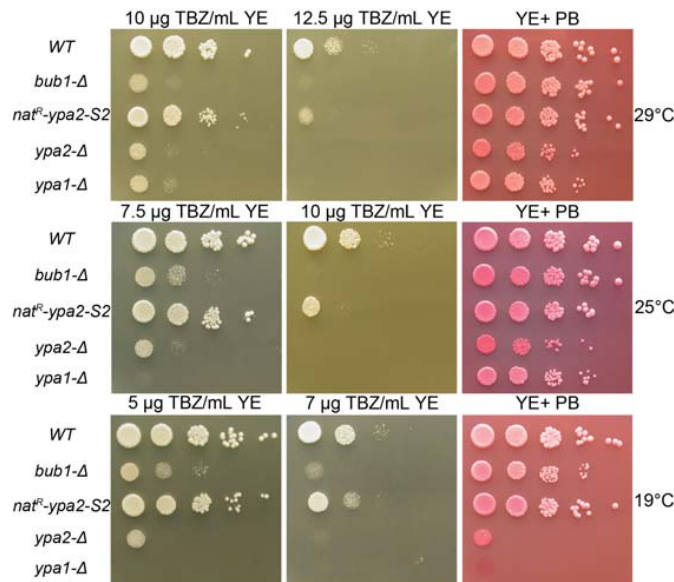


Fig. 3:6 TBZ-sensitivity test of the PTPA mutants. The deletion mutant *bub1-Δ* was reported to be TBZ sensitive (Yamagishi et al., 2012), which can be observed at all tested temperatures. Notice that *ypa1-Δ* and *ypa2-Δ* are TBZ sensitive at 25°C and 29°C; these strains do not grow at 19°C (Bernal et al., 2012; Goyal and Simanis, 2012). *nat^R-ypa2-S2* is TBZ sensitive at all tested temperatures. YE+PB control plates were spotted to verify the growth of the mutants.

To simplify the identification of *ypa2-S2* in genetic crosses, the *nat^R* gene was integrated 341 nt upstream of its START codon (see section 2.5.2). We chose the upstream region, because there is transcriptional overlap between *ypa2* and the downstream gene, *phb1*. Although *nat^R* is placed 109 nt upstream into the long 3' UTR of *cox24*, it is found distal to the main polyadenylation site of *cox24* (Wood et al., 2012). Similar to *ypa2-S2*, *nat^R-ypa2-S2* is TBZ-sensitive (data not shown and Fig. 3:6), however, to determine whether the rescue of SIN alleles by *ypa2-S2* was affected by placing *nat^R* upstream of its CDS, we compared the ability of *nat^R-ypa2-*

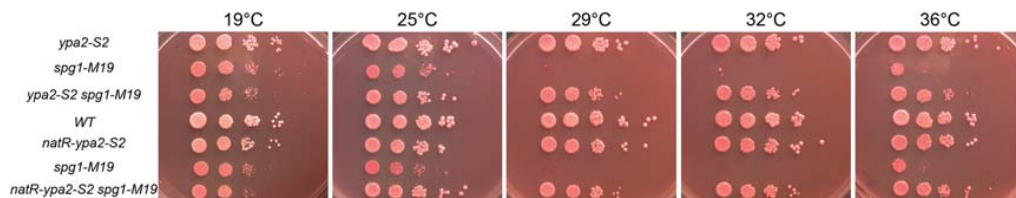


Figure 3:7 Cell growth assays showing the validation of *nat^R-ypa2-S2*. The cell growth assays were performed as described in section 2.2.2. The untagged and *nat^R*-tagged *ypa2-S2* rescue the hs phenotype of *spg1-M19*, in a similar manner.

S2 and *ypa2-S2* to rescue the mutant *spg1-M19*. Both *ypa2-S2* alleles rescued the SIN mutant (Fig. 3:7), therefore we concluded that *nat^R-ypa2-S2* is functional.

3.6 Characterization of the allele *ypa2-S2*

3.6.1 Is *ypa2-S2* advanced into mitotic commitment?

In fission yeast cell length is indicative of the cell cycle stage and mutants that are advanced into mitotic commitment divide as short as 7.6 μm (for example, *wee1- Δ*) (Russell and Nurse, 1987b). *ypa2- Δ* was reported to divide at reduced cell length, as compared to *WT*. This observation and the fact *ypa2- Δ* is synthetic lethal with the mutant *wee1-50*, that is also advanced into mitosis, implicated Ypa2p in the control of mitotic commitment (Bernal et al., 2012; Goyal and Simanis, 2012; Nurse, 1975).

To examine whether *ypa2-S2* is altered in commitment to mitosis, cell length and width measurements were performed for *ypa2-S2*, *ypa2- Δ* and *ypa2⁺* (Fig. 3:8).

A	cell length		cell width		B	cell length		cell width	
	<i>ypa2⁺</i>	<i>ypa2-Δ</i>	<i>ypa2⁺</i>	<i>ypa2-Δ</i>		<i>ypa2⁺</i>	<i>ypa2-S2</i>	<i>ypa2⁺</i>	<i>ypa2-S2</i>
AVG	13.4	9.7	3.8	4.5	13.8	12.5	3.8	3.9	
ST DEV	0.8	0.9	0.4	0.5	1.1	1	0.4	0.4	
M	13.4	9.6	3.8	4.5	13.7	12.4	3.8	3.9	
P-value	6.16E-217		1.0551E-59		5.26016E-46		0.003		

Figure 3:8 Cell length and width measurements of *ypa2- Δ* , *ypa2⁺* and *ypa2-S2*. Cultures grown at 29°C were used for cell length and width measurements, where 100 cells were measured in each of three different experiments, for each genotype. AVG, ST DEV and M are given in μm . The P-value was calculated with the Student's t-test between *ypa2⁺* and *ypa2-S2* or *ypa2- Δ* , for cell length and width respectively (see section 2:6). "E" stands for exponential function.

Similar to published observations, we found that *ypa2- Δ* divides at reduced cell length and increased width (Fig. 3:8 A), and that length and width of *ypa2-S2* also differed in a statistically significant manner from *WT* (Fig. 3:8 B). While cell length of *ypa2- Δ* was reduced by 3.7 μm and width increased by 0.7 μm , the values of *ypa2-S2* were 1.3 μm and respectively 0.1 μm . This suggested that *ypa2-S2* might be advanced into mitosis, therefore we investigated whether *ypa2-S2* interacts genetically with mutants that alter commitment to mitosis.

Some mutations that lead to inefficient inhibition of Cdc2p, by Wee1p (for example, *cdc2-1w*, *wee1-50*) or to bypass of the requirement for Cdc25p, in Cdc2p activation (for example, *cdc2-3w*), allow cells to divide at reduced cell length (Fantès, 1981; Nurse, 1975; Russell and Nurse, 1987b). In contrast to *ypa2- Δ wee1-50*, *nat^R-ypa2-S2 wee1-50* is viable, however with impaired colony formation at 36°C (Fig. 3:9). Examination of cell morphology on the plate indicated that *nat^R-ypa2-S2 wee1-50*, was shorter than *WT* at all temperatures, similar to *wee1-50* (Nurse, 1975). Consistently, a reduction in colony size was found also for *nat^R-ypa2-S2 cdc2-1w*, at

19°C and 36°C. No genetic interaction was observed between *nat^R-ypa2-S2* and *cdc2-3w* (Fig. 3:9).

PP2A inhibits mitotic commitment by influencing the phosphorylation status of Wee1p and Cdc25p (Bollen et al., 2009; Chica et al., 2016; Jeong and Yang, 2013; Kinoshita et al., 1993). Given that *nat^R-ypa2-S2* negatively interacted with mutants that alter mitotic commitment via Wee1p but not with *cdc2-3w*, indicated that *nat^R-ypa2-S2* might alter the ability of PP2A (or another phosphatase), to inhibit Cdc25p activation. In agreement with this hypothesis, *nat^R-ypa2-S2* did not show a genetic interaction with *cdc25-22* (Fig. 3:9); this allele cannot enter mitosis when incubated at 36°C, therefore elongated, G2-arrested cells accumulate at this temperature (Fantès, 1979). Microscopic examination on plates indicated that *nat^R-ypa2-S2 cdc25-22* has the phenotype of *cdc25-22*.

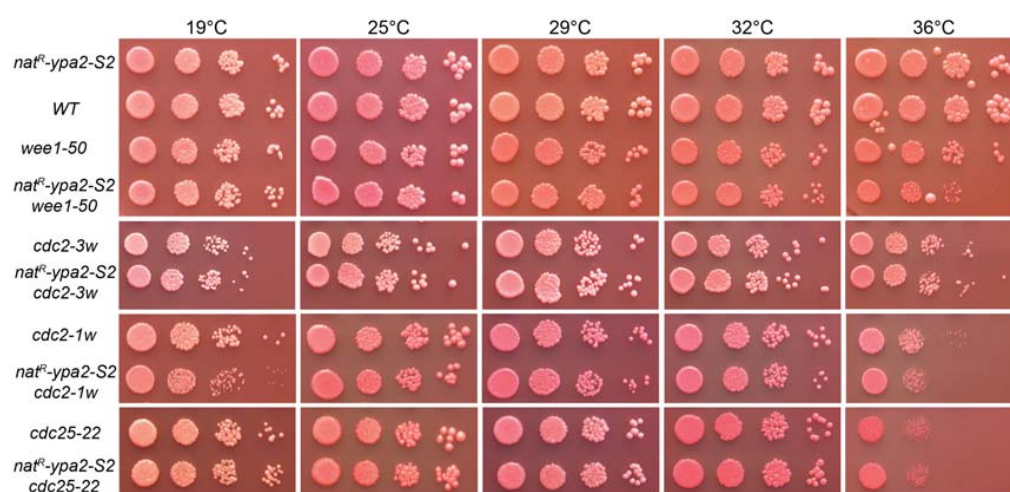


Figure 3:9 Cell growth assays of double mutants between *nat^R-ypa2-S2* and *hs* mutants that alter mitotic commitment. The cell growth assays were performed as described in section 2:2.2. Note the impaired ability of colony formation, for the double mutants *nat^R-ypa2-S2 cdc2-1w* (at 19°C and 36°C) and *nat^R-ypa2-S2 wee1-50* (at 36°C). The alleles *cdc2-3w* and *cdc25-22* do not interact genetically with *nat^R-ypa2-S2*.

3.6.2 Does *nat^R-ypa2-S2* have altered cell polarity?

Deletion of *ypa2* leads to altered cell morphology, which results from changes in the distribution of actin and MTs (Bernal et al., 2012; Goyal and Simanis, 2012).

Consistent with the involvement of Ypa2p in the regulation of cell polarity, double mutants between *ypa2-Δ* and *tea1-Δ*, *tea4-Δ* and *for3-Δ* were found to have strong negative genetic interaction (Bernal et al., 2012). Fig. 3:2 suggests that *ypa2-S2* does not have altered cell polarity, however, we investigated whether minor defects were concealed in this allele.

The double mutants *nat^R-ypa2-S2 tea4-Δ* and *nat^R-ypa2-S2 for3-Δ* were able to form colonies that were similar in size to the single mutants; microscopic examination of the colonies did not reveal major morphological differences between the parental strains and the double mutant (Fig. 3:10). Although detailed analysis of the morphology of the double mutants in culture is required, these observations indicate that there are no major polarity defects in the *nat^R-ypa2-S2* mutant.

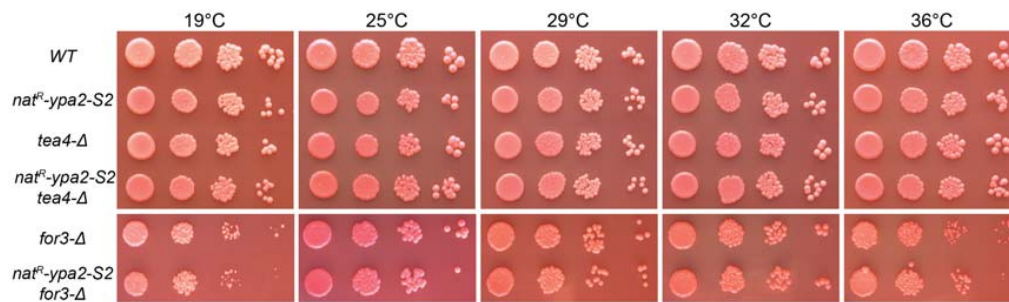


Figure 3:10 Cell growth assays of double mutants between *nat^R-ypa2-S2* with deletion mutants that have altered cell polarity. The cell growth assays were performed as described in section 2.2.2. As compared to the parental strains, no colony formation defect was observed for *nat^R-ypa2-S2 tea4-Δ* and *nat^R-ypa2-S2 for3-Δ*.

Although no obvious negative genetic interaction was found between *nat^R-ypa2-S2* and *tea4-Δ* or *for3-Δ*, the sensitivity of *nat^R-ypa2-S2* to TBZ (Fig. 3:6) indicated that there might be defects in the organization of MTs. As shown in Fig. 3:6, *ypa2-Δ* is also TBZ-sensitive and localization studies of GFP-Atb2p indicated that MTs are shorter in this mutant (Goyal and Simanis, 2012). To understand if there is alteration in the organization of MTs in the *ypa2-S2* mutant, we examined the localization of GFP-Atb2p (Krapp et al., 2006). Analysis of 275 *WT* and 301 *ypa2-S2* cells, at 29°C, showed that there were no abnormal MT figures in the 78% *WT* interphase cells, while 3.65% out of 77% *ypa2-S2* interphase cells had criss-crossed MTs (Fig. 3:11). Another difference was the presence of 4% mitotic and 19% postanaphase cells in *ypa2-S2*, in contrast to 8% and 14% respectively, in *WT*. These results indicate that a small number of interphase cells have alterations of MT organization and that there are less mitotic and more postanaphase cells in *ypa2-S2*.

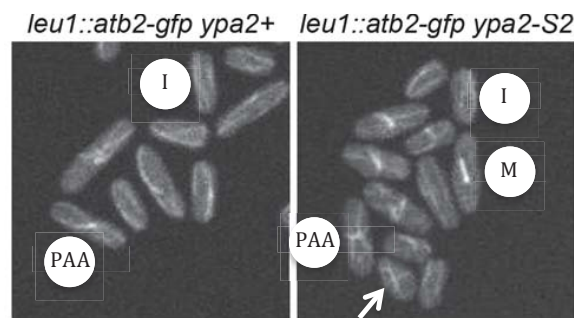


Fig. 3:11 Analysis of GFP-Atb2p in *WT* and *ypa2-S2*. The samples were analyzed as described in section 2.7.2. Indicated is the MT organization specific to interphase (I), mitotic (M) or postanaphase (PAA) cell. White arrow indicates altered MT organization in an interphase cell, whereby a microtubule is placed perpendicular to the short axis of the cell.

3.6.3 Analysis of the genetic interaction of *nat^R-ypa2-S2* with PP2A mutants

Deletion mutants of the major catalytic and regulatory subunits of PP2A were previously shown to negatively interact with *ypa2-Δ* (Goyal and Simanis, 2012). Since *nat^R-ypa2-S2* is a hypomorphic allele, we investigated its interaction with PP2A mutants (Fig. 3:12).

A negative genetic interaction was found between *nat^R-ypa2-S2* and each of the catalytic subunit deletion mutants, however the nature of the interaction differs. No additive phenotypic interaction with *ppa1-Δ* was observed at $\geq 29^{\circ}\text{C}$. At $\leq 25^{\circ}\text{C}$ the double mutant cells were shorter than *WT* and had oval/roundish morphology, although each single mutant appeared morphologically *WT*. In addition, *nat^R-ypa2-S2 ppa1-Δ* colony formation was impaired at 19°C (data not shown and Fig. 3:12). Previous studies did not describe a negative genetic interaction between *ypa2-Δ* and *ppa1-Δ*, because *ypa2-Δ* is *cs* (Goyal and Simanis, 2012).

The mutant *ppa2-Δ* divides at shorter cell length than *WT* (Kinoshita et al., 1990) and *nat^R-ypa2-S2 ppa2-Δ* had the phenotype of *ppa2-Δ* at $\geq 29^{\circ}\text{C}$. However, at 29°C there were lysing cells and the colony formation of the double mutant was impaired (Fig. 3:12). At $\leq 25^{\circ}\text{C}$ the phenotype of *nat^R-ypa2-S2 ppa2-Δ* was similar to *ypa2-Δ*, including the inability to form colonies at 19°C (data not shown and Fig. 3:12). The fact that *nat^R-ypa2-S2* shows a negative interaction with *ppa2-Δ* supports the notion that *nat^R-ypa2-S2* is a hypomorphic allele, because *ypa2-Δ ppa2-Δ* is *cs* and sick at $\leq 25^{\circ}\text{C}$ (Goyal and Simanis, 2012).

Cells deleted for the B regulatory subunit are sterile (Kinoshita et al., 1996), therefore *pab1-Δ* complemented with *pab1⁺* from *lys1*, was used to obtain the strain *nat^R-ypa2-S2 pab1-Δ*. The double mutant had the short and round morphology of *pab1-Δ* at all temperatures and although colony size of the double mutant did not differ from that of the parental strains at $\geq 25^{\circ}\text{C}$, its growth was decreased at 19°C . The double mutant *nat^R-ypa2-S2 par1-Δ* showed a negative interaction at most tested temperatures, however colony formation was most affected at 19°C (Fig. 3:12).

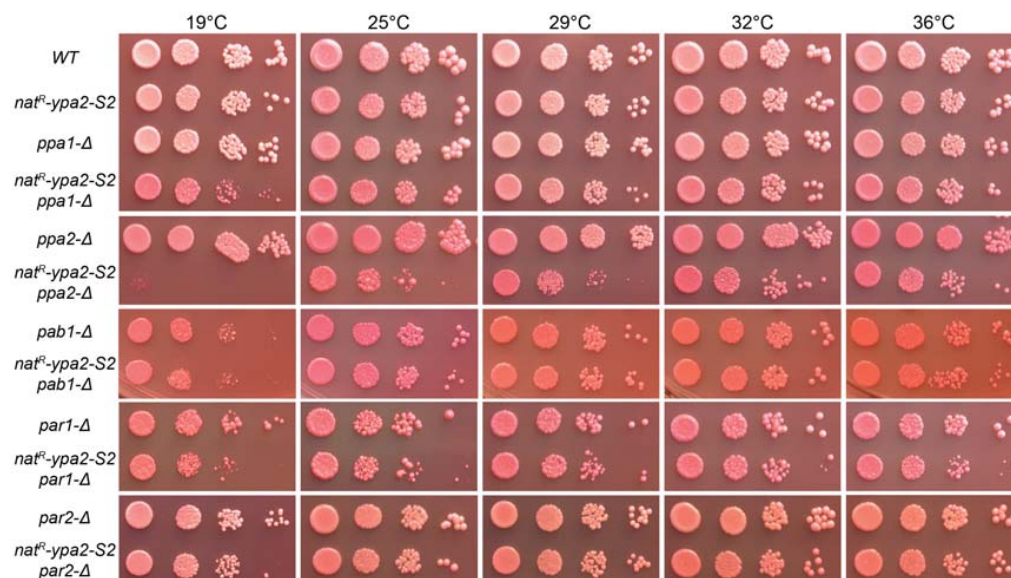


Figure 3:12 Cell growth assays showing the interaction between *nat^R-ypa2-S2* and PP2A deletion mutants. The cell growth assays were performed as described in section 2.2.2. Notice the reduction in colony size and darker PB colony color of *nat^R-ypa2-S2 ppa1-Δ*, at 19°C . With *ppa2-Δ* and *par1-Δ*, *nat^R-ypa2-S2* shows negative interaction at all tested temperatures. No reduction of colony size was observed in the *nat^R-ypa2-S2 par2-Δ* double mutant.

Although observations made microscopically on the plate indicated that the phenotype of the double mutant was similar to that of *par1-Δ* (generally longer cells than *WT*, with misplaced division septum, septum found more towards one of the two cell ends or wider cell on one or both sides of the septum) (Jiang and Hallberg, 2001), future analysis of fixed cells will address the nature of morphological and division defects in detail. No genetic interaction was found between *nat^R-ypa2-S2* and *par2-Δ* (Fig. 3:12).

3.6.4 Does *nat^R-ypa2-S2* interact with the SIP?

The PP2A-related SIP complex was shown to influence the asymmetric localization of some SIN components and to affect the phosphorylation status of Cdc11p (Singh et al., 2011; Wachowicz et al., 2015). Since PTPA could regulate the SIP, deletion mutants of SIP subunits were crossed into the *nat^R-ypa2-S2* background (Fig. 3:13). The colony size of the double mutant *nat^R-ypa2-S2 csc3-Δ* was smaller than that of each single mutant, at 19°C and 36°C and *nat^R-ypa2-S2 csc2-Δ* formed smaller colonies at 19°C. The colony size of *nat^R-ypa2-S2 csc4-Δ* was similar to *nat^R-ypa2-S2*, which may indicate that *ypa2* is epistatic to *csc4*. No interaction genetic interaction was found between *nat^R-ypa2-S2* and *csc1-Δ* (Fig. 3:13). The negative genetic interaction described here between *nat^R-ypa2-S2* and deletion mutants of SIP regulatory subunits could be due to deregulation of SIN signaling, since a common target of the SIP and PP2A/PTPA is the SIN (Goyal and Simanis, 2012; Singh et al., 2011).

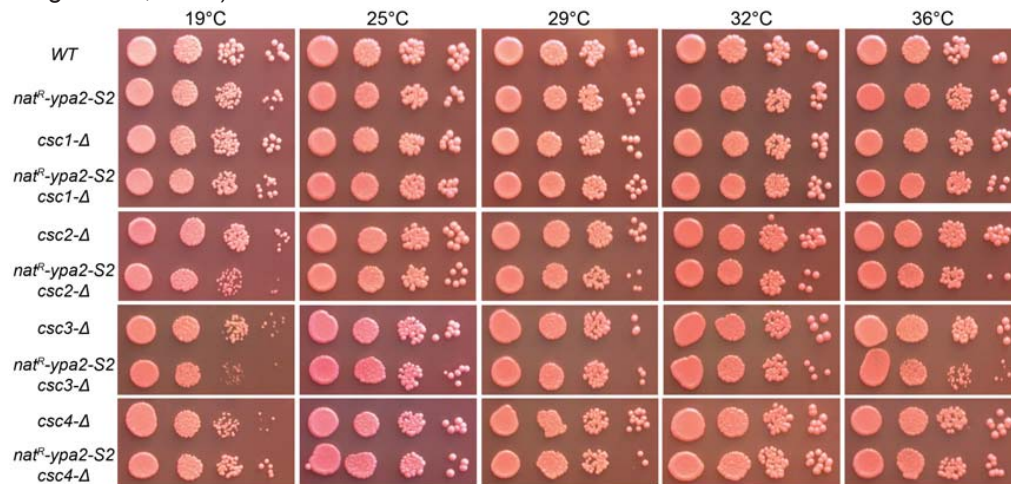


Fig. 3:13 Cell growth assays showing the interaction between *nat^R-ypa2-S2* and SIP mutants. The cell growth assays were performed as described in section 2.2.2. Notice the synthetic sick interaction of *nat^R-ypa2-S2* with *csc3-Δ*, at 19°C and 36°C, and with *csc2-Δ*, at 19°C. Note also that *nat^R-ypa2-S2* is epistatic to *csc4-Δ*, because the size of the double is similar to that of *nat^R-ypa2-S2*.

3.6.5 Is the localization of SIN proteins altered in the *nat^R-ypa2-S2* allele?

Previous reports have shown that the localization of Cdc7p and Sid2p changes in alleles of the major catalytic and B' subunits of PP2A and in *ypa2-Δ* (Goyal and Simanis, 2012; Jiang and Hallberg, 2001; Wachowicz et al., 2015), therefore we examined the localization of GFP-tagged SIN alleles, in *nat^R-ypa2-S2*. Synchronized

G2 cells were imaged as they progressed through mitosis and the GFP signal on the SPB(s) was measured as described in section 2.7.

Similar to previously published observations (Wachowicz et al., 2015), we found that in *WT* a large fraction of cells have asymmetric Cdc7p-GFP (Sohrmann et al., 1998) in the early stages of mitosis and that all cells have asymmetric signal in the late stages (Fig. 3:14). Among the cells that did not have asymmetric Cdc7p there were mostly cells with no signal in our sample, while (Wachowicz et al., 2015) reported no signal, asymmetric and symmetric localization. The difference could be due to the fact that the experiments presented here were done once, while (Wachowicz et al., 2015) present data obtained from at least two repeats. No major differences can be observed in the localization of Cdc7p to the SPBs between *nat^R-ypa2-S2* and *WT*, although the early mitotic cells that did not establish Cdc7p asymmetry show heterogeneity of states in *nat^R-ypa2-S2* (Fig. 3:14).

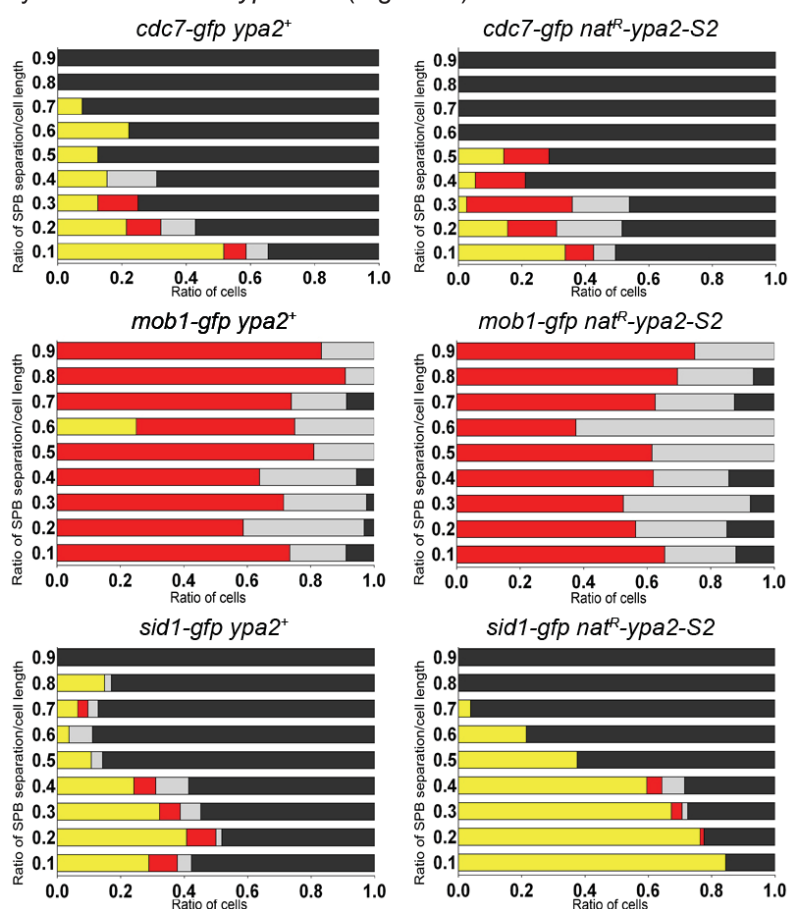


Fig. 3:14 Analysis of the localization of Cdc7p-GFP, Mob1p-GFP and GFP-Sid1p in *WT* and *nat^R-ypa2-S2*, throughout mitosis. The graphs were generated as described in section 2.7. No major difference exists in the localization of Cdc7p-GFP, between the mutant and *WT* backgrounds. A larger fraction of cells were in a transition or asymmetric state for Mob1p-GFP and there was a larger fraction of cells with asymmetric GFP-Sid1p in *nat^R-ypa2-S2*, as compared to *WT*. Color legend: yellow, no signal; red, symmetric; grey, transition; black, asymmetric.

To understand whether the localization of the terminal signaling module within the SIN is altered, we analyzed localization of Mob1p-GFP. Throughout mitosis, Mob1p-

GFP (Salimova et al., 2000) was symmetric on the SPBs in most cells and a small fraction was in a transition or asymmetric state (Fig. 3:14), similar to what reported by (Wachowicz et al., 2015). In *nat^R-ypa2-S2*, the majority of cells had also symmetric Mob1p, however a larger fraction of cells were found in a transition or asymmetric state, than in *WT* (Fig. 3:14).

We also examined the localization of GFP-Sid1p (Guertin et al., 2000); in approximately half of the early mitotic cells no signal was observed, with asymmetry being established in all cells by the latest mitotic stages (Fig. 3:14) (Wachowicz et al., 2015). In *nat^R-ypa2-S2* a larger fraction of cells had no signal throughout mitosis, than *WT* (Fig. 3:14). Although these experiments have to be repeated (see section 2.7), they suggest that localization of Sid1p and Mob1p is altered in the *nat^R-ypa2-S2* background, while localization of Cdc7p is unaffected.

3.7 SGA, to identify genetic interactions of *nat^R-ypa2-S2*

3.7.1 Screening and identification of control interactions

To identify genetic interactors of *ypa2*, a SGA was performed, whereby *nat^R-ypa2-S2* was crossed to version five of *S. pombe* non-essential, genome-wide deletion library purchased from the Bioneer corporation (Kim et al., 2010). The deletion library contains 3576 deletion mutants, which represents 73.9% of the *S. pombe* genes.

Synthetic lethal and sick interactions of *nat^R-ypa2-S2* were identified, which are expected to be genes that normally compensate for the hypomorphic features of this allele. The hits were scored from 19°C and 29°C (see section 2.4), because the library was generated at 29°C (Kim et al., 2010) and *ypa2* is essential at 19°C (Bernal et al., 2012; Goyal and Simanis, 2012) (Fig. 3:5).

To identify the sick and lethal interactions, we selected for the deletion library mutants and for the double mutants. The library strains are G418 resistant (Kim et al., 2010), and *nat^R-ypa2-S2* is able to grow on NAT-containing plates. Inability of deletion mutants to mate and sporulate, as well as the presence of parental strains, diploid meiotic intermediates and the unwanted genotypes would have interfered with the analysis, therefore we used the PEM-2 counterselection system (Roguev et al., 2007).

PEM-2 is based on the ability of CYH to inhibit the ribosomal protein Rpl42p, which renders *WT* cells sensitive to this drug. The library strains are *rpl42⁺* and of *h⁺* mating type; in *nat^R-ypa2-S2* a CYH-resistant, recessive allele of *rpl42* was expressed from the endogenous locus and *rpl42⁺* was inserted next to the *mat1P* locus, expressing the *h⁻* mating information (Roguev et al., 2007; Styrkarsdottir et al., 1993). Both the library strain and *nat^R-ypa2-S2*, diploid cells formed upon their mating, as well as any spores that expressed *rpl42⁺* were sensitive to CYH. The progenies that only expressed the recessive allele of *rpl42*, and were of *h⁺* mating type, were able to grow on CYH-containing plates. When crossed into the *nat^R-ypa2-S2* background, the PEM-2 selection markers did not affect the phenotype of *nat^R-ypa2-S2* (data not shown). In the SGA selection was done on YE plates supplemented 1) with CYH and G418, which selected the library deletion mutants and 2) CYH, G418 and NAT, to select the double mutant between *nat^R-ypa2-S2* and the deletion mutant.

The analysis of the selective plates was done as described in section 2.4.3.1, from which we identified two hundred twelve synthetic lethal and sick hits (Table 3:2), ninety-seven mutants that did not grow on either selective plate (Table 3:5) and two hundred and six null mutants that were represented by a low number of colonies (Table 3:8); these numbers represent the total between 19°C and 29°C, for each category. The bioinformatics analysis of these genes was done as described in section 2.4.3.2 and the results are described in section 3.7.2. To confirm the identity of the hits, PCR-verification of the library deletion mutants was performed as described in section 2.4.3.3. The validation of any interactions described below, in this section and in section 3.7.3 was done as indicated in section 2.4.3.3.

Among the SGA hits we expected to find the synthetic lethal and sick interactions described in sections 3.6.2- 3.6.4. The synthetic lethal interaction with *ypa1-Δ* was identified at 29°C (see section 3:2 and Table 3:2) and *ypa1* is correctly deleted (data not shown). *ypa1-Δ* also appears in the list with non-growers from 19°C, because it is cs (Table 3:5 and Fig. 3.16) (Goyal and Simanis, 2012).

The only gene that scored as synthetic lethal at both 19°C and 29°C was *ypa2-Δ*, which is correctly deleted. At high temperature this outcome was expected, because *ypa2-Δ* and *nat^R-ypa2-S2* are located at the same locus. However, considering that *ypa2-Δ* does not grow at 19°C (3:4), we expected to find *ypa2-Δ* among the non-growers from 19°C. The cells that grew on the plate YE supplemented with CYH and G418, at 19°C, had the morphology specific to *ypa2-Δ* (data not shown and section 3.1) (Bernal et al., 2012; Goyal and Simanis, 2012). Although not formally reported in yeast, growth of *ypa2-Δ* at 19°C probably occurred due to a crowding effect, resulting from the plating of a large number of spores. Numerous cell viability assays performed throughout this study showed that *ypa2-Δ* undergoes a few more divisions than *ypa1-Δ*, at 19°C, before lysing (data not shown); this could account for the fact that *ypa1-Δ* scored in the cs list (Table 3:5).

The negative genetic interaction described between *nat^R-ypa2-S2* and *ppa1-Δ* (Fig. 3:12) was not recapitulated in the screen. The strain is correctly deleted and manual reconstruction of *nat^R-ypa2-S2 ppa1-Δ* showed reduced colony size at 19°C and that cells were shorter than *WT* at ≤ 25°C, (Fig. 3:15 and data not shown). However, at 19°C the colonies of the double mutant obtained with *ppa1-Δ* from the laboratory's stock of strains (Kinoshita et al., 1990) were darker red than of the double mutant obtained with the library *ppa1-Δ* (compare *nat^R-ypa2-S2 ppa1-Δ* from Fig. 3:12 and Fig. 3:15); this indicates that there might be a stronger negative genetic interaction with the former double mutant and future studies will examine the phenotype of fixed cells. The explanation for these differences could be that Kinoshita et al. disrupted the ORF of *ppa1*, while > than 80% of the ORF was deleted in the library strain (Kim et al., 2010). The failure to retrieve the weak sick interaction between *nat^R-ypa2-S2* and *ppa1-Δ* (Fig. 3:15) indicates that mild synthetic sick interactions were probably not recovered. As presumed above in this section, for the growth of *ypa2-Δ* at 19°C, this might be an effect of spotting a large number of colonies on a restricted spotting area.

In the SGA, *nat^R-ypa2-S2 ppa2-Δ* was synthetic sick, at 19°C (Table 3:2 and Fig. 3:15). The strain is correctly deleted and has a shorter cell length than *WT*, as reported for *ppa2-Δ* (data not shown) (Kinoshita et al., 1990). Some differences exist between the double mutants *nat^R-ypa2-S2* with *ppa2-Δ* from the laboratory stock of strains (Kinoshita et al., 1990), compared to the library mutant (compare *nat^R-ypa2-S2 ppa2-Δ* from Fig. 3:12 and Fig. 3:15). Detailed characterization of fixed cultures is needed, however microscopic of the colonies showed that: 1) although mostly lysing, the double mutant obtained with the library strain appears to undergo a few more divisions at 19°C, as compared to the double mutant presented in Fig. 3:12; 2) *nat^R-ypa2-S2 ppa2-Δ* obtained with the strain from the laboratory's stock had the morphology of *ppa2-Δ* at ≥ 29°C and was short and round at ≤ 25°C, while the double mutant shown in Fig. 3:15 was short and round, at all temperatures; 3) at 36°C growth was strongly affected for the double mutant obtained with the library strain. As presented above for *ppa1-Δ*, these differences probably resulted from the fact that the laboratory *ppa2-Δ* is a disruption (Kinoshita et al., 1990). Although the validation experiment indicated that *nat^R-ypa2-S2 ppa2-Δ* is slower growing at 29°C (Fig. 3:15), this was not identified in the SGA, which is in agreement with the observation made immediately above (for *ppa1-Δ*) whereby reduced synthetic sick interactions were not identified in the SGA.

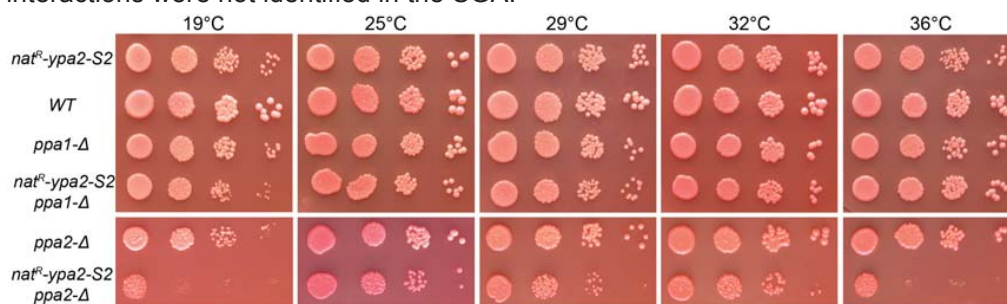


Fig. 3:15 Cell growth assays showing the negative genetic interactions of *nat^R-ypa2-S2* with PP2A deletion mutants, that were recapitulated in and which validate the SGA. The cell growth assays were performed as described in section 2.2.2. Notice that *nat^R-ypa2-S2 ppa1-Δ* colonies have a reduced size at 19°C; *nat^R-ypa2-S2 ppa2-Δ* growth is impaired at 19°C and 36°C and the colony size is reduced at 29°C.

The strain *pab1-Δ* is present in the library; since disruption of *pab1* renders cells sterile (Kinoshita et al., 1996), this gene should have appeared in the non-growers list. In the spot corresponding to *pab1-Δ*, colonies grew on both selective plates, at 19°C and 29°C. PCR-verification of this strain showed that it is not correctly deleted (data not shown). In the SGA no genetic interaction was found between *nat^R-ypa2-S2* and *par2-Δ*; however, although consistent with the observations made previously (Fig. 3:13), *par2-Δ* was not correctly deleted (data not shown).

Furthermore, the synthetic sick interactions between *nat^R-ypa2-S2* and both *par1-Δ* and *for3-Δ* (described previously in Fig. 3:13 and Fig. 3:10) were recovered in the screen, at 19°C; both strains were correctly deleted (data not shown). Other deletion mutants whose phenotype in the *nat^R-ypa2-S2* background was previously characterized (Fig. 3:10 and Fig. 3:15) do not exist in the library: *tea4-Δ*, *csc1-Δ*, *csc2-Δ*, *csc3-Δ*.

The mutant *ppa3-Δ* is provided in the library but did not interact negatively with *nat^R-ypa2-S2* (data not shown). Ppa3p encodes for a catalytic subunit of PP2A and of the SIP complex (Singh et al., 2011); although it was not verified previously whether *nat^R-ypa2-S2* and *ppa3-Δ* interact genetically, a weak sick interaction (similar to those described above in this section, for *ppa1-Δ* -at 19°C- and *ppa2-Δ* -at 29°C-) cannot be excluded.

Consistent with the negative genetic interaction between *wee1-50* and *nat^R-ypa2-S2* (Fig. 3:9), *wee1-Δ* scored as synthetic sick, at 19°C. The double mutant was not reconstructed, nor was the deletion verified, however the phenotype of the putative *wee1-Δ* is characteristic to that observed previously for this mutant (data not shown) (Russell and Nurse, 1987b).

3.7.2 Bioinformatics analysis

The BP and FYPO were retrieved for the hits, non-growers and the deletion mutants represented by a reduced number of colonies (Table 3:2, 3:5 and 3:8, respectively). This information was used to understand the functions in which their gene products are involved (BP) and the phenotypes associated with their gene deletion (FYPO).

No colony grew on either selective plate, for ninety-seven null mutants: ten did not form colonies at 29°C, twenty-one at 19°C and the rest did not grow at both temperatures (Table 3:5). Eight of ten deletion mutants that did not grow at 29°C were listed among those with a reduced number of colonies at 19°C (Table 3:8); the other two were represented at 19°C by a number of colonies above the threshold set for the category of reduced number of colonies. Twenty-two, out of twenty-four, BPs listed for these strains were enriched (see section 2.4.3.2); among these, nine were involved in mating (Table 3:6). The highest enriched FYPO annotations indicated that deletion of these genes decreases mating efficiency or renders cells sterile; also enriched and consistent with the failure to grow in the SGA were the sensitivity to stresses, inability to sustain starvation and altered cell morphology (see section 2.4.3.2 and Table 3:7). Among the deletion mutants that cluster in the sensitivity to different cellular stresses and in the FYPOs related to survival in the growth or mating conditions of the screen are the genes *exo2*, *sty1* and *ypa1*, which are assigned to several of these categories (Table 3:7). Exo2p and Sty1p were previously involved in mating (Wood et al., 2012) and Ypa1p was identified in a screen for genes that are required to survive starvation (Shimanuki et al., 2007). Polarized cell growth requires both the actin and MT cytoskeleton (Snell and Nurse, 1993, 1994; Verde et al., 1995); previous reports showed that polarized growth is essential in mating (Merlini et al., 2013; Petersen et al., 1998; Snell and Nurse, 1993).

The genes in the group of deletion mutants for which the analysis was based upon a reduced number of colonies numbered fifty-four at 19°C, fifty-nine at 29°C and ninety-two at both temperatures (Table 3:8). Enrichment for the BPs regulated by these genes showed mating, vacuole organization and chromatin remodeling (Table 3:9). FYPO enrichment indicated their involvement in mating, stress response, cell polarity and viability (Table 3:10). As explained above for non-growers, the genes involved in stress response, as well as those involved in cell polarity, can have an impact on mating efficiency.

From the two hundred twelve hits scored in the SGA, seventeen were found at 29°C, eight were common to 19°C and 29°C and one hundred eighty-seven were identified at 19°C (Table 3:2). The larger number of hits identified at low temperature is consistent with the proposed hypomorphic nature of *nat^R-ypa2-S2* (see section 3.6.2), since *ypa2* is required for colony formation at 19°C (Bernal et al., 2012; Goyal and Simanis, 2012).

The enriched BP (see section 2.4.3.2 and Table 3:3) in which the hits function were: regulation of mitotic cell cycle, protein dephosphorylation, positive regulation of GTPase activity, regulation of transcription from the RNA polymerase II promoter, chromatin silencing and remodeling, protein folding in the endoplasmic reticulum, fungal-type cell wall biogenesis, mRNA processing, vesicle-mediated transport, endosome to vacuole transport, vacuole organization and fusion, negative regulation of transcription by glucose, negative regulation of G0 to G1 transition, regulation of filamentous growth, negative regulation of G2/M transition of mitotic cell cycle, phosphorelay signal transduction, signal transduction. Of the two hundred and twelve hits, twenty-five were previously reported to interact genetically with *ypa2-Δ* and none of these is covered by the eight BPs mentioned immediately above (Table 3:2 and Table 3:3). The hits identified at 29°C and those common to 19°C and 29°C clustered into most of the enriched BPs (Table 3:3) and to understand the degree to which the screen interactions can be reconstructed, we validated these (see section 3.7.3).

Among the enriched FYPOs of the hits (see section 2.4.3.2 and Table 3:4), several were sensitivities to cell stressing agents: tacrolimus, caffeine, carbendazim, potassium chloride and calcofluor white. Tacrolimus/FK-506 inhibits the phosphatase PP2B/Calcineurin, which was found to interact with the SIN. PP2B promotes cytokinesis, because SIN mutants grown on FK-506 containing plates lyse with a SIN phenotype, at the permissive temperature. Also, SIN hypomorphic alleles in a background with disrupted PP2B activity are lethal, while constitutive activation of PP2B rescues SIN mutants, at the restrictive temperature (Lu et al., 2002; Plochocka-Zulinska et al., 1995; Yoshida et al., 1994). A previous screen for null mutants which are hypersensitive to FK-506 did not identify *ypa2-Δ* (Ma et al., 2011), however, given that hits from our SGA are sensitive to FK-506 we tested whether alleles of PTPA are sensitive to this drug. Similar to SIN mutants, which lyse in the presence of FK-506 (Lu et al., 2002), *ypa2-Δ* was sensitive; colony formation by *nat^R-ypa2-S2* and *ypa1-Δ* was unaffected by FK-506, except 19°C where the latter mutant does not grow (Fig. 3:16). Although PP2B and PP2A/PTPA appear to have antagonistic effects on the SIN (Goyal and Simanis, 2012; Jiang and Hallberg, 2000; Lahoz et al., 2010; Le Goff et al., 2001; Lu et al., 2002; Yoshida et al., 1994), the sensitivity of *ypa2-Δ* to FK-506 indicates that PP2A/PTPA and PP2B have similar functions on a common target.

Similar to TBZ, carbendazim impairs assembly of MTs (Walker, 1982); as shown in Fig. 3:6 PTPA alleles are sensitive to TBZ and although not tested here, it is possible that they are also sensitive to carbendazim. The annotation “sensitive to TBZ” is not among the enriched FYPOs described in this section, because its statistical values are found below the thresholds set for the analysis discussed here (see section 2.4.3.2). Other enriched FYPOs (see section 2.4.3.2 and Table 3:4) are: abolished

protein localization to cell tip, abolished protein localization to cell tip (with protein mislocalized to cytoplasm), normal protein localization to cell tip, MT bundles present in greater numbers, abnormal actin cortical patch localization; the interactors that belong in these groups might have to do with the mitotic advancement and the defects in MT organization of *nat^R-ypa2-S2* (see sections 3.6.1 and 3.6.2).

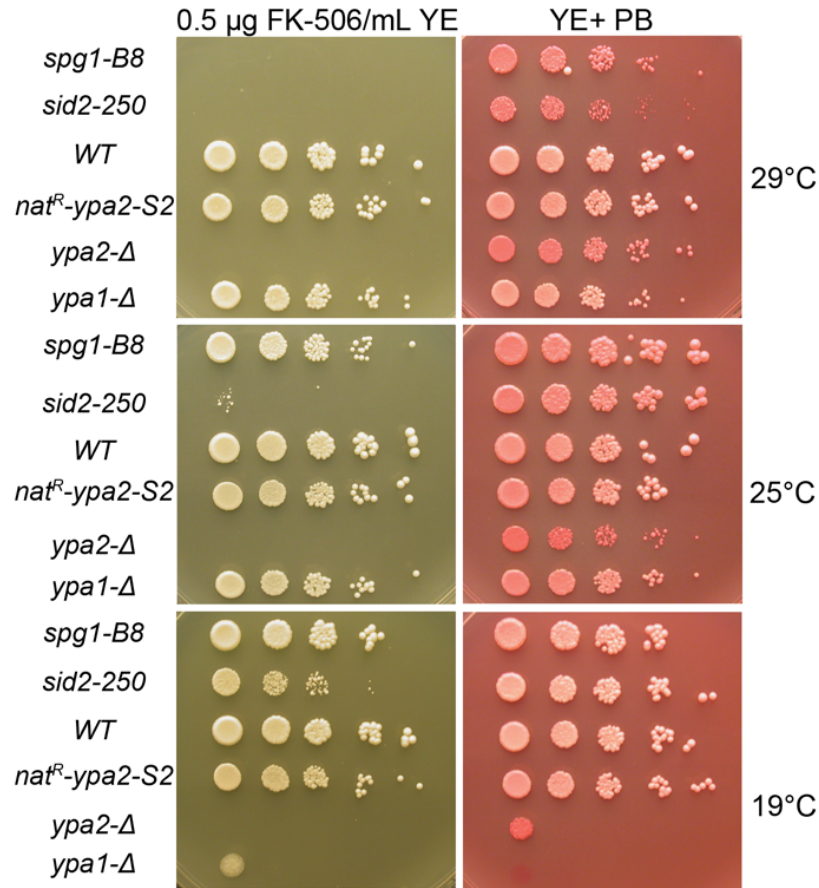


Fig. 3:16 FK-506 sensitivity assay for PTPA mutants. The cell growth assays were performed as described in section 2.2.2. The SIN mutants *spg1-B8* and *sid2-250* are sensitive to FK-506 at 29°C (Lu et al., 2002) and the sensitivity persists down to 19°C for *sid2-250*. *ypa2-Δ*, but not *ypa1-Δ* and *nat^R-ypa2-S2*, is sensitive at 25°C and 29°C. At 19°C *ypa1-Δ* and *ypa2-Δ* do not grow (Bernal et al., 2012; Goyal and Simanis, 2012) and *nat^R-ypa2-S2* was not sensitive.

FYPOs, such as decreased chromatin silencing at telomere, abolished histone H3-K4 methylation, normal chromatin silencing at silent mating-type cassette, abnormal mitotic cell cycle arrest with unreplicated DNA, decreased H3-K9 methylation at centromere outer repeat, increased protein level during vegetative growth, pseudohyphal growth abolished, increased protein phosphorylation during vegetative growth, increased RNA level during nitrogen starvation, increased spontaneous diploidization (Table 3:4) await characterization while mislocalized septum during vegetative growth, abnormal cell separation after cytokinesis and small vacuoles present in greater numbers during vegetative growth (Table 3:4) might be involved in cytokinesis. The FYPO decreased cell population growth during glucose starvation was probably generated by the selection conditions of the SGA, whereby a large number of cells were grown on a limited area of the selective plates (Table 3:4).

3.7.3 Validation of the hits found at 29°C

The validation was done as described in section 2.4.3.3 for the twenty-four synthetic lethal and sick interactions identified at 29°C and those common to 19°C and 29°C (Table 3:2, Table 3:11 and Fig. 3:17). The assessment of a synthetic sick interaction was made based upon reduced colony size or by additive morphological differences observed for the double mutant, as compared to the parental strains. The images of colony formation assays are presented in this section, while the observations about cell morphology are mentioned based on microscopic examination of the colonies, on the plates.

Four strains were not correctly deleted: *paf1*, *fip1*, *lsm1* and *ipk1* (data not shown). However, if a negative genetic interaction would be reconstructed with the strains provided in the Bioneer library as deletion mutants of these genes, inverse PCR (Jong et al., 2002) could be performed, to understand which gene's deletion interacted with *nat^R-ypa2-S2*. The presumed *paf1-Δ* and *fip1-Δ* were crossed into the *nat^R-ypa2-S2* background and cell growth assays showed that they do not interact genetically with *nat^R-ypa2-S2* (data not shown).

Although identified as synthetic sick at 29°C, manual reconstruction showed that double mutants of *nat^R-ypa2-S2* with the strain indicated in the library as *lsm1-Δ*, had reduced colony size only at 19°C (Fig. 3:17 and Table 3:11). Lsm1p was not characterized in *S. pombe*, however it is predicted to encode for a subunit of the mRNA decapping complex (Wood et al., 2012); PP2A and PP1 were shown to regulate the spliceosomal complex in other organisms (Naro and Sette, 2013). The double mutant *nat^R-ypa2-S2 ipk1-Δ* was synthetic sick: colony formation of the double mutant was similar to the parental strains (Fig. 3:17 and Table 3:11) but in contrast to these the double mutant cells were shorter. Fission yeast Ipk1p is involved in the inositol phosphate biosynthetic process and has orthologs in *S. cerevisiae* (Ives et al., 2000) and humans (Wood et al., 2012). Since the strains provided in the library as *lsm1-Δ* and *ipk1-Δ* showed a negative genetic interaction with *nat^R-ypa2-S2* it is of future interest to understand what is the deleted gene in these strains.

The strain *nat^R-ypa2-S2 hus5-Δ* could not be reconstructed, because the genetic markers of the strains did not segregate properly in any of the tetrads analyzed. This may be due to the abnormal segregation of sister chromatids, which has been reported for *hus5-Δ* (al-Khodairy et al., 1995).

The colony size of the double mutant between *nat^R-ypa2-S2* and *arp42-Δ* was reduced at 36°C. Although in the screen it scored as synthetic sick at 19°C, *arp42-Δ* and the double mutant do not grow at this temperature (Table 3:11 and Fig. 3:17) and was previously reported to be non-grower at 16°C (Monahan et al., 2008). This could be explained by a cell density effect (as was the case for *ypa2-Δ*; see section 3.7.1) that allowed growth in the SGA. At 19°C, both *arp42-Δ* and the double mutant lysed with a *WT* morphology. At 25°C- 32°C, *arp42-Δ* cells were morphologically similar to *WT*, while at 36°C they had a larger volume. The morphology of the double mutant was similar to *WT* at 25°C and the cells were shorter at ≥ 29°C, with additional polarity defects at 36°C. Arp42p is part of the SWI/SNF and RSC

chromatin remodeling complexes (Monahan et al., 2008), which regulate transcription in mammalian and yeast cells. In mitosis, some subunits of SWI/SNF are inhibited by phosphorylation and it was shown, *in vitro*, that PP2A can dephosphorylate and activate these subunits (Sif et al., 1998). In *S. pombe* a negative genetic interaction was found between *arp42-Δ* and *par1-Δ* (Ryan et al., 2012).

Table 3:11 Summary of the reconstructed interactions found in the SGA. Cell growth assays were performed as described in section 2:2.2; sick interactions were evaluated based on smaller colony size, darker PB colony color or change in the morphology of the double mutant, as compared to parental strains (see also Fig. 3:17). n.d. stands for not done.

Deletion mutant	Correctly deleted?	Was the interaction validated at the temperature where identified?	Is there an interaction at other temperature(s)? If yes, specify it.
<i>ypa1-Δ</i>	Yes	Yes	n.d.
<i>ypa2-Δ</i>	Yes	n.d.	n.d.
<i>paf1-Δ</i>	No	No	No
<i>fip1-Δ</i>	No	No	No
<i>lsm1-Δ</i>	No	No	19°C
<i>ipk1-Δ</i>	No	Yes	At all tested temperatures.
<i>flp1-Δ</i>	Yes	Yes	At all tested temperatures.
<i>ckb1-Δ</i>	Yes	Yes	≥ 29°C
<i>arp42-Δ</i>	Yes	Not at 19°C, yes at 29°C.	≥ 29°C
<i>hus5-Δ</i>	Yes	n.d.	n.d.
<i>inp2-Δ</i>	Yes	No	No
<i>fio1-Δ</i>	Yes	Yes	19°C
<i>SPAC27E2.11c-Δ</i>	Yes	Yes	At all tested temperatures.
<i>kgd2-Δ</i>	Yes	Yes	At all tested temperatures.
<i>eca39-Δ</i>	Yes	No	36°C
<i>erp5/6-Δ</i>	Yes	No	19°C and 36°C
<i>apm1-Δ</i>	Yes	Yes	32°C
<i>pfa3-Δ</i>	Yes	Yes	At all tested temperatures.
<i>rex3-Δ</i>	Yes	Yes	At all tested temperatures.
<i>SPAC13G6.09-Δ</i>	Yes	Yes	≤ 25°C
<i>rrp14-Δ</i>	Yes	No	36°C
<i>rpl3201-Δ</i>	Yes	Yes	At all tested temperatures.
<i>rpl1201-Δ</i>	Yes	Yes	19°C and 36°C
<i>rpl15-Δ</i>	Yes	Yes	At all tested temperatures.

The reconstructed *nat^R-ypa2-S2 inp2-Δ* mutant did not show a synthetic sick interaction. Fission yeast Inp2p is a predicted protein of the myosin binding vezatin family, which are involved in peroxisome inheritance (Wood et al., 2012) and localizes at the cell tips and cell division site (Matsuyama et al., 2006). Yeast peroxisomes contain enzymes that contribute in the metabolism of carbon sources such as choline and ethanalamine (Zwart et al., 1983); in *S. cerevisiae* INP2 cooperates with Myo2p in peroxisome inheritance into the bud (Saraya et al., 2010). It is unclear whether Inp2p interacts with PP2A or whether it is an indirect hit, generated by the spotting of a high density of spores.

nat^R-ypa2-S2 fio1-Δ grew in smaller colonies at 19°C and 29 °C (Table 3:11 and Fig. 3:17) and single and double mutants had *WT* morphology. Fio1p, together with Fip1p (see above, Fip1p), constitute the fission yeast system for high affinity iron transport (Askwith and Kaplan, 1997). It is worth noting that Fe²⁺, in the presence of ascorbate, is required for the activation of the PP2A catalytic activity *in vitro* (Yu, 1998).

The mutant *nat^R-ypa2-S2 kgd2-Δ* grew in smaller colonies at all tested temperatures, although less well visible in the image for 36°C (Table 3:11 and Fig. 3:17). At all temperatures, the parental strains had *WT* morphology and the double mutant was shorter; at 36°C, *nat^R-ypa2-S2 kgd2-Δ* had also cell polarity defects (Wood et al., 2012). Kgd2p is a conserved mitochondrial component, and its only known interactor in fission yeast is Imp1p, a nucleocytoplasmic importin required for spindle disassembly (Lucena et al., 2015). In *S. cerevisiae* *kgd2* encodes for α-ketoglutarate dehydrogenase, which is involved in respiration and biosynthesis, and is transcriptionally regulated by glucose (Heublein et al., 2014; Tretter and Adam-Vizi, 2005).

The gene encoded by *SPAC27E2.11c* does not have apparent orthologs in other organisms (Wood et al., 2012) and is part of the cell membrane (De Groot et al., 2003) and of the mitochondrion (Matsuyama et al., 2006). Similar to previously published data, we found that *SPAC27E2.11c-Δ* has altered cell morphology (Hayles et al., 2013) at all tested temperatures. The double mutant *nat^R-ypa2-S2 SPAC27E2.11c-Δ* had also cell polarity defects, and was shorter than the parental strains at 32°C and 36°C (Table 3:11); at all temperatures the colonies of the double mutant were smaller than those of the parental strains (Fig. 3:17) and had lysing cells.

Eca39p is a branched chain aminoacid transferase, required for the synthesis of Leu, Ile and Val (Eden and Benvenisty, 1998). *nat^R-ypa2-S2 eca39-Δ* colonies were reduced in size only at 36°C, however microscopic examination showed that the cell length was shorter and presented cell polarity defects at all temperatures (Table 3:11, Fig. 3:17). By itself *eca39-Δ* looked *WT* at all temperatures except 36°C, where it had polarity defects. Eca39p was found to physically interact with Csc3p in fission yeast (Singh et al., 2011); in budding yeast the deletion mutant grows faster and has a shorter G1 phase, without affecting other cell cycle stages (Schuldiner et al., 1996).

The growth of *nat^R-ypa2-S2 apm1-Δ* was reduced at 19°C (Table 3:11 and Fig. 3:17); at 29°C and 32°C the double mutant cells were shorter than parental strains, which had a *WT* morphology at all temperatures. Both the double mutant and *apm1-Δ* lysed at 36°C, with a morphology that appeared similar to *WT*. Fission yeast Apm1p is a

subunit of the clathrin-associated adaptor protein-1 (AP-1) complex, which functions in the selection of cargo to be transported from Golgi and in the formation of intracellular transport vesicles (Boehm and Bonifacino, 2001; Kita et al., 2004).

When reconstructed, *nat^R-ypa2-S2 pfa3-Δ* was found to grow in smaller colonies at all tested temperatures (Table 3:11 and Fig. 3:17) and both *pfa3-Δ* and the double mutant cells were morphologically similar to *WT*. Pfa3p is a predicted palmitoyltransferase, involved in ER membrane organization and membrane fusion; the deletion mutant was reported to have abnormal cell shape, however there is not much knowledge about its interactors in *S pombe* (Wood et al., 2012).

The double mutant *nat^R-ypa2-S2 erp5/6-Δ* grew in smaller colonies at 19°C and 36°C (Table 3:11 and Fig. 3:17). Except for 25°C, where no major polarity defects were observed for *erp5/6-Δ* or for the double mutant, at all tested temperatures the double mutant had more obvious polarity defects than *erp5/6-Δ* (Ucisik-Akkaya et al., 2014). Erp5/6p is involved in ER exit during meiosis and the deletion mutant has defects in the forespore membrane formation, which wraps each of the four spores found in an ascus (Ucisik-Akkaya et al., 2014).

The sick interaction between *SPAC13G6.09-Δ* and *nat^R-ypa2-S2* was also validated and the double mutant was sick by colony size, down to 19°C (Table 3:11 and Fig. 3:17); the morphology of *SPAC13G6.09-Δ* and of the double mutant was similar to *WT*. Rex3p is predicted to encode a conserved exonuclease, involved in RNA processing and ribosome biogenesis (Wood et al., 2012). The colonies of *nat^R-ypa2-S2 rex3-Δ* were of similar size to each parental strain, however the double mutant cells were shorter at all tested temperatures (Table 3:11 and Fig. 3:17).

Reconstruction of *nat^R-ypa2-S2 rrp14-Δ* showed that it was sick only at 36°C (Table 3:11 and Fig. 3:17). Similar to *rrp14-Δ*, the double mutant had *WT* morphology at ≥ 29°C and the cells had a larger volume at ≤ 25°C. Both *rrp14* and *SPAC13G6.09* are predicted to be involved in ribosome biogenesis (Wood et al., 2012). TSR4 is the *S. cerevisiae* homolog of *SPAC13G6.09* and conditionally altered TSR4 was associated with defective ribosome assembly (Li et al., 2009). In budding yeast, RRP14 was implicated in the synthesis of 60S ribosomal subunits and in polarized cell growth; the deletion mutant grows slowly (Yamada et al., 2007), similar to fission yeast *rrp14-Δ* (fig. 3:17). In *S. cerevisiae* the deletion mutant of the PP2A scaffold subunit, *tpd3-Δ*, has cytokinetic defects at low temperature and impaired transcription by RNA polymerase III. This polymerase transcribes rRNA, among other types of RNA, which implicates PP2A in the regulation of ribosome biogenesis (van Zyl et al., 1992).

The synthetic sick interactions identified in the SGA between *nat^R-ypa2-S2* and *rpl3201-Δ*, *rpl1201-Δ* or *rpl15-Δ* were validated. These interactions occurred also at other temperatures (Table 3:11 and Fig. 3:17) and cell morphology of the single and double mutants was similar to *WT*. Rpl3201p, Rpl1201p and Rpl15p are conserved in humans and budding yeast and encode for 60S ribosomal subunits (Wood et al., 2012). It is noteworthy that several *rpl* genes were found among the hits identified in a screen looking for fission yeast deletion mutants sensitive to the cell wall synthesis inhibitor micafungin and among these there was *rpl15-Δ* (Zhou et al., 2013).

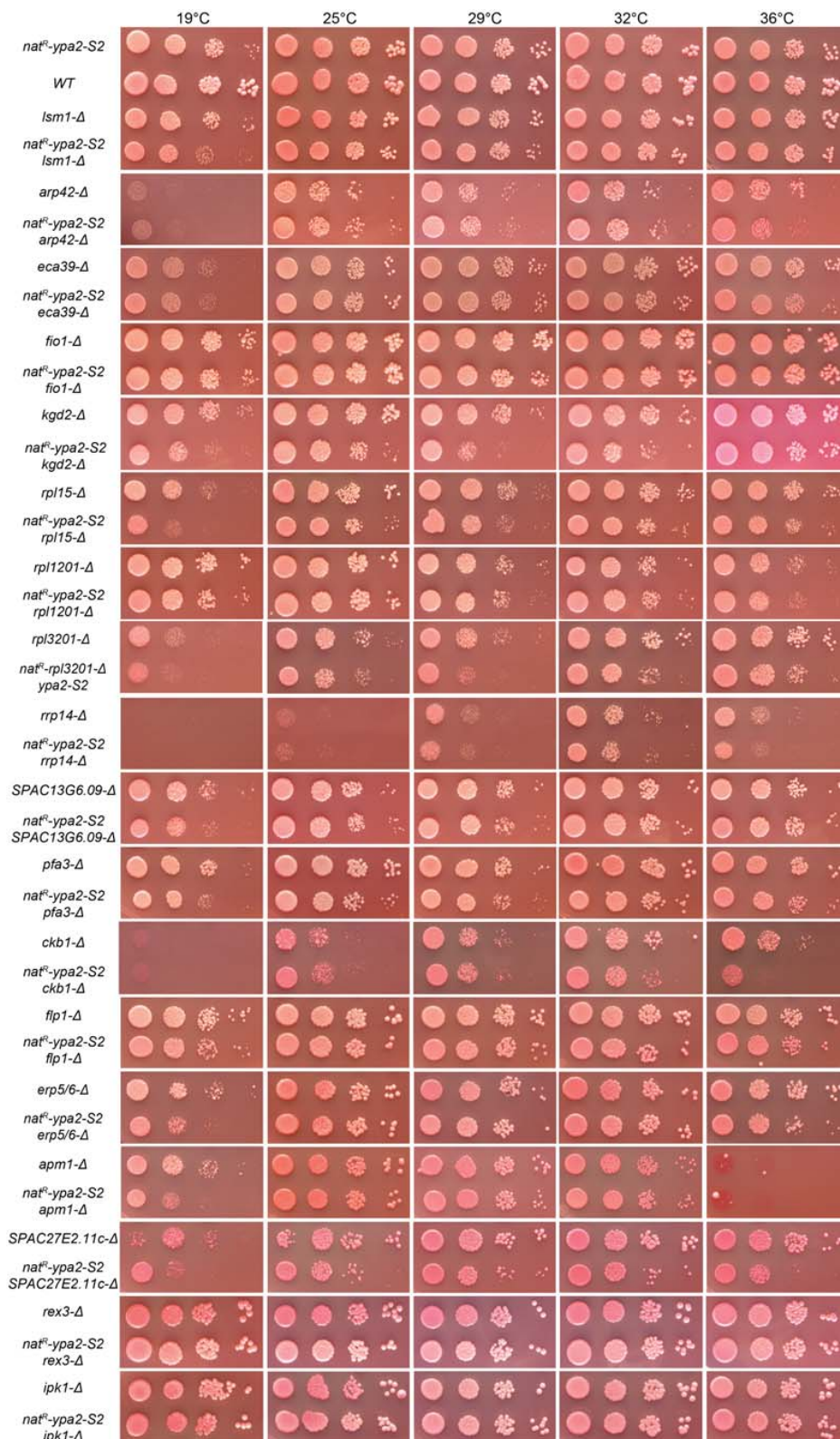


Fig. 3:17 Cell growth assays of double mutants between *nat^R-ypa2-S2* and hits identified in the SGA, at 29°C and 19°C and 29°C. The cell growth assays were performed

as described in section 2.2.2. Notice the synthetic sick interaction of *nat^R-ypa2-S2* with: *flp1-Δ*, *kgd2-Δ*, *pfa3-Δ*, *rpl3201-Δ*, *rrp15-Δ* and *SPAC27E2.11c* at all tested temperatures; *lsm1-Δ* and *flp1-Δ*, at 19°C; *erp5/6-Δ*, at 19°C and 36°C; *rpl1201-Δ*, at 19°C and 32°C; *SPAC13G6.09-Δ*, at ≤ 25°C; *ckb1-Δ* and *arp42-Δ*, at ≥ 29°C; *apm1-Δ*, at 19°C; *rrp14-Δ*, at ≥ 32°C; *eca39-Δ*, at 36°C. The following deletion mutants did not grow by themselves, and in the *nat^R-ypa2-S2* background: *apm1-Δ*, at 36°C; *arp42-Δ*, at 19°C; *rrp14-Δ*, at 19°C and 25°C; *ckb1-Δ*, at 19°C. Notice that, at 19°C and 25°C the 1st and 2nd highest dilutions of *SPAC27E2.11c* were inverted, in error.

Although scarcely visible at low temperatures in Fig. 3:17, the double mutant *nat^R-ypa2-S2 flp1-Δ* had darker red colony color at all tested temperatures (Table 3:11 and Fig. 3:17). *flp1-Δ* was shown to interact with SIN mutants (Chen et al., 2008; Cueille et al., 2001; Mishra et al., 2005) and similar to the SIN, Flp1p is involved in assuring completion of cytokinesis upon mild perturbation of the CAR (Mishra et al., 2004). Flp1p is also involved in mitotic commitment (Esteban et al., 2004); despite their synergistic effects in the control of cell division, an interaction between Flp1p and PTPA/PP2A was not characterized previously. Further characterization between the two phosphatases is presented in section 3.7.4.

The growth of the double mutant *nat^R-ypa2-S2 ckb1-Δ* was reduced at 32°C and strongly impaired at 36°C (Table 3:11 and Fig. 3:17). Microscopic examination indicated that the double mutant had strongly altered cell polarity at ≥ 29°C, and phenotype similar to *ypa2-Δ* at ≤ 25°C (data not shown). By itself, *ckb1-Δ* also has polarity defects and is shorter than *WT* cells (Fig. 3:26 B) at most temperatures, except 19°C, where the mutant lyses with one of the following phenotypes: multicompartmented, cells that are wider on one of the two sides of the division septum or they have a larger volume and polarity defects (Fig. 3:26 B). Ckb1p is one of the two regulatory subunits of CK II; the second regulatory subunit is Ckb2p. The catalytic subunit is encoded by *cka1/orb5* (Cipak et al., 2013; Roussou and Draetta, 1994; Snell and Nurse, 1994). *cka1* is essential (Snell and Nurse, 1994) and is involved in cell polarity establishment, while previous characterization indicated that disrupted *ckb1-Δ* is cs, has cell polarity defects or becomes multicompartmented; OE of Ckb1p generates multicompartmented cells, which indicates that Ckb1p inhibits cytokinesis (Roussou and Draetta, 1994). Given these phenotypes and the fact that Ypa2p has a predicted CK II phosphorylation site (Dinkel et al., 2016), we decided to characterize the interaction of CK II with PP2A/PTPA and the SIN (see section 3.7.5).

3.7.4 Characterization of the interaction between *flp1-Δ* and PP2A/PTPA mutants

3.7.4.1 Phenotypic characterization of the double mutant *nat^R-ypa2-S2 flp1-Δ*

The morphology of *flp1-Δ* is similar to *WT* and *nat^R-ypa2-S2 flp1-Δ* was largely rod-shaped. However, unequal sized daughter cells were generated in the double mutant culture, as a result of septum mispositioning; also, a large number of unseparated sister cells was observed in these cultures (Fig. 3:18). Cell count indicated that in *WT* 4% of the cells were not separated, while in the single mutant cultures of *nat^R-ypa2-S2* and *flp1-Δ* the percentage was 14 and 18 respectively. In the *nat^R-ypa2-S2 flp1-Δ* culture this phenotype represented 45% of the population.

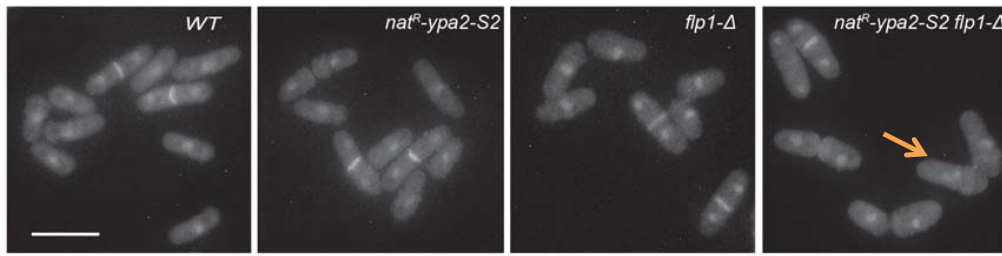


Figure 3:18 Phenotypic characterization of the double mutant *nat^R-ypa2-S2 flp1-Δ*. Exponentially growing cultures from 29°C were imaged as described in section 2.6. Notice that all genotypes have a rod-shaped cell morphology. In the image of the double mutant there are many unseparated cells; the orange arrow indicates a cell in early mitosis, while its attached sister cell remains in interphase, which suggests delayed sister cells separation. Unequal sister cells can also be observed in the double mutant culture. Scale bar: 10 μm.

3.7.4.2 The genetic interaction between *flp1-Δ* and *ypa1-Δ* and *dis2-Δ*
 Prompted by the interaction identified between *flp1-Δ* and *nat^R-ypa2-S2*, we investigated whether *flp1-Δ* interacts genetically with the deletion mutant of the second PTPA gene. Similar to *ypa1-Δ*, *flp1-Δ ypa1-Δ* did not grow at 19°C (Fig. 3:19 A); however, in contrast to the *WT*-shaped parental strains, *flp1-Δ ypa1-Δ* was shorter in length and with cell polarity defects (Fig. 3:19 B) at all tested temperatures and had darker red colony color (Fig. 3:19 A).

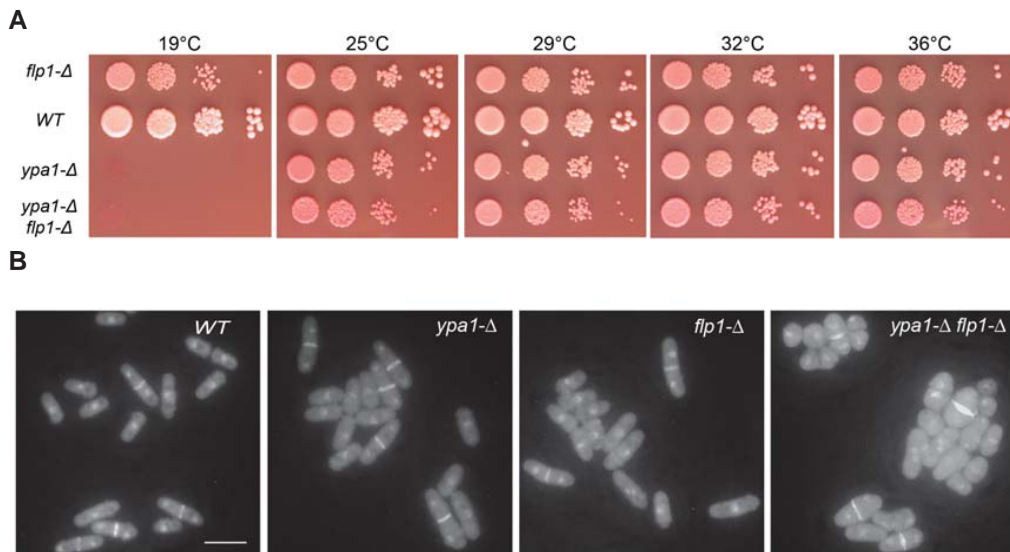


Fig. 3:19 A) Cell growth assay showing the genetic interaction between the *flp1-Δ* and *ypa1-Δ*. The cell growth assays were performed as described in section 2.2.2. The double mutant did not grow at 19°C, similar to *ypa1-Δ*, and had darker red colony color at all temperatures. **B) Phenotypic characterization of the double mutant *flp1-Δ ypa1-Δ*, at 29°C.** Exponentially growing cultures from 29°C were imaged as described in section 2.6. Notice that in contrast to the rod-shaped single mutant alleles, the double mutant cells are shorter and round/oval. Scale bar: 10 μm.

Since Dis2p is involved in the activation of PP2A-Pab1p and PP2A-Par1p holoenzymes (Grallert et al., 2015) to promote mitotic progression, we created the double mutant *flp1-Δ dis2-Δ*. This strain had impaired colony formation at 19°C (Fig. 3:20 A), where cells had varied phenotypes, that indicated altered cytokinesis:

thin/thick division septum or incomplete septa, whereby the septum is seen as a dotted line instead of a continuous structure (Fig. 3:20 B). Such phenotypes were also found in the *dis2-Δ* culture (Fig. 3:20 B); to our knowledge, it is the first time when such defects are reported for *dis2-Δ*. Also, as previously reported by (Ohkura et al., 1989), the *dis2-Δ* mutant had cells with non-disjoined sister chromatids (Fig. 3:20B). Other phenotypes observed for *dis2-Δ* and *flp1-Δ dis2-Δ* cells was a larger volume, generated by wider and/or longer cells (Fig. 3:20 B) and cell wall material deposited at other sites in the cell than the division plane (e.g. at the cell tip, at a cell side) for the double mutant (Fig. 3:20 B).

The finding that there is a negative interaction between null alleles of *dis2* and *flp1*, prompted us to examine whether such an interaction also existed between *dis2* and *ypa2*. The growth and morphology of *dis2-Δ nat^R-ypa2-S2* was similar to that of the parental strains, at all tested temperatures (Fig. 3:20 A and data not shown). Although the phenotype of the strain *ypa2-Δ dis2-Δ* has to be examined, the results presented above (this section and section 3.7.4.2) indicate that if Flp1p and Ypa2p activate PP2A, as does Dis2p, then Ypa2p and Dis2p are probably within the same pathway, while Flp1p would function in a parallel pathway to Ypa2p-Dis2p.

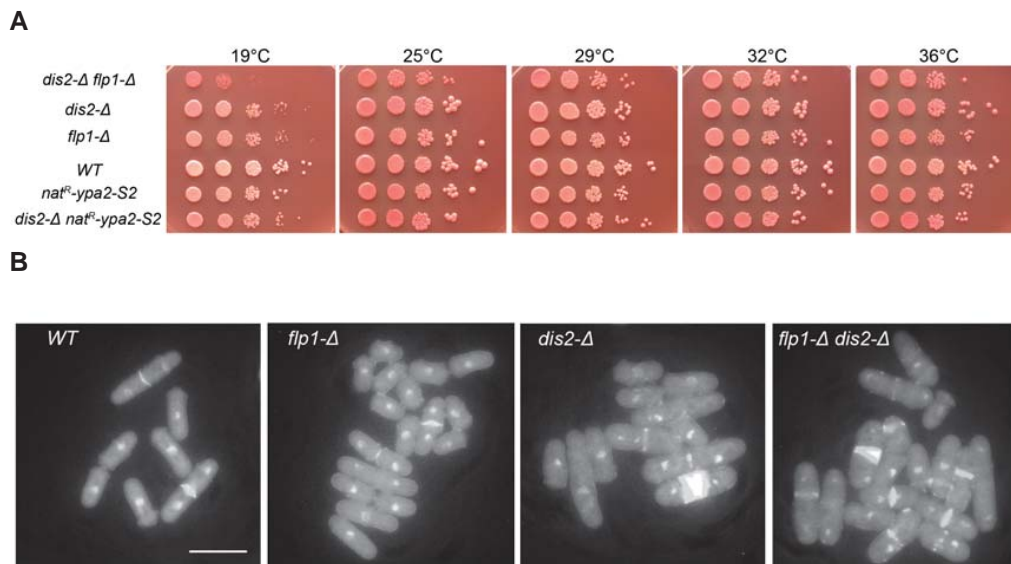


Fig. 3:20 A) Cell growth assays showing the genetic interaction between *dis2-Δ* and *flp1-Δ* and *nat^R-ypa2-S2*. The cell growth assays were performed as described in section 2.2.2. The double mutant *dis2-Δ flp1-Δ* shows a synthetic sick interaction at $\leq 25^{\circ}\text{C}$. The *dis2-Δ nat^R-ypa2-S2* colonies grow in a similar manner to the single mutants. **B) Phenotypic characterization of the double mutant *flp1-Δ dis2-Δ*, at 19°C .** Exponentially growing cultures from 29°C were used to set-up cultures at 19°C , which were fixed after three generations. Fixed samples were imaged as described in section 2.6. Notice that *dis2-Δ* and *flp1-Δ dis2-Δ* cells have larger volume, as compared to *WT* and *flp1-Δ*. The mutants *dis2-Δ* and *flp1-Δ dis2-Δ* have abnormal septa; notice also the failure of *dis2-Δ*, to separate sister chromatids (arrow) and cell wall material deposited at the cell tip in *flp1-Δ dis2-Δ* interphase cell (arrow) Scale bar: 10 μm

3.7.4.3 Analysis of the genetic interaction between *flp1-Δ* and PP2A mutants

To understand whether *flp1-Δ* interacts with PP2A, double mutants were obtained with null alleles of PP2A subunits. With *ppa1-Δ*, *flp1-Δ* interacted only at 19°C, where colony size was reduced and had darker red color (Fig. 3:21); microscopic examination of the colonies showed that the double mutant cells were shorter, as compared to parental strains. Although *ppa2-Δ* is shorter than *WT*, this phenotype was enhanced in *flp1-Δ ppa2-Δ*, at all temperatures, as assessed by microscopic examination of the double mutant colonies; consistent with a synthetic sick interaction, the colony color of the double mutant was darker red at 19°C (Fig. 3:21).

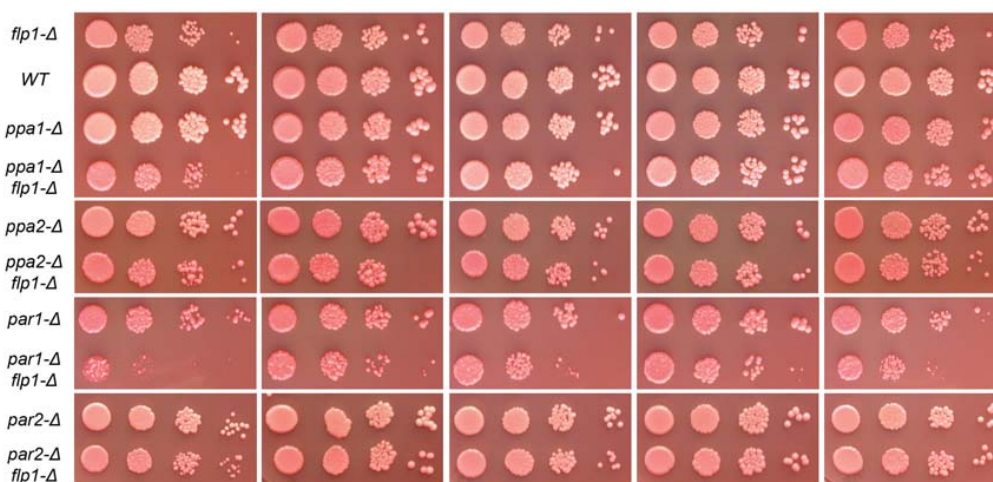


Fig. 3:21 Cell growth assays showing the genetic interaction between *flp1-Δ* and PP2A deletion mutants. The cell growth assays were performed as described in section 2.2.2. Notice that growth of *flp1-Δ ppa1-Δ* and *flp1-Δ ppa2-Δ* is impaired at 19°C, although to a reduced extent for the latter. The strain *flp1-Δ par1-Δ* does not survive at 19°C and reduced colony size was observed at the other tested temperatures. *flp1-Δ par2-Δ* had slightly darker red colony color.

The strain *flp1-Δ pab1-Δ* formed microcolonies, which could not be propagated; microscopic examination showed that the cells were short and round, which is a phenotype characteristic to *pab1-Δ*; in contrast to *pab1-Δ* in the double mutant colony there were lysing cells. The double mutant *flp1-Δ par1-Δ* had the homogenous morphology defects of *par1-Δ* (cell polarity defects and misplaced septa), at all tested temperatures (Fig. 3:22); while colony formation was strongly impaired at 19°C, the colony size was reduced at the other temperatures (Fig. 3:21). At the permissive temperature the prevalent phenotype in the double mutant culture was misplaced division septum (Fig. 3:22). Examination of cultures grown for three generations at 19°C indicated that, except for the morphology (larger volume and misshapen cells) and cytokinesis defects (failure in cell separation or misplaced septa) specific to *par1-Δ* at this temperature, in the double mutant culture there were also cells with a SIN phenotype (Fig. 3:22). Except for a slightly darker red colony color of the double mutant (Fig. 3:21), no interaction was observed between *flp1-Δ* and *par2-Δ*.

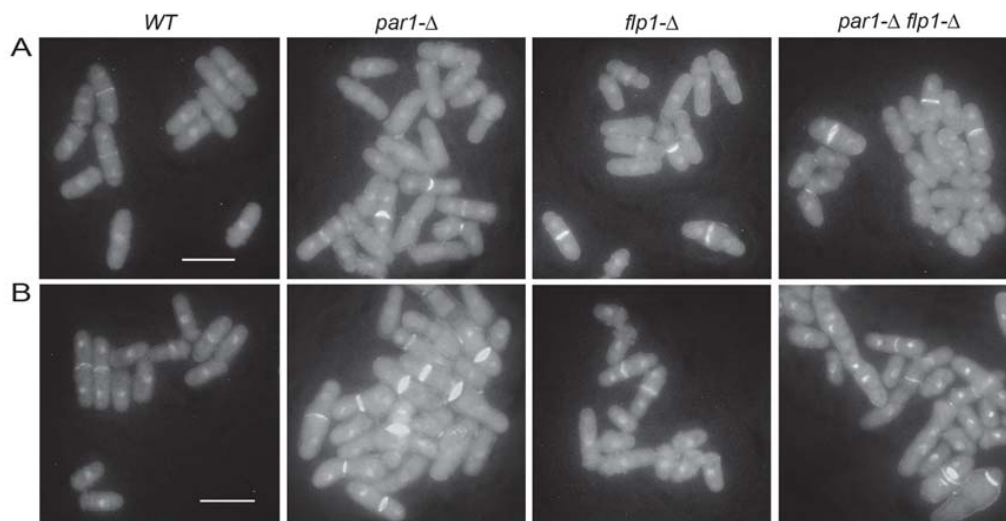


Fig. 3:22 Phenotypic characterization of the double mutant *flp1-Δ par1-Δ*. Exponentially growing cultures from 32°C were used for fixation and to set-up cultures at 19°C, which were fixed after three generations. Fixed samples were imaged as described in section 2.6. **A) Samples from 32°C.** The mutant *par1-Δ* is largely similar to *WT*, however alterations in cell polarity and division septum placed closer to one cell end can also be observed; in the double mutant culture the displacement of the division septum is a frequent defect. **B) Samples from 19°C.** The culture *par1-Δ* comprised the following alterations: cells with larger volume, division septum placed closer to one cell end and cell separation defects. In addition to the defects described for *par1-Δ*, in the double mutant culture there were also cells with SIN phenotype. Scale bar: 10 μm.

3.7.5 Characterization of the interaction between *ckb1-Δ* and alleles of PP2A/PTPA/Dis2p, SIN and Cdc2p

3.7.5.1 Phenotypic characterization of the double mutant *nat^R-ypa2-S2 ckb1-Δ*

The single mutant *ckb1-Δ* has altered cell polarity and also generates unequal sized daughter cells, as a result of misplaced division septum (Fig. 3:23). *nat^R-ypa2-S2 ckb1-Δ* cells are short and have cell polarity defects but also a higher septation index (Fig. 3:23). In the *WT* culture 9% of the cells had a division septum, while *nat^R-ypa2-S2* and *ckb1-Δ* had each 16% septated cells. In double mutant culture, the septation index reached to 28%.

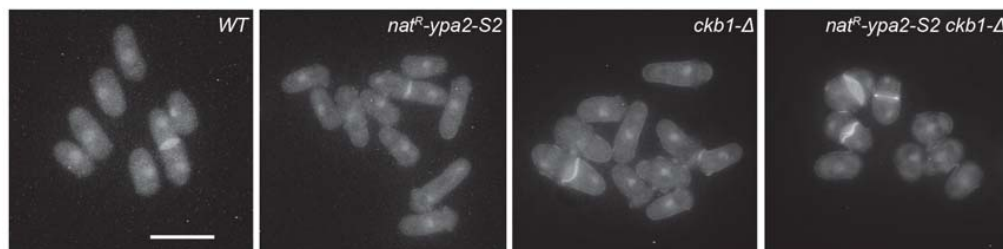


Figure 3:23 Phenotypic characterization of the double mutant *nat^R-ypa2-S2 ckb1-Δ*. Exponentially growing cultures from 29°C were imaged as described in section 2.6. Notice that *ckb1-Δ* had cell polarity defects and generated daughter cells of unequal size. The double mutant becomes short and has a higher septation index. Scale bar: 10 μm.

3.7.5.2 The interaction of *natR-ypa2-S2* with *cka1-12*

To understand whether *ypa2* interacts also with the catalytic subunit of CK II, we crossed *nat^R-ypa2-S2* into the *cka1-12* background. This mutant is hs, thus the cross was dissected at 25°C; similar to *cka1-12*, the double mutant did not grow at ≥ 32°C and, in addition, showed a reduction in colony size at 19°C (Fig. 3:24).

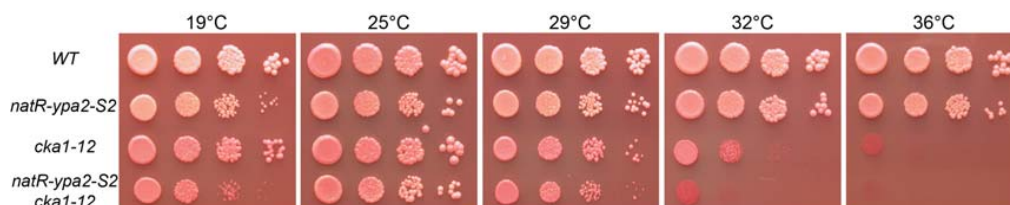


Fig. 3:24 Cell growth assays showing the genetic interaction between *nat^R-ypa2-S2* and *cka1-12*. The cell growth assays were performed as described in section 2.2.2. *cka1-12* and the double mutant with *nat^R-ypa2-S2* do not grow at ≥ 32°C and have reduced colony size at 29°C. A synthetic sick interaction can be observed between *nat^R-ypa2-S2* and *cka1-12* at 19°C, as judged by the reduced colony size of the double mutant.

3.7.5.3 The genetic interaction between *ckb1-Δ* and PP2A/PTPA mutants

We also analyzed the genetic interaction between *ckb1-Δ* and PP2A/PTPA deletion mutants (Fig. 3:25 A and B). Consistent with the negative genetic interaction between *ckb1-Δ* and *nat^R-ypa2-S2*, the double mutant *ckb1-Δ ypa2-Δ* forms very

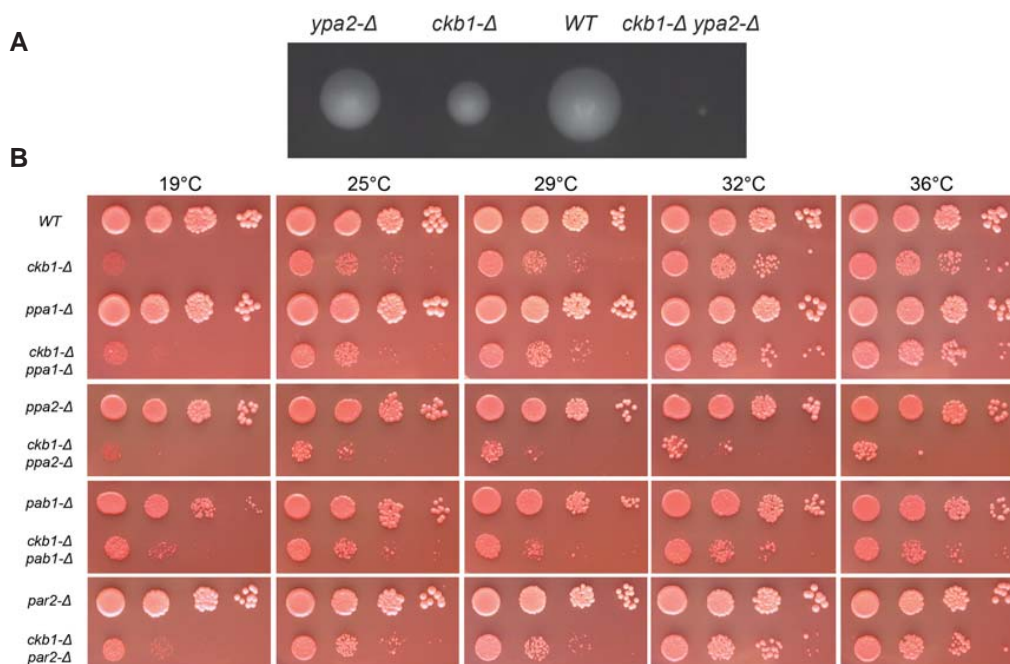


Fig. 3:25 Cell growth assays showing the genetic interaction between *ckb1-Δ* and PP2A/PTPA deletion mutants. A) Three tetrads, with genotypes labeled above each colony, are shown from the cross *ckb1-Δ* with *ypa2-Δ*. B) The cell growth assays were performed as described in section 2.2.2. Notice that growth of *ckb1-Δ ppa2-Δ* is strongly impaired at all temperatures. Reduction in colony size occurs for *ckb1-Δ pab1-Δ* at all temperatures, with residual growth at 19°C. No negative genetic interaction was observed between *ckb1-Δ* and *ppa1-Δ* or *par2-Δ*.

small colonies of short and round cells, most of which lysed (Fig. 3:25 A). No additive genetic interaction was found between *ckb1-Δ* and *ppa1-Δ* and *par2-Δ*, and the double mutants had the phenotype of *ckb1-Δ* at all temperatures (data not shown and Fig. 3:25 B). The double mutant *ckb1-Δ par1-Δ* was lethal, and generated only 1-4 short cells, some of which were round (data not shown). A strong negative genetic interaction was observed also between *ckb1-Δ* and *ppa2-Δ* (Fig. 3:25 B); the cells were mostly lysing and analysis of the morphology of the double indicated that cells were short and round and had polarity defects (data not shown). *ckb1-Δ pab1-Δ* cells were short and round, however, the volume of the cells was larger than that of *pab1-Δ*. Although there was lysis at all temperatures, the morphology of *ckb1-Δ pab1-Δ* and the fact that some cell divisions occur at 19°C indicates that *pab1* is epistatic to *ckb1* (Fig. 3:25 B).

3.7.5.4 Is there an interaction between *ckb1-Δ* and *dis2-Δ*?

Since *ckb1* is an interactor of *ypa2*, we tested whether a genetic interaction existed between *ckb1-Δ* and *dis2-Δ*. We found that colony formation by the double mutant is strongly affected at 25°C and 29°C and that the double mutant is not able to grow at 19°C, similar to *ckb1-Δ* (Fig. 3:26 A).

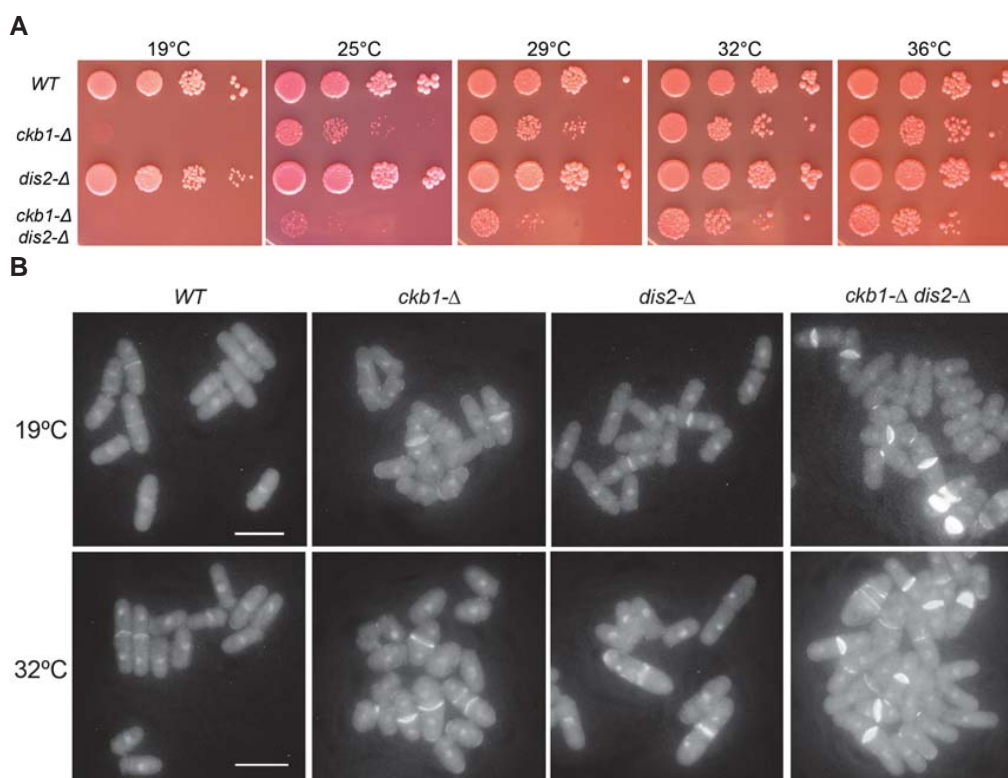


Fig. 3:26 A) Cell growth assays showing the genetic interaction between *ckb1-Δ* and *dis2-Δ*. The cell growth assays were performed as described in section 2.2.2. Colony formation by the double mutant is strongly reduced at 25°C and 29°C; at 19°C *ckb1-Δ dis2-Δ* does not grow, similar to *ckb1-Δ*. **B) Phenotypic characterization of the double mutant *ckb1-Δ dis2-Δ*, at 19°C.** Exponentially growing cultures from 32°C were used to fix cells and to set-up cultures at 19°C, which were fixed after three generations. Fixed samples were imaged as described in section 2.6. Notice that at both permissive and restrictive temperature, the double mutant cells have cell separation defects or cell wall material deposited at one cell

end. Also, at 19°C, the double mutant cells have a larger volume, which can also be observed for the parental strains. Scale bar: 10 μm

Examination of cells from 19°C and 32°C suggested that the double mutant has defects in cell separation, as indicated by cells that have several nuclei and by presence of more than one septum; also, septum material was also deposited at other sites than the medial region, often at one cell end (Fig. 3:26 B).

3.7.5.5 The genetic interaction between *ckb1-Δ* and alleles of *cdc2*
 Given the reduction in cell length observed for the *nat^R-ypa2-S2 ckb1-Δ* mutant, we investigated whether a negative genetic interaction occurs between *ckb1-Δ* and mutants that alter mitotic commitment. The double mutant *ckb1-Δ cdc2-1w*, could not be recovered and generated microcolonies of short cells (data not shown). *ckb1-Δ cdc2-3w* was picked and cell growth assays showed that there is a reduction in colony size at $\geq 32^\circ\text{C}$. At 25°C and 29°C the colony size is similar to that of *ckb1-Δ*, while at 19°C there is residual growth of the double mutant (Fig. 3:27). The phenotype of *ckb1-Δ cdc2-3w* was similar to that of *cdc2-3w*, which has a reduced cell length (Fantes, 1981).

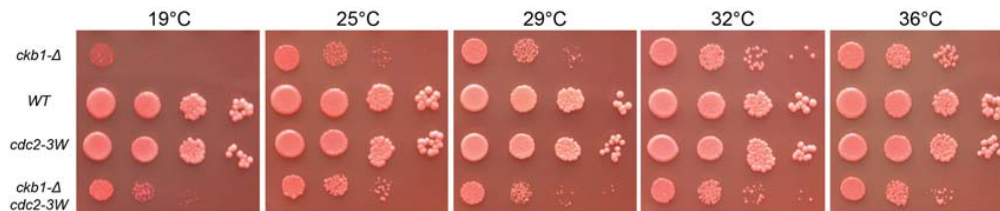


Fig. 3:27 Cell growth assays showing the genetic interaction between *ckb1-Δ* and *cdc2-3W*. The cell growth assays were performed as described in section 2.2.2. The colony size of *cdc2-3W ckb1-Δ* was reduced as compared to *ckb1-Δ* $\geq 32^\circ\text{C}$. Similar colony size was observed for the double mutant and *ckb1-Δ* at 25°C and 29°C. *ckb1-Δ* does not grow at 19°C; although colony formation is impaired, the double mutant undergoes residual division.

3.7.5.6 The genetic interaction between *ckb1-Δ* and SIN mutants
 Since there was a genetic interaction between *ckb1-Δ* and PP2A we investigated whether there were interactions between SIN mutants and *ckb1-Δ*. To test this we crossed SIN mutants into the *ckb1-Δ* background. The crosses were dissected at 25°C, which is the lowest permissive temperature of *ckb1-Δ* (Fig. 3: 17 and Fig. 3:25, Fig. 3:27 and Fig. 3:28), because the SIN alleles are hs (Fig. 3:1 and Fig. 3:28). The double mutants *ckb1-Δ sid2-250*, *ckb1-Δ sid4-SA1* and *ckb1-Δ cdc11-136* were picked, while *ckb1-Δ cdc7-24* and *ckb1Δ cdc14-118* generated microcolonies and could not be propagated (data not shown). At $\geq 29^\circ\text{C}$, *ckb1-Δ sid4-SA1* did not form colonies, similar to *sid4-SA1*. The phenotypes of the two strains differed at 36°C; while *sid4-SA1* lysed with a SIN phenotype, the double mutant cells comprised of very elongated and “branched” or “swollen” cells. A similar phenotype was observed at 36°C for *ckb1-Δ cdc11-136* and *ckb1-Δ cdc7-24* and for *ckb1-Δ sid2-250* $\geq 29^\circ\text{C}$ (data not shown). Interestingly, although the cell morphology was altered (data not shown), *sid2-250* rescued *ckb1-Δ* at 19°C and enhanced growth at 25°C (Fig. 3:28). With *cdc11-136*, *ckb1-Δ* showed a strong negative genetic interaction at $\geq 25^\circ\text{C}$ and was unable to grow at 19°C.

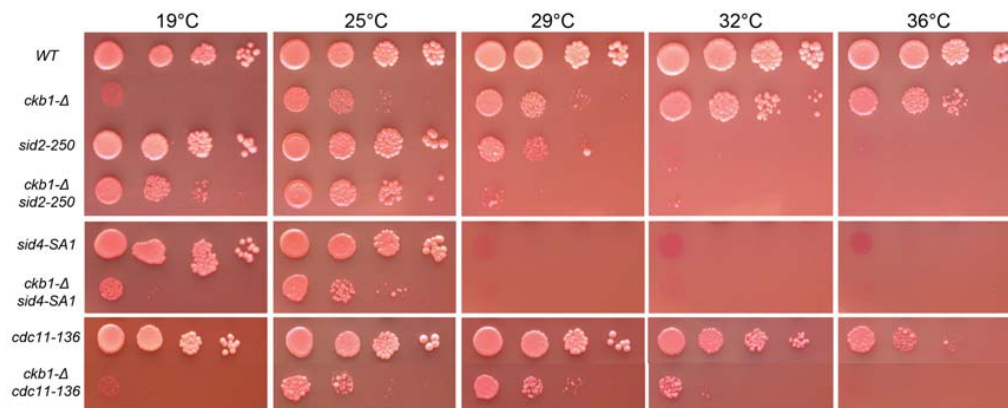


Fig. 3:28 Cell growth assays showing the genetic interaction between *ckb1-Δ* and SIN alleles. The cell growth assays were performed as described in section 2.2.2. Similar to *sid2-250*, the double mutant with *ckb1-Δ* could not grow at $\geq 32^\circ\text{C}$ and its growth was impaired at 29°C ; the inability of *ckb1-Δ* to grow at 19°C was rescued by *sid2-250*. Both *ckb1-Δ sid4-SA1* and *sid4-SA1* were not able to form colonies at $\geq 29^\circ\text{C}$; at 25°C the double mutant colonies have a better fitness than *ckb1-Δ*, whereas at 19°C the growth of the double mutant is impaired. The double mutant *ckb1-Δ cdc11-136* decreases the restrictive temperature of *cdc11-136* to 32°C , is sick at 25°C and unable to grow at 19°C .

4 Discussion

4.1 What are the characteristics of the *nat^R-ypa2-S2* allele?

It was previously shown that loss-of-function alleles of PP2A and PTPA rescue SIN mutants that cannot undergo cytokinesis and that null alleles of the major subunit of PTPA and of the catalytic subunit of PP2A become synthetic lethal in a mutant background of the mitotic regulator Wee1p. Ypa2p, the major subunit of PTPA (Goyal and Simanis, 2012), is also implicated in the establishment of cell polarity and cell growth (Bernal et al., 2012; Goyal and Simanis, 2012). Here we characterized the allele *ypa2-S2* and its genetically tagged version (*nat^R-ypa2-S2*), which rescues SIN mutants (see section 3.1) but has less effect upon mitotic control (see section 3.6.1) and in the establishment of cell polarity (see section 3.6.2). The hypomorphic character of *nat^R-ypa2-S2* was suggested by lethal interaction with the deletion mutant of the minor subunit of PTPA (see section 3.6.3), since previous studies have shown that fission yeast cannot tolerate the lack of both PTPA proteins (Bernal et al., 2012; Goyal and Simanis, 2012). We found that *nat^R-ypa2-S2* is dominant with respect to the rescue of SIN mutations (see section 3.3), which indicates reduced activity towards the SIN. Such an effect could result if Ypa2p-S2 would bind PP2A (or another phosphatase) but would not lead to phosphatase activation; thus, in *nat^R-ypa2-S2* the effective phosphatase concentration could be reduced or the phosphatase(s) would be titrated away.

Ypa2p is essential at 19°C (Bernal et al., 2012; Goyal and Simanis, 2012), thus the ability of *nat^R-ypa2-S2* to grow at this temperature (see section 3:1) allowed us to get more insight into the functions of Ypa2p. We identified a synthetic lethal interaction with the null mutant of the major catalytic subunit of PP2A, and demonstrated the rescue of the SIN mutant *etd1-Δ*, at 19°C (see section 3:1). The biochemical function of Etd1p is unknown, therefore one can not say with precision why *nat^R-ypa2-S2* rescues *etd1-Δ* but it is noteworthy that the loss-of-function allele of the B regulatory subunit of PP2A, *pab1-4*, rescues *etd1-Δ* (Lahoz et al., 2010).

The findings summarized above indicate that *nat^R-ypa2-S2* is a separation-of-function allele, with greater defects in the regulation of cytokinesis.

4.2 SGA, to identify non-essential genes that show a negative genetic interaction with *nat^R-ypa2-S2*

4.2.1 Concept of the SGA

The mutant *nat^R-ypa2-S2* was used in a SGA with the non-essential, whole genome deletion library, from which we identified synthetic sick and lethal interactions. However, we failed to identify a weak negative interaction that we would have expected (see section 3.6.3); this suggests that the protocol that we used may have missed some weaker interactions. To uncover such interactions a second, lower dilution should be spotted in future screens. The screen was done at low and high temperature, with the idea of identifying networks that could contribute to the requirement for *ypa2* at low temperature. Consistent with this, a higher number of hits were identified at 19°C than at 29°C (see section 3.7.2).

The accepted logic underlying SGA screens suggests that the hits are genes which compensate for reduction in the function of Ypa2p in *nat^R-ypa2-S2*; they may be regulated by *ypa2*, or one of its targets, or be regulators of *ypa2* (future studies would have to address whether the *ypa2-S2* mutation affects the steady state level of Ypa2p).

4.2.2 Analysis of the hits

4.2.2.1 What are the BPs in which the hits identified in the SGA cluster? How do these compare to data obtained in other studies?

Two hundred and twelve hits were identified, of which roughly 90% are novel interactors of *ypa2* (see section 3.7.2). The clustering of the hits into several BPs (see section 3.7.2) is consistent with the involvement of PTPA in the regulation of multiple processes (Bernal et al., 2012; Goyal and Simanis, 2012; Wood et al., 2012).

A mass spectrometry study that cross-correlated physical interactors of the PP2A scaffold Paa1p with proteins that change their phosphorylation status between *WT* and the mutants *ypa2-Δ* and *pab1-4*, found hits that are classified in similar BPs (Bernal et al., 2014). Among the enriched annotations were “regulation of mitotic cycle”, “cellular aminoacid metabolic process”, and “ribosome biogenesis” (Bernal et al., 2014), which are also enriched among the hits of the SGA described in this study (see section 3.7.2). BPs such as “nucleobase-containing small molecule metabolic process”, “carbohydrate metabolic process”, “generation of precursor metabolites and energy” and “cofactor metabolic process” are enriched in the (Bernal et al., 2014) study but not in our screen; this could be due to the fact that although it is a hypomorphic allele (see sections 3.1 and 3.2), *ypa2-S2* does not phenocopy *ypa2-Δ* (see sections 3.1, 3.6.1 and 3.6.2) and to differences that arise from the screening method. Although hypomorphic, Ypa2p-S2 could lead to the activation of a certain level of PP2A complexes, which would be enough to satisfy its function in some biological processes but not others. This could explain also the fact that *ypa2-S2* is mainly altered in the regulation of cytokinesis signaling (see sections 3.1, 3.3, 3.4, 3.6.5) and to a reduced extent in the control of other processes (see sections 3.6.1 and 3.6.2).

Apart from the composite ATPase activity shown by PTPA and PP2A catalytic subunit (Chao et al., 2006), the peptidyl cis-trans isomerase activity of PTPA towards Pro 190 of the PP2A catalytic subunit also leads to the activation of PP2A (Jordens et al., 2006). However, it is not known whether other substrates are targeted by the isomerase activity of PTPA (*ypa1/ypa2*). Mass spectrometry analysis of affinity purified *WT* and isomerase-dead *ypa2* should indicate these substrates, among which is expected to find the PP2A catalytic subunit. Whether some of the hits generated in the SGA presented here were generated by reduced isomerase activity in *ypa2-S2* is not clear at the moment, however future analysis will reveal if this is the case.

Given that the non-essential genome-wide deletion library was used for screening of mutants sensitive to chemical agents that target different pathways (Deshpande et al., 2009; Kennedy et al., 2008; Kim et al., 2016; Lee et al., 2012b; Ma et al., 2011; Mojardin et al., 2015; Pan et al., 2012; Rallis et al., 2014; Tay et al., 2013; Zhou et al.,

2013), bioinformatic analysis that compares hits obtained in these studies with the interactors of *ypa2-S2* could identify the links in pathways controlled by this gene. For example, considering that *ypa2-Δ* is sensitive to FK-506 (see section 3.7.2), cross-correlation between the hits obtained in our SGA and those identified in a screen for deletion mutants that are hypersensitive to this drug (Ma et al., 2011) could point out which protein(s) are the targets of PP2A and PP2B; it is possible that among the common hits will be genes involved in membrane trafficking, since both screens generated such hits.

Regarding the biases of the screening method, a SGA can identify both direct and indirect interactors of the favorite gene, while phosphoproteome analysis has limitations related to the degradation of phosphorylated proteins or related to the extraction method. Therefore, cross-correlation studies between genetic and mass spectrometry analyses should give an integrated view on the interactors of the gene studied.

4.2.2.2 What can be learnt about *ypa2*, from the FYPO analysis of the hits?

Among the enriched FYPOs of the hits was sensitivity to FK-506 and subsequent testing showed that *ypa2-Δ* is sensitive to this drug (see section 3.7.2), which indicates cross-talk between PP2A/PTPA and PP2B.

Although not tested here, hypotheses can be drawn on other enriched FYPOs (see section 3.7.2). Null mutants which render fission yeast sensitive to caffeine are involved in stress signaling, chromatin remodeling and cell morphology; *ypa2-Δ* is sensitive to caffeine (Calvo et al., 2009) and the BPs and FYPOs of the hits from our screen indicate that Ypa2p is involved in these processes. Of these processes, the best described is the involvement of Ypa2p in the control of cell morphology (Bernal et al., 2012).

A target of caffeine in fission yeast is the DNA repair pathway that operates in S and G2, upon damage or incomplete DNA replication (Osman and McCready, 1998). The phosphorylation status of the DNA damage responsive protein Chk1p is regulated by PP2A in HeLa cells (Leung-Pineda et al., 2006); although Chk1p was not described as a PP2A substrate in fission yeast, the PP2A activator Dis2p (Grallert et al., 2015) affects the phosphorylation status of Chk1p (den Elzen and O'Connell, 2004). Potassium chloride affects the membrane potential and high concentrations of potassium chloride renders fission yeast resistant to drugs (Alao et al., 2015). Three of the four hits that belong in the FYPO of mutants sensitive to potassium chloride (Table 3:4) are involved in chromatin remodeling (Table 3:3).

Transcriptional regulation was reported for cells grown in the presence of potassium chloride (Johnsson et al., 2006), therefore this FYPO might reflect the role of PTPA in the regulation of transcription. Calcofluor white compromises the cell wall of fungal cells, by binding β-linked polymers (Kingsbury et al., 2012). No alleles of PTPA were reported to be sensitive to calcofluor white in fission yeast to date; future studies will examine this point.

Although we discussed enriched FYPOs of certain statistical values (see section 2.4.3.2), the limits can be set lower, as indicated by the FYPO “sensitive to thiabendazole”. In section 3.5 we describe that PTPA alleles are sensitive to TBZ and this FYPO has values under the thresholds discussed (see section 2.4.3.2 and Table 3:4). A similar case is that of the FYPO that comprises hits sensitive to the cytotoxic compound 5-FU; 5-FU causes G1/S arrest and deletion mutants with chromosome segregation defects are sensitive to this drug (Mojardin et al., 2015). Consistent with the idea that *ypa2* mutants might be sensitive to this drug is the fact that *ypa2-Δ* showed a nine fold increase over *WT*, in chromosome loss assays performed at 29°C (Prof. Viesturs Simanis; unpublished data; personal communication). Therefore, further analysis of the FYPOs of the hits generated in the SGA will provide information on the functions of *ypa2*.

4.2.3 The validation of hits from the SGA

Although the number of hits that belonged to each BP was increased at low temperature, the hits from 29°C clustered to the same annotations (see section 3.7.2). In the time available we focused on the hits obtained at 29°C; validation experiments revealed that over 80% of the interactions can be reconstructed (see section 3.7.2).

Ypa2p was shown to regulate the protein levels and activity of the GTPase Cdc42p (Bernal et al., 2012), which is involved in the control of polarized growth. This process requires the tethering of secretory vesicles to the cell tips where growth occurs and Cdc42p controls the formation of growth zones (Bendezu and Martin, 2011; Estravis et al., 2011; Miller and Johnson, 1994; Pruyne et al., 2004). The hits identified in the SGA with *nat^R-ypa2-S2*, which are involved in vesicular transport, are *pfa3*, *erp5/6* and *apm1* (section 3.7.3). While *pfa3* was not described in fission yeast, some reports indicate the involvement of the other two in cytokinesis. The morphological defects of the deletion mutant implicates Apm1p in several processes: vacuole fusion, cytokinesis and cell integrity (Kita et al., 2004). Although disruption of *gef3*, which is an activator of Rho3p, has cell separation defects by itself, when in the *apm1-Δ* background these become additive and the cell viability decreases (Munoz et al., 2014). Also, *apm1-Δ* is synthetic lethal in the background of disrupted PP2B and is sensitive to FK-506. *erp5/6* is required for the forespore formation in *S. pombe* meiosis (Ucisik-Akkaya et al., 2014), a process in which SIN signaling is essential (Krapp et al., 2006; Krapp and Simanis, 2014). It is noteworthy that the meiotic Sid2p homolog, Slk1p is involved in forespore membrane formation and one of the mechanisms by which this works could be vesicle trafficking at the forespore membrane (Perez-Hidalgo et al., 2008); vesicles trafficking from the sites of polarized growth to the cell division site in mitosis was previously found to require the SIN (Gachet and Hyams, 2005). Whether Ypa2p is required to regulate the transport of endocytic vesicles at the site of forespore membrane assembly and at the cell division site remains to be tested.

PP2A was shown to regulate the assembly of ribosomal complexes in *S. cerevisiae* (van Zyl et al., 1992), however such a function was not documented for PP2A in fission yeast. In *S. pombe* *rpl15-Δ* was identified in a screen looking for deletion mutants sensitive to the beta-1,3-glucan synthase, micafungin. Interestingly, this

mutant was not further sensitive to β -glucanase, a hydrolyze that degrades the division septum (Baladron et al., 2002; Martin-Cuadrado et al., 2003). *rpl15*- Δ one of the hits identified in the SGA (section 3.7.3) and it would be interesting to understand whether the other four ribosomal proteins (some of which predicted) identified in the SGA are required for cell separation and whether ribosomal biogenesis is regulated by or regulates PTPA/PP2A.

The interaction of *nat^R-ypa2-S2* with the transmembrane transporters Fio1p and Eca39p (section 3.7.3), which are required for iron and branched chain aminoacid transport respectively could be the effect of TOR signaling inactivation. Starvation of yeast cells for nitrogen and of mammalian cells for branched chain aminoacids inhibits TOR signaling (De Virgilio and Loewith, 2006; Petersen and Nurse, 2007). Also, in human cells grown in media depleted for iron TORC1 signaling is suppressed, which is mediated by PP2A (Watson et al., 2016). Active TOR signaling was shown to promote PP2A activity and thus, inhibit mitotic entry in fission yeast (Chica et al., 2016). If lack of branched chain aa would inactivate TOR and promote PP2A activity, the negative interaction between *eca39* and *nat^R-ypa2-S2* could be due to a reduction in the levels of active PP2A in the cell. Conversely, if PP2A would turn off TOR signaling in response to lack of iron, the synthetic sick interaction between *nat^R-ypa2-S2* and *fio1* could be due to inefficient activation of PP2A in the *nat^R-ypa2-S2* background, which would fail to inactivate TOR. It is not known what biological process *kgd2* is involved in, however it is a predicted dihydrolipoamide S-succinyltransferase, which might be involved in the metabolism of cellular aminoacids. Therefore, future studies should shed light on the interaction between *kgd2* and *ypa2*.

It remains to be verified which genes are deleted in the strains provided in the library as *lsm1*- Δ and *ipk1*- Δ , because a synthetic sick interaction between these mutants and *nat^R-ypa2-S2* was validated (section 3.7.3). It is also important to investigate whether chromatin remodeling regulates expression of PP2A/PTPA genes or vice-versa; this question is prompted by the synthetic negative interaction found between the SWI/SNF chromatin remodeling complex protein Arp42p and *nat^R-ypa2-S2*, but also by the negative genetic interaction found between *par1*- Δ and *arp42*- Δ (Ryan et al., 2012).

Given the greater detail to which they were characterized, the hits Flp1p and Ckb1p are discussed below. In summary, the genes that were validated encode proteins that are involved in chromatin remodeling, RNA processing, assembly of ribosomal complexes, respiration, aa and iron transport, vesicular transport, signal transduction and protein dephosphorylation (see section 3.7.2).

4.2.4 Characterization of the genetic interactions between Flp1p and PP2A/PTPA

4.2.4.1 What could generate the cell separation defect identified in *nat^R-ypa2-S2 flp1*- Δ ?

The synthetic sick interaction between *nat^R-ypa2-S2* and *flp1*- Δ is due at least in part, to inefficient cell separation (see section 3.7.5.4). At 19°C, cell separation defects were also reported for *ypa2*- Δ (Goyal and Simanis, 2012); similarly, mutants of the

exocyst (Wang et al., 2002), the transcription factor *sep1* (Ribar et al., 1997; Yoshida et al., 1994), the glucanase pathway (Dekker et al., 2004), PP2B (*ppb1*) (Yoshida et al., 1994), the MAPK *pmk1* (Toda et al., 1996) and of the MAPK phosphatase *pmp1* (Sugiura et al., 1998) have cell separation defects.

The experiments presented here reveal that *ypa2-Δ* is sensitive to FK-506 (see section 3.7.2) and indicate an interaction between PP2A/PTPA and PP2B. Interestingly, previous screens looked for the deletion library mutants that are sensitive to FK-506 and identified *flp1-Δ* and *par1-Δ* but not *ypa2-Δ*. It is not specified which version of the non-essential deletion library was used in the study of (Ma et al., 2011), but the reason for which *ypa2-Δ* was not among their hits could be that the mutant was not provided in the library or that it was not correctly deleted. The relationship between Flp1p, PP2A/PTPA and PP2B will be addressed.

In *X. laevis* it was previously shown that OE of Cdc14p (homolog of Flp1p) prevents the recruitment of the exocyst to the site of cell separation and thus, hampers cell division (Krasinska et al., 2007). Whether Flp1p and PP2A/PTPA cooperate in trafficking of vesicles to the site of cell division remains to be tested. Also, whether Flp1p and PP2A/PTPA interact with *sep1*, glucanases and the MAPK pathway will be assayed.

4.2.4.2 What could be the nature of the genetic interaction between Flp1p and PP2A/PTPA mutants?

We uncovered genetic interactions which indicate that Flp1p contributes, with different subunits of PP2A/PTPA, in the regulation of several processes (Fig. 4:1).

Flp1p and Ypa2p contribute to efficient cell separation (see section 3.7.4.1 and 4.2.4.1), while preliminary analysis shows that Flp1p and the minor regulatory subunit of PTPA (Ypa1p) regulate mitotic commitment and cell polarity (see section 3.7.4.2.).

Whether the interaction between the null alleles of PTPA and *flp1-Δ* results from deregulation of the PP2A holoenzymes formed in one or the other PTPA mutant is not clear. Although no phosphorylated sites were detected for Ypa1p, we found that Ypa2p is phosphorylated on Ser 254 and Ser 337 (data not shown). It would be interesting to see if in the absence of one PTPA protein the steady state of the other changes and whether Ypa1p and Ypa2p are regulated by Flp1p-mediated dephosphorylation.

We found that Flp1p and the PP2A activator Dis2p (Grallert et al., 2015) are involved in the control of cytokinesis, at low temperature (section 3.7.4.1). Dis2p is inhibited by phosphorylation on Thr 316, which is catalyzed by CDK1 (Grallert et al., 2015). Although previous studies have shown that Dis2p can autoreactivate in mitosis (Wu et al., 2009), Flp1p could contribute to this process. It would be interesting to examine the kinetics of Dis2p activation in *flp1-Δ*. Flp1p is also phosphorylated (Broadus and Gould, 2012; Chen et al., 2008; Koch et al., 2011) and auto-catalytic activity has been reported (Wolfe et al., 2006); however, contribution of Dis2p in Flp1p dephosphorylation may occur.

Consistent with their involvement in mitotic control, there was an additive phenotypic defect in mitotic commitment, between *flp1-Δ* and the null mutant of the major catalytic subunit of PP2A, *ppa2* (see section 3.7.4.3) (Cueille et al., 2001; Kinoshita et al., 1990; Kinoshita et al., 1993). Preliminary results in the *flp1-Δ* background also revealed a potential role of the minor catalytic subunit of PP2A (Ppa1p) in mitotic control, at 19°C (see section 3.7.4.3), although this is also inferred from the slight reduction in cell length of *ppa1-Δ* (Chica et al., 2016). The genetic interaction between Flp1p and the PP2A catalytic subunits could result from deregulated PTPA, in the *flp1-Δ* background.

The double mutant *flp1-Δ pab1-Δ* is not viable; such a phenotype could arise if Flp1p were redundant to PP2A-Pab1p or because Flp1p is required to activate another phosphatase. It would be interesting to see whether *pab1-Δ dis2-Δ* is also lethal.

A strong negative genetic interaction was found between *flp1-Δ* and *par1-Δ* (see section 3.7.4.3); at the permissive temperature and the prevalent phenotype was misoriented division septum, while at the restrictive temperature there were additional cell separation defects: cells with several nuclei and one septum or cells with a SIN phenotype. (see section 3.7.4.3). The misplaced division septum reminds of the *pom1-Δ* phenotype of (Bahler and Pringle, 1998); whether a change in the phosphorylation status of Pom1p generates a misplaced division septum in *flp1-Δ par1-Δ* will be tested. The cells with several nuclei and one septum and the cells with a SIN phenotype observed in *flp1-Δ par1-Δ* indicate that the two genes promote septation. Whether Flp1p and PP2A- Par1p activate each other or they promote in parallel septum formation has to be tested.

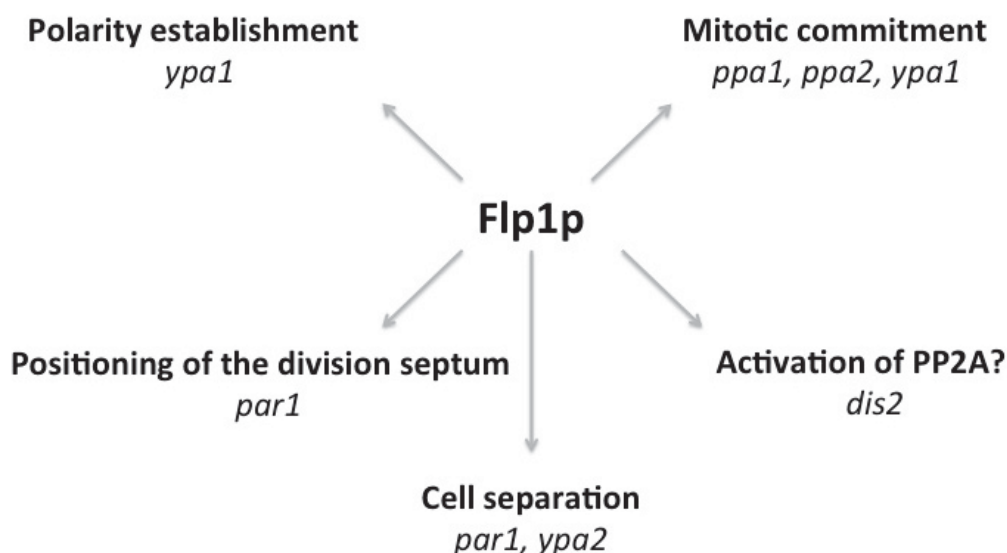


Fig. 4:1 Summary of the interaction between Flp1p and PP2A/PTPA. Flp1p contributes in polarity establishment, mitotic commitment, positioning of the division septum, cell separation and potentially in the activation of PP2A, together with the genes mentioned below each process.

4.2.5 Characterization of the genetic interaction between Ckb1p and PP2A/PTPA

4.2.5.1 Ckb1p: a link between cell growth, mitotic commitment and SIN signaling?

We uncovered a link between Ckb1p and mitotic control, SIN signaling and PP2A/PTPA. It is possible that Ckb1p is involved in mitotic control, because the double mutant *ckb1-Δ cdc2-1w* was synthetic lethal (see section 3.7.5.5), therefore, future studies are required to understand the relationship between Ckb1p and genes involved in mitotic control. Given that Ckb1p encodes for a regulatory subunit of CK II one possibility would be phosphorylation and activation of Wee1p, by CK II. Wee1p was previously shown to be activated and stabilized by phosphorylation, in response to DNA damage (Raleigh and O'Connell, 2000). If Ckb1p regulates Wee1p it remains to be determined what is the regulatory input to which CK II responds. Given that all three subunits of this kinase (Cka1p, Ckb1p, Ckb2p) were shown to interact with the MOR protein Nak1p (Cipak et al., 2013) and because of the involvement of Cka1p in polarized growth (Snell and Nurse, 1994), one possibility is that CK II contributes to signaling the "growth status" to the cell size control. Consistent with such a model, Cka1p localizes at the cell tips and cell division site. Also, Cka1p localizes in the nucleolus and at the SPBs throughout the cell cycle (Cipak et al., 2013), which could explain the feedback to the SIN.

4.2.5.2 Does Ckb1p promote SIN signaling? Is there feedback signaling from the SIN to Ckb1p? Ckb1p as a potential link between the SIN and PP2B

The fact that double mutants of *ckb1-Δ* with SIN alleles were very sick (see section 3.7.5.6) could indicate that Ckb1p is required to promote SIN signaling.

Phosphorylation was reported for the SIN proteins Cdc11p (Carpy et al., 2014; Chen et al., 2013; Feoktistova et al., 2012; Koch et al., 2011; Krapp et al., 2003), Cdc7p (Beltrao et al., 2009; Koch et al., 2011), Sid2p (Beltrao et al., 2009; Carpy et al., 2014; Hou et al., 2004; Koch et al., 2011) and Etd1p (Koch et al., 2011), although the importance of phosphorylation to SIN signaling was only reported for Cdc11p (Krapp et al., 2003) and Sid2p (Hou et al., 2004). CK II could phosphorylate Cdc11p, which would allow recruitment of SIN components to the SPB, or would activate Sid2p. This view is supported by the strong negative genetic between *ckb1-Δ* and *cdc11-136* and *sid2-250* (see section 3.7.5.6). SIN regulation by CK II would occur downstream of Sid4p, because the double mutant *ckb1-Δ sid4-SA1* has a growth pattern similar to the SIN mutant (see section 3.7.5.6). Although a heat-sensitive mutant, the allele *sid2-250* is also defective at the permissive temperature (Mishra et al., 2004); the fact that *sid2-250* rescues the lethality of *ckb1-Δ* at low temperature indicates that Sid2p/Mob1p could feedback to CK II. In this context, it is noteworthy that phosphorylation was detected on the catalytic subunit of CK II, Cka1p (Cipak et al., 2013). Whether there is feedback regulation between the SIN and CK II will be analyzed by combining localization studies of the relevant SIN proteins in CK II mutant backgrounds, and the reverse, and by mass spectrometry and mutational analysis.

Interestingly, the morphology of the double mutants between *ckb1-Δ* and SIN alleles was different than that of the SIN mutants, because the cells were elongated and

branched (see section 3.7.5.6). At the permissive temperature the *ckb1-Δ* mutant has also some multicompartmented cells (Roussou and Draetta, 1994), which indicates failure in cell separation (see section 3.7.5.1 and 3.7.5.4). It is noteworthy that disruption of PP2B also leads to the generation of multicompartmented and branched cells (Yoshida et al., 1994). Consistent with the view that CK II might be involved in cell separation is also the finding that *ckb1-Δ* is sensitive to micafungin (Ma et al., 2011). A link between SIN signaling and PP2B was previously suggested (Lu et al., 2002) and whether CK II functions between the SIN and PP2B will be investigated.

4.2.5.3 Ckb1p interacts with PP2A activators and with the major catalytic and regulatory subunits of PP2A

The strong synthetic negative interaction between *ckb1-Δ* and *dis2-Δ*, *ypa2-Δ*, *ppa2-Δ* and *par1-Δ* (see section 3.7.5.1, section 3.7.5.3 and section 3.7.5.4) indicates that CK II could act in the activation of PP2A holoenzymes Paa1p-Ppa2p-Par1p or the reverse; alternatively, CK II and PP2A could target common substrates. It is currently unclear whether CK II is regulated by phosphorylation in *S. pombe* and whether PP2A would influence this process, however regulation of PP2A activators and subunits in response to phosphorylation is emerging, to which CK II could contribute. Interestingly, regulation of CK II by phosphorylation and by the activity of the Pin1p isomerase was reported in other systems (Tarrant et al., 2012).

The biochemical mechanism by which Ypa2p activates PP2A was not elucidated in fission yeast. As discussed in section 4.2.4.2, phosphorylation might represent a way to regulate PTPA; if this will turn out to be the case, whether CK II contributes in this regulation will be investigated. Phosphorylation of a CDK1-targeted site on Dis2p was found to have implications in its activation (Grallert et al., 2015). If CK II were to phosphorylate Dis2p, the effect would be to halt septation, because among the cell separation defects of *ckb1-Δ dis2-Δ* has, more than one septum or septum material deposited at other sites than the cell center.

In mammals, phosphorylation of the PP2A catalytic subunit on Tyr 307 inhibits formation of heterotrimeric PP2A complexes, while phosphorylation on Thr 304 promotes it (Longin et al., 2007). No phosphorylation sites have yet been mapped on the three fission yeast catalytic subunits and Ppa2p has no predicted CK II phosphorylation sites (data not shown) (Dinkel et al., 2016); if conserved in *S. pombe*, phosphorylation of the PP2A catalytic subunit on Thr 304 and Tyr 307 could be targeted by CK II, and by a Tyr kinase, given that CK II is a Ser/Thr kinase (Roussou and Draetta, 1994).

Pab1p was found to be phosphorylated on Ser 134, Ser 136, Ser 139, Thr 146 (Kettenbach et al., 2015; Wilson-Grady et al., 2008); the effects of phosphorylation on these residues were not characterized and although there are three highly conserved CK II phosphorylation sites on Pab1p, they do not map any of these residues (data not shown) (Dinkel et al., 2016). The mutant *ckb1-Δ pab1-Δ* has a phenotype similar to *pab1-Δ* and, in contrast to *ckb1-Δ*, is able to grow at 19°C. This indicates that Pab1p is a potential inhibitor of the second regulatory subunit of CK II, Ckb2p or that Ckb1p and Pab1p have a common substrate, which is in an active form by default. Whether Ckb1p is phosphorylated was not reported, however, the catalytic subunit of CK II, Cka1p, is phosphorylated on Thr 4 (Cipak et al., 2013). If

mutagenesis of this residue indicates that it is important for the activity of CK II, PP2A-Pab1p could dephosphorylate it and thus, inactivate CK II. This hypothesis would only fit with the negative interaction between *ckb1-Δ* and *dis2-Δ*, *ypa2-Δ*, *ppa2-Δ* and *par1-Δ* if the latter four genes modulate/balance the activity of of PP2A-Pab1p.

Although dephosphorylation of Ser 378 of Par1p was shown to be important for PP2A-Par1p activation, other phosphorylation sites were mapped: Ser 26, Ser 29, Ser 93, Ser 94, Tyr 96, Ser 99, Ser 109, Ser 542, Ser 545 (Beltrao et al., 2009; Carpy et al., 2014; Kettenbach et al., 2015; Koch et al., 2011; Wilson-Grady et al., 2008). However, none of these sites map within a predicted CK II phosphorylation site (data not shown) (Dinkel et al., 2016). To better understand the regulation between CK II and PP2A/PTPA, biochemical studies are required, such as the quantification of Pab1p protein levels in *par1-Δ* and the reverse, but also mutagenesis of the phosphorylation sites of Cka1p, Pab1p and Par1p.

4.2.6 Concluding remarks

This study uncovered what could represent an extended phosphatase relay to that described by (Grallert et al., 2015), implicated in the control of mitotic commitment and cytokinesis, where Flp1p is a potential activator of PP2A or could function as a redundant phosphatase to the latter. Moreover, we have connected CK II genetically to PP2A/PTPA and Flp1p; CK II is implicated in mitotic control cell separation, polar growth and could add to coordination of cell growth with mitotic commitment.

4.2.7 Future directions

More information should be extracted from the FYPO analysis of the hits generated in the SGA (see section 4.2.2.2), which will allow a better understanding of Ypa2p functions. Also, biochemical analysis of the PTPA activity towards PP2A regulation is needed. Whether the isomerase function of PTPA regulates other substrates than PP2A, should also be addressed; such a question can be answered by analysis of physical interactors between *WT* and an isomerase-dead mutant of *ypa2*.

Bioinformatic analysis between our hits and those obtained by (Ryan et al., 2012), in where *ypa1-Δ* was used as bait against the deletion library, will hint common and different pathways in which *ypa1* and *ypa2* function.

To understand if the catalytic activity of Flp1p is required for the genetic interactions described here, the double mutants will be reconstructed with a Flp1p allele which catalytically inactive (Wolfe et al., 2006). If the phosphatase activity of Flp1p is important for these interactions, it should be verified whether similar to Dis2p, Flp1p could contribute in the activation of PP2A complexes, by dephosphorylating specific residues of the PP2A regulatory subunits. An important question however, remains the stoichiometry of PP2A subunits, in null alleles of the PP2A B and B' subunits and will be solved by mass spectrometry.

Phosphomapping of the CK II subunits and mutational analysis will indicate how CK II activity is regulated. The interaction between CK II and the SIN will be followed initially by localization studies of CK II subunits in SIN alleles and the reverse. The link between Flp1p and CK II should also be identified, because *ckb1-Δ flp1-Δ* is lethal. Whether PP2A is a common target of Ckb1p and Flp1p remains to be solved.

5 References

- Agarwal, M.L., Taylor, W.R., Chernov, M.V., Chernova, O.B., and Stark, G.R. (1998). The p53 network. *The Journal of biological chemistry* 273, 1-4.
- al-Khodairy, F., Enoch, T., Hagan, I.M., and Carr, A.M. (1995). The *Schizosaccharomyces pombe* hus5 gene encodes a ubiquitin conjugating enzyme required for normal mitosis. *Journal of cell science* 108 (Pt 2), 475-486.
- Alao, J.P., Weber, A.M., Shabro, A., and Sunnerhagen, P. (2015). Suppression of sensitivity to drugs and antibiotics by high external cation concentrations in fission yeast. *PloS one* 10, e0119297.
- Alcaide-Gavilan, M., Lahoz, A., Daga, R.R., and Jimenez, J. (2014). Feedback regulation of SIN by Etd1 and Rho1 in fission yeast. *Genetics* 196, 455-470.
- Alexandru, G., Zachariae, W., Schleiffer, A., and Nasmyth, K. (1999). Sister chromatid separation and chromosome re-duplication are regulated by different mechanisms in response to spindle damage. *The EMBO journal* 18, 2707-2721.
- Almonacid, M., Celton-Morizur, S., Jakubowski, J.L., Dingli, F., Loew, D., Mayeux, A., Chen, J.S., Gould, K.L., Clifford, D.M., and Paoletti, A. (2011). Temporal control of contractile ring assembly by Plo1 regulation of myosin II recruitment by Mid1/anillin. *Current biology : CB* 21, 473-479.
- Almonacid, M., Moseley, J.B., Janvore, J., Mayeux, A., Fraissier, V., Nurse, P., and Paoletti, A. (2009). Spatial control of cytokinesis by Cdr2 kinase and Mid1/anillin nuclear export. *Current biology : CB* 19, 961-966.
- Alonso-Nunez, M.L., An, H., Martin-Cuadrado, A.B., Mehta, S., Petit, C., Sipiczki, M., del Rey, F., Gould, K.L., and de Aldana, C.R. (2005). Ace2p controls the expression of genes required for cell separation in *Schizosaccharomyces pombe*. *Molecular biology of the cell* 16, 2003-2017.
- Alvarez-Tabares, I., Grallert, A., Ortiz, J.M., and Hagan, I.M. (2007). *Schizosaccharomyces pombe* protein phosphatase 1 in mitosis, endocytosis and a partnership with Wsh3/Tea4 to control polarised growth. *Journal of cell science* 120, 3589-3601.
- Arai, R., and Mabuchi, I. (2002). F-actin ring formation and the role of F-actin cables in the fission yeast *Schizosaccharomyces pombe*. *Journal of cell science* 115, 887-898.
- Arellano, M., Duran, A., and Perez, P. (1996). Rho 1 GTPase activates the (1-3)beta-D-glucan synthase and is involved in *Schizosaccharomyces pombe* morphogenesis. *The EMBO journal* 15, 4584-4591.
- Askwith, C., and Kaplan, J. (1997). An oxidase-permease-based iron transport system in *Schizosaccharomyces pombe* and its expression in *Saccharomyces cerevisiae*. *The Journal of biological chemistry* 272, 401-405.
- Bahler, J. (2005). A transcriptional pathway for cell separation in fission yeast. *Cell cycle (Georgetown, Tex)* 4, 39-41.
- Bahler, J., and Pringle, J.R. (1998). Pom1p, a fission yeast protein kinase that provides positional information for both polarized growth and cytokinesis. *Genes & development* 12, 1356-1370.
- Bahler, J., Steever, A.B., Wheatley, S., Wang, Y., Pringle, J.R., Gould, K.L., and McCollum, D. (1998a). Role of polo kinase and Mid1p in determining the site of cell division in fission yeast. *The Journal of cell biology* 143, 1603-1616.
- Bahler, J., Wu, J.Q., Longtine, M.S., Shah, N.G., McKenzie, A., 3rd, Steever, A.B., Wach, A., Philippsen, P., and Pringle, J.R. (1998b). Heterologous modules for

efficient and versatile PCR-based gene targeting in *Schizosaccharomyces pombe*. *Yeast* (Chichester, England) *14*, 943-951.

Baladron, V., Ufano, S., Duenas, E., Martin-Cuadrado, A.B., del Rey, F., and Vazquez de Aldana, C.R. (2002). Eng1p, an endo-1,3-beta-glucanase localized at the daughter side of the septum, is involved in cell separation in *Saccharomyces cerevisiae*. *Eukaryotic cell* *1*, 774-786.

Balasubramanian, M.K., McCollum, D., Chang, L., Wong, K.C., Naqvi, N.I., He, X., Sazer, S., and Gould, K.L. (1998). Isolation and characterization of new fission yeast cytokinesis mutants. *Genetics* *149*, 1265-1275.

Bamps, S., Westerling, T., Pihlak, A., Tafforeau, L., Vandenhoute, J., Makela, T.P., and Hermand, D. (2004). Mcs2 and a novel CAK subunit Pmh1 associate with Skp1 in fission yeast. *Biochemical and biophysical research communications* *325*, 1424-1432.

Bardin, A.J., Visintin, R., and Amon, A. (2000). A mechanism for coupling exit from mitosis to partitioning of the nucleus. *Cell* *102*, 21-31.

Barr, F.A., Sillje, H.H., and Nigg, E.A. (2004). Polo-like kinases and the orchestration of cell division. *Nature reviews Molecular cell biology* *5*, 429-440.

Baumer, M., Braus, G.H., and Irniger, S. (2000). Two different modes of cyclin clb2 proteolysis during mitosis in *Saccharomyces cerevisiae*. *FEBS letters* *468*, 142-148.

Beltraminelli, N., Murone, M., and Simanis, V. (1999). The *S. pombe* *zfs1* gene is required to prevent septation if mitotic progression is inhibited. *Journal of cell science* *112 Pt 18*, 3103-3114.

Beltrao, P., Trinidad, J.C., Fiedler, D., Roguev, A., Lim, W.A., Shokat, K.M., Burlingame, A.L., and Krogan, N.J. (2009). Evolution of phosphoregulation: comparison of phosphorylation patterns across yeast species. *PLoS biology* *7*, e1000134.

Bendezu, F.O., and Martin, S.G. (2011). Actin cables and the exocyst form two independent morphogenesis pathways in the fission yeast. *Molecular biology of the cell* *22*, 44-53.

Berlin, A., Paoletti, A., and Chang, F. (2003). Mid2p stabilizes septin rings during cytokinesis in fission yeast. *The Journal of cell biology* *160*, 1083-1092.

Bernal, M., Sanchez-Romero, M.A., Salas-Pino, S., and Daga, R.R. (2012). Regulation of fission yeast morphogenesis by PP2A activator pta2. *PloS one* *7*, e32823.

Bernal, M., Zhurinsky, J., Iglesias-Romero, A.B., Sanchez-Romero, M.A., Flor-Parra, I., Tomas-Gallardo, L., Perez-Pulido, A.J., Jimenez, J., and Daga, R.R. (2014). Proteome-wide search for PP2A substrates in fission yeast. *Proteomics* *14*, 1367-1380.

Bi, E., Maddox, P., Lew, D.J., Salmon, E.D., McMillan, J.N., Yeh, E., and Pringle, J.R. (1998). Involvement of an actomyosin contractile ring in *Saccharomyces cerevisiae* cytokinesis. *The Journal of cell biology* *142*, 1301-1312.

Blanco, M.A., Sanchez-Diaz, A., de Prada, J.M., and Moreno, S. (2000). APC(*ste9/srw1*) promotes degradation of mitotic cyclins in G(1) and is inhibited by *cdc2* phosphorylation. *The EMBO journal* *19*, 3945-3955.

Bloecher, A., Venturi, G.M., and Tatchell, K. (2000). Anaphase spindle position is monitored by the BUB2 checkpoint. *Nature cell biology* *2*, 556-558.

Bloom, J., and Cross, F.R. (2007). Multiple levels of cyclin specificity in cell-cycle control. *Nature reviews Molecular cell biology* *8*, 149-160.

Boehm, M., and Bonifacino, J.S. (2001). Adaptins: the final recount. *Molecular biology of the cell* *12*, 2907-2920.

Bohnert, K.A., Grzegorzewska, A.P., Willet, A.H., Vander Kooi, C.W., Kovar, D.R., and Gould, K.L. (2013). SIN-dependent phosphoinhibition of formin multimerization controls fission yeast cytokinesis. *Genes Dev* *27*, 2164-2177.

Bollen, M., Gerlich, D.W., and Lesage, B. (2009). Mitotic phosphatases: from entry guards to exit guides. *Trends in cell biology* *19*, 531-541.

Booher, R., and Beach, D. (1988). Involvement of *cdc13+* in mitotic control in *Schizosaccharomyces pombe*: possible interaction of the gene product with microtubules. *The EMBO journal* *7*, 2321-2327.

Booher, R., and Beach, D. (1989). Involvement of a type 1 protein phosphatase encoded by *bws1+* in fission yeast mitotic control. *Cell* *57*, 1009-1016.

Booher, R.N., Alfa, C.E., Hyams, J.S., and Beach, D.H. (1989). The fission yeast *cdc2/cdc13/suc1* protein kinase: regulation of catalytic activity and nuclear localization. *Cell* *58*, 485-497.

Boyne, J.R., Yosuf, H.M., Bieganowski, P., Brenner, C., and Price, C. (2000). Yeast myosin light chain, *Mlc1p*, interacts with both IQGAP and class II myosin to effect cytokinesis. *Journal of cell science* *113 Pt 24*, 4533-4543.

Broadus, M.R., and Gould, K.L. (2012). Multiple protein kinases influence the redistribution of fission yeast *Clp1/Cdc14* phosphatase upon genotoxic stress. *Molecular biology of the cell* *23*, 4118-4128.

Buck, V., Russell, P., and Millar, J.B. (1995). Identification of a cdk-activating kinase in fission yeast. *The EMBO journal* *14*, 6173-6183.

Cabib, E. (2004). The septation apparatus, a chitin-requiring machine in budding yeast. *Archives of biochemistry and biophysics* *426*, 201-207.

Cabib, E., Roberts, R., and Bowers, B. (1982). Synthesis of the yeast cell wall and its regulation. *Annual review of biochemistry* *51*, 763-793.

Calonge, T.M., Nakano, K., Arellano, M., Arai, R., Katayama, S., Toda, T., Mabuchi, I., and Perez, P. (2000). *Schizosaccharomyces pombe* rho2p GTPase regulates cell wall alpha-glucan biosynthesis through the protein kinase *pck2p*. *Molecular biology of the cell* *11*, 4393-4401.

Calvo, I.A., Gabrielli, N., Iglesias-Baena, I., Garcia-Santamarina, S., Hoe, K.L., Kim, D.U., Sanso, M., Zuin, A., Perez, P., Ayte, J., *et al.* (2009). Genome-wide screen of genes required for caffeine tolerance in fission yeast. *PloS one* *4*, e6619.

Carmena, M., Wheelock, M., Funabiki, H., and Earnshaw, W.C. (2012). The chromosomal passenger complex (CPC): from easy rider to the godfather of mitosis. *Nature reviews Molecular cell biology* *13*, 789-803.

Carnahan, R.H., and Gould, K.L. (2003). The PCH family protein, *Cdc15p*, recruits two F-actin nucleation pathways to coordinate cytokinetic actin ring formation in *Schizosaccharomyces pombe*. *The Journal of cell biology* *162*, 851-862.

Carpy, A., Krug, K., Graf, S., Koch, A., Popic, S., Hauf, S., and Macek, B. (2014). Absolute proteome and phosphoproteome dynamics during the cell cycle of *Schizosaccharomyces pombe* (Fission Yeast). *Molecular & cellular proteomics : MCP* *13*, 1925-1936.

Carr, C.M., and Rizo, J. (2010). At the junction of SNARE and SM protein function. *Current opinion in cell biology* *22*, 488-495.

Cassimeris, L. (1999). Accessory protein regulation of microtubule dynamics throughout the cell cycle. *Current opinion in cell biology* *11*, 134-141.

Celton-Morizur, S., Racine, V., Sibarita, J.B., and Paoletti, A. (2006). Pom1 kinase links division plane position to cell polarity by regulating Mid1p cortical distribution. *Journal of cell science* *119*, 4710-4718.

Cerutti, L., and Simanis, V. (1999). Asymmetry of the spindle pole bodies and spg1p GAP segregation during mitosis in fission yeast. *Journal of cell science* *112 (Pt 14)*, 2313-2321.

Chang, F., Woollard, A., and Nurse, P. (1996). Isolation and characterization of fission yeast mutants defective in the assembly and placement of the contractile actin ring. *Journal of cell science* *109 (Pt 1)*, 131-142.

Chang, L., and Gould, K.L. (2000). Sid4p is required to localize components of the septation initiation pathway to the spindle pole body in fission yeast. *Proceedings of the National Academy of Sciences of the United States of America* *97*, 5249-5254.

Chang, L., Morrell, J.L., Feoktistova, A., and Gould, K.L. (2001). Study of cyclin proteolysis in anaphase-promoting complex (APC) mutant cells reveals the requirement for APC function in the final steps of the fission yeast septation initiation network. *Molecular and cellular biology* *21*, 6681-6694.

Chao, Y., Xing, Y., Chen, Y., Xu, Y., Lin, Z., Li, Z., Jeffrey, P.D., Stock, J.B., and Shi, Y. (2006). Structure and mechanism of the phosphotyrosyl phosphatase activator. *Molecular cell* *23*, 535-546.

Chatr-Aryamontri, A., Breitkreutz, B.J., Oughtred, R., Boucher, L., Heinicke, S., Chen, D., Stark, C., Breitkreutz, A., Kolas, N., O'Donnell, L., *et al.* (2015). The BioGRID interaction database: 2015 update. *Nucleic acids research* *43*, D470-478.

Chen, C.T., Feoktistova, A., Chen, J.S., Shim, Y.S., Clifford, D.M., Gould, K.L., and McCollum, D. (2008). The SIN kinase Sid2 regulates cytoplasmic retention of the *S. pombe* Cdc14-like phosphatase Clp1. *Current biology : CB* *18*, 1594-1599.

Chen, C.T., Hehnlly, H., and Doxsey, S.J. (2012). Orchestrating vesicle transport, ESCRTs and kinase surveillance during abscission. *Nat Rev Mol Cell Biol* *13*, 483-488.

Chen, J.S., Broadus, M.R., McLean, J.R., Feoktistova, A., Ren, L., and Gould, K.L. (2013). Comprehensive proteomics analysis reveals new substrates and regulators of the fission yeast clp1/cdc14 phosphatase. *Molecular & cellular proteomics : MCP* *12*, 1074-1086.

Cheney, R.E., and Mooseker, M.S. (1992). Unconventional myosins. *Current opinion in cell biology* *4*, 27-35.

Cheng, H.C., Qi, R.Z., Paudel, H., and Zhu, H.J. (2011). Regulation and function of protein kinases and phosphatases. *Enzyme research* *2011*, 794089.

Cherfils, J., and Zeghouf, M. (2013). Regulation of small GTPases by GEFs, GAPs, and GDIs. *Physiological reviews* *93*, 269-309.

Chica, N., Rozalen, A.E., Perez-Hidalgo, L., Rubio, A., Novak, B., and Moreno, S. (2016). Nutritional Control of Cell Size by the Greatwall-Endosulfine-PP2A.B55 Pathway. *Current biology : CB* *26*, 319-330.

Chin, C.F., and Yeong, F.M. (2010). Safeguarding entry into mitosis: the antephase checkpoint. *Mol Cell Biol* *30*, 22-32.

Chuang, J.S., and Schekman, R.W. (1996). Differential trafficking and timed localization of two chitin synthase proteins, Chs2p and Chs3p. *The Journal of cell biology* *135*, 597-610.

Cipak, L., Gupta, S., Rajovic, I., Jin, Q.W., Anrather, D., Ammerer, G., McCollum, D., and Gregan, J. (2013). Crosstalk between casein kinase II and Ste20-related kinase Nak1. *Cell cycle (Georgetown, Tex)* *12*, 884-888.

Cipak, L., Polakova, S., Hyppa, R.W., Smith, G.R., and Gregan, J. (2014). Synchronized fission yeast meiosis using an ATP analog-sensitive Pat1 protein kinase. *Nature protocols* *9*, 223-231.

Coffman, V.C., Nile, A.H., Lee, I.J., Liu, H., and Wu, J.Q. (2009). Roles of formin nodes and myosin motor activity in Mid1p-dependent contractile-ring assembly during fission yeast cytokinesis. *Molecular biology of the cell* *20*, 5195-5210.

Cortes, J.C., Ishiguro, J., Duran, A., and Ribas, J.C. (2002). Localization of the (1,3)beta-D-glucan synthase catalytic subunit homologue Bgs1p/Cps1p from fission yeast suggests that it is involved in septation, polarized growth, mating, spore wall formation and spore germination. *Journal of cell science* *115*, 4081-4096.

Cortes, J.C., Konomi, M., Martins, I.M., Munoz, J., Moreno, M.B., Osumi, M., Duran, A., and Ribas, J.C. (2007). The (1,3)beta-D-glucan synthase subunit Bgs1p is responsible for the fission yeast primary septum formation. *Molecular microbiology* *65*, 201-217.

Coudreuse, D., and Nurse, P. (2010). Driving the cell cycle with a minimal CDK control network. *Nature* *468*, 1074-1079.

Crandall, M., Egel, R., and Mackay, V.L. (1977). Physiology of mating in three yeasts. *Advances in microbial physiology* *15*, 307-398.

Creanor, J., and Mitchison, J.M. (1996). The kinetics of the B cyclin p56cdc13 and the phosphatase p80cdc25 during the cell cycle of the fission yeast *Schizosaccharomyces pombe*. *Journal of cell science* *109 (Pt 6)*, 1647-1653.

Cueille, N., Salimova, E., Esteban, V., Blanco, M., Moreno, S., Bueno, A., and Simanis, V. (2001). Flp1, a fission yeast orthologue of the *s. cerevisiae* CDC14 gene, is not required for cyclin degradation or rum1p stabilisation at the end of mitosis. *Journal of cell science* *114*, 2649-2664.

Cuif, M.H., Possmayer, F., Zander, H., Bordes, N., Jollivet, F., Couedel-Courteille, A., Janoueix-Lerosey, I., Langsley, G., Bornens, M., and Goud, B. (1999). Characterization of GAPCenA, a GTPase activating protein for Rab6, part of which associates with the centrosome. *The EMBO journal* *18*, 1772-1782.

Cundell, M.J., and Price, C. (2014). The budding yeast amphiphysin complex is required for contractile actin ring (CAR) assembly and post-contraction GEF-independent accumulation of Rho1-GTP. *PloS one* *9*, e97663.

Cuthbertson, B.J., Liao, Y., Birnbaumer, L., and Blackshear, P.J. (2008). Characterization of zfs1 as an mRNA-binding and -destabilizing protein in *Schizosaccharomyces pombe*. *The Journal of biological chemistry* *283*, 2586-2594.

D'Aquino, K.E., Monje-Casas, F., Paulson, J., Reiser, V., Charles, G.M., Lai, L., Shokat, K.M., and Amon, A. (2005). The protein kinase Kin4 inhibits exit from mitosis in response to spindle position defects. *Molecular cell* *19*, 223-234.

Daga, R.R., and Chang, F. (2005). Dynamic positioning of the fission yeast cell division plane. *Proceedings of the National Academy of Sciences of the United States of America* *102*, 8228-8232.

Daga, R.R., and Jimenez, J. (1999). Translational control of the cdc25 cell cycle phosphatase: a molecular mechanism coupling mitosis to cell growth. *Journal of cell science* *112 Pt 18*, 3137-3146.

Daga, R.R., Lahoz, A., Munoz, M.J., Moreno, S., and Jimenez, J. (2005). Etd1p is a novel protein that links the SIN cascade with cytokinesis. *The EMBO journal* *24*, 2436-2446.

Damagnez, V., Makela, T.P., and Cottarel, G. (1995). Schizosaccharomyces pombe Mop1-Mcs2 is related to mammalian CAK. *The EMBO journal* *14*, 6164-6172.

de Carcer, G., Escobar, B., Higuero, A.M., Garcia, L., Anson, A., Perez, G., Mollejo, M., Manning, G., Melendez, B., Abad-Rodriguez, J., *et al.* (2011). Plk5, a polo box domain-only protein with specific roles in neuron differentiation and glioblastoma suppression. *Molecular and cellular biology* *31*, 1225-1239.

De Groot, P.W., Hellingwerf, K.J., and Klis, F.M. (2003). Genome-wide identification of fungal GPI proteins. *Yeast (Chichester, England)* *20*, 781-796.

De Virgilio, C. (2012). The essence of yeast quiescence. *FEMS microbiology reviews* *36*, 306-339.

De Virgilio, C., and Loewith, R. (2006). The TOR signalling network from yeast to man. *The international journal of biochemistry & cell biology* *38*, 1476-1481.

De Wulf, P., Montani, F., and Visintin, R. (2009). Protein phosphatases take the mitotic stage. *Current opinion in cell biology* *21*, 806-815.

Dechant, R., and Glotzer, M. (2003). Centrosome separation and central spindle assembly act in redundant pathways that regulate microtubule density and trigger cleavage furrow formation. *Dev Cell* *4*, 333-344.

Dekker, N., Speijer, D., Grun, C.H., van den Berg, M., de Haan, A., and Hochstenbach, F. (2004). Role of the alpha-glucanase Agn1p in fission-yeast cell separation. *Molecular biology of the cell* *15*, 3903-3914.

Demeter, J., and Sazer, S. (1998). imp2, a new component of the actin ring in the fission yeast Schizosaccharomyces pombe. *The Journal of cell biology* *143*, 415-427.

den Elzen, N., Kosoy, A., Christopoulos, H., and O'Connell, M.J. (2004). Resisting arrest: recovery from checkpoint arrest through dephosphorylation of Chk1 by PP1. *Cell cycle (Georgetown, Tex)* *3*, 529-533.

den Elzen, N.R., and O'Connell, M.J. (2004). Recovery from DNA damage checkpoint arrest by PP1-mediated inhibition of Chk1. *The EMBO journal* *23*, 908-918.

Deshpande, G.P., Hayles, J., Hoe, K.L., Kim, D.U., Park, H.O., and Hartsuiker, E. (2009). Screening a genome-wide S. pombe deletion library identifies novel genes and pathways involved in genome stability maintenance. *DNA repair* *8*, 672-679.

Dewey, E.B., Taylor, D.T., and Johnston, C.A. (2015). Cell Fate Decision Making through Oriented Cell Division. *Journal of developmental biology* *3*, 129-157.

Dhonukshe, P., Baluska, F., Schlicht, M., Hlavacka, A., Samaj, J., Friml, J., and Gadella, T.W., Jr. (2006). Endocytosis of cell surface material mediates cell plate formation during plant cytokinesis. *Developmental cell* *10*, 137-150.

Ding, R., West, R.R., Morphew, D.M., Oakley, B.R., and McIntosh, J.R. (1997). The spindle pole body of Schizosaccharomyces pombe enters and leaves the nuclear envelope as the cell cycle proceeds. *Molecular biology of the cell* *8*, 1461-1479.

Dinkel, H., Van Roey, K., Michael, S., Kumar, M., Uyar, B., Altenberg, B., Milchevskaya, V., Schneider, M., Kuhn, H., Behrendt, A., *et al.* (2016). ELM 2016--data update and new functionality of the eukaryotic linear motif resource. *Nucleic acids research* *44*, D294-300.

Dischinger, S., Krapp, A., Xie, L., Paulson, J.R., and Simanis, V. (2008). Chemical genetic analysis of the regulatory role of Cdc2p in the *S. pombe* septation initiation network. *Journal of cell science* *121*, 843-853.

Dominguez-Brauer, C., Thu, K.L., Mason, J.M., Blaser, H., Bray, M.R., and Mak, T.W. (2015). Targeting Mitosis in Cancer: Emerging Strategies. *Molecular cell* *60*, 524-536.

Ducommun, B., Draetta, G., Young, P., and Beach, D. (1990). Fission yeast *cdc25* is a cell-cycle regulated protein. *Biochemical and biophysical research communications* *167*, 301-309.

Eden, A., and Benvenisty, N. (1998). Characterization of a branched-chain amino-acid aminotransferase from *Schizosaccharomyces pombe*. *Yeast (Chichester, England)* *14*, 189-194.

El Kasmi, F., Krause, C., Hiller, U., Stierhof, Y.D., Mayer, U., Conner, L., Kong, L., Reichardt, I., Sanderfoot, A.A., and Jurgens, G. (2013). SNARE complexes of different composition jointly mediate membrane fusion in *Arabidopsis* cytokinesis. *Molecular biology of the cell* *24*, 1593-1601.

Enami, K., Ichikawa, M., Uemura, T., Kutsuna, N., Hasezawa, S., Nakagawa, T., Nakano, A., and Sato, M.H. (2009). Differential expression control and polarized distribution of plasma membrane-resident SYP1 SNAREs in *Arabidopsis thaliana*. *Plant & cell physiology* *50*, 280-289.

Epp, J.A., and Chant, J. (1997). An IQGAP-related protein controls actin-ring formation and cytokinesis in yeast. *Current biology* : CB *7*, 921-929.

Esteban, V., Blanco, M., Cueille, N., Simanis, V., Moreno, S., and Bueno, A. (2004). A role for the Cdc14-family phosphatase Flp1p at the end of the cell cycle in controlling the rapid degradation of the mitotic inducer Cdc25p in fission yeast. *Journal of cell science* *117*, 2461-2468.

Estravis, M., Rincon, S.A., Santos, B., and Perez, P. (2011). Cdc42 regulates multiple membrane traffic events in fission yeast. *Traffic (Copenhagen, Denmark)* *12*, 1744-1758.

Falk, J.E., Tsuchiya, D., Verdaasdonk, J., Lacefield, S., Bloom, K., and Amon, A. (2016). Spatial signals link exit from mitosis to spindle position. *Elife* *5*.

Fankhauser, C., Marks, J., Reymond, A., and Simanis, V. (1993). The *S. pombe* *cdc16* gene is required both for maintenance of p34cdc2 kinase activity and regulation of septum formation: a link between mitosis and cytokinesis? *The EMBO journal* *12*, 2697-2704.

Fankhauser, C., Reymond, A., Cerutti, L., Utzig, S., Hofmann, K., and Simanis, V. (1995). The *S. pombe* *cdc15* gene is a key element in the reorganization of F-actin at mitosis. *Cell* *82*, 435-444.

Fankhauser, C., and Simanis, V. (1993). The *Schizosaccharomyces pombe* *cdc14* gene is required for septum formation and can also inhibit nuclear division. *Molecular biology of the cell* *4*, 531-539.

Fankhauser, C., and Simanis, V. (1994). The *cdc7* protein kinase is a dosage dependent regulator of septum formation in fission yeast. *The EMBO journal* *13*, 3011-3019.

Fantes, P. (1979). Epistatic gene interactions in the control of division in fission yeast. *Nature* *279*, 428-430.

Fantes, P., and Nurse, P. (1977). Control of cell size at division in fission yeast by a growth-modulated size control over nuclear division. *Experimental cell research* *107*, 377-386.

Fantes, P.A. (1981). Isolation of cell size mutants of a fission yeast by a new selective method: characterization of mutants and implications for division control mechanisms. *Journal of bacteriology* 146, 746-754.

Featherstone, C., and Russell, P. (1991). Fission yeast p107wee1 mitotic inhibitor is a tyrosine/serine kinase. *Nature* 349, 808-811.

Feilolter, H., Nurse, P., and Young, P.G. (1991). Genetic and molecular analysis of *cdr1/nim1* in *Schizosaccharomyces pombe*. *Genetics* 127, 309-318.

Fennessy, D., Grallert, A., Krapp, A., Cokoja, A., Bridge, A.J., Petersen, J., Patel, A., Tallada, V.A., Boke, E., Hodgson, B., *et al.* (2014). Extending the *Schizosaccharomyces pombe* molecular genetic toolbox. *PloS one* 9, e97683.

Feoktistova, A., Morrell-Falvey, J., Chen, J.S., Singh, N.S., Balasubramanian, M.K., and Gould, K.L. (2012). The fission yeast septation initiation network (SIN) kinase, Sid2, is required for SIN asymmetry and regulates the SIN scaffold, Cdc11. *Molecular biology of the cell* 23, 1636-1645.

Fesquet, D., Fitzpatrick, P.J., Johnson, A.L., Kramer, K.M., Toyn, J.H., and Johnston, L.H. (1999). A Bub2p-dependent spindle checkpoint pathway regulates the Dbf2p kinase in budding yeast. *The EMBO journal* 18, 2424-2434.

Fisher, D., and Nurse, P. (1995). Cyclins of the fission yeast *Schizosaccharomyces pombe*. *Seminars in cell biology* 6, 73-78.

Fisher, D.L., and Nurse, P. (1996). A single fission yeast mitotic cyclin B p34cdc2 kinase promotes both S-phase and mitosis in the absence of G1 cyclins. *The EMBO journal* 15, 850-860.

Forsburg, S.L., and Rhind, N. (2006). Basic methods for fission yeast. *Yeast (Chichester, England)* 23, 173-183.

Fournier, N., Cerutti, L., Beltraminelli, N., Salimova, E., and Simanis, V. (2001). Bypass of the requirement for *cdc16p* GAP function in *Schizosaccharomyces pombe* by mutation of the septation initiation network genes. *Archives of microbiology* 175, 62-69.

Fraschini, R., Formenti, E., Lucchini, G., and Piatti, S. (1999). Budding yeast Bub2 is localized at spindle pole bodies and activates the mitotic checkpoint via a different pathway from Mad2. *The Journal of cell biology* 145, 979-991.

Frenz, L.M., Lee, S.E., Fesquet, D., and Johnston, L.H. (2000). The budding yeast Dbf2 protein kinase localises to the centrosome and moves to the bud neck in late mitosis. *Journal of cell science* 113 Pt 19, 3399-3408.

Furge, K.A., Cheng, Q.C., Jwa, M., Shin, S., Song, K., and Albright, C.F. (1999). Regions of Byr4, a regulator of septation in fission yeast, that bind Spg1 or Cdc16 and form a two-component GTPase-activating protein with Cdc16. *The Journal of biological chemistry* 274, 11339-11343.

Furge, K.A., Wong, K., Armstrong, J., Balasubramanian, M., and Albright, C.F. (1998). Byr4 and Cdc16 form a two-component GTPase-activating protein for the Spg1 GTPase that controls septation in fission yeast. *Current biology : CB* 8, 947-954.

Furnari, B.A., Russell, P., and Leatherwood, J. (1997). Pch1(+), a second essential C-type cyclin gene in *Schizosaccharomyces pombe*. *The Journal of biological chemistry* 272, 12100-12106.

Gachet, Y., and Hyams, J.S. (2005). Endocytosis in fission yeast is spatially associated with the actin cytoskeleton during polarised cell growth and cytokinesis. *Journal of cell science* 118, 4231-4242.

Garcia-Cortes, J.C., and McCollum, D. (2009). Proper timing of cytokinesis is regulated by *Schizosaccharomyces pombe* Etd1. *The Journal of cell biology* *186*, 739-753.

Ge, W., and Balasubramanian, M.K. (2008). Pxl1p, a paxillin-related protein, stabilizes the actomyosin ring during cytokinesis in fission yeast. *Molecular biology of the cell* *19*, 1680-1692.

Geymonat, M., Spanos, A., Walker, P.A., Johnston, L.H., and Sedgwick, S.G. (2003). In vitro regulation of budding yeast Bfa1/Bub2 GAP activity by Cdc5. *The Journal of biological chemistry* *278*, 14591-14594.

Gladfelter, A.S., Bose, I., Zyla, T.R., Bardes, E.S., and Lew, D.J. (2002). Septin ring assembly involves cycles of GTP loading and hydrolysis by Cdc42p. *The Journal of cell biology* *156*, 315-326.

Glotzer, M. (2004). Cleavage furrow positioning. *J Cell Biol* *164*, 347-351.

Glover, C.V., 3rd (1998). On the physiological role of casein kinase II in *Saccharomyces cerevisiae*. *Progress in nucleic acid research and molecular biology* *59*, 95-133.

Godin, M., Delgado, F.F., Son, S., Grover, W.H., Bryan, A.K., Tzur, A., Jorgensen, P., Payer, K., Grossman, A.D., Kirschner, M.W., *et al.* (2010). Using buoyant mass to measure the growth of single cells. *Nature methods* *7*, 387-390.

Gomez, M., Gomez, V., and Hergovich, A. (2014). The Hippo pathway in disease and therapy: cancer and beyond. *Clinical and translational medicine* *3*, 22.

Gould, K.L., Moreno, S., Owen, D.J., Sazer, S., and Nurse, P. (1991). Phosphorylation at Thr167 is required for *Schizosaccharomyces pombe* p34cdc2 function. *The EMBO journal* *10*, 3297-3309.

Gould, K.L., and Nurse, P. (1989). Tyrosine phosphorylation of the fission yeast cdc2+ protein kinase regulates entry into mitosis. *Nature* *342*, 39-45.

Goyal, A., and Simanis, V. (2012). Characterization of ypa1 and ypa2, the *Schizosaccharomyces pombe* orthologs of the peptidyl prolyl isomerases that activate PP2A, reveals a role for Ypa2p in the regulation of cytokinesis. *Genetics* *190*, 1235-1250.

Goyal, A., Takaine, M., Simanis, V., and Nakano, K. (2011). Dividing the spoils of growth and the cell cycle: The fission yeast as a model for the study of cytokinesis. *Cytoskeleton (Hoboken, NJ)* *68*, 69-88.

Grallert, A., Boke, E., Hagting, A., Hodgson, B., Connolly, Y., Griffiths, J.R., Smith, D.L., Pines, J., and Hagan, I.M. (2015). A PP1-PP2A phosphatase relay controls mitotic progression. *Nature* *517*, 94-98.

Grallert, A., Chan, K.Y., Alonso-Nunez, M.L., Madrid, M., Biswas, A., Alvarez-Tabares, I., Connolly, Y., Tanaka, K., Robertson, A., Ortiz, J.M., *et al.* (2013). Removal of centrosomal PP1 by NIMA kinase unlocks the MPF feedback loop to promote mitotic commitment in *S. pombe*. *Curr Biol* *23*, 213-222.

Grallert, A., and Hagan, I.M. (2002). *Schizosaccharomyces pombe* NIMA-related kinase, Fin1, regulates spindle formation and an affinity of Polo for the SPB. *The EMBO journal* *21*, 3096-3107.

Grallert, A., Krapp, A., Bagley, S., Simanis, V., and Hagan, I.M. (2004). Recruitment of NIMA kinase shows that maturation of the *S. pombe* spindle-pole body occurs over consecutive cell cycles and reveals a role for NIMA in modulating SIN activity. *Genes & development* *18*, 1007-1021.

Gromley, A., Jurczyk, A., Sillibourne, J., Halilovic, E., Mogensen, M., Groisman, I., Blomberg, M., and Doxsey, S. (2003). A novel human protein of the maternal

centriole is required for the final stages of cytokinesis and entry into S phase. *The Journal of cell biology* 161, 535-545.

Gromley, A., Yeaman, C., Rosa, J., Redick, S., Chen, C.T., Mirabelle, S., Guha, M., Sillibourne, J., and Doxsey, S.J. (2005). Centriolin anchoring of exocyst and SNARE complexes at the midbody is required for secretory-vesicle-mediated abscission. *Cell* 123, 75-87.

Gruneberg, U., Campbell, K., Simpson, C., Grindlay, J., and Schiebel, E. (2000). Nud1p links astral microtubule organization and the control of exit from mitosis. *The EMBO journal* 19, 6475-6488.

Guertin, D.A., Chang, L., Irshad, F., Gould, K.L., and McCollum, D. (2000). The role of the sid1p kinase and cdc14p in regulating the onset of cytokinesis in fission yeast. *The EMBO journal* 19, 1803-1815.

Guertin, D.A., Venkatram, S., Gould, K.L., and McCollum, D. (2002). Dma1 prevents mitotic exit and cytokinesis by inhibiting the septation initiation network (SIN). *Developmental cell* 3, 779-790.

Guizetti, J., and Gerlich, D.W. (2010). Cytokinetic abscission in animal cells. *Seminars in cell & developmental biology* 21, 909-916.

Guo, F., Stanevich, V., Wlodarchak, N., Sengupta, R., Jiang, L., Satyshur, K.A., and Xing, Y. (2014). Structural basis of PP2A activation by PTPA, an ATP-dependent activation chaperone. *Cell research* 24, 190-203.

Gupta, S., Mana-Capelli, S., McLean, J.R., Chen, C.T., Ray, S., Gould, K.L., and McCollum, D. (2013). Identification of SIN pathway targets reveals mechanisms of crosstalk between NDR kinase pathways. *Current biology : CB* 23, 333-338.

Gupta, S., and McCollum, D. (2011). Crosstalk between NDR kinase pathways coordinates cell cycle dependent actin rearrangements. *Cell division* 6, 19.

Gutz, H., and Doe, F.J. (1973). Two Different h Mating Types in SCHIZOSACCHAROMYCES POMBE. *Genetics* 74, 563-569.

Haccard, O., and Jessus, C. (2011). Greatwall kinase, ARPP-19 and protein phosphatase 2A: shifting the mitosis paradigm. *Results and problems in cell differentiation* 53, 219-234.

Hachet, O., and Simanis, V. (2008). Mid1p/anillin and the septation initiation network orchestrate contractile ring assembly for cytokinesis. *Genes & development* 22, 3205-3216.

Hagan, I., and Yanagida, M. (1995). The product of the spindle formation gene *sad1+* associates with the fission yeast spindle pole body and is essential for viability. *The Journal of cell biology* 129, 1033-1047.

Hagan, I.M. (1998). The fission yeast microtubule cytoskeleton. *Journal of cell science* 111 (Pt 12), 1603-1612.

Hagan, I.M. (2008). The spindle pole body plays a key role in controlling mitotic commitment in the fission yeast *Schizosaccharomyces pombe*. *Biochemical Society transactions* 36, 1097-1101.

Hagan, I.M., and Hyams, J.S. (1996). Forces acting on the fission yeast anaphase spindle. *Cell motility and the cytoskeleton* 34, 69-75.

Hanna, D.E., Rethinaswamy, A., and Glover, C.V. (1995). Casein kinase II is required for cell cycle progression during G1 and G2/M in *Saccharomyces cerevisiae*. *The Journal of biological chemistry* 270, 25905-25914.

Hannig, G., Otilie, S., and Erikson, R.L. (1994). Negative regulation of mitosis in fission yeast by catalytically inactive *pyp1* and *pyp2* mutants. *Proceedings of the National Academy of Sciences of the United States of America* 91, 10084-10088.

Hanyu, Y., Imai, K.K., Kawasaki, Y., Nakamura, T., Nakaseko, Y., Nagao, K., Kokubu, A., Ebe, M., Fujisawa, A., Hayashi, T., *et al.* (2009). Schizosaccharomyces pombe cell division cycle under limited glucose requires Ssp1 kinase, the putative CaMKK, and Sds23, a PP2A-related phosphatase inhibitor. *Genes to cells : devoted to molecular & cellular mechanisms* 14, 539-554.

Hartwell, L.H., and Unger, M.W. (1977). Unequal division in Saccharomyces cerevisiae and its implications for the control of cell division. *J Cell Biol* 75, 422-435.

Harvey, K.F., Zhang, X., and Thomas, D.M. (2013). The Hippo pathway and human cancer. *Nature reviews Cancer* 13, 246-257.

Hayles, J., and Nurse, P. (1992). Genetics of the fission yeast Schizosaccharomyces pombe. *Annual review of genetics* 26, 373-402.

Hayles, J., Wood, V., Jeffery, L., Hoe, K.L., Kim, D.U., Park, H.O., Salas-Pino, S., Heichinger, C., and Nurse, P. (2013). A genome-wide resource of cell cycle and cell shape genes of fission yeast. *Open biology* 3, 130053.

He, X., Patterson, T.E., and Sazer, S. (1997). The Schizosaccharomyces pombe spindle checkpoint protein mad2p blocks anaphase and genetically interacts with the anaphase-promoting complex. *Proceedings of the National Academy of Sciences of the United States of America* 94, 7965-7970.

Heitz, M.J., Petersen, J., Valovin, S., and Hagan, I.M. (2001). MTOC formation during mitotic exit in fission yeast. *J Cell Sci* 114, 4521-4532.

Hentges, P., Van Driessche, B., Tafforeau, L., Vandenhoute, J., and Carr, A.M. (2005). Three novel antibiotic marker cassettes for gene disruption and marker switching in Schizosaccharomyces pombe. *Yeast (Chichester, England)* 22, 1013-1019.

Hergovich, A. (2013). Regulation and functions of mammalian LATS/NDR kinases: looking beyond canonical Hippo signalling. *Cell & bioscience* 3, 32.

Hergovich, A., Stegert, M.R., Schmitz, D., and Hemmings, B.A. (2006). NDR kinases regulate essential cell processes from yeast to humans. *Nature reviews Molecular cell biology* 7, 253-264.

Hermant, D., Pihlak, A., Westerling, T., Damagnez, V., Vandenhoute, J., Cottarel, G., and Makela, T.P. (1998). Fission yeast Csk1 is a CAK-activating kinase (CAKAK). *The EMBO journal* 17, 7230-7238.

Hermeking, H., Lengauer, C., Polyak, K., He, T.C., Zhang, L., Thiagalingam, S., Kinzler, K.W., and Vogelstein, B. (1997). 14-3-3sigma is a p53-regulated inhibitor of G2/M progression. *Molecular cell* 1, 3-11.

Heublein, M., Burguillos, M.A., Vogtle, F.N., Teixeira, P.F., Imhof, A., Meisinger, C., and Ott, M. (2014). The novel component Kgd4 recruits the E3 subunit to the mitochondrial alpha-ketoglutarate dehydrogenase. *Molecular biology of the cell* 25, 3342-3349.

Hirata, D., Kishimoto, N., Suda, M., Sogabe, Y., Nakagawa, S., Yoshida, Y., Sakai, K., Mizunuma, M., Miyakawa, T., Ishiguro, J., *et al.* (2002). Fission yeast Mor2/Cps12, a protein similar to Drosophila Furry, is essential for cell morphogenesis and its mutation induces Wee1-dependent G(2) delay. *The EMBO journal* 21, 4863-4874.

Ho, C.M., Hotta, T., Guo, F., Roberson, R.W., Lee, Y.R., and Liu, B. (2011). Interaction of antiparallel microtubules in the phragmoplast is mediated by the microtubule-associated protein MAP65-3 in Arabidopsis. *The Plant cell* 23, 2909-2923.

Ho, C.M., Lee, Y.R., Kiyama, L.D., Dinesh-Kumar, S.P., and Liu, B. (2012). Arabidopsis microtubule-associated protein MAP65-3 cross-links antiparallel microtubules toward their plus ends in the phragmoplast via its distinct C-terminal microtubule binding domain. *The Plant cell* *24*, 2071-2085.

Hochstenbach, F., Klis, F.M., van den Ende, H., van Donselaar, E., Peters, P.J., and Klausner, R.D. (1998). Identification of a putative alpha-glucan synthase essential for cell wall construction and morphogenesis in fission yeast. *Proceedings of the National Academy of Sciences of the United States of America* *95*, 9161-9166.

Hoffman, C.S., Wood, V., and Fantes, P.A. (2015). An Ancient Yeast for Young Geneticists: A Primer on the *Schizosaccharomyces pombe* Model System. *Genetics* *201*, 403-423.

Hofken, T., and Schiebel, E. (2002). A role for cell polarity proteins in mitotic exit. *The EMBO journal* *21*, 4851-4862.

Horisberger, M., and Rouvet-Vauthey, M. (1984). Localization of glycosylated kappa-casein on thin sections of casein micelles by lectin-labelled gold markers. *Histochemistry* *80*, 523-526.

Hotz, M., and Barral, Y. (2014). The Mitotic Exit Network: new turns on old pathways. *Trends in cell biology* *24*, 145-152.

Hotz, M., Leisner, C., Chen, D., Manatschal, C., Wegleiter, T., Ouellet, J., Lindstrom, D., Gottschling, D.E., Vogel, J., and Barral, Y. (2012a). Spindle pole bodies exploit the mitotic exit network in metaphase to drive their age-dependent segregation. *Cell* *148*, 958-972.

Hotz, M., Lengefeld, J., and Barral, Y. (2012b). The MEN mediates the effects of the spindle assembly checkpoint on Kar9-dependent spindle pole body inheritance in budding yeast. *Cell cycle (Georgetown, Tex)* *11*, 3109-3116.

Hou, M.C., Guertin, D.A., and McCollum, D. (2004). Initiation of cytokinesis is controlled through multiple modes of regulation of the Sid2p-Mob1p kinase complex. *Molecular and cellular biology* *24*, 3262-3276.

Hou, M.C., Salek, J., and McCollum, D. (2000). Mob1p interacts with the Sid2p kinase and is required for cytokinesis in fission yeast. *Current biology : CB* *10*, 619-622.

Hou, M.C., Wiley, D.J., Verde, F., and McCollum, D. (2003). Mob2p interacts with the protein kinase Orb6p to promote coordination of cell polarity with cell cycle progression. *Journal of cell science* *116*, 125-135.

Hu, F., Wang, Y., Liu, D., Li, Y., Qin, J., and Elledge, S.J. (2001). Regulation of the Bub2/Bfa1 GAP complex by Cdc5 and cell cycle checkpoints. *Cell* *107*, 655-665.

Hug, N., and Lingner, J. (2006). Telomere length homeostasis. *Chromosoma* *115*, 413-425.

Humbel, B.M., Konomi, M., Takagi, T., Kamasawa, N., Ishijima, S.A., and Osumi, M. (2001). In situ localization of beta-glucans in the cell wall of *Schizosaccharomyces pombe*. *Yeast (Chichester, England)* *18*, 433-444.

Hwa Lim, H., Yeong, F.M., and Surana, U. (2003). Inactivation of mitotic kinase triggers translocation of MEN components to mother-daughter neck in yeast. *Molecular biology of the cell* *14*, 4734-4743.

Ishiguro, J., Saitou, A., Duran, A., and Ribas, J.C. (1997). *cps1+*, a *Schizosaccharomyces pombe* gene homolog of *Saccharomyces cerevisiae* FKS genes whose mutation confers hypersensitivity to cyclosporin A and papulacandin B. *Journal of bacteriology* *179*, 7653-7662.

Ives, E.B., Nichols, J., Wente, S.R., and York, J.D. (2000). Biochemical and functional characterization of inositol 1,3,4,5, 6-pentakisphosphate 2-kinases. *The Journal of biological chemistry* 275, 36575-36583.

Jahn, R., and Scheller, R.H. (2006). SNAREs--engines for membrane fusion. *Nature reviews Molecular cell biology* 7, 631-643.

Jensen, S., Geymonat, M., Johnson, A.L., Segal, M., and Johnston, L.H. (2002). Spatial regulation of the guanine nucleotide exchange factor *Lte1* in *Saccharomyces cerevisiae*. *Journal of cell science* 115, 4977-4991.

Jeong, A.L., and Yang, Y. (2013). PP2A function toward mitotic kinases and substrates during the cell cycle. *BMB Rep* 46, 289-294.

Jiang, W., and Hallberg, R.L. (2000). Isolation and characterization of *par1(+)* and *par2(+)*: two *Schizosaccharomyces pombe* genes encoding B' subunits of protein phosphatase 2A. *Genetics* 154, 1025-1038.

Jiang, W., and Hallberg, R.L. (2001). Correct regulation of the septation initiation network in *Schizosaccharomyces pombe* requires the activities of *par1* and *par2*. *Genetics* 158, 1413-1429.

Jin, Q.W., and McCollum, D. (2003). *Scw1p* antagonizes the septation initiation network to regulate septum formation and cell separation in the fission yeast *Schizosaccharomyces pombe*. *Eukaryotic cell* 2, 510-520.

Jin, Q.W., Ray, S., Choi, S.H., and McCollum, D. (2007). The nucleolar *Net1/Cfi1*-related protein *Dnt1* antagonizes the septation initiation network in fission yeast. *Molecular biology of the cell* 18, 2924-2934.

Jin, Q.W., Zhou, M., Bimbo, A., Balasubramanian, M.K., and McCollum, D. (2006). A role for the septation initiation network in septum assembly revealed by genetic analysis of *sid2-250* suppressors. *Genetics* 172, 2101-2112.

John, J., Rensland, H., Schlichting, I., Vetter, I., Borasio, G.D., Goody, R.S., and Wittinghofer, A. (1993). Kinetic and structural analysis of the Mg(2+)-binding site of the guanine nucleotide-binding protein p21H-ras. *The Journal of biological chemistry* 268, 923-929.

Johnson, A.E., and Gould, K.L. (2011). *Dma1* ubiquitinates the SIN scaffold, *Sid4*, to impede the mitotic localization of *Plo1* kinase. *The EMBO journal* 30, 341-354.

Johnsson, A., Xue-Franzen, Y., Lundin, M., and Wright, A.P. (2006). Stress-specific role of fission yeast *Gcn5* histone acetyltransferase in programming a subset of stress response genes. *Eukaryotic cell* 5, 1337-1346.

Jong, A.Y., T'Ang, A., Liu, D.P., and Huang, S.H. (2002). Inverse PCR. *Genomic DNA cloning. Methods in molecular biology (Clifton, NJ)* 192, 301-307.

Jordens, J., Janssens, V., Longin, S., Stevens, I., Martens, E., Bultynck, G., Engelborghs, Y., Lescrinier, E., Waelkens, E., Goris, J., *et al.* (2006). The protein phosphatase 2A phosphatase activator is a novel peptidyl-prolyl cis/trans-isomerase. *The Journal of biological chemistry* 281, 6349-6357.

Jourdain, I., Dooley, H.C., and Toda, T. (2012). Fission yeast *sec3* bridges the exocyst complex to the actin cytoskeleton. *Traffic (Copenhagen, Denmark)* 13, 1481-1495.

Kafri, R., Levy, J., Ginzberg, M.B., Oh, S., Lahav, G., and Kirschner, M.W. (2013). Dynamics extracted from fixed cells reveal feedback linking cell growth to cell cycle. *Nature* 494, 480-483.

Kamasaki, T., Osumi, M., and Mabuchi, I. (2007). Three-dimensional arrangement of F-actin in the contractile ring of fission yeast. *The Journal of cell biology* 178, 765-771.

Kanai, M., Kume, K., Miyahara, K., Sakai, K., Nakamura, K., Leonhard, K., Wiley, D.J., Verde, F., Toda, T., and Hirata, D. (2005). Fission yeast MO25 protein is localized at SPB and septum and is essential for cell morphogenesis. *The EMBO journal* 24, 3012-3025.

Kanoh, J., and Russell, P. (1998). The protein kinase Cdr2, related to Nim1/Cdr1 mitotic inducer, regulates the onset of mitosis in fission yeast. *Molecular biology of the cell* 9, 3321-3334.

Karagiannis, J., and Balasubramanian, M.K. (2007). A cyclin-dependent kinase that promotes cytokinesis through modulating phosphorylation of the carboxy terminal domain of the RNA Pol II Rpb1p sub-unit. *PloS one* 2, e433.

Karagiannis, J., Bimbo, A., Rajagopalan, S., Liu, J., and Balasubramanian, M.K. (2005). The nuclear kinase Lsk1p positively regulates the septation initiation network and promotes the successful completion of cytokinesis in response to perturbation of the actomyosin ring in *Schizosaccharomyces pombe*. *Molecular biology of the cell* 16, 358-371.

Karagiannis, J., Oulton, R., and Young, P.G. (2002). The Scw1 RNA-binding domain protein regulates septation and cell-wall structure in fission yeast. *Genetics* 162, 45-58.

Katayama, S., Hirata, D., Arellano, M., Perez, P., and Toda, T. (1999). Fission yeast alpha-glucan synthase Mok1 requires the actin cytoskeleton to localize the sites of growth and plays an essential role in cell morphogenesis downstream of protein kinase C function. *The Journal of cell biology* 144, 1173-1186.

Kelly, M., Burke, J., Smith, M., Klar, A., and Beach, D. (1988). Four mating-type genes control sexual differentiation in the fission yeast. *The EMBO journal* 7, 1537-1547.

Kemp, H.A., and Sprague, G.F., Jr. (2003). Far3 and five interacting proteins prevent premature recovery from pheromone arrest in the budding yeast *Saccharomyces cerevisiae*. *Molecular and cellular biology* 23, 1750-1763.

Kennedy, P.J., Vashisht, A.A., Hoe, K.L., Kim, D.U., Park, H.O., Hayles, J., and Russell, P. (2008). A genome-wide screen of genes involved in cadmium tolerance in *Schizosaccharomyces pombe*. *Toxicological sciences : an official journal of the Society of Toxicology* 106, 124-139.

Kettenbach, A.N., Deng, L., Wu, Y., Baldissard, S., Adamo, M.E., Gerber, S.A., and Moseley, J.B. (2015). Quantitative phosphoproteomics reveals pathways for coordination of cell growth and division by the conserved fission yeast kinase pom1. *Molecular & cellular proteomics : MCP* 14, 1275-1287.

Kim, D.M., Kim, H., Yeon, J.H., Lee, J.H., and Park, H.O. (2016). Identification of a Mitochondrial DNA Polymerase Affecting Cardiotoxicity of Sunitinib Using a Genome-Wide Screening on *S. pombe* Deletion Library. *Toxicological sciences : an official journal of the Society of Toxicology* 149, 4-14.

Kim, D.U., Hayles, J., Kim, D., Wood, V., Park, H.O., Won, M., Yoo, H.S., Duhig, T., Nam, M., Palmer, G., *et al.* (2010). Analysis of a genome-wide set of gene deletions in the fission yeast *Schizosaccharomyces pombe*. *Nature biotechnology* 28, 617-623.

King, R.W., Deshaies, R.J., Peters, J.M., and Kirschner, M.W. (1996). How proteolysis drives the cell cycle. *Science* 274, 1652-1659.

Kingsbury, J.M., Heitman, J., and Pinnell, S.R. (2012). Calcofluor white combination antifungal treatments for *Trichophyton rubrum* and *Candida albicans*. *PloS one* 7, e39405.

Kinoshita, K., Nemoto, T., Nabeshima, K., Kondoh, H., Niwa, H., and Yanagida, M. (1996). The regulatory subunits of fission yeast protein phosphatase 2A (PP2A) affect cell morphogenesis, cell wall synthesis and cytokinesis. *Genes to cells : devoted to molecular & cellular mechanisms* 1, 29-45.

Kinoshita, N., Ohkura, H., and Yanagida, M. (1990). Distinct, essential roles of type 1 and 2A protein phosphatases in the control of the fission yeast cell division cycle. *Cell* 63, 405-415.

Kinoshita, N., Yamano, H., Niwa, H., Yoshida, T., and Yanagida, M. (1993). Negative regulation of mitosis by the fission yeast protein phosphatase ppa2. *Genes & development* 7, 1059-1071.

Kita, A., Sugiura, R., Shoji, H., He, Y., Deng, L., Lu, Y., Sio, S.O., Takegawa, K., Sakaue, M., Shuntoh, H., *et al.* (2004). Loss of Apm1, the micro1 subunit of the clathrin-associated adaptor-protein-1 complex, causes distinct phenotypes and synthetic lethality with calcineurin deletion in fission yeast. *Molecular biology of the cell* 15, 2920-2931.

Ko, L.J., and Prives, C. (1996). p53: puzzle and paradigm. *Genes & development* 10, 1054-1072.

Koch, A., Krug, K., Pengelley, S., Macek, B., and Hauf, S. (2011). Mitotic substrates of the kinase aurora with roles in chromatin regulation identified through quantitative phosphoproteomics of fission yeast. *Science signaling* 4, rs6.

Kohli, J., Hottinger, H., Munz, P., Strauss, A., and Thuriaux, P. (1977). Genetic Mapping in SCHIZOSACCHAROMYCES POMBE by Mitotic and Meiotic Analysis and Induced Haploidization. *Genetics* 87, 471-489.

Kohli, J., and Nurse, P. (1995). Genetic nomenclature guide. *Schizosaccharomyces pombe*. *Trends in genetics : TIG*, 9-10.

Kovar, D.R., Sirotkin, V., and Lord, M. (2011). Three's company: the fission yeast actin cytoskeleton. *Trends in cell biology* 21, 177-187.

Kovelman, R., and Russell, P. (1996). Stockpiling of Cdc25 during a DNA replication checkpoint arrest in *Schizosaccharomyces pombe*. *Molecular and cellular biology* 16, 86-93.

Krapp, A., Cano, E., and Simanis, V. (2003). Mitotic hyperphosphorylation of the fission yeast SIN scaffold protein cdc11p is regulated by the protein kinase cdc7p. *Current biology : CB* 13, 168-172.

Krapp, A., Cano, E., and Simanis, V. (2004). Analysis of the *S. pombe* signalling scaffold protein Cdc11p reveals an essential role for the N-terminal domain in SIN signalling. *FEBS letters* 565, 176-180.

Krapp, A., Collin, P., Cano Del Rosario, E., and Simanis, V. (2008). Homeostasis between the GTPase Spg1p and its GAP in the regulation of cytokinesis in *S. pombe*. *Journal of cell science* 121, 601-608.

Krapp, A., Collin, P., Cokoja, A., Dischinger, S., Cano, E., and Simanis, V. (2006). The *Schizosaccharomyces pombe* septation initiation network (SIN) is required for spore formation in meiosis. *Journal of cell science* 119, 2882-2891.

Krapp, A., Schmidt, S., Cano, E., and Simanis, V. (2001). *S. pombe* cdc11p, together with sid4p, provides an anchor for septation initiation network proteins on the spindle pole body. *Current biology : CB* 11, 1559-1568.

Krapp, A., and Simanis, V. (2014). Dma1-dependent degradation of SIN proteins during meiosis in *Schizosaccharomyces pombe*. *Journal of cell science* 127, 3149-3161.

Krasinska, L., de Bettignies, G., Fisher, D., Abrieu, A., Fesquet, D., and Morin, N. (2007). Regulation of multiple cell cycle events by Cdc14 homologues in vertebrates. *Experimental cell research* 313, 1225-1239.

Kumar, M., Pushpa, K., and Mylavarapu, S.V. (2015). Splitting the cell, building the organism: Mechanisms of cell division in metazoan embryos. *IUBMB life* 67, 575-587.

Kuzmin, E., Costanzo, M., Andrews, B., and Boone, C. (2016). Synthetic Genetic Arrays: Automation of Yeast Genetics. *Cold Spring Harbor protocols* 2016, pdb top086652.

Labib, K., and Moreno, S. (1996). rum1: a CDK inhibitor regulating G1 progression in fission yeast. *Trends in cell biology* 6, 62-66.

Lahoz, A., Alcaide-Gavilan, M., Daga, R.R., and Jimenez, J. (2010). Antagonistic roles of PP2A-Pab1 and Etd1 in the control of cytokinesis in fission yeast. *Genetics* 186, 1261-1270.

Laporte, D., Coffman, V.C., Lee, I.J., and Wu, J.Q. (2011). Assembly and architecture of precursor nodes during fission yeast cytokinesis. *The Journal of cell biology* 192, 1005-1021.

Laporte, D., Ojkic, N., Vavylonis, D., and Wu, J.Q. (2012). alpha-Actinin and fimbrin cooperate with myosin II to organize actomyosin bundles during contractile-ring assembly. *Molecular biology of the cell* 23, 3094-3110.

Le Goff, X., Buvelot, S., Salimova, E., Guerry, F., Schmidt, S., Cueille, N., Cano, E., and Simanis, V. (2001). The protein phosphatase 2A B'-regulatory subunit par1p is implicated in regulation of the *S. pombe* septation initiation network. *FEBS letters* 508, 136-142.

Le Goff, X., Woollard, A., and Simanis, V. (1999). Analysis of the *cps1* gene provides evidence for a septation checkpoint in *Schizosaccharomyces pombe*. *Molecular & general genetics : MGG* 262, 163-172.

Lee, I.J., Coffman, V.C., and Wu, J.Q. (2012a). Contractile-ring assembly in fission yeast cytokinesis: Recent advances and new perspectives. *Cytoskeleton (Hoboken, NJ)* 69, 751-763.

Lee, J., Hwang, H.S., Kim, J., and Song, K. (1999). Ibd1p, a possible spindle pole body associated protein, regulates nuclear division and bud separation in *Saccharomyces cerevisiae*. *Biochimica et biophysica acta* 1449, 239-253.

Lee, J.H., Yeon, J.H., Kim, H., Roh, W., Chae, J., Park, H.O., and Kim, D.M. (2012b). The natural anticancer agent plumbagin induces potent cytotoxicity in MCF-7 human breast cancer cells by inhibiting a PI-5 kinase for ROS generation. *PLoS one* 7, e45023.

Lee, K.W., Chen, W., Junn, E., Im, J.Y., Grosso, H., Sonsalla, P.K., Feng, X., Ray, N., Fernandez, J.R., Chao, Y., *et al.* (2011). Enhanced phosphatase activity attenuates alpha-synucleinopathy in a mouse model. *The Journal of neuroscience : the official journal of the Society for Neuroscience* 31, 6963-6971.

Lee, S.E., Frenz, L.M., Wells, N.J., Johnson, A.L., and Johnston, L.H. (2001a). Order of function of the budding-yeast mitotic exit-network proteins Tem1, Cdc15, Mob1, Dbf2, and Cdc5. *Current biology : CB* 11, 784-788.

Lee, S.E., Jensen, S., Frenz, L.M., Johnson, A.L., Fesquet, D., and Johnston, L.H. (2001b). The Bub2-dependent mitotic pathway in yeast acts every cell cycle and regulates cytokinesis. *Journal of cell science* 114, 2345-2354.

Leonhard, K., and Nurse, P. (2005). Ste20/GCK kinase Nak1/Orb3 polarizes the actin cytoskeleton in fission yeast during the cell cycle. *Journal of cell science* *118*, 1033-1044.

Leulliot, N., Vicentini, G., Jordens, J., Quevillon-Cheruel, S., Schiltz, M., Barford, D., van Tilbeurgh, H., and Goris, J. (2006). Crystal structure of the PP2A phosphatase activator: implications for its PP2A-specific PPIase activity. *Molecular cell* *23*, 413-424.

Leung-Pineda, V., Ryan, C.E., and Piwnicka-Worms, H. (2006). Phosphorylation of Chk1 by ATR is antagonized by a Chk1-regulated protein phosphatase 2A circuit. *Molecular and cellular biology* *26*, 7529-7538.

Levine, A.J. (1997). p53, the cellular gatekeeper for growth and division. *Cell* *88*, 323-331.

Li, C., Furge, K.A., Cheng, Q.C., and Albright, C.F. (2000). Byr4 localizes to spindle-pole bodies in a cell cycle-regulated manner to control Cdc7 localization and septation in fission yeast. *The Journal of biological chemistry* *275*, 14381-14387.

Li, R. (1999). Bifurcation of the mitotic checkpoint pathway in budding yeast. *Proceedings of the National Academy of Sciences of the United States of America* *96*, 4989-4994.

Li, Z., Lee, I., Moradi, E., Hung, N.J., Johnson, A.W., and Marcotte, E.M. (2009). Rational extension of the ribosome biogenesis pathway using network-guided genetics. *PLoS biology* *7*, e1000213.

Lippincott, J., and Li, R. (1998). Sequential assembly of myosin II, an IQGAP-like protein, and filamentous actin to a ring structure involved in budding yeast cytokinesis. *The Journal of cell biology* *140*, 355-366.

Liu, G., and Young, D. (2012). Conserved Orb6 phosphorylation sites are essential for polarized cell growth in *Schizosaccharomyces pombe*. *PloS one* *7*, e37221.

Liu, J., Tang, X., Wang, H., Oliferenko, S., and Balasubramanian, M.K. (2002). The localization of the integral membrane protein Cps1p to the cell division site is dependent on the actomyosin ring and the septation-inducing network in *Schizosaccharomyces pombe*. *Molecular biology of the cell* *13*, 989-1000.

Liu, J., Wang, H., and Balasubramanian, M.K. (2000). A checkpoint that monitors cytokinesis in *Schizosaccharomyces pombe*. *Journal of cell science* *113 (Pt 7)*, 1223-1230.

Liu, J., Wang, H., McCollum, D., and Balasubramanian, M.K. (1999). Drc1p/Cps1p, a 1,3-beta-glucan synthase subunit, is essential for division septum assembly in *Schizosaccharomyces pombe*. *Genetics* *153*, 1193-1203.

Liu, N.N., Han, T.X., Du, L.L., and Zhou, J.Q. (2010). A genome-wide screen for *Schizosaccharomyces pombe* deletion mutants that affect telomere length. *Cell research* *20*, 963-965.

Longin, S., Zwaenepoel, K., Louis, J.V., Dilworth, S., Goris, J., and Janssens, V. (2007). Selection of protein phosphatase 2A regulatory subunits is mediated by the C terminus of the catalytic subunit. *The Journal of biological chemistry* *282*, 26971-26980.

Longtine, M.S., DeMarini, D.J., Valencik, M.L., Al-Awar, O.S., Fares, H., De Virgilio, C., and Pringle, J.R. (1996). The septins: roles in cytokinesis and other processes. *Current opinion in cell biology* *8*, 106-119.

Loog, M., and Morgan, D.O. (2005). Cyclin specificity in the phosphorylation of cyclin-dependent kinase substrates. *Nature* *434*, 104-108.

Lopez-Girona, A., Furnari, B., Mondesert, O., and Russell, P. (1999). Nuclear localization of Cdc25 is regulated by DNA damage and a 14-3-3 protein. *Nature* 397, 172-175.

Low, C., Quistgaard, E.M., Kovermann, M., Anandapadamanaban, M., Balbach, J., and Nordlund, P. (2014). Structural basis for PTPA interaction with the invariant C-terminal tail of PP2A. *Biological chemistry* 395, 881-889.

Lu, L.X., Domingo-Sananes, M.R., Huzarska, M., Novak, B., and Gould, K.L. (2012). Multisite phosphoregulation of Cdc25 activity refines the mitotic entrance and exit switches. *Proceedings of the National Academy of Sciences of the United States of America* 109, 9899-9904.

Lu, Y., Sugiura, R., Yada, T., Cheng, H., Sio, S.O., Shuntoh, H., and Kuno, T. (2002). Calcineurin is implicated in the regulation of the septation initiation network in fission yeast. *Genes to cells : devoted to molecular & cellular mechanisms* 7, 1009-1019.

Luca, F.C., Mody, M., Kurischko, C., Roof, D.M., Giddings, T.H., and Winey, M. (2001). *Saccharomyces cerevisiae* Mob1p is required for cytokinesis and mitotic exit. *Molecular and cellular biology* 21, 6972-6983.

Lucena, R., Dephoure, N., Gygi, S.P., Kellogg, D.R., Tallada, V.A., Daga, R.R., and Jimenez, J. (2015). Nucleocytoplasmic transport in the midzone membrane domain controls yeast mitotic spindle disassembly. *The Journal of cell biology* 209, 387-402.

Lundgren, K., Walworth, N., Booher, R., Dembski, M., Kirschner, M., and Beach, D. (1991). mik1 and wee1 cooperate in the inhibitory tyrosine phosphorylation of cdc2. *Cell* 64, 1111-1122.

Ma, Y., Jiang, W., Liu, Q., Ryuko, S., and Kuno, T. (2011). Genome-wide screening for genes associated with FK506 sensitivity in fission yeast. *PloS one* 6, e23422.

MacIver, F.H., Tanaka, K., Robertson, A.M., and Hagan, I.M. (2003). Physical and functional interactions between polo kinase and the spindle pole component Cut12 regulate mitotic commitment in *S. pombe*. *Genes & development* 17, 1507-1523.

Mah, A.S., Jang, J., and Deshaies, R.J. (2001). Protein kinase Cdc15 activates the Dbf2-Mob1 kinase complex. *Proceedings of the National Academy of Sciences of the United States of America* 98, 7325-7330.

Malumbres, M., and Barbacid, M. (2009). Cell cycle, CDKs and cancer: a changing paradigm. *Nature reviews Cancer* 9, 153-166.

Marks, J., Hagan, I.M., and Hyams, J.S. (1986). Growth polarity and cytokinesis in fission yeast: the role of the cytoskeleton. *Journal of cell science Supplement* 5, 229-241.

Martin, S.G., and Arkowitz, R.A. (2014). Cell polarization in budding and fission yeasts. *FEMS microbiology reviews* 38, 228-253.

Martin, S.G., and Berthelot-Grosjean, M. (2009). Polar gradients of the DYRK-family kinase Pom1 couple cell length with the cell cycle. *Nature* 459, 852-856.

Martin, S.G., and Chang, F. (2005). New end take off: regulating cell polarity during the fission yeast cell cycle. *Cell cycle (Georgetown, Tex)* 4, 1046-1049.

Martin-Cuadrado, A.B., Duenas, E., Sipiczki, M., Vazquez de Aldana, C.R., and del Rey, F. (2003). The endo-beta-1,3-glucanase eng1p is required for dissolution of the primary septum during cell separation in *Schizosaccharomyces pombe*. *Journal of cell science* 116, 1689-1698.

Martin-Cuadrado, A.B., Morrell, J.L., Konomi, M., An, H., Petit, C., Osumi, M., Balasubramanian, M., Gould, K.L., Del Rey, F., and de Aldana, C.R. (2005). Role of septins and the exocyst complex in the function of hydrolytic enzymes responsible for fission yeast cell separation. *Molecular biology of the cell* *16*, 4867-4881.

Martin-Garcia, R., Coll, P.M., and Perez, P. (2014). F-BAR domain protein Rga7 collaborates with Cdc15 and Imp2 to ensure proper cytokinesis in fission yeast. *Journal of cell science* *127*, 4146-4158.

Martin-Garcia, R., and Santos, B. (2016). The price of independence: cell separation in fission yeast. *World journal of microbiology & biotechnology* *32*, 65.

Matsuyama, A., Arai, R., Yashiroda, Y., Shirai, A., Kamata, A., Sekido, S., Kobayashi, Y., Hashimoto, A., Hamamoto, M., Hiraoka, Y., *et al.* (2006). ORFeome cloning and global analysis of protein localization in the fission yeast *Schizosaccharomyces pombe*. *Nature biotechnology* *24*, 841-847.

McKay, H.F., and Burgess, D.R. (2011). 'Life is a highway': membrane trafficking during cytokinesis. *Traffic (Copenhagen, Denmark)* *12*, 247-251.

McMurray, M.A., and Thorner, J. (2009). Septins: molecular partitioning and the generation of cellular asymmetry. *Cell division* *4*, 18.

Mehta, S., and Gould, K.L. (2006). Identification of functional domains within the septation initiation network kinase, Cdc7. *The Journal of biological chemistry* *281*, 9935-9941.

Meitinger, F., Boehm, M.E., Hofmann, A., Hub, B., Zentgraf, H., Lehmann, W.D., and Pereira, G. (2011). Phosphorylation-dependent regulation of the F-BAR protein Hof1 during cytokinesis. *Genes & development* *25*, 875-888.

Meitinger, F., Petrova, B., Lombardi, I.M., Bertazzi, D.T., Hub, B., Zentgraf, H., and Pereira, G. (2010). Targeted localization of Inn1, Cyk3 and Chs2 by the mitotic-exit network regulates cytokinesis in budding yeast. *Journal of cell science* *123*, 1851-1861.

Mendoza, M., Redemann, S., and Brunner, D. (2005). The fission yeast MO25 protein functions in polar growth and cell separation. *European journal of cell biology* *84*, 915-926.

Merlini, L., Dudin, O., and Martin, S.G. (2013). Mate and fuse: how yeast cells do it. *Open biology* *3*, 130008.

Mierzwa, B., and Gerlich, D.W. (2014). Cytokinetic abscission: molecular mechanisms and temporal control. *Dev Cell* *31*, 525-538.

Millar, J.B., Lenaers, G., and Russell, P. (1992). Pyp3 PTPase acts as a mitotic inducer in fission yeast. *The EMBO journal* *11*, 4933-4941.

Millar, J.B., McGowan, C.H., Lenaers, G., Jones, R., and Russell, P. (1991). p80cdc25 mitotic inducer is the tyrosine phosphatase that activates p34cdc2 kinase in fission yeast. *The EMBO journal* *10*, 4301-4309.

Miller, P.J., and Johnson, D.I. (1994). Cdc42p GTPase is involved in controlling polarized cell growth in *Schizosaccharomyces pombe*. *Molecular and cellular biology* *14*, 1075-1083.

Minet, M., Nurse, P., Thuriaux, P., and Mitchison, J.M. (1979). Uncontrolled septation in a cell division cycle mutant of the fission yeast *Schizosaccharomyces pombe*. *Journal of bacteriology* *137*, 440-446.

Miserey-Lenkei, S., Couedel-Courteille, A., Del Nery, E., Bardin, S., Piel, M., Racine, V., Sibarita, J.B., Perez, F., Bornens, M., and Goud, B. (2006). A role for the Rab6A'

GTPase in the inactivation of the Mad2-spindle checkpoint. *The EMBO journal* *25*, 278-289.

Mishra, M., Huang, J., and Balasubramanian, M.K. (2014). The yeast actin cytoskeleton. *FEMS microbiology reviews* *38*, 213-227.

Mishra, M., Karagiannis, J., Sevugan, M., Singh, P., and Balasubramanian, M.K. (2005). The 14-3-3 protein rad24p modulates function of the cdc14p family phosphatase clp1p/flp1p in fission yeast. *Current biology : CB* *15*, 1376-1383.

Mishra, M., Karagiannis, J., Trautmann, S., Wang, H., McCollum, D., and Balasubramanian, M.K. (2004). The Clp1p/Flp1p phosphatase ensures completion of cytokinesis in response to minor perturbation of the cell division machinery in *Schizosaccharomyces pombe*. *Journal of cell science* *117*, 3897-3910.

Mitchison, J.M. (1957). The growth of single cells. I. *Schizosaccharomyces pombe*. *Experimental cell research* *13*, 244-262.

Mitchison, J.M. (1970). Chapter 7 Physiological and Cytological Methods for *Schizosaccharomyces pombe*. In *Methods in Cell Biology*, M.P. David, ed. (Academic Press), pp. 131-165.

Mitchison, J.M., and Nurse, P. (1985). Growth in cell length in the fission yeast *Schizosaccharomyces pombe*. *Journal of cell science* *75*, 357-376.

Mojardin, L., Botet, J., Moreno, S., and Salas, M. (2015). Chromosome segregation and organization are targets of 5'-Fluorouracil in eukaryotic cells. *Cell cycle (Georgetown, Tex)* *14*, 206-218.

Monahan, B.J., Villen, J., Marguerat, S., Bahler, J., Gygi, S.P., and Winston, F. (2008). Fission yeast SWI/SNF and RSC complexes show compositional and functional differences from budding yeast. *Nature structural & molecular biology* *15*, 873-880.

Moorhead, G.B., De Wever, V., Templeton, G., and Kerk, D. (2009). Evolution of protein phosphatases in plants and animals. *The Biochemical journal* *417*, 401-409.

Moorhead, G.B., Trinkle-Mulcahy, L., and Ulke-Lemee, A. (2007). Emerging roles of nuclear protein phosphatases. *Nature reviews Molecular cell biology* *8*, 234-244.

Moreno, S., Klar, A., and Nurse, P. (1991). Molecular genetic analysis of fission yeast *Schizosaccharomyces pombe*. *Methods in enzymology* *194*, 795-823.

Moreno, S., and Nurse, P. (1991). Clues to action of cdc25 protein. *Nature* *351*, 194.

Moreno, S., and Nurse, P. (1994). Regulation of progression through the G1 phase of the cell cycle by the rum1+ gene. *Nature* *367*, 236-242.

Moreno, S., Nurse, P., and Russell, P. (1990). Regulation of mitosis by cyclic accumulation of p80cdc25 mitotic inducer in fission yeast. *Nature* *344*, 549-552.

Morgan, D.O. (1995). Principles of CDK regulation. *Nature* *374*, 131-134.

Morgan, D.O. (1997). Cyclin-dependent kinases: engines, clocks, and microprocessors. *Annual review of cell and developmental biology* *13*, 261-291.

Morrell, J.L., Nichols, C.B., and Gould, K.L. (2004a). The GIN4 family kinase, Cdr2p, acts independently of septins in fission yeast. *Journal of cell science* *117*, 5293-5302.

Morrell, J.L., Tomlin, G.C., Rajagopalan, S., Venkatram, S., Feoktistova, A.S., Tasto, J.J., Mehta, S., Jennings, J.L., Link, A., Balasubramanian, M.K., *et al.* (2004b). Sid4p-

Cdc11p assembles the septation initiation network and its regulators at the *S. pombe* SPB. *Current biology* : CB 14, 579-584.

Moseley, J.B., Mayeux, A., Paoletti, A., and Nurse, P. (2009). A spatial gradient coordinates cell size and mitotic entry in fission yeast. *Nature* 459, 857-860.

Motegi, F., Nakano, K., and Mabuchi, I. (2000). Molecular mechanism of myosin-II assembly at the division site in *Schizosaccharomyces pombe*. *Journal of cell science* 113 (Pt 10), 1813-1825.

Muller, S., and Jurgens, G. (2016). Plant cytokinesis-No ring, no constriction but centrifugal construction of the partitioning membrane. *Seminars in cell & developmental biology* 53, 10-18.

Mullins, J.M., and Biesele, J.J. (1977). Terminal phase of cytokinesis in D-98s cells. *J Cell Biol* 73, 672-684.

Mulvihill, D.P., Petersen, J., Ohkura, H., Glover, D.M., and Hagan, I.M. (1999). Plo1 kinase recruitment to the spindle pole body and its role in cell division in *Schizosaccharomyces pombe*. *Molecular biology of the cell* 10, 2771-2785.

Munoz, S., Manjon, E., and Sanchez, Y. (2014). The putative exchange factor Gef3p interacts with Rho3p GTPase and the septin ring during cytokinesis in fission yeast. *The Journal of biological chemistry* 289, 21995-22007.

Murone, M., and Simanis, V. (1996). The fission yeast *dma1* gene is a component of the spindle assembly checkpoint, required to prevent septum formation and premature exit from mitosis if spindle function is compromised. *The EMBO journal* 15, 6605-6616.

Naro, C., and Sette, C. (2013). Phosphorylation-mediated regulation of alternative splicing in cancer. *International journal of cell biology* 2013, 151839.

Nasmyth, K.A. (1979). A control acting over the initiation of DNA replication in the yeast *Schizosaccharomyces pombe*. *J Cell Sci* 36, 155-168.

Navarro, F.J., and Nurse, P. (2012). A systematic screen reveals new elements acting at the G2/M cell cycle control. *Genome Biol* 13, R36.

Nefsky, B., and Beach, D. (1996). Pub1 acts as an E6-AP-like protein ubiquitin ligase in the degradation of *cdc25*. *The EMBO journal* 15, 1301-1312.

Nelson, B., Kurischko, C., Horecka, J., Mody, M., Nair, P., Pratt, L., Zougman, A., McBroom, L.D., Hughes, T.R., Boone, C., *et al.* (2003). RAM: a conserved signaling network that regulates Ace2p transcriptional activity and polarized morphogenesis. *Molecular biology of the cell* 14, 3782-3803.

Ng, S.S., Papadopoulou, K., and McInerney, C.J. (2006). Regulation of gene expression and cell division by Polo-like kinases. *Current genetics* 50, 73-80.

Nishihama, R., Schreiter, J.H., Onishi, M., Vallen, E.A., Hanna, J., Moravcevic, K., Lippincott, M.F., Han, H., Lemmon, M.A., Pringle, J.R., *et al.* (2009). Role of Inn1 and its interactions with Hof1 and Cyk3 in promoting cleavage furrow and septum formation in *S. cerevisiae*. *The Journal of cell biology* 185, 995-1012.

Norden, C., Mendoza, M., Dobbelaere, J., Kotwaliwale, C.V., Biggins, S., and Barral, Y. (2006). The NoCut pathway links completion of cytokinesis to spindle midzone function to prevent chromosome breakage. *Cell* 125, 85-98.

Normand, G., and King, R.W. (2010). Understanding cytokinesis failure. *Advances in experimental medicine and biology* 676, 27-55.

Nurse, P. (1975). Genetic control of cell size at cell division in yeast. *Nature* 256, 547-551.

Nurse, P. (1990). Universal control mechanism regulating onset of M-phase. *Nature* 344, 503-508.

Nurse, P., and Bissett, Y. (1981). Gene required in G1 for commitment to cell cycle and in G2 for control of mitosis in fission yeast. *Nature* 292, 558-560.

Nurse, P., and Thuriaux, P. (1977). Controls over the timing of DNA replication during the cell cycle of fission yeast. *Exp Cell Res* 107, 365-375.

Nurse, P., and Thuriaux, P. (1980). Regulatory genes controlling mitosis in the fission yeast *Schizosaccharomyces pombe*. *Genetics* 96, 627-637.

Nurse, P., Thuriaux, P., and Nasmyth, K. (1976). Genetic control of the cell division cycle in the fission yeast *Schizosaccharomyces pombe*. *Molecular & general genetics : MGG* 146, 167-178.

Ohkura, H., Adachi, Y., Kinoshita, N., Niwa, O., Toda, T., and Yanagida, M. (1988). Cold-sensitive and caffeine-supersensitive mutants of the *Schizosaccharomyces pombe* dis genes implicated in sister chromatid separation during mitosis. *The EMBO journal* 7, 1465-1473.

Ohkura, H., Hagan, I.M., and Glover, D.M. (1995). The conserved *Schizosaccharomyces pombe* kinase *plp1*, required to form a bipolar spindle, the actin ring, and septum, can drive septum formation in G1 and G2 cells. *Genes & development* 9, 1059-1073.

Ohkura, H., Kinoshita, N., Miyatani, S., Toda, T., and Yanagida, M. (1989). The fission yeast *dis2+* gene required for chromosome disjoining encodes one of two putative type 1 protein phosphatases. *Cell* 57, 997-1007.

Ohkura, H., and Yanagida, M. (1991). *S. pombe* gene *sds22+* essential for a midmitotic transition encodes a leucine-rich repeat protein that positively modulates protein phosphatase-1. *Cell* 64, 149-157.

Oliferenko, S., and Balasubramanian, M.K. (2001). Cell cycle: the Flp side of *Cdc14*. *Curr Biol* 11, R872-874.

Oliferenko, S., Chew, T.G., and Balasubramanian, M.K. (2009). Positioning cytokinesis. *Genes & development* 23, 660-674.

Onishi, M., Ko, N., Nishihama, R., and Pringle, J.R. (2013). Distinct roles of *Rho1*, *Cdc42*, and *Cyk3* in septum formation and abscission during yeast cytokinesis. *The Journal of cell biology* 202, 311-329.

Onishi, M., Koga, T., Hirata, A., Nakamura, T., Asakawa, H., Shimoda, C., Bahler, J., Wu, J.Q., Takegawa, K., Tachikawa, H., *et al.* (2010). Role of septins in the orientation of forespore membrane extension during sporulation in fission yeast. *Molecular and cellular biology* 30, 2057-2074.

Osman, F., and McCreedy, S. (1998). Differential effects of caffeine on DNA damage and replication cell cycle checkpoints in the fission yeast *Schizosaccharomyces pombe*. *Molecular & general genetics : MGG* 260, 319-334.

Padmanabhan, A., Bakka, K., Sevugan, M., Naqvi, N.I., D'Souza, V., Tang, X., Mishra, M., and Balasubramanian, M.K. (2011). IQGAP-related *Rng2p* organizes cortical nodes and ensures position of cell division in fission yeast. *Current biology : CB* 21, 467-472.

Padte, N.N., Martin, S.G., Howard, M., and Chang, F. (2006). The cell-end factor *pom1p* inhibits *mid1p* in specification of the cell division plane in fission yeast. *Current biology : CB* 16, 2480-2487.

Painter, R.B. (1986). Inhibition of mammalian cell DNA synthesis by ionizing radiation. *International journal of radiation biology and related studies in physics, chemistry, and medicine* 49, 771-781.

Pan, X., Lei, B., Zhou, N., Feng, B., Yao, W., Zhao, X., Yu, Y., and Lu, H. (2012). Identification of novel genes involved in DNA damage response by screening a

genome-wide *Schizosaccharomyces pombe* deletion library. *BMC genomics* *13*, 662.

Paoletti, A., and Chang, F. (2000). Analysis of mid1p, a protein required for placement of the cell division site, reveals a link between the nucleus and the cell surface in fission yeast. *Molecular biology of the cell* *11*, 2757-2773.

Pardee, A.B. (1974). A restriction point for control of normal animal cell proliferation. *Proceedings of the National Academy of Sciences of the United States of America* *71*, 1286-1290.

Paulovich, A.G., and Hartwell, L.H. (1995). A checkpoint regulates the rate of progression through S phase in *S. cerevisiae* in response to DNA damage. *Cell* *82*, 841-847.

Peggie, M.W., MacKelvie, S.H., Bloecher, A., Knatko, E.V., Tatchell, K., and Stark, M.J. (2002). Essential functions of Sds22p in chromosome stability and nuclear localization of PP1. *Journal of cell science* *115*, 195-206.

Pereira, G., Hofken, T., Grindlay, J., Manson, C., and Schiebel, E. (2000). The Bub2p spindle checkpoint links nuclear migration with mitotic exit. *Molecular cell* *6*, 1-10.

Pereira, G., Manson, C., Grindlay, J., and Schiebel, E. (2002). Regulation of the Bfa1p-Bub2p complex at spindle pole bodies by the cell cycle phosphatase Cdc14p. *The Journal of cell biology* *157*, 367-379.

Pereira, G., and Schiebel, E. (2005). Kin4 kinase delays mitotic exit in response to spindle alignment defects. *Molecular cell* *19*, 209-221.

Pereira, G., Tanaka, T.U., Nasmyth, K., and Schiebel, E. (2001). Modes of spindle pole body inheritance and segregation of the Bfa1p-Bub2p checkpoint protein complex. *The EMBO journal* *20*, 6359-6370.

Pereira, G., and Yamashita, Y.M. (2011). Fly meets yeast: checking the correct orientation of cell division. *Trends in cell biology* *21*, 526-533.

Perez, P., Cortes, J.C., Martin-Garcia, R., and Ribas, J.C. (2016). Overview of Fission Yeast Septation. *Cellular microbiology*.

Perez, P., Portales, E., and Santos, B. (2015). Rho4 interaction with exocyst and septins regulates cell separation in fission yeast. *Microbiology (Reading, England)* *161*, 948-959.

Perez-Hidalgo, L., Rozalen, A.E., Martin-Castellanos, C., and Moreno, S. (2008). Slk1 is a meiosis-specific Sid2-related kinase that coordinates meiotic nuclear division with growth of the forespore membrane. *Journal of cell science* *121*, 1383-1392.

Petersen, J., Heitz, M.J., and Hagan, I.M. (1998). Conjugation in *S. pombe*: identification of a microtubule-organising centre, a requirement for microtubules and a role for Mad2. *Current biology : CB* *8*, 963-966.

Petersen, J., and Nurse, P. (2007). TOR signalling regulates mitotic commitment through the stress MAP kinase pathway and the Polo and Cdc2 kinases. *Nature cell biology* *9*, 1263-1272.

Peti, W., Nairn, A.C., and Page, R. (2013). Structural basis for protein phosphatase 1 regulation and specificity. *The FEBS journal* *280*, 596-611.

Piekny, A.J., and Glotzer, M. (2008). Anillin is a scaffold protein that links RhoA, actin, and myosin during cytokinesis. *Current biology : CB* *18*, 30-36.

Pinar, M., Coll, P.M., Rincon, S.A., and Perez, P. (2008). *Schizosaccharomyces pombe* Pxl1 is a paxillin homologue that modulates Rho1 activity and participates in cytokinesis. *Molecular biology of the cell* *19*, 1727-1738.

Plochocka-Zulinska, D., Rasmussen, G., and Rasmussen, C. (1995). Regulation of calcineurin gene expression in *Schizosaccharomyces pombe*. Dependence on the ste11 transcription factor. *The Journal of biological chemistry* 270, 24794-24799.

Proctor, S.A., Minc, N., Boudaoud, A., and Chang, F. (2012). Contributions of turgor pressure, the contractile ring, and septum assembly to forces in cytokinesis in fission yeast. *Current biology : CB* 22, 1601-1608.

Pruyne, D., Legesse-Miller, A., Gao, L., Dong, Y., and Bretscher, A. (2004). Mechanisms of polarized growth and organelle segregation in yeast. *Annual review of cell and developmental biology* 20, 559-591.

Rachfall, N., Johnson, A.E., Mehta, S., Chen, J.S., and Gould, K.L. (2014). Cdk1 promotes cytokinesis in fission yeast through activation of the septation initiation network. *Molecular biology of the cell* 25, 2250-2259.

Raleigh, J.M., and O'Connell, M.J. (2000). The G(2) DNA damage checkpoint targets both Wee1 and Cdc25. *Journal of cell science* 113 (Pt 10), 1727-1736.

Rallis, C., Lopez-Maury, L., Georgescu, T., Pancaldi, V., and Bahler, J. (2014). Systematic screen for mutants resistant to TORC1 inhibition in fission yeast reveals genes involved in cellular ageing and growth. *Biology open* 3, 161-171.

Rasmussen, C.G., Wright, A.J., and Muller, S. (2013). The role of the cytoskeleton and associated proteins in determination of the plant cell division plane. *The Plant journal : for cell and molecular biology* 75, 258-269.

Ray, S., Kume, K., Gupta, S., Ge, W., Balasubramanian, M., Hirata, D., and McCollum, D. (2010). The mitosis-to-interphase transition is coordinated by cross talk between the SIN and MOR pathways in *Schizosaccharomyces pombe*. *The Journal of cell biology* 190, 793-805.

Rehman, A., Archbold, J.K., Hu, S.H., Norwood, S.J., Collins, B.M., and Martin, J.L. (2014). Reconciling the regulatory role of Munc18 proteins in SNARE-complex assembly. *IUCrj* 1, 505-513.

Ren, L., Willet, A.H., Roberts-Galbraith, R.H., McDonald, N.A., Feoktistova, A., Chen, J.S., Huang, H., Guillen, R., Boone, C., Sidhu, S.S., *et al.* (2015). The Cdc15 and Imp2 SH3 domains cooperatively scaffold a network of proteins that redundantly ensure efficient cell division in fission yeast. *Molecular biology of the cell* 26, 256-269.

Ribar, B., Banrevi, A., and Sipiczki, M. (1997). sep1+ encodes a transcription-factor homologue of the HNF-3/forkhead DNA-binding-domain family in *Schizosaccharomyces pombe*. *Gene* 202, 1-5.

Rivals, I., Personnaz, L., Taing, L., and Potier, M.-C. (2007). Enrichment or depletion of a GO category within a class of genes: which test? *Bioinformatics* 23, 401-407.

Roberts-Galbraith, R.H., Chen, J.S., Wang, J., and Gould, K.L. (2009). The SH3 domains of two PCH family members cooperate in assembly of the *Schizosaccharomyces pombe* contractile ring. *The Journal of cell biology* 184, 113-127.

Roberts-Galbraith, R.H., and Gould, K.L. (2008). Stepping into the ring: the SIN takes on contractile ring assembly. *Genes & development* 22, 3082-3088.

Roguev, A., Wiren, M., Weissman, J.S., and Krogan, N.J. (2007). High-throughput genetic interaction mapping in the fission yeast *Schizosaccharomyces pombe*. *Nature methods* 4, 861-866.

Rosenberg, J.A., Tomlin, G.C., McDonald, W.H., Snyderman, B.E., Muller, E.G., Yates, J.R., 3rd, and Gould, K.L. (2006). Ppc89 links multiple proteins, including the

septation initiation network, to the core of the fission yeast spindle-pole body. *Molecular biology of the cell* 17, 3793-3805.

Roussou, I., and Draetta, G. (1994). The Schizosaccharomyces pombe casein kinase II alpha and beta subunits: evolutionary conservation and positive role of the beta subunit. *Molecular and cellular biology* 14, 576-586.

Russell, P., and Nurse, P. (1986). cdc25+ functions as an inducer in the mitotic control of fission yeast. *Cell* 45, 145-153.

Russell, P., and Nurse, P. (1987a). The mitotic inducer nim1+ functions in a regulatory network of protein kinase homologs controlling the initiation of mitosis. *Cell* 49, 569-576.

Russell, P., and Nurse, P. (1987b). Negative regulation of mitosis by wee1+, a gene encoding a protein kinase homolog. *Cell* 49, 559-567.

Rustici, G., Mata, J., Kivinen, K., Lio, P., Penkett, C.J., Burns, G., Hayles, J., Brazma, A., Nurse, P., and Bahler, J. (2004). Periodic gene expression program of the fission yeast cell cycle. *Nature genetics* 36, 809-817.

Ryan, C.J., Roguev, A., Patrick, K., Xu, J., Jahari, H., Tong, Z., Beltrao, P., Shales, M., Qu, H., Collins, S.R., *et al.* (2012). Hierarchical modularity and the evolution of genetic interactomes across species. *Molecular cell* 46, 691-704.

Salimova, E., Sohrmann, M., Fournier, N., and Simanis, V. (2000). The S. pombe orthologue of the S. cerevisiae mob1 gene is essential and functions in signalling the onset of septum formation. *Journal of cell science* 113 (Pt 10), 1695-1704.

Sambrook, J., Fritsch, E.F., and Maniatis, T. (1989). *Molecular cloning*, 2nd Ed. edn (New York: Cold Spring Harbor Laboratory Press).

Samuels, A.L., Giddings, T.H., Jr., and Staehelin, L.A. (1995). Cytokinesis in tobacco BY-2 and root tip cells: a new model of cell plate formation in higher plants. *The Journal of cell biology* 130, 1345-1357.

Sanchez, Y., Wong, C., Thoma, R.S., Richman, R., Wu, Z., Piwnicka-Worms, H., and Elledge, S.J. (1997). Conservation of the Chk1 checkpoint pathway in mammals: linkage of DNA damage to Cdk regulation through Cdc25. *Science (New York, NY)* 277, 1497-1501.

Sangodkar, J., Farrington, C.C., McClinch, K., Galsky, M.D., Kastrinsky, D.B., and Narla, G. (2016). All roads lead to PP2A: exploiting the therapeutic potential of this phosphatase. *The FEBS journal* 283, 1004-1024.

Santos, B., Martin-Cuadrado, A.B., Vazquez de Aldana, C.R., del Rey, F., and Perez, P. (2005). Rho4 GTPase is involved in secretion of glucanases during fission yeast cytokinesis. *Eukaryotic cell* 4, 1639-1645.

Saraya, R., Cepinska, M.N., Kiel, J.A., Veenhuis, M., and van der Klei, I.J. (2010). A conserved function for Inp2 in peroxisome inheritance. *Biochimica et biophysica acta* 1803, 617-622.

Sasabe, M., Boudolf, V., De Veylder, L., Inze, D., Genschik, P., and Machida, Y. (2011). Phosphorylation of a mitotic kinesin-like protein and a MAPKKK by cyclin-dependent kinases (CDKs) is involved in the transition to cytokinesis in plants. *Proceedings of the National Academy of Sciences of the United States of America* 108, 17844-17849.

Sasabe, M., and Machida, Y. (2006). MAP65: a bridge linking a MAP kinase to microtubule turnover. *Current opinion in plant biology* 9, 563-570.

Sburlati, A., and Cabib, E. (1986). Chitin synthetase 2, a presumptive participant in septum formation in Saccharomyces cerevisiae. *The Journal of biological chemistry* 261, 15147-15152.

Schiebel, E. (2000). gamma-tubulin complexes: binding to the centrosome, regulation and microtubule nucleation. *Current opinion in cell biology* *12*, 113-118.

Schmidt, M., Bowers, B., Varma, A., Roh, D.H., and Cabib, E. (2002). In budding yeast, contraction of the actomyosin ring and formation of the primary septum at cytokinesis depend on each other. *Journal of cell science* *115*, 293-302.

Schmidt, S., Sohrmann, M., Hofmann, K., Woollard, A., and Simanis, V. (1997). The Spg1p GTPase is an essential, dosage-dependent inducer of septum formation in *Schizosaccharomyces pombe*. *Genes & development* *11*, 1519-1534.

Schuldiner, O., Eden, A., Ben-Yosef, T., Yanuka, O., Simchen, G., and Benvenisty, N. (1996). ECA39, a conserved gene regulated by c-Myc in mice, is involved in G1/S cell cycle regulation in yeast. *Proceedings of the National Academy of Sciences of the United States of America* *93*, 7143-7148.

Schwab, M., Lutum, A.S., and Seufert, W. (1997). Yeast Hct1 is a regulator of Clb2 cyclin proteolysis. *Cell* *90*, 683-693.

Sents, W., Ivanova, E., Lambrecht, C., Haesen, D., and Janssens, V. (2013). The biogenesis of active protein phosphatase 2A holoenzymes: a tightly regulated process creating phosphatase specificity. *The FEBS journal* *280*, 644-661.

Seshacharyulu, P., Pandey, P., Datta, K., and Batra, S.K. (2013). Phosphatase: PP2A structural importance, regulation and its aberrant expression in cancer. *Cancer letters* *335*, 9-18.

Shannon, K.B., and Li, R. (1999). The multiple roles of Cyk1p in the assembly and function of the actomyosin ring in budding yeast. *Molecular biology of the cell* *10*, 283-296.

Shannon, K.B., and Li, R. (2000). A myosin light chain mediates the localization of the budding yeast IQGAP-like protein during contractile ring formation. *Current biology : CB* *10*, 727-730.

Shimanuki, M., Chung, S.Y., Chikashige, Y., Kawasaki, Y., Uehara, L., Tsutsumi, C., Hatanaka, M., Hiraoka, Y., Nagao, K., and Yanagida, M. (2007). Two-step, extensive alterations in the transcriptome from G0 arrest to cell division in *Schizosaccharomyces pombe*. *Genes to cells : devoted to molecular & cellular mechanisms* *12*, 677-692.

Shirayama, M., Toth, A., Galova, M., and Nasmyth, K. (1999). APC(Cdc20) promotes exit from mitosis by destroying the anaphase inhibitor Pds1 and cyclin Clb5. *Nature* *402*, 203-207.

Shou, W., Azzam, R., Chen, S.L., Huddleston, M.J., Baskerville, C., Charbonneau, H., Annan, R.S., Carr, S.A., and Deshaies, R.J. (2002). Cdc5 influences phosphorylation of Net1 and disassembly of the RENT complex. *BMC molecular biology* *3*, 3.

Shou, W., Seol, J.H., Shevchenko, A., Baskerville, C., Moazed, D., Chen, Z.W., Jang, J., Shevchenko, A., Charbonneau, H., and Deshaies, R.J. (1999). Exit from mitosis is triggered by Tem1-dependent release of the protein phosphatase Cdc14 from nucleolar RENT complex. *Cell* *97*, 233-244.

Sif, S., Stukenberg, P.T., Kirschner, M.W., and Kingston, R.E. (1998). Mitotic inactivation of a human SWI/SNF chromatin remodeling complex. *Genes & development* *12*, 2842-2851.

Silar, P., and Thiele, D.J. (1991). New shuttle vectors for direct cloning in *Saccharomyces cerevisiae*. *Gene* *104*, 99-102.

Simanis, V. (2015). *Pombe's thirteen* - control of fission yeast cell division by the septation initiation network. *Journal of cell science* *128*, 1465-1474.

Singh, N.S., Shao, N., McLean, J.R., Sevugan, M., Ren, L., Chew, T.G., Bimbo, A., Sharma, R., Tang, X., Gould, K.L., *et al.* (2011). SIN-inhibitory phosphatase complex promotes Cdc11p dephosphorylation and propagates SIN asymmetry in fission yeast. *Current biology : CB* *21*, 1968-1978.

Sio, S.O., Suehiro, T., Sugiura, R., Takeuchi, M., Mukai, H., and Kuno, T. (2005). The role of the regulatory subunit of fission yeast calcineurin for in vivo activity and its relevance to FK506 sensitivity. *The Journal of biological chemistry* *280*, 12231-12238.

Sipiczki, M., and Bozsik, A. (2000). The use of morphomutants to investigate septum formation and cell separation in *Schizosaccharomyces pombe*. *Archives of microbiology* *174*, 386-392.

Sipiczki, M., Grallert, B., and Miklos, I. (1993). Mycelial and syncytial growth in *Schizosaccharomyces pombe* induced by novel septation mutations. *Journal of cell science* *104 (Pt 2)*, 485-493.

Skop, A.R., Liu, H., Yates, J., 3rd, Meyer, B.J., and Heald, R. (2004). Dissection of the mammalian midbody proteome reveals conserved cytokinesis mechanisms. *Science* *305*, 61-66.

Smedley, D., Haider, S., Durinck, S., Pandini, L., Provero, P., Allen, J., Arnaiz, O., Awedh, M.H., Baldock, R., Barbiera, G., *et al.* (2015). The BioMart community portal: an innovative alternative to large, centralized data repositories. *Nucleic acids research* *43*, W589-598.

Smertenko, A.P., Deeks, M.J., and Hussey, P.J. (2010). Strategies of actin reorganisation in plant cells. *Journal of cell science* *123*, 3019-3028.

Smertenko, A.P., Piette, B., and Hussey, P.J. (2011). The origin of phragmoplast asymmetry. *Current biology : CB* *21*, 1924-1930.

Smith, G.R. (2009). Genetic analysis of meiotic recombination in *Schizosaccharomyces pombe*. *Methods in molecular biology (Clifton, NJ)* *557*, 65-76.

Snell, V., and Nurse, P. (1993). Investigations into the control of cell form and polarity: the use of morphological mutants in fission yeast. *Development (Cambridge, England) Supplement*, 289-299.

Snell, V., and Nurse, P. (1994). Genetic analysis of cell morphogenesis in fission yeast--a role for casein kinase II in the establishment of polarized growth. *The EMBO journal* *13*, 2066-2074.

Sohrmann, M., Fankhauser, C., Brodbeck, C., and Simanis, V. (1996). The *dmf1/mid1* gene is essential for correct positioning of the division septum in fission yeast. *Genes & development* *10*, 2707-2719.

Sohrmann, M., Schmidt, S., Hagan, I., and Simanis, V. (1998). Asymmetric segregation on spindle poles of the *Schizosaccharomyces pombe* septum-inducing protein kinase Cdc7p. *Genes & development* *12*, 84-94.

Somers, W.G., and Saint, R. (2003). A RhoGEF and Rho family GTPase-activating protein complex links the contractile ring to cortical microtubules at the onset of cytokinesis. *Dev Cell* *4*, 29-39.

Son, S., Tzur, A., Weng, Y., Jorgensen, P., Kim, J., Kirschner, M.W., and Manalis, S.R. (2012). Direct observation of mammalian cell growth and size regulation. *Nature methods* *9*, 910-912.

Song, K., Mach, K.E., Chen, C.Y., Reynolds, T., and Albright, C.F. (1996). A novel suppressor of *ras1* in fission yeast, *byr4*, is a dosage-dependent inhibitor of cytokinesis. *The Journal of cell biology* *133*, 1307-1319.

Sontag, J.M., and Sontag, E. (2014). Protein phosphatase 2A dysfunction in Alzheimer's disease. *Frontiers in molecular neuroscience* 7, 16.

Sparks, C.A., Morphew, M., and McCollum, D. (1999). Sid2p, a spindle pole body kinase that regulates the onset of cytokinesis. *The Journal of cell biology* 146, 777-790.

Staehelin, L.A., and Hepler, P.K. (1996). Cytokinesis in higher plants. *Cell* 84, 821-824.

Stark, C., Breitzkreutz, B.J., Reguly, T., Boucher, L., Breitzkreutz, A., and Tyers, M. (2006). BioGRID: a general repository for interaction datasets. *Nucleic acids research* 34, D535-539.

Stearns, T., Evans, L., and Kirschner, M. (1991). Gamma-tubulin is a highly conserved component of the centrosome. *Cell* 65, 825-836.

Stegmeier, F., Visintin, R., and Amon, A. (2002). Separase, polo kinase, the kinetochore protein Slk19, and Spo12 function in a network that controls Cdc14 localization during early anaphase. *Cell* 108, 207-220.

Steigemann, P., and Gerlich, D.W. (2009). Cytokinetic abscission: cellular dynamics at the midbody. *Trends in cell biology* 19, 606-616.

Stone, E.M., Yamano, H., Kinoshita, N., and Yanagida, M. (1993). Mitotic regulation of protein phosphatases by the fission yeast sds22 protein. *Current biology : CB* 3, 13-26.

Streiblova, E., and Wolf, A. (1972). Cell wall growth during the cell cycle of *Schizosaccharomyces pombe*. *Zeitschrift fur allgemeine Mikrobiologie* 12, 673-684.

Styrkarsdottir, U., Egel, R., and Nielsen, O. (1993). The smt-0 mutation which abolishes mating-type switching in fission yeast is a deletion. *Current genetics* 23, 184-186.

Sudhof, T.C., and Rothman, J.E. (2009). Membrane fusion: grappling with SNARE and SM proteins. *Science (New York, NY)* 323, 474-477.

Sugawara, T., Sato, M., Takagi, T., Kamasaki, T., Ohno, N., and Osumi, M. (2003). In situ localization of cell wall alpha-1,3-glucan in the fission yeast *Schizosaccharomyces pombe*. *Journal of electron microscopy* 52, 237-242.

Sugiura, R., Sio, S.O., Shuntoh, H., and Kuno, T. (2002). Calcineurin phosphatase in signal transduction: lessons from fission yeast. *Genes to cells : devoted to molecular & cellular mechanisms* 7, 619-627.

Sugiura, R., Toda, T., Shuntoh, H., Yanagida, M., and Kuno, T. (1998). pmp1+, a suppressor of calcineurin deficiency, encodes a novel MAP kinase phosphatase in fission yeast. *The EMBO journal* 17, 140-148.

Sur, S., and Agrawal, D.K. (2016). Phosphatases and kinases regulating CDC25 activity in the cell cycle: clinical implications of CDC25 overexpression and potential treatment strategies. *Molecular and cellular biochemistry* 416, 33-46.

Sveiczzer, A., Novak, B., and Mitchison, J.M. (1996). The size control of fission yeast revisited. *Journal of cell science* 109 (Pt 12), 2947-2957.

Szankasi, P., Heyer, W.D., Schuchert, P., and Kohli, J. (1988). DNA sequence analysis of the ade6 gene of *Schizosaccharomyces pombe*. Wild-type and mutant alleles including the recombination host spot allele ade6-M26. *Journal of molecular biology* 204, 917-925.

Tajadura, V., Garcia, B., Garcia, I., Garcia, P., and Sanchez, Y. (2004). *Schizosaccharomyces pombe* Rgf3p is a specific Rho1 GEF that regulates cell wall

beta-glucan biosynthesis through the GTPase Rho1p. *Journal of cell science* *117*, 6163-6174.

Tamm, T., Grallert, A., Grossman, E.P., Alvarez-Tabares, I., Stevens, F.E., and Hagan, I.M. (2011). Brr6 drives the *Schizosaccharomyces pombe* spindle pole body nuclear envelope insertion/extrusion cycle. *The Journal of cell biology* *195*, 467-484.

Tanaka, K., and Okayama, H. (2000). A *pcl*-like cyclin activates the Res2p-Cdc10p cell cycle "start" transcriptional factor complex in fission yeast. *Molecular biology of the cell* *11*, 2845-2862.

Tanaka, K., Petersen, J., MacIver, F., Mulvihill, D.P., Glover, D.M., and Hagan, I.M. (2001). The role of Plo1 kinase in mitotic commitment and septation in *Schizosaccharomyces pombe*. *The EMBO journal* *20*, 1259-1270.

Tarrant, M.K., Rho, H.S., Xie, Z., Jiang, Y.L., Gross, C., Culhane, J.C., Yan, G., Qian, J., Ichikawa, Y., Matsuoka, T., *et al.* (2012). Regulation of CK2 by phosphorylation and O-GlcNAcylation revealed by semisynthesis. *Nature chemical biology* *8*, 262-269.

Tasto, J.J., Morrell, J.L., and Gould, K.L. (2003). An anillin homologue, Mid2p, acts during fission yeast cytokinesis to organize the septin ring and promote cell separation. *The Journal of cell biology* *160*, 1093-1103.

Tay, Z., Eng, R.J., Sajiki, K., Lim, K.K., Tang, M.Y., Yanagida, M., and Chen, E.S. (2013). Cellular robustness conferred by genetic crosstalk underlies resistance against chemotherapeutic drug doxorubicin in fission yeast. *PloS one* *8*, e55041.

Taylor, W.R., and Stark, G.R. (2001). Regulation of the G2/M transition by p53. *Oncogene* *20*, 1803-1815.

Thiele, K., Wanner, G., Kindzierski, V., Jurgens, G., Mayer, U., Pachl, F., and Assaad, F.F. (2009). The timely deposition of callose is essential for cytokinesis in *Arabidopsis*. *The Plant journal : for cell and molecular biology* *58*, 13-26.

Thiyagarajan, S., Munteanu, E.L., Arasada, R., Pollard, T.D., and O'Shaughnessy, B. (2015). The fission yeast cytokinetic contractile ring regulates septum shape and closure. *Journal of cell science* *128*, 3672-3681.

Toda, T., Dhut, S., Superti-Furga, G., Gotoh, Y., Nishida, E., Sugiura, R., and Kuno, T. (1996). The fission yeast *pmk1+* gene encodes a novel mitogen-activated protein kinase homolog which regulates cell integrity and functions coordinately with the protein kinase C pathway. *Molecular and cellular biology* *16*, 6752-6764.

Tolic-Norrelykke, I.M., Sacconi, L., Stringari, C., Raabe, I., and Pavone, F.S. (2005). Nuclear and division-plane positioning revealed by optical micromanipulation. *Current biology : CB* *15*, 1212-1216.

Tolliday, N., VerPlank, L., and Li, R. (2002). Rho1 directs formin-mediated actin ring assembly during budding yeast cytokinesis. *Current biology : CB* *12*, 1864-1870.

Toyn, J.H., and Johnston, L.H. (1994). The Dbf2 and Dbf20 protein kinases of budding yeast are activated after the metaphase to anaphase cell cycle transition. *The EMBO journal* *13*, 1103-1113.

Tran, P.T., Marsh, L., Doye, V., Inoue, S., and Chang, F. (2001). A mechanism for nuclear positioning in fission yeast based on microtubule pushing. *The Journal of cell biology* *153*, 397-411.

Trautmann, S., and McCollum, D. (2005). Distinct nuclear and cytoplasmic functions of the *S. pombe* Cdc14-like phosphatase Clp1p/Flp1p and a role for nuclear shuttling in its regulation. *Current biology : CB* *15*, 1384-1389.

Trautmann, S., Rajagopalan, S., and McCollum, D. (2004). The *S. pombe* Cdc14-like phosphatase Clp1p regulates chromosome biorientation and interacts with Aurora kinase. *Developmental cell* 7, 755-762.

Trautmann, S., Wolfe, B.A., Jorgensen, P., Tyers, M., Gould, K.L., and McCollum, D. (2001). Fission yeast Clp1p phosphatase regulates G2/M transition and coordination of cytokinesis with cell cycle progression. *Current biology : CB* 11, 931-940.

Tretter, L., and Adam-Vizi, V. (2005). Alpha-ketoglutarate dehydrogenase: a target and generator of oxidative stress. *Philosophical transactions of the Royal Society of London Series B, Biological sciences* 360, 2335-2345.

Trinkle-Mulcahy, L., and Lamond, A.I. (2006). Mitotic phosphatases: no longer silent partners. *Current opinion in cell biology* 18, 623-631.

Ucisik-Akkaya, E., Leatherwood, J.K., and Neiman, A.M. (2014). A genome-wide screen for sporulation-defective mutants in *Schizosaccharomyces pombe*. *G3 (Bethesda, Md)* 4, 1173-1182.

Uehara, R., Goshima, G., Mabuchi, I., Vale, R.D., Spudich, J.A., and Griffis, E.R. (2010). Determinants of myosin II cortical localization during cytokinesis. *Curr Biol* 20, 1080-1085.

Van Damme, D., Gadeyne, A., Vanstraelen, M., Inze, D., Van Montagu, M.C., De Jaeger, G., Russinova, E., and Geelen, D. (2011). Adaptin-like protein TPLATE and clathrin recruitment during plant somatic cytokinesis occurs via two distinct pathways. *Proceedings of the National Academy of Sciences of the United States of America* 108, 615-620.

van Zyl, W., Huang, W., Sneddon, A.A., Stark, M., Camier, S., Werner, M., Marck, C., Sentenac, A., and Broach, J.R. (1992). Inactivation of the protein phosphatase 2A regulatory subunit A results in morphological and transcriptional defects in *Saccharomyces cerevisiae*. *Molecular and cellular biology* 12, 4946-4959.

Vardy, L., Fujita, A., and Toda, T. (2002). The gamma-tubulin complex protein Alp4 provides a link between the metaphase checkpoint and cytokinesis in fission yeast. *Genes to cells : devoted to molecular & cellular mechanisms* 7, 365-373.

Vavylonis, D., Wu, J.Q., Hao, S., O'Shaughnessy, B., and Pollard, T.D. (2008). Assembly mechanism of the contractile ring for cytokinesis by fission yeast. *Science (New York, NY)* 319, 97-100.

Verde, F., Mata, J., and Nurse, P. (1995). Fission yeast cell morphogenesis: identification of new genes and analysis of their role during the cell cycle. *The Journal of cell biology* 131, 1529-1538.

Verde, F., Wiley, D.J., and Nurse, P. (1998). Fission yeast orb6, a ser/thr protein kinase related to mammalian rho kinase and myotonic dystrophy kinase, is required for maintenance of cell polarity and coordinates cell morphogenesis with the cell cycle. *Proceedings of the National Academy of Sciences of the United States of America* 95, 7526-7531.

Verlhac, M.H., and Terret, M.E. (2016). Oocyte Maturation and Development. *F1000Research* 5.

Vermeulen, K., Van Bockstaele, D.R., and Berneman, Z.N. (2003). The cell cycle: a review of regulation, deregulation and therapeutic targets in cancer. *Cell proliferation* 36, 131-149.

VerPlank, L., and Li, R. (2005). Cell cycle-regulated trafficking of Chs2 controls actomyosin ring stability during cytokinesis. *Molecular biology of the cell* *16*, 2529-2543.

Vigil, D., Cherfils, J., Rossman, K.L., and Der, C.J. (2010). Ras superfamily GEFs and GAPs: validated and tractable targets for cancer therapy? *Nature reviews Cancer* *10*, 842-857.

Visintin, R., and Amon, A. (2001). Regulation of the mitotic exit protein kinases Cdc15 and Dbf2. *Molecular biology of the cell* *12*, 2961-2974.

Visintin, R., Stegmeier, F., and Amon, A. (2003). The role of the polo kinase Cdc5 in controlling Cdc14 localization. *Molecular biology of the cell* *14*, 4486-4498.

Wachowicz, P., Chasapi, A., Krapp, A., Cano Del Rosario, E., Schmitter, D., Sage, D., Unser, M., Xenarios, I., Rougemont, J., and Simanis, V. (2015). Analysis of *S. pombe* SIN protein association to the SPB reveals two genetically separable states of the SIN. *Journal of cell science* *128*, 741-754.

Walde, S., and King, M.C. (2014). The KASH protein Kms2 coordinates mitotic remodeling of the spindle pole body. *Journal of cell science* *127*, 3625-3640.

Walker, G.M. (1982). Cell cycle specificity of certain antimicrotubular drugs in *Schizosaccharomyces pombe*. *Journal of general microbiology* *128*, 61-71.

Wang, H., Tang, X., and Balasubramanian, M.K. (2003a). Rho3p regulates cell separation by modulating exocyst function in *Schizosaccharomyces pombe*. *Genetics* *164*, 1323-1331.

Wang, H., Tang, X., Liu, J., Trautmann, S., Balasundaram, D., McCollum, D., and Balasubramanian, M.K. (2002). The multiprotein exocyst complex is essential for cell separation in *Schizosaccharomyces pombe*. *Molecular biology of the cell* *13*, 515-529.

Wang, N., Wang, M., Zhu, Y.H., Grosel, T.W., Sun, D., Kudryashov, D.S., and Wu, J.Q. (2015). The Rho-GEF Gef3 interacts with the septin complex and activates the GTPase Rho4 during fission yeast cytokinesis. *Molecular biology of the cell* *26*, 238-255.

Wang, P., Malumbres, M., and Archambault, V. (2014). The Greatwall-PP2A axis in cell cycle control. *Methods in molecular biology* (Clifton, NJ) *1170*, 99-111.

Wang, Y., Li, W.Z., Johnson, A.E., Luo, Z.Q., Sun, X.L., Feoktistova, A., McDonald, W.H., McLeod, I., Yates, J.R., 3rd, Gould, K.L., *et al.* (2012). Dnt1 acts as a mitotic inhibitor of the spindle checkpoint protein dma1 in fission yeast. *Molecular biology of the cell* *23*, 3348-3356.

Wang, Y., Shirogane, T., Liu, D., Harper, J.W., and Elledge, S.J. (2003b). Exit from exit: resetting the cell cycle through Amn1 inhibition of G protein signaling. *Cell* *112*, 697-709.

Watson, A., Lipina, C., McArdle, H.J., Taylor, P.M., and Hundal, H.S. (2016). Iron depletion suppresses mTORC1-directed signalling in intestinal Caco-2 cells via induction of REDD1. *Cellular signalling* *28*, 412-424.

Watson, A.T., Garcia, V., Bone, N., Carr, A.M., and Armstrong, J. (2008). Gene tagging and gene replacement using recombinase-mediated cassette exchange in *Schizosaccharomyces pombe*. *Gene* *407*, 63-74.

Weilguny, D., Praetorius, M., Carr, A., Egel, R., and Nielsen, O. (1991). New vectors in fission yeast: application for cloning the his2 gene. *Gene* *99*, 47-54.

White, E.A., and Glotzer, M. (2012). Centralspindlin: at the heart of cytokinesis. *Cytoskeleton* (Hoboken) *69*, 882-892.

Willer, M., Hoffmann, L., Styrkarsdottir, U., Egel, R., Davey, J., and Nielsen, O. (1995). Two-step activation of meiosis by the *mat1* locus in *Schizosaccharomyces pombe*. *Molecular and cellular biology* *15*, 4964-4970.

Willet, A.H., McDonald, N.A., Bohnert, K.A., Baird, M.A., Allen, J.R., Davidson, M.W., and Gould, K.L. (2015). The F-BAR Cdc15 promotes contractile ring formation through the direct recruitment of the formin Cdc12. *The Journal of cell biology* *208*, 391-399.

Wilson-Grady, J.T., Villen, J., and Gygi, S.P. (2008). Phosphoproteome analysis of fission yeast. *Journal of proteome research* *7*, 1088-1097.

Wlodarchak, N., and Xing, Y. (2016). PP2A as a master regulator of the cell cycle. *Critical reviews in biochemistry and molecular biology* *51*, 162-184.

Wolfe, B.A., McDonald, W.H., Yates, J.R., 3rd, and Gould, K.L. (2006). Phosphoregulation of the Cdc14/Clp1 phosphatase delays late mitotic events in *S. pombe*. *Developmental cell* *11*, 423-430.

Wood, V., Harris, M.A., McDowall, M.D., Rutherford, K., Vaughan, B.W., Staines, D.M., Aslett, M., Lock, A., Bahler, J., Kersey, P.J., *et al.* (2012). PomBase: a comprehensive online resource for fission yeast. *Nucleic acids research* *40*, D695-699.

Wu, J.Q., Guo, J.Y., Tang, W., Yang, C.S., Freel, C.D., Chen, C., Nairn, A.C., and Kornbluth, S. (2009). PP1-mediated dephosphorylation of phosphoproteins at mitotic exit is controlled by inhibitor-1 and PP1 phosphorylation. *Nature cell biology* *11*, 644-651.

Wu, J.Q., Kuhn, J.R., Kovar, D.R., and Pollard, T.D. (2003). Spatial and temporal pathway for assembly and constriction of the contractile ring in fission yeast cytokinesis. *Developmental cell* *5*, 723-734.

Wu, J.Q., Sirotkin, V., Kovar, D.R., Lord, M., Beltzner, C.C., Kuhn, J.R., and Pollard, T.D. (2006). Assembly of the cytokinetic contractile ring from a broad band of nodes in fission yeast. *The Journal of cell biology* *174*, 391-402.

Wu, L., and Russell, P. (1993). Nim1 kinase promotes mitosis by inactivating Wee1 tyrosine kinase. *Nature* *363*, 738-741.

Wu, S.Z., and Bezanilla, M. (2014). Myosin VIII associates with microtubule ends and together with actin plays a role in guiding plant cell division. *eLife* *3*.

Xie, X., Harrison, D.H., Schlichting, I., Sweet, R.M., Kalabokis, V.N., Szent-Gyorgyi, A.G., and Cohen, C. (1994). Structure of the regulatory domain of scallop myosin at 2.8 Å resolution. *Nature* *368*, 306-312.

Xu, S., Huang, H.K., Kaiser, P., Latterich, M., and Hunter, T. (2000). Phosphorylation and spindle pole body localization of the Cdc15p mitotic regulatory protein kinase in budding yeast. *Current biology : CB* *10*, 329-332.

Yamada, H., Horigome, C., Okada, T., Shirai, C., and Mizuta, K. (2007). Yeast Rrp14p is a nucleolar protein involved in both ribosome biogenesis and cell polarity. *RNA (New York, NY)* *13*, 1977-1987.

Yamagishi, Y., Yang, C.H., Tanno, Y., and Watanabe, Y. (2012). MPS1/Mph1 phosphorylates the kinetochore protein KNL1/Spc7 to recruit SAC components. *Nature cell biology* *14*, 746-752.

Yamaguchi, S., Okayama, H., and Nurse, P. (2000). Fission yeast Fizzy-related protein *srw1p* is a G(1)-specific promoter of mitotic cyclin B degradation. *The EMBO journal* *19*, 3968-3977.

Yamano, H., Gannon, J., and Hunt, T. (1996). The role of proteolysis in cell cycle progression in *Schizosaccharomyces pombe*. *The EMBO journal* *15*, 5268-5279.

Yamano, H., Ishii, K., and Yanagida, M. (1994). Phosphorylation of dis2 protein phosphatase at the C-terminal cdc2 consensus and its potential role in cell cycle regulation. *The EMBO journal* *13*, 5310-5318.

Yang, J., and Kornbluth, S. (1999). All aboard the cyclin train: subcellular trafficking of cyclins and their CDK partners. *Trends in cell biology* *9*, 207-210.

Yeong, F.M., Lim, H.H., Padmashree, C.G., and Surana, U. (2000). Exit from mitosis in budding yeast: biphasic inactivation of the Cdc28-Clb2 mitotic kinase and the role of Cdc20. *Molecular cell* *5*, 501-511.

Yonetani, A., and Chang, F. (2010). Regulation of cytokinesis by the formin cdc12p. *Current biology : CB* *20*, 561-566.

Yoshida, S., Ichihashi, R., and Toh-e, A. (2003). Ras recruits mitotic exit regulator Lte1 to the bud cortex in budding yeast. *The Journal of cell biology* *161*, 889-897.

Yoshida, S., Kono, K., Lowery, D.M., Bartolini, S., Yaffe, M.B., Ohya, Y., and Pellman, D. (2006). Polo-like kinase Cdc5 controls the local activation of Rho1 to promote cytokinesis. *Science (New York, NY)* *313*, 108-111.

Yoshida, S., and Toh-e, A. (2001). Regulation of the localization of Dbf2 and mob1 during cell division of *saccharomyces cerevisiae*. *Genes & genetic systems* *76*, 141-147.

Yoshida, S., and Toh-e, A. (2002). Budding yeast Cdc5 phosphorylates Net1 and assists Cdc14 release from the nucleolus. *Biochemical and biophysical research communications* *294*, 687-691.

Yoshida, T., Toda, T., and Yanagida, M. (1994). A calcineurin-like gene *ppb1+* in fission yeast: mutant defects in cytokinesis, cell polarity, mating and spindle pole body positioning. *Journal of cell science* *107 (Pt 7)*, 1725-1735.

Yu, J.S. (1998). Activation of protein phosphatase 2A by the Fe²⁺/ascorbate system. *Journal of biochemistry* *124*, 225-230.

Zeng, K., Bastos, R.N., Barr, F.A., and Gruneberg, U. (2010). Protein phosphatase 6 regulates mitotic spindle formation by controlling the T-loop phosphorylation state of Aurora A bound to its activator TPX2. *The Journal of cell biology* *191*, 1315-1332.

Zeng, Y., Forbes, K.C., Wu, Z., Moreno, S., Piwnicka-Worms, H., and Enoch, T. (1998). Replication checkpoint requires phosphorylation of the phosphatase Cdc25 by Cds1 or Chk1. *Nature* *395*, 507-510.

Zhang, G., Kashimshetty, R., Ng, K.E., Tan, H.B., and Yeong, F.M. (2006). Exit from mitosis triggers Chs2p transport from the endoplasmic reticulum to mother-daughter neck via the secretory pathway in budding yeast. *The Journal of cell biology* *174*, 207-220.

Zhou, X., Ma, Y., Fang, Y., gerile, W., Jaiseng, W., Yamada, Y., and Kuno, T. (2013). A genome-wide screening of potential target genes to enhance the antifungal activity of micafungin in *Schizosaccharomyces pombe*. *PloS one* *8*, e65904.

Zhou, Z., Munteanu, E.L., He, J., Ursell, T., Bathe, M., Huang, K.C., and Chang, F. (2015). The contractile ring coordinates curvature-dependent septum assembly during fission yeast cytokinesis. *Molecular biology of the cell* *26*, 78-90.

Zilahi, E., Salimova, E., Simanis, V., and Sipiczki, M. (2000). The *S. pombe* *sep1* gene encodes a nuclear protein that is required for periodic expression of the *cdc15* gene. *FEBS letters* *481*, 105-108.

Zitouni, S., Nabais, C., Jana, S.C., Guerrero, A., and Bettencourt-Dias, M. (2014). Polo-like kinases: structural variations lead to multiple functions. *Nature reviews Molecular cell biology* *15*, 433-452.

Zwart, K.B., Veenhuis, M., and Harder, W. (1983). Significance of yeast peroxisomes in the metabolism of choline and ethanolamine. *Antonie van Leeuwenhoek* 49, 369-385.

Appendix

Table 3:1 List of strains used in this study

Genotype	Source
<i>apm1-Δ</i>	Bioneer deletion collection
<i>arp42-Δ</i>	Bioneer deletion collection
<i>cdc7-24</i>	(Nurse et al., 1976)
<i>cdc7-A20</i>	(Fankhauser and Simanis, 1994)
<i>cdc11-136</i>	(Nurse et al., 1976)
<i>cdc14-118</i>	(Nurse et al., 1976)
<i>cdc2-1w</i>	(Fantes, 1981)
<i>cdc2-3w</i>	(Russell and Nurse, 1987b)
<i>cdc16-116</i>	(Minet et al., 1979)
<i>cdc25-22</i>	(Fantes, 1979)
<i>ckb1-Δ</i>	Bioneer deletion collection
<i>csc1-Δ</i>	(Singh et al., 2011)
<i>csc2-Δ</i>	(Singh et al., 2011)
<i>csc3-Δ</i>	(Singh et al., 2011)
<i>csc4-Δ</i>	(Singh et al., 2011)
<i>dis2-Δ</i>	Yanagida lab
<i>eca39-Δ</i>	Bioneer deletion collection
<i>erp5/6-Δ</i>	Bioneer deletion collection
<i>etd1-Δ</i>	(Daga and Chang, 2005)
<i>flp1-Δ</i>	(Cueille et al., 2001)
<i>fio1-Δ</i>	Bioneer deletion collection
<i>for3-Δ</i>	From Sophie Martin, Lausanne
<i>kgd2-Δ</i>	Bioneer deletion collection
<i>mob1-R4</i>	(Salimova et al., 2000)
<i>mat2p-102</i>	Lab stock (from Peter Fantès, Edinburgh)
<i>ppa1-Δ</i>	(Kinoshita et al., 1990)
<i>ppa2-Δ</i>	(Kinoshita et al., 1990)
<i>pab1-Δ</i>	(Kinoshita et al., 1996)
<i>par1-Δ</i>	(Le Goff et al., 2001)
<i>par2-Δ</i>	Bioneer deletion collection
<i>pfa3-Δ</i>	Bioneer deletion collection
<i>rpl15-Δ</i>	Bioneer deletion collection
<i>rpl1201-Δ</i>	Bioneer deletion collection
<i>rpl3201-Δ</i>	Bioneer deletion collection
<i>rrp14-Δ</i>	Bioneer deletion collection
<i>sid2-1</i>	(Balasubramanian et al., 1998)
<i>sid2-250</i>	(Balasubramanian et al., 1998)
<i>sid4-SA1</i>	(Balasubramanian et al., 1998)
<i>SPAC13G6.09-Δ</i>	Bioneer deletion collection
<i>SPBC3D6.08c-Δ</i>	Bioneer deletion collection
<i>spg1-B8</i>	(Schmidt et al., 1997)
<i>spg1-M19</i>	(Grote, Krapp and Simanis, unpublished)
<i>tea4-Δ</i>	From Sophie Martin, Lausanne
<i>wee1-50</i>	(Nurse, 1975)
<i>WT</i>	Lab strain
<i>ypa1-Δ</i>	(Goyal and Simanis, 2012)
<i>ypa2-Δ</i>	(Goyal and Simanis, 2012)
<i>ypa2-S2</i>	(Grote, Krapp and Simanis, unpublished)

<i>cdc7-gfp</i>	(Sohrmann et al., 1998)
<i>mob1-gfp</i>	(Salimova et al., 2000)
<i>gfp-sid1</i>	(Guertin et al., 2000)
<i>leu1::gfp-atb2</i>	(Krapp et al., 2006)

Table 3:2 Information on the hits from the SGA (attached to the online version of this document)

Table 3:3 BP of the hits from the SGA (attached to the online version of this document)

Table 3:4 FYPO of the deletion mutants identified as hits in the SGA (attached to the online version of this document)

Table 3:5 Information on the non-growers from the SGA (attached to the online version of this document)

Table 3:6 BP of the non-growers from the SGA (attached to the online version of this document)

Table 3:7 FYPO of the deletion mutants, which did not grow in the SGA (attached to the online version of this document)

Table 3:8 Information on the genes that generated a reduced number of colonies in the SGA (attached to the online version of this document)

Table 3:9 BP of the genes that generated a reduced number of colonies in the SGA (attached to the online version of this document)

Table 3:10 FYPO of the deletion mutants, for the genes that generated a reduced number of colonies in the SGA (attached to the online version of this document)

Table 3:11 Summary of the reconstructed interactions found in the SGA (section 3.7.3)

Table 3:12 List of primers used in this study

In bold is indicated the sequence corresponding to the restriction site.

Primer	Sequence	Purpose
VS 713	5` -ACC GGC GCA GGA ACA CTG- 3`	<i>kanR</i> + internal primer
VS 1598	5`-CAT GTC GAC CTT TAG TAG TCG AAA TTA TTT CC- 3`	Cloning of <i>ypa2</i> -S2 in DW232
VS 1599	5`-CAT GAA TTC CTC AAA ATT ATG ATT TGT CAC C- 3`	Cloning of <i>ypa2</i> -S2 in DW232
VS 1621	5`- GGG ATA TCA GTA CCT CTC TTT	Cloning of the <i>ypa2</i> +

	T C- 3'	promoter into <i>ypa2-S2</i> -containing INT K1
VS 1622	5'-CTC TTC TCT AGA AAG CAT GTT GGC- 3'	Cloning of the <i>ypa2+</i> promoter into <i>ypa2-S2</i> containing INT K1
VS 1649	5'-CAT TGT ACA AGC TTG CCT CGT CCC CGC CGG GT- 3'	Insertion of <i>natR+</i> upstream of <i>ypa2-S2</i>
VS 1650	5'-CAT TGT ACA ACT GGA TGG CGG CGT TAG TAT CG- 3'	Insertion of <i>natR+</i> upstream of <i>ypa2-S2</i>
VS 1686	5'-TGT TTT TCA GTT TGG TAA AAA CTG G- 3'	Verification of Bioneer <i>ypa1-Δ</i>
VS 1687	5'-AAC TGT ACT TCT CAG CAT TTA TGC G- 3'	Verification of Bioneer <i>ppa2-Δ</i>
VS 1695	5' - CTA CAA AGT GTC ACT GTC ACA CCT G- 3'	Verification of Bioneer <i>ckb1-Δ</i>
VS 1696	5' - AGC ATC TAG AGA AAA ATC AAT TGG C- 3'	Verification of Bioneer <i>hus5-Δ</i>
VS 1697	5' -GAT TAG GGT AGC TTT AAA GGT CCG G- 3'	Verification of Bioneer <i>flp1-Δ</i>
VS 1705	5' -AAG AAA GCT CTT GGC ATA ACA GTC G- 3'	Verification of Bioneer <i>SPAC13G6.09-Δ</i>
VS 1706	5' -CCC CTG GTA CCT GTC CTC TTA ATT A- 3'	Verification of Bioneer <i>SPAC27E2.11c-Δ</i>
VS 1707	5' -TAT AGT CAA GGC GAA TAT TTC TGC A- 3'	Verification of Bioneer <i>inp2-Δ</i>
VS 1708	5' -AGG TGT CAA TAC TTG TGC AAG TCG A- 3'	Verification of Bioneer <i>erp5/6-Δ</i>
VS 1709	5' - TGA AAA TTT GCT TAC CAA AAA ATC A- 3'	Verification of Bioneer <i>paf1-Δ</i>
VS 1710	5' - AAT GAA AAT ATC AAA TTC GCA CAG A- 3'	Verification of Bioneer <i>pfa3-Δ</i>
VS 1711	5' - TTC AAT GAA CTA ATC CGC TTA TGA T- 3'	Verification of Bioneer <i>ism1-Δ</i>
VS 1712	5' - ATG CCT GAA ACT TAG AGT ACG AAC C- 3'	Verification of Bioneer <i>rrp14-Δ</i>
VS 1713	5' - TTT ATT GGA TTA GAG CAC TAT GCC G- 3'	Verification of Bioneer <i>rpl1201-Δ</i>
VS 1714	5' -GTT CAC TTG CTT TCG GTA AAA	Verification of Bioneer

	ATG A- 3`	<i>rpl15-Δ</i>
VS 1716	5` - TCA TTT TTG CTG TCT TTA CAT CAC A- 3`	Verification of Bioneer <i>kgd2-Δ</i>
VS 1717	5` - GAT TTG ACG AAC CGA TCC ATT AAA G- 3`	Verification of Bioneer <i>fio1-Δ</i>
VS 1718	5` -TGG ATG CTC AAA GCA CCT G- 3`	Verification of Bioneer <i>ipk1-Δ</i>
VS 1719	5` -AAT GCA AAA AAA CTG CTT ATT CAA G- 3`	Verification of Bioneer <i>arp42-Δ</i>
VS 1720	5` -ACT GGT TTA AAT GGC AGT TTT TAC A- 3`	Verification of Bioneer <i>rex3-Δ</i>
VS 1721	5` -TCA CTT TGG TTT TAT CAT TGG TGA A- 3`	Verification of Bioneer <i>apm1-Δ</i>
VS 1723	5` -CTT TGA AAG GAA AAT TTG AGT TTG C- 3`	Verification of Bioneer <i>rpl3201-Δ</i>
VS 1724	5` -TTC ATC AGA TAT GCT CCT TAG GGT A- 3`	Verification of Bioneer <i>fip1-Δ</i>
VS 1725	5` -ACT AAA GCT ATG CCA ATG GTA CTC A- 3`	Verification of Bioneer <i>eca39-Δ</i>
VS 1732	5` -TAA AAG AGA CTC GAC TGT AAC TGC G- 3`	Verification of Bioneer <i>atp18-Δ</i>
VS 1733	5` -ATT ACG CTT TTT TTC AGA AAT TTG G- 3`	Verification of Bioneer <i>par1-Δ</i>
VS 1734	5` -GTT TTG CTT CAT TTG CCA AAC ATA A- 3`	Verification of Bioneer <i>par2-Δ</i>
VS 1735	5` -TAA GGT TTC ATT AAT GGG AAA TTG C- 3`	Verification of Bioneer <i>pab1-Δ</i>
VS 1736	5` -CCA TAC CTT TCA ACC TTC ATA CAA A- 3`	Verification of Bioneer <i>ppa1-Δ</i>
VS 1737	5` -AGA AAT AAG GTT TTT GTT TTG CTG G- 3`	Verification of Bioneer <i>for3-Δ</i>
VS 1739	5` -CTT TTT GAT TAT CCA AGA GCA TCA A- 3`	Verification of Bioneer <i>ckb2-Δ</i>
VS 1740	5` -TAT TAC AAT ACC TCC ATC TTT GGC C- 3`	Verification of Bioneer <i>ypa2-Δ</i>

Curriculum vitae **Manuela Moraru**

Date of birth: 19.09.1987
Nationality: Romanian
Av. de Cour 15
1007 Lausanne
manuela.moraru87@gmail.com



Education

2012 - 2016 PhD Studies in Molecular Life Sciences

Polytechnic Federal School of Lausanne, Switzerland

PhD thesis: "Identification of genetic interactors of *ypa2* in *Schizosaccharomyces pombe*" (in the lab of Prof. Viesturs Simanis)

2009 - 2011 Master Studies in Developmental and Cell Biology Biology

University of Fribourg, Switzerland

Dissertation: "An *in vitro* model to study proliferation control in *Drosophila* neuroblasts" (in the lab of Prof. Simon G. Sprecher)

2006 - 2009 Bachelor Studies in Biology and Teaching Training

University of Constanta, Romania

Bachelor thesis: "Structural and functional aspects of *Magnetospirillum gryphiswaldense*, cultured on 1 μ M and 100 μ M iron" (in the lab of Prof. Ioan I. Ardelean)

Technical skills

Schizosaccharomyces pombe: genetics, molecular biology (DNA extraction, polymerase chain reaction, gene deletion, DNA cloning, generation of recombinant proteins), biochemistry (protein extraction, affinity purification, Western-blotting), SILAC labelling, immunostaining

Drosophila melanogaster: larval brain dissection, primary cell culture, immunohistochemistry

Escherichia coli: transformation, isolation of plasmid DNA

Microscopy: epifluorescence and confocal

Computer Skills: Microsoft Office (Word, Excel, PowerPoint), Adobe PhotoShop, ImageJ, GraphPad Prism, Scaffold Viewer

Teaching experience

2012 - 2013: Teaching assistant (235 hours) for "Laboratoire intégré en sciences de la vie", Polytechnic Federal School of Lausanne, Switzerland

2014 and 2015: Project supervisor (one week/each year) in the program “La Science Appelle les Jeunes”, Polytechnic Federal School of Lausanne, Switzerland

2015: Project supervisor (8 weeks) in the “Summer Research Program for Undergraduate Life Science Students”, Polytechnic Federal School of Lausanne, Switzerland

Publications

Egger B, van Giesen L, **Moraru M**, Sprecher SG, In vitro imaging of primary neural cell culture from *Drosophila*, Nature Protocols, 2013 May;8(5):958-65. doi: 10.1038/nprot.2013.052.

Moraru M, Egger B, Bao DB, Sprecher SG, Analysis of cell identity, morphology, apoptosis and mitotic activity in a primary neural cell culture system in *Drosophila*, Neural Development, 2012 Jun 20;7:14. doi: 10.1186/1749-8104-7-14

Meetings attended

March 2016: French and UK *pombe* clubs, Carry-le-Rouet, France

March 2016: Cancer and Immunology PhD students retreat, Les Diablerets, Switzerland

September 2015: EMBO Meeting, Birmingham, United Kingdom

March 2015: Cancer and Immunology PhD students retreat, Les Diablerets, Switzerland

September 2013: Cancer Summer Course, CHUV, Lausanne, Switzerland

July 2012: EMBO Course on Molecular genetics in fission yeast, Paris, France

September 2011: Workshop in Marine Developmental Biology, Banyuls-sur-mer, France

January 2011: Bern-Fribourg Colloquium on Neuro- and Developmental biology, Leysin, Switzerland

August 2010: Neurobiology Labs Retreat, Archachon, France

November 2008: Meeting on the Impact of Environmental Factors on Biodiversity, Bucharest, Romania

Languages

Romanian: native; **English** and **French:** fluent; **Spanish:** basic